NEW MEXICO BUREAU OF GEOLOGY AND MINERAL RESOURCES
Memoir 51 2024

Geology of the Quebradas Region, Socorro County, Central New Mexico

Steven M. Cather and Daniel J. Koning, editors

GEOLOGY

Geology of the Quebradas Region, Socorro County, Central New Mexico

Steven M. Cather and Daniel J. Koning, editors

Memoir 51
December 2024

New Mexico Bureau of Geology and Mineral Resources
A research and service division of New Mexico Institute of Mining and Technology

Memoir 51—Geology of the Quebradas Region, Socorro County, Central New Mexico

Editors: Steven M. Cather and Daniel J. Koning

New Mexico Bureau of Geology and Mineral Resources
A research and service division of New Mexico Institute of Mining and Technology

Mapping/Graphics/Data Support: Ann D. (Andi) Knight, Phil Miller, Elizabeth Roybal, Mark Mansell, Leo Gabaldon, Stephanie Chavez, Allison Walsh, and Brigitte Felix

Copyediting: Carrin Rich and Frank Sholedice

Design and Layout: Lauri Logan

Publications Program Manager: Barbara J. Horowitz

Cover Photograph: Overturned fold in the Los Vallos Formation (upper Yeso Group) in the Lomas de las Cañas quadrangle. View is to the southwest from 334936E, 3766503N (zone 13, NAD 27). *Photo by S.M. Cather*

Project Funding: Funding for this project was provided by the U.S. Geological Survey STATEMAP program and the New Mexico Bureau of Geology and Mineral Resources.

Suggested Citation: Cather, S.M., and Koning, D.J., eds., 2024, Geology of the Quebradas Region, Socorro County, Central New Mexico: New Mexico Bureau of Geology and Mineral Resources Memoir 51, 206 p. https://doi.org/10.58799/M-51

PREFACE

The eastern rift flank of the Socorro Basin is referred to by local inhabitants as the Quebradas, short for *las tierras quebradas*—the broken lands. An apt physiographic description, the name is also appropriate in a geologic sense. In my 45 years of experience as a field geologist, I have seen no region of comparable stratigraphic diversity and structural complexity elsewhere in New Mexico. As an undergraduate student at the New Mexico Institute of Mining and Technology in the mid-1970s, I often wondered why no detailed map and report existed for the Quebradas region; it lies, after all, right across the river from the school. I now know why.

I am fortunate to have been allowed sufficient time and resources by the New Mexico Bureau of Geology and Mineral Resources (NMBGMR) to map the six quadrangles that form the basis of this memoir. The work was done piecemeal. It began with mapping of the Bosquecito pumice in 1988, continued with mapping of upper Cenozoic basin-fill deposits in the mid-1990s, and culminated with STATEMAP-supported mapping of mostly bedrock areas between 2002 and 2014. It is fortunate that the bedrock mapping began relatively late in my career; I did not possess sufficient knowledge of structural geology and regional stratigraphy to have attempted it earlier. That said, there are parts of the mapped area that require more detailed study or remapping at larger scales. I regard the present map as a detailed reconnaissance in some areas of limited access or great structural complexity.

Several renowned geologists, paleontologists, and geochronologists contributed their expertise to the research and writing of this memoir. They are Gary Axen, Matt Heizler, Gretchen Hoffman, Steve Hook, Bill McIntosh, Ginger McLemore, and the late Bill Cobban. I thank various private landholders and the Sevilleta National Wildlife Refuge for access to lands. Steve Hook wishes to acknowledge Greg Mack for helpful interpretation and Atarque Geologic Consulting LLC, the New Mexico Bureau of Geology and Mineral Resources, and K.C. McKinney (core collections manager, U.S. Geological Survey) for support. Parts of the memoir were reviewed by Gary Axen, Doug Bland, Martha Cather, Richard Chamberlin, Bill Chenowith, Kent Condie, Bob Eveleth, Andy Heckert, Karl Karlstrom, Shari Kelley, Dan Koning, Karl Krainer, Barry Kues, Neil Landman, Tim Lawton, Mark Leckie, Dave Love, John Nelson, Bob Osburn, and Kate Zeigler. The authors thank these reviewers for their useful comments and revisions.

Dan Koning kindly agreed to serve as co-editor of this memoir. Cartography was done by Ann D. (Andi) Knight and Elizabeth Roybal. The late Mark Mansell prepared the digital elevation maps. Leo Gabaldon, Stephanie Chavez, and Brigitte Felix created the figures. Editorial comments by Jennifer Eoff, Carrin Rich, and Frank Sholedice were greatly appreciated. I benefited from valuable discussions with numerous geoscientists, most notably Bruce Allen, Gary Axen, Richard Chamberlin, Chuck Chapin, Bob Colpitts, Santiago Flores, Mark Green, John Hawley, Karl Karlstrom, Shari Kelley, Barry Kues, Dave Love, Spencer Lucas, John Nelson, Bob Osburn, Peter Scholle, Dana Ulmer-Scholle, and the late Clay T. Smith. Curtis Verploegh provided field assistance on some of the longer traverses and piloting on overflights. Mapping was greatly expedited by my equine friends Sasquatch, Vicky, Lucy, Star, and Rojo. Their company was greatly appreciated.

This memoir is a companion to the *Geologic Map of the Quebradas Region, Socorro County, Central New Mexico* (Plates 1 and 2), which is available for download at **https://geoinfo.nmt.edu/publications/monographs/memoirs/51/**.

This memoir is dedicated to the memory of Chuck Chapin and Bob Folk—longtime mentors, facilitators, and friends.

Steve Cather
Socorro, New Mexico
Spring 2024

CONTENTS

Figures

Tables

ABSTRACT

The Quebradas region lies east of Socorro, New Mexico, and encompasses the eastern part of the Socorro Basin of the Rio Grande rift and the adjacent rift shoulder. Exposed rocks are of Proterozoic, Pennsylvanian, Permian, Middle and Late Triassic, Late Jurassic, Late Cretaceous, Paleogene, Neogene, and Quaternary age. Tectonic episodes recorded in the study area include Proterozoic plutonism and deformation, Pennsylvanian (Ancestral Rocky Mountain) and Late Cretaceous–middle Eocene (Laramide) dextral-oblique contraction, middle Eocene–middle Miocene top-east detachment faulting, and Neogene–Quaternary rift-related extension.

Proterozoic rocks crop out in several small exposures on fault blocks along the east margin of the Socorro Basin. The west-central part of the study area exposes the Tajo granite, and biotite gneiss crops out to the north. Both rock units are undated.

Pennsylvanian strata nonconformably overlie Proterozoic rocks in the study area and consist of sandstone, mudstone, and limestone of the Sandia, Gray Mesa, Atrasado, and Bursum Formations. These Desmoinesian to lower-Wolfcampian beds were deposited in fluvial, coastal-plain, nearshore, and open-marine environments during the Ancestral Rocky Mountain orogeny. Despite their relative thinness, most members of the Gray Mesa and Atrasado Formations can be correlated over a broad region of central and southern New Mexico. This great lateral continuity suggests that Pennsylvanian member-scale lithostratigraphic variation reflects mostly eustatic, paleoclimatic, and/or epeirogenic influences rather than local orogenic ones. Paleocurrent data, maximum clast-size distribution, isopach data, and lithofacies trends from the Bursum Formation indicate that a Late Pennsylvanian uplift (herein termed the San Antonio Uplift) occupied much of what is now the Socorro Basin, south of the long-known Joyita Uplift.

Permian stratigraphic units include the Abo Formation, the Yeso Group (consisting of the Meseta Blanca Sandstone and Los Vallos Formations), the Glorieta Sandstone, the San Andres Formation, and the Artesia Group. Fluvial deposits of the Abo Formation filled relict basins and lapped onto Ancestral Rocky Mountain uplifts in central New Mexico. The Yeso Group, Glorieta Sandstone, San Andres Formation, and Artesia Group represent eolian, coastal-plain, sabkha, and marine deposition on a stable shelf northwest of the Delaware Basin of southeastern New Mexico.

Mesozoic strata are apportioned among the Middle Triassic Moenkopi Formation, the Upper Triassic Chinle Formation, the Upper Jurassic Morrison Formation, and the Upper Cretaceous Dakota Sandstone, Mancos Shale, Tres Hermanos Formation, Gallup Sandstone, and Crevasse Canyon Formation. Both the Moenkopi and Chinle were deposited by mostly fluvial processes in an evolving retro-arc basin. The Morrison Formation in the study area accumulated as fluvial deposits on the southern feather-edge of the broad Morrison basin. Upper Cretaceous strata record three transgressive–regressive cycles in the southwestern part of the Late Cretaceous Western Interior Seaway. Upper Cretaceous marine rocks in the Quebradas area range in age from middle Cenomanian to early Coniacian.

Red beds of the middle Eocene Baca Formation accumulated in the late Laramide Carthage–La Joya Basin. The Baca Formation consists of fluvial deposits mostly derived from the Sierra Uplift, a transpressional uplift now largely subsided within the Socorro Basin. Also preserved are axial-river deposits that may represent a regional paleoriver system with headwaters to the west in Arizona. In the southern part of the Carthage–La Joya Basin, Baca sediments accumulated in half grabens related to hanging-wall splays of a regional top-east detachment fault, the Quebradas detachment.

Thick sections of middle Eocene to upper Oligocene volcanic and volcaniclastic rocks are exposed in the study area and provide a good representation of the stratigraphy of the northeastern Mogollon–Datil volcanic field. These rocks consist of the volcaniclastic Spears Group and the overlying, ignimbrite-dominated Datil and Mogollon Groups. $^{40}Ar/^{39}Ar$ ages for Paleogene volcanic, volcaniclastic, and intrusive rocks in the study area range from approximately 43 to 27.7 Ma. A Pliocene basalt was erupted about 3.7 Ma at Black Mesa and post-dates local slip on the Montosa fault.

Neogene deposits in the study area are assigned to the Santa Fe Group (the Popotosa and Sierra Ladrones Formations). The Popotosa Formation (undated in the study area, but regionally of late Oligocene to late Miocene age) may be related to the final episode of slip on the Quebradas detachment fault rather than Rio Grande rifting. The upper Miocene–lower Pleistocene Sierra Ladrones Formation consists of piedmont deposits and interfingered ancestral Rio Grande deposits in the eastern part of the Socorro Basin. The Sierra Ladrones Formation contains pumiceous flood deposits related to the 1.6 Ma eruption of the lower Bandelier Tuff (Otowi Member). Incision of the Rio Grande and its tributaries began about 800 ka, marking the end of Santa Fe Group deposition. Santa Fe Group deposition was followed by middle Pleistocene to Holocene episodes of alternating aggradation and degradation during which sand, mud, and gravel were deposited in the Rio Grande valley as several generations of inset piedmont and terrace deposits.

The structural geology of the Quebradas region is complex. Structures include (1) Laramide west-up reverse faults and associated fault-propagation folds, fault-bend folds, and monoclines; (2) northeast-striking zones of dextral Laramide strike-slip faults with linking contractile and extensional step-overs; (3) a regional middle Eocene to middle Miocene, top-east decollement (herein termed the Quebradas detachment fault) developed mostly within the gypsiferous upper Yeso Group that is associated with splay faults and rollover anticlines in its hanging wall; and (4) Neogene and Quaternary normal faults related to rifting.

Two mining districts (Socorro and Chupadero) and two coal fields (Carthage and Jornada del Muerto) are present in the Quebradas region. Known mineral deposits include Rio Grande rift copper-silver (± uranium) veins, disseminated uranium and rare earth elements (REE), sandstone uranium, volcanogenic uranium, Rio Grande rift barite-fluorite-galena (± silver, copper), sedimentary copper, sedimentary clay deposits, and gypsum. Coal was produced primarily from the Carthage coal field, with intermittent production between the 1880s and 1960s. With the possible exception of U-REE deposits in the Tajo granite, little or no potential for mineral or coal production exists in the Quebradas region under current market conditions.

INTRODUCTION AND PREVIOUS WORK

This report describes the geology of six 7.5-minute quadrangles—Mesa del Yeso (Cather et al., 2004), Sierra de la Cruz (Cather et al., 2012), Loma de las Cañas (Cather and Colpitts, 2005), Bustos Well (Cather et al., 2014), San Antonio (Cather, 2002), and Cañon Agua Buena (Cather et al., 2007). These geologic quadrangles, compiled at a scale of 1:36,000 on Plate 1, encompass about 950 km^2 in what is herein termed the Quebradas region—the eastern part of the Socorro Basin and its uplifted eastern rift flank (Fig. 1).

Wilpolt and Wanek (1951) were the first to map the geology of the Quebradas region; they did so as part of a larger oil and gas investigation. Several thesis and dissertation maps were subsequently completed by students at the New Mexico Institute of Mining and Technology and the University of New Mexico (Fig. 2). Unpublished geologic maps of local areas were kindly supplied by R.M. Colpitts, S. Flores, M.W. Green, and G.R. Osburn.

The quality of exposure is good in most places. Except along U.S. Route 380, access is by dirt roads, some of which are graded but many are unimproved. Several areas are only accessible by foot or horseback. Most of the Quebradas region is federal or state lands, with scattered private inholdings. The northern part of the study area lies within the Sevilleta National Wildlife Refuge, for which access permission is required.

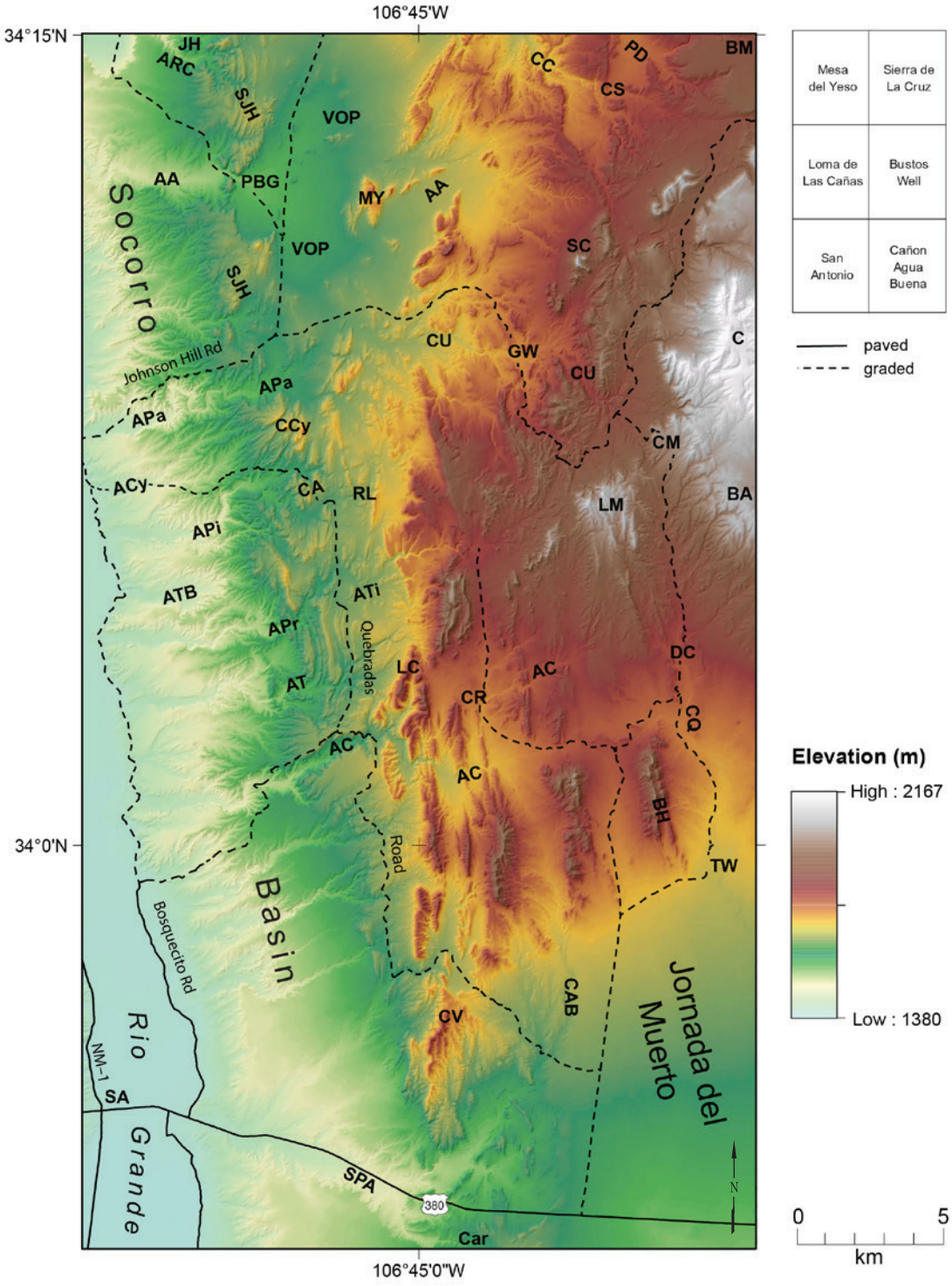

Figure 1. Color-ramped digital elevation model of the Quebradas study area showing 7.5-minute quadrangle maps, selected place names, and roads. **AA**—Arroyo de Alamillo, **AC**—Arroyo de las Cañas, **ACy**—Arroyo del Coyote, **APa**—Arroyo de la Parida, **APi**—Arroyo de los Pinos, **APr**—Arroyo de la Presilla, **ARC**—Arroyo Rosa de Castillo, **AT**—Arroyo del Tajo, **ATB**—Arroyo Tio Bartolo, **ATi**—Arroyo Tinajas, **BA**—Bordo Atravesado, **BH**—Blackington Hills, **BM**—Black Mesa, **C**—La Cebolla, **CA**—Cerros de Amado, **CAB**—Cañon Agua Buena, **Car**—Carthage (abandoned townsite), **CC**—Cibola Canyon, **CCy**—Cerrillos del Coyote, **CM**—Cuesta de la McBride, **CQ**—Cañada Quemada, **CR**—Las Cañas Ranch, **CS**—Cibola Spring, **CU**—Cañoncito de la Uva, **CV**—Cerro del Viboro, **DC**—Del Curto Ranch, **GW**—Gallina Well, **JH**—Joyita Hills, **LC**—Loma de las Cañas, **LM**—La Montanera, **MY**—Mesa del Yeso, **PBG**—Puertecito of Bowling Green, **PD**—Palo Duro Canyon, **RL**—Rancho de Lopez, **SA**—San Antonio village, **SC**—Sierra de la Cruz, **SJH**—southern Joyita Hills, **SPA**—San Pedro Arroyo, **TW**—Taylor Well, **VOP**—Valle del Ojo de la Parida.

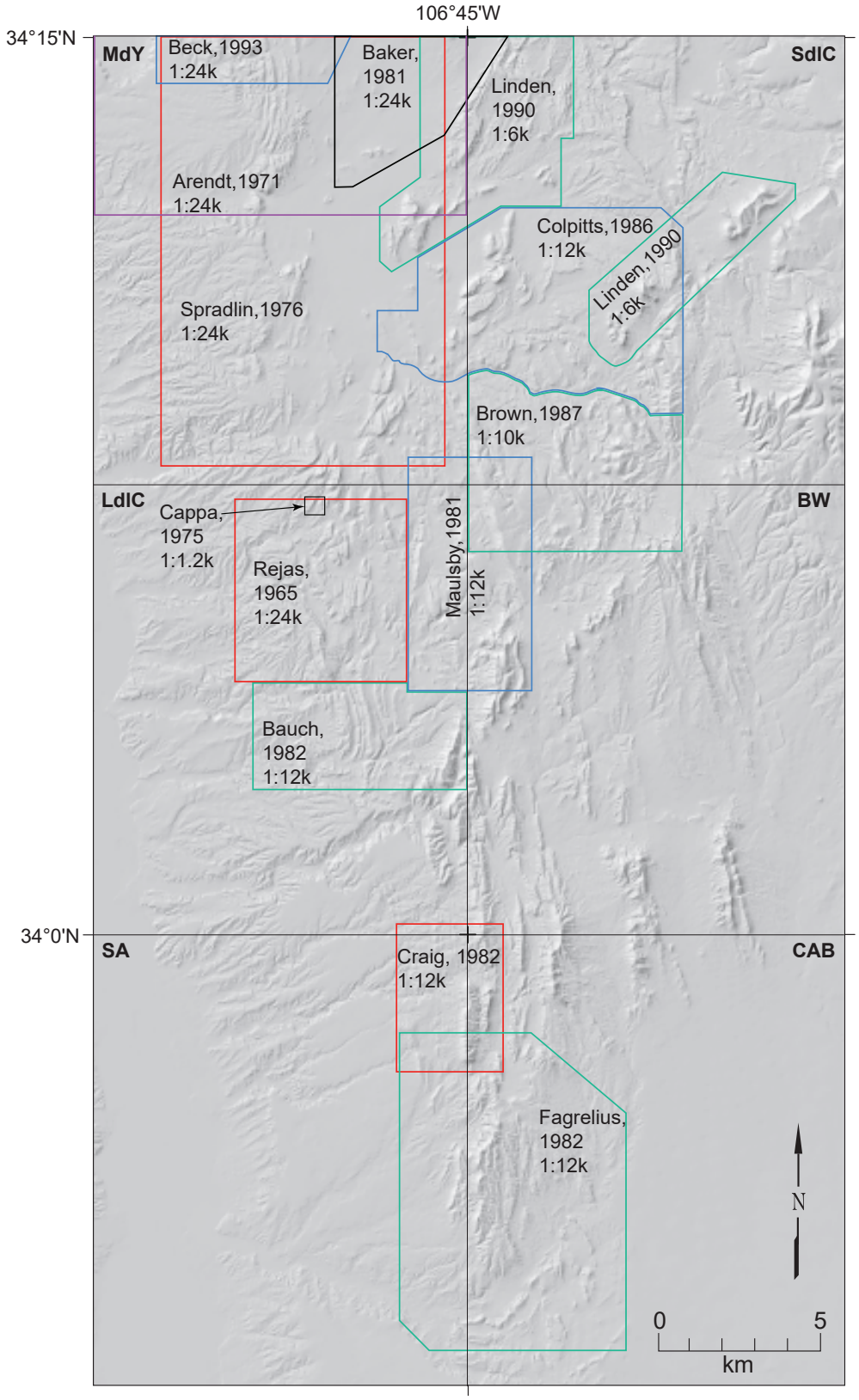

Figure 2. Digital elevation model of the Quebradas study area showing boundaries of geologic quadrangle maps and location and scale of thesis mapping. Geologic quadrangle maps are **BW**—Bustos Well (Cather et al., 2014), **CAB**—Cañon Agua Buena (Cather et al., 2007), **LdlC**—Loma de las Cañas (Cather and Colpitts, 2005), **MdY**—Mesa del Yeso (Cather et al., 2004), **SA**—San Antonio (Cather, 2002), and **SdlC**—Sierra de la Cruz (Cather et al., 2012).

View to the southeast across the northern Jornada del Muerto with Sierra Oscura (right) and Mockingbird Gap on the skyline. Photo taken from astride Vicky, a gaited Morgan mare, from the northwestern Cañon Agua Buena quadrangle. *Photo by Steve Cather*

CHAPTER I: PROTEROZOIC ROCKS OF THE QUEBRADAS REGION

Steven M. Cather

INTRODUCTION

Precambrian rocks of central New Mexico are within the 1.7–1.6 Ga Mazatzal province, one of a series of terranes that were accreted to the southern margin of Laurentia during the Proterozoic (Karlstrom et al., 2004). Several exposures of Proterozoic rocks are present in the study area; all are in fault blocks along the eastern margin of the Socorro Basin of the Rio Grande rift.

TAJO PLUTON

Six small exposures of the granitic Tajo pluton of Condie and Budding (1979) crop out in the central part of the Loma de las Cañas quadrangle, in the drainages of Arroyo del Tajo, Arroyo de la Presilla, and Arroyo de Tio Bartolo. Each exposure is bounded on the west by a west-down, rift-related normal fault, and most are nonconformably overlain by east-dipping strata of the Pennsylvanian Sandia Formation (Fig. 3). These Precambrian exposures lie within the core of the Laramide Tajo structural zone (see Chapter 5) and owe much of their structural elevation to Laramide reverse faulting. The Tajo structural zone was a salient on the eastern flank of the Laramide Sierra Uplift, which contained widespread exposures of Proterozoic rocks that have since been structurally inverted within the Socorro Basin (Cather, 1983).

The Tajo pluton consists mostly of quartz, alkali feldspar, and plagioclase (with an average respective ratio of about 35/37/27) and minor biotite, muscovite, and magnetite (Condie and Budding, 1979). The Tajo pluton was described by most previous workers as quartz monzonite (Condie and Budding, 1979; Bauch; 1982; McLemore, 1983a). Based on the present International Union of Geological Sciences (IUGS) classification (Le Maitre et al., 1989), however, it is granite. The Tajo pluton is grayish-orange, medium to coarse grained, weakly foliated, and commonly highly fractured and jointed (Fig. 4). It is locally sericitized and stained by iron oxides and contains metamorphic xenoliths, rare pegmatites, and aplites (McLemore, 1983a). Barite and fluorite veins and uranium mineralization also occur locally (McLemore, 1983a; see Chapter 6). An exposure of the Tajo pluton in NE1/4 sec. 3, T. 3 S., R. 1 E. yielded an apatite fission-track cooling age of 8.2 ± 4.8 Ma, which may reflect cooling following fluorite mineralization in the nearby Gonzales prospect (Kelley et al., 1992). The Tajo pluton has not been dated, but is texturally more similar to 1.65 Ga granites in the Manzano and Los Pinos Mountains to the north than to megacrystic 1.4 Ga granites of the region (K.E. Karlstrom, written communication, 2018).

BIOTITE GNEISS

In the Mesa del Yeso quadrangle, Proterozoic biotite gneiss crops out in the footwall of the East Joyita fault, in and near Arroyo de Rosa Castillo in the Joyita Hills. These rocks grade northward into a larger expanse of foliated Proterozoic granite (the La Joyita pluton of Condie and Budding [1979]) that extends about 5 km beyond the study area to the north (Herber, 1963a, 1963b; Arendt, 1971; Condie and Budding, 1979). Proterozoic rocks exposed in the Joyita Hills owe their penetrative fabrics to a combination of the 1.65 Ga Mazatzal and 1.45 Ga Picuris orogenies (Karlstrom et al., 2016) and their structural height to a combination of Ancestral Rocky Mountain, Laramide, and rift tectonism (Beck and Chapin, 1994).

Biotite gneiss in the study area is medium to coarse grained and in places contains microcline porphyroblasts as long as 2 cm. It also hosts sparse amphibolite units as much as 10 m thick and small intrusions of granite similar to the La Joyita pluton.

Figure 3. Proterozoic Tajo granite (orange rocks on left) overlain by east-dipping beds of the Pennsylvanian Sandia Formation. View is to the north across Arroyo del Tajo from 333745E, 3768160N (zone 13, NAD 27).

Foliation in the biotite gneiss generally strikes northeast, dips moderately or steeply to the southeast (Herber, 1963b), and is locally mylonitic (Beck, 1993; Beck and Chapin, 1994). Foliation orientations are more diverse in areas to the north of the study area (Beck, 1993; Beck and Chapin, 1994). Proterozoic rocks in the Joyita Hills display ubiquitous stretching lineations that plunge moderately to the southeast (Herber, 1963b); these rocks were termed L- and L>S tectonites by Beck (1993) and Beck and Chapin (1994). These fabrics may represent a southwestern extension of the Monte Largo shear zone of the Manzano Mountains (de Moor et al., 2005).

Condie and Budding (1979) interpreted the biotite gneiss exposed in the Arroyo de Rosa Castillo area as a large xenolith of biotite schist that was partially granitized and recrystallized by the La Joyita pluton. The age of the pluton has not been determined. Apatite fission-track analysis indicates the Proterozoic core of the Joyita Hills cooled through the approximately 120°C isotherm from around 27 to 22 Ma (Kelley et al., 1992), and apatite (U-Th)/He thermochronology shows overlying Triassic strata cooled through the approximately 70°C isotherm from about 26 to 14 Ma (Ricketts et al., 2016). Both results are consistent with exhumation and cooling during early Rio Grande rifting and/or during postvolcanic relaxation of isotherms.

Figure 4. Jointed Proterozoic granite of the Tajo pluton exposed in Arroyo del Tajo. View is to the northwest from 333634E, 3768413N (zone 13, NAD 27), Loma de las Cañas quadrangle.

CHAPTER 2: PALEOZOIC ROCKS

PENNSYLVANIAN STRATA OF THE QUEBRADAS REGION

Steven M. Cather

Introduction

Pennsylvanian deposits in the Quebradas region accumulated near the paleoequator during the Ancestral Rocky Mountain orogeny (Ye et al., 1996), which affected much of south-central and southwestern Laurentia during an approximately 25 Myr interval from Early Pennsylvanian (Morrowan) through Early Permian time (Wolfcampian). This orogenic event produced numerous, mostly north-trending basins and uplifts in New Mexico resulting from northeast-southwest crustal shortening and associated dextral strike-slip faulting (Woodward et al., 1999; Cather et al., 2006; Leary et al., 2017).

Pennsylvanian strata are exposed in all six quadrangles of the study area. These strata represent most of the time interval of the Ancestral Rocky Mountain orogeny, except for the Morrowan. Only the Loma de las Cañas quadrangle contains relatively complete exposures of the Pennsylvanian section, which is approximately 600–700 m thick. Elsewhere, typically only the upper part of the Pennsylvanian section is exposed. The Pennsylvanian succession in the Quebradas region consists of limestone, mudstone, sandstone, and minor conglomerate that were deposited in open-marine, nearshore, fluvial, lacustrine, and coastal-plain environments. No major unconformities are apparent in the Pennsylvanian section, except at the basal contact of the youngest unit (the uppermost Pennsylvanian Bursum Formation).

Pennsylvanian stratigraphic nomenclature of central New Mexico has evolved considerably over the past century (Table 1). This evolution has been described in recent publications (Kues, 2001; Lucas et al., 2009a; Cather et al., 2013) and will not be repeated here (see summary in Fig. 5). In the present study, the Sandia Formation, Gray Mesa Formation, Atrasado Formation, and Bursum Formation were mapped (Plate 1). Members of the Gray Mesa Formation and the Atrasado Formation (Table 1; Lucas et al., 2009a) are recognizable in most places, but were not mapped separately.

Sandia Formation

The Pennsylvanian Sandia Formation is a heterolithic succession of drab mudstone, sandstone, fossiliferous limestone, and minor quartz-pebble conglomerate. It represents the base of the Phanerozoic in the study area (Figs. 3 and 6). Locally, the basal lag conglomerate contains granitic clasts as large as 20 cm. Sandstone is mostly quartzose, but Rejas (1965) noted the presence of a few subarkosic beds, and Krainer and Lucas (2013) described rare beds of lithic arenite. The Sandia crops out primarily in the central part of the Loma de las Cañas quadrangle, within the Laramide Tajo structural zone (see Chapter 5), where it overlies Proterozoic granite with profound nonconformity. A small, isolated exposure of probable Sandia Formation is also present in a fault block in the NW1/4 sec. 23, T. 3 S., R. 2 E. in the southwestern part of the Bustos Well quadrangle (Wilpolt and Wanek, 1951).

Four complete sections of the Sandia Formation were measured by previous workers in the central Loma de las Cañas quadrangle, each separated by about a kilometer. Measured thicknesses (Table 1) are, from northwest to southeast, 177.1 m (Rejas, 1965; NE1/4 sec. 3 and NW1/4 sec. 2, T. 2 S., R. 1 E.), 135.7 m (Rejas, 1965; NE1/4 sec. 2, T. 2 S., R. 1 E.), 162 m (Lucas et al., 2009a; NE1/4 sec. 11 and NW1/4 sec. 12, T. 3 S., R. 1 E.), and 86.1 m (Bauch, 1982; SW1/4 sec. 12, T. 3 S., R. 1 E.). The three northwestern measured sections are of comparable thickness and contain 7–24% marine limestone, which occurs mostly in the middle and upper part of the Sandia Formation.

Table 1. Thicknesses of Pennsylvanian stratigraphic units of the Quebradas region.

Formation	Member[1]	Thickness (m)							
		Rejas, 1965	Maulsby, 1981	Fagrelius, 1982	Bauch, 1982	Colpitts, 1986	Brown, 1987	Altares, 1990	Lucas et al., 2009a
Bursum		**61.0**[3]	**76.7**	**59.0**	**>32.6**	**57.9–63.2**	**46.0**	**41–88**	**25–120**[8]
Atrasado		**~227–254**[4]			**268.5**[4]				**~290**[9]
	Moya	23.5	26.8		42.8		>33.6		18.0
	Del Cuerto*	17.4	6.2–11.8		27.2[5]		7.5		7.0
	Story	12.1	9.5–13.2				6.0[6]		6.0
	Burrego*	11.2–25.9	>102.4		60.0		>69.4[7]		13.0
	Council Spring	6.1			10.4		>2.0		2.0–12.7
	Tinajas*[2]	78.7–91.2			34.8				72.4–104
	Amado	10.6			18.3				3.3–17.9
	Bartolo*	67.0			75.0				67.0
Gray Mesa		**~133–151**[4]			**186.7**[4]				**>184.6**[10]
	Garcia	61.3			91.4				103.0
	Whiskey Canyon	32.9			41.5				25.0
	Elephant Butte	38.7–57.0			53.8				93.0
Sandia		**135.7–177.1**			**86.1**				**162**

*Siliciclastic-dominated members; others are mostly limestone.
[1] Nomenclature of Lucas et al. (2009a).
[2] "Adobe-Coane undifferentiated" of earlier workers.
[3] Thickness estimated from cross section.
[4] Sum of reported member thicknesses.
[5] Combined thickness of Del Cuerto Member and Story Member; the upper limestone part of the Story Member is not present.
[6] Upper limestone part of Story Member only.
[7] Combined thickness of Burrego Member and lower siliciclastic part of Story Member.
[8] 120 m thickness may be from a fault-repeated section (see text).
[9] Reported formation thickness (Lucas et al., 2009a, p. 193); member thicknesses sum to 188.7–245.6 m.
[10] Reported formation thickness (Lucas et al., 2009a, p. 190); member thicknesses sum to 221 m.

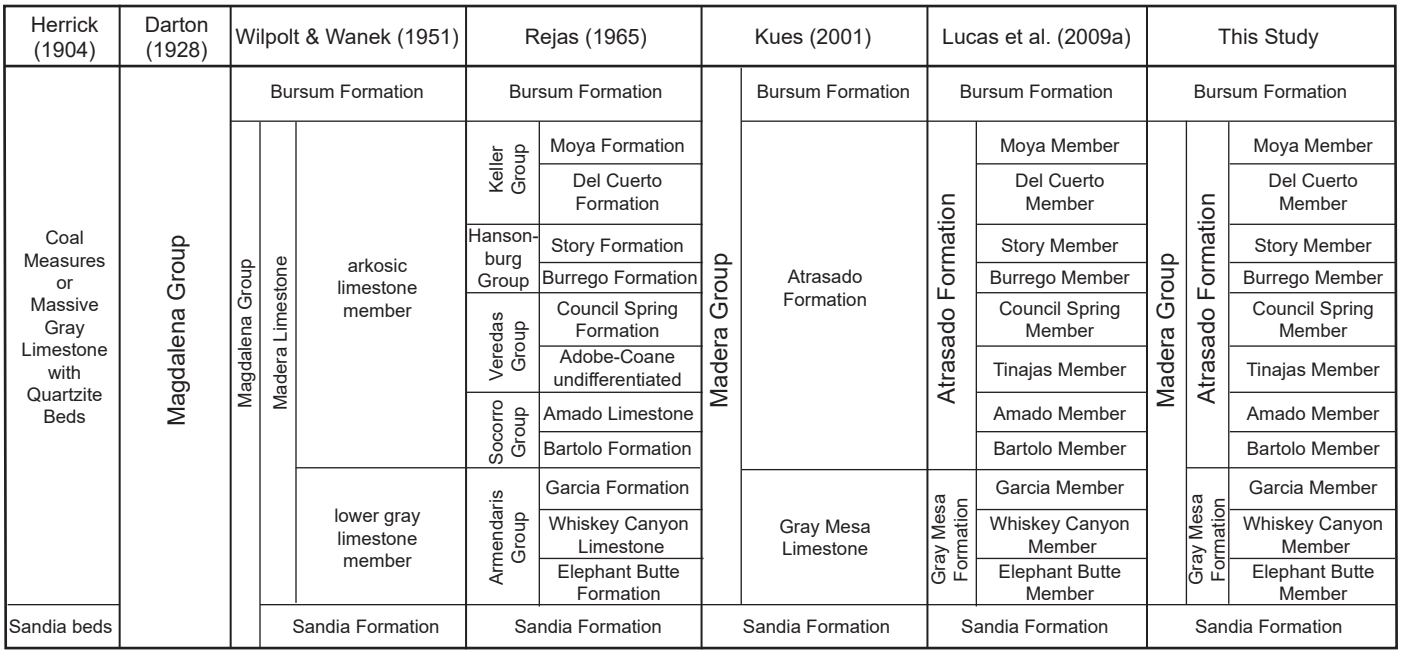

Figure 5. Stratigraphic chart showing the evolution of nomenclature for Pennsylvanian strata in central New Mexico. Modified from Lucas et al. (2009a).

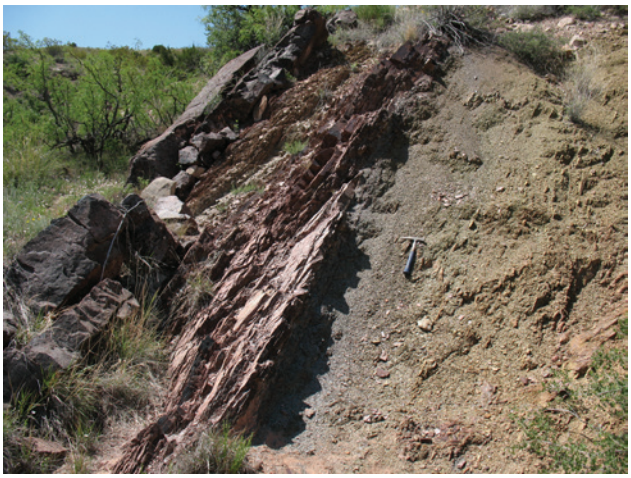

Figure 6. East-dipping beds of sandstone and mudstone of the lower Sandia Formation at Arroyo del Tajo. View is to the south from 333678E, 3768366N (zone 13, NAD 27).

In contrast, the southern measured section is significantly thinner and contains more limestone (approximately 39% of the section), primarily in the lower and middle part of the unit (Bauch, 1982). Rejas (1965) also noted that the grain size of sandstones and bed thickness of limestones in the Sandia Formation increase somewhat toward the west. Lateral variations of thickness and lithofacies in the Sandia Formation are common and have been noted in other areas by Kues (2001) and Krainer and Lucas (2013). No laterally extensive marker beds have been recognized.

The Sandia Formation in the study area consists of open-marine, marginal-marine, and coastal-plain deposits. No detailed depositional or paleocurrent analyses have yet been attempted for these beds. Sandstone and mudstone in the basal part of the unit form a transgressive succession, which locally contains plant fossils, including lycopsids (Herrick, 1904; Lucas et al., 2009a, 2009b). Cross-bedded, upward-fining sandstones in the Sandia Formation are largely of fluvial origin. Marine limestone and mudstone locally contain fossils of brachiopods, bryozoans, crinoids, rugose corals, fusulinids, gastropods, sponge spicules, fishes, and conodonts (Bauch, 1982; Ivanov et al., 2009; Lucas et al., 2009a; Krainer and Lucas, 2013).

Regionally, the Sandia Formation ranges in age from late Morrowan to Atokan (Krainer and Lucas, 2013). In the study area, conodonts from the lower part of the Sandia Formation are of late Atokan age (Lucas et al., 2009a, 2022a). The upper part of the unit has not been dated but is conformably overlain by the lower Desmoinesian Elephant Butte Member of the Gray Mesa Formation.

Gray Mesa Formation

The Gray Mesa Formation is the lower part of the Madera Group in central New Mexico, where it forms the resistant cap on several rift-shoulder uplifts such as the Sandia, Manzano, and Oscura Mountains. In the study area, the Gray Mesa Formation is approximately 130–220 m thick (Table 1) and consists of three members (in ascending order, the Elephant Butte, Whiskey Canyon, and Garcia Members). These member-rank terms are derived from stratigraphic units first identified by Thompson (1942; he considered them formations) in the Mud Springs Mountains near Truth or Consequences, about 110 km to the south (Rejas, 1965; Lucas et al., 2009a). The members can be discriminated primarily by their siliciclastic content (greater in the Elephant Butte and Garcia Members) and their chert content (greater in the Whiskey Canyon Member). The lower contact of the Gray Mesa Formation is placed at the base of the first thick chert-bearing limestone above the siliciclastic-dominated Sandia Formation. The main outcrop belt of Gray Mesa in the study area extends southward from Ojo de Amado to the north side of Arroyo del Tajo in the Loma de las Cañas quadrangle.

The Gray Mesa Formation was mostly deposited in open-marine conditions. The age range of the Gray Mesa Formation varies somewhat regionally, but in central New Mexico its base is no older than late Atokan and its top no younger than early Missourian (Nelson et al., 2013). Within the study area, the Gray Mesa Formation is Desmoinesian in age based on its fusulinid content (Rejas, 1965; Lucas and Estep, 2000). Conodont biostratigraphy indicates the Gray Mesa Formation is mostly early Desmoinesian in age, but the upper part of the Garcia Member in the study area was deposited during the late Desmoinesian (Lucas et al., 2009a, 2022a).

The **Elephant Butte Member** is an approximately 39–93 m succession of gray marine limestone and gray mudstone, with a prominent, around 10-m-thick, indistinctly cross-bedded quartzarenite about 30 m above the base of the unit. Limestones locally contain chert nodules and commonly exhibit fossil crinoids,

bryozoans, brachiopods, solitary corals, and algal laminations. Mudstones are generally poorly exposed. The thickness and siliciclastic content of the Elephant Butte Member increase eastward across the Amado fault zone (Rejas, 1965), probably resulting from structural juxtaposition by Laramide dextral faulting (see Chapter 5).

The **Whiskey Canyon Member** is approximately 25–42 m thick and is distinguished by a dominance of very cherty, thin- to medium-bedded, cliff-forming limestone and by a scarcity of siliciclastic beds (it has only a few thin beds of gray mudstone). Fossils include phylloid algae, crinoids, solitary corals, fusulinids, and bryozoans.

The **Garcia Member** (Fig. 7) is approximately 61–103 m of interbedded limestone and gray mudstone, with several 1- to 4-m-thick arkosic sandstones in its middle and upper parts (beginning with the Garcia Member and continuing upsection through the Abo Formation, arkose and subarkose are the dominant types of sandstone). Limestones commonly contain fossil crinoids, solitary corals, phylloid algae, bryozoans, and fusulinids. In the central part of the Loma de las Cañas quadrangle, the thickness and clastic content of the Garcia Member decrease toward the north (Bauch, 1982). The clastic content of the lower part of the Garcia Member also decreases westward across the Amado fault zone (Rejas, 1965).

Atrasado Formation

The Atrasado Formation (upper Madera Group) conformably overlies the Gray Mesa Formation in the study area. It consists of interbedded arkosic sandstone, mudstone, and carbonate rocks totaling around 225–270 m in thickness (Table 1; see Krainer et al. [2017] for petrographic analyses of these rocks). Sediment-dispersal patterns and environments of deposition have not been adequately studied for some siliciclastic parts of the Atrasado Formation. In most places in the study area, the Atrasado Formation can be divided into as many as eight members (in ascending order, the Bartolo, Amado, Tinajas, Council Spring, Burrego, Story, Del Cuerto, and Moya Members; see Lucas et al. [2009a] for a history of these terms). The contacts between these members appear conformable. Outcrops of the Atrasado are widely distributed in uplifted fault blocks in the central and northern portions of the map area, but complete sections are exposed only in the central part of the Loma de las Cañas quadrangle.

The **Bartolo Member** is the basal unit of the Atrasado Formation in the study area and, like the overlying Amado and Tinajas Members, crops out only in the central part of the Loma de las Cañas quadrangle. There, the Bartolo Member is approximately 67–75 m thick (Table 1) and consists mostly of brownish-gray mudstone with subordinate, thin beds of arkosic sandstone and fossiliferous limestone (Fig. 8). The abundance and grain size of sandstones in the Bartolo Member increase somewhat to the east (Rejas, 1965; Lucas et al., 2009a). Limestone occurs mostly in the upper half of the unit. Marine fossils are preserved in most limestones and some sandstones and include crinoids, brachiopods, bryozoans, algae, gastropods, corals, conodonts, and foraminifera (Rejas, 1965; Bauch, 1982; Lucas et al., 2009a). Plant fossils have also been collected and described in the Bartolo Member (Lucas et al., 2009a; DiMichele et al., 2017). Lithofacies and fossils indicate the Bartolo Member is of mixed coastal-plain and marine origin, with greater marine influence during deposition of the upper half of the unit. Conodont biostratigraphy suggests the Bartolo Member is late Desmoinesian in age (Lucas et al., 2009a, 2022a; Barrick et al., 2013).

The **Amado Member**, a prominent, laterally continuous unit in the study area, is approximately 3–18 m of cherty marine limestone and minor gray mudstone that form a conspicuous set of ledges (Fig. 8). Fossils include brachiopods, crinoids, bryozoans, algae, gastropods, and corals. Conodonts recovered from the Amado Member indicate a late Desmoinesian to early Missourian age (Barrick et al., 2013; Lucas et al., 2022a).

The **Tinajas Member** ("Adobe-Coane undifferentiated" of early workers; see Lucas et al. [2009a]) is approximately 35–104 m (Table 1) of olive-gray to black mudstone, marine limestone, and minor arkosic sandstone and gypsum. The lower Tinajas Member locally contains lacustrine carbonaceous shale beds and sabkha-related gypsiferous carbonate beds, both of which contain fossils, including silicified wood (Lerner et al., 2009; Falcon-Lang et al., 2011; DiMichele et al., 2017).

Figure 7. Limestone and mudstone of the Garcia Member of the Gray Mesa Formation. View is to the north-northwest across a tributary of Arroyo de los Pinos from 332593E, 3773978N (zone 13, NAD 27), Loma de las Cañas quadrangle.

Figure 8. Lower Atrasado Formation near Cerros de Amado in the Loma de las Cañas quadrangle near the Cerros de Amado C measured section of Lucas et al. (2009a). View to the north from near 332600E, 3774300N (zone 13, NAD 27). The prominent limestone bed near the skyline is the Amado Member. The Bartolo Member forms the underlying slope.

Limestone composes most of the Tinajas Member west of the Amado fault zone in SW1/4 sec. 26, T. 2 S., R. 1 E. (Rejas, 1965), but it occurs only as scattered, thin beds in exposures about 1.5 km to the east (Rejas, 1965; Lucas et al., 2009a) and appears to be absent in a poorly exposed, thin Tinajas Member section about 5 km farther to the southeast (Bauch, 1982). Fossils in limestone include brachiopods, bryozoans, echinoderms, crinoids, ostracods, conodonts, and algae (Rejas, 1965; Lucas et al., 2009a). Fossil fishes, terrestrial vertebrates, plants, crustaceans, insects, ostracods, bivalves, a cnidarian, and vertebrate coprolites are locally present in the lower and middle parts of the Tinajas Member (Lerner et al., 2009; Schneider et al., 2017; Harris and Lucas, 2022). Conodont biostratigraphy indicates the Tinajas Member is Missourian in age (Lucas et al., 2022a).

Exposures of the Tinajas Member with markedly differing carbonate content are closely juxtaposed across the Amado fault zone in S1/2 sec. 26 and N1/2 sec. 35, T. 2 S., R. 1 E. (Rejas, 1965). This juxtaposition provides the best evidence for postdepositional, probably dextral separation along a strand of the Amado fault zone (Cather and Colpitts, 2005; see Chapter 5).

The **Council Spring Member** is a widespread and distinctive unit in the study area. It consists of approximately 2–13 m of cliff-forming, typically light-gray marine limestone that contains fossil brachiopods, crinoids, and algae (Lucas et al., 2009a). Fusulinids (*Triticites*) from the Council Spring Member suggest an early to middle Missourian age (Kues et al., 2002), but conodont biostratigraphy indicates the Council Spring Member is upper Missourian (Lucas et al., 2009a, 2022a). A major phylloid algal bioherm in the Council Spring Member near Ojo de Amado (SE1/4 sec. 27, T. 2 S., R. 1 E.) was described by Hambleton (1959, 1962). This mound was subsequently placed in the Tinajas Member by Krainer et al. (2017).

The **Burrego Member** consists of ledge- and slope-forming, subarkosic sandstone, mudstone, and marine limestone. Thickness and lithology vary greatly (Table 1). In two measured sections in NW1/4, SW1/4 sec. 26, T. 2 S., R. 1 E., west of the Amado fault zone, the Burrego Member is 13.0–25.9 m thick and consists dominantly of mudstone and sandstone (Rejas, 1965; Lucas et al., 2009a). About 2.2 km to the east in NE1/4, SW1/4 sec. 25, T. 2 S., R. 1 E., the Burrego is 11.2 m thick and becomes dominantly carbonate (Rejas, 1965). A few kilometers farther to the east and northeast, Maulsby (1981) measured two incomplete sections in the Burrego Member in W1/2, W1/2, W1/2 sec. 29, T. 2 S., R. 2 E. and SE1/4, NW1/4 sec. 21, T. 2 S., R. 2 E. These partial sections are 81.1 m and 102.4 m thick, respectively, and both are dominantly siliciclastic with a few thin marine limestones. Also in sec. 21, T. 2 S., R. 2 E., Brown (1987) measured a partial section in the Burrego Member that is 69.4 m thick and consists mostly of mudstone and sandstone with a few thin marine limestone beds. To the south in NE1/4, SE1/4 sec. 12, T. 3 S., R. 1 E., the Burrego Member is 60 m thick and entirely siliciclastic (Bauch, 1982), although Brown (1987) noted a few thin carbonate grainstone beds near Bauch's measured section.

Fossils in the Burrego Member occur mostly in limestone and include crinoids, brachiopods, bryozoans, solitary corals, algae, and gastropods. Maulsby (1981) reported the fusulinid *Triticites* in the Burrego Member, which he regarded as early Virgilian in age. Conodonts from the Burrego Member indicate an early Virgilian age (Barrick et al., 2013). Lucas et al. (2022a) placed the Missourian–Virgilian boundary within the Burrego Member.

The depositional environments of the Burrego Member have not been adequately studied. Siliciclastics in the Burrego Member appear to be mostly coastal-plain and nearshore deposits. Limestones were deposited in marine environments following transgressive events. In the northeastern part of the Loma de las Cañas quadrangle, Lucas and Tanner (2021) noted local calcareous paleosols in red floodplain mudstone of the Burrego Member, which they suggest are indicative of a seasonally dry, monsoonal paleoclimate.

Throughout most of the study area, the **Story Member** is approximately 6–13 m thick and consists of a lower part of arkosic sandstone and mudstone and a distinctive upper limestone (Fig. 9), both of similar thickness. There is, however, considerable lateral variation within the unit. In the Cerros de Amado region, Rejas (1965) noted the lower, siliciclastic part of the Story Member thins and becomes coarser-grained to the east. To the northeast, this lower siliciclastic part becomes indistinguishable from the underlying Burrego Member; for this

reason, it was mapped as the upper part of the Burrego Member by Brown (1987). To the south of the Cerros de Amado region, the upper limestone part of the Story Member pinches out, which caused Bauch (1982) to map the siliciclastic beds of the Story Member as part of the overlying Del Cuerto Member. Fossils in the upper part of the Story Member include crinoids, bryozoans, solitary corals, ostracods, algae, bivalves, foraminifera, and calcispheres (Rejas, 1965; Maulsby, 1981) as well as Virgilian conodonts (Lucas et al., 2009a, 2022a; Barrick et al., 2013). The Story Member appears to represent a transgressive, nearshore, and open-marine succession (e.g., Lucas and Krainer, 2009).

The **Del Cuerto Member** (Fig. 9) is an approximately 6- to 20-m-thick, slope-forming, heterolithic succession of arkosic sandstone, mudstone, and limestone. Rejas (1965) proposed dividing the Del Cuerto, which he considered a formation, into three members: lower and upper, mostly siliciclastic members and a medial, limestone-dominated member. These members, however, cannot be recognized in adjacent areas (see Bauch [1982] and Lucas et al. [2009a]) and thus should be abandoned. Crinoidal biosparites in the middle part of the Del Cuerto Member are indicative of open-marine conditions, above wave base. The depositional paleoenvironments of the siliciclastic parts of the Del Cuerto Member are unstudied. The Del Cuerto Member is middle Virgilian in age (Lucas et al., 2009a, 2022a; Barrick et al., 2013).

The uppermost part of the Atrasado Formation, the **Moya Member**, is approximately 18–43 m of gray marine limestone interbedded with subordinate mudstone and minor arkosic sandstone (Fig. 9). In some areas, it is possible to divide the Moya Member into two units separated by a thin arkosic sandstone or its corresponding covered interval (Rejas, 1965; Maulsby, 1981). In other areas, such subdivision is not possible (Bauch, 1982; Brown, 1987; Lucas et al., 2009a). The Moya Member was deposited largely in an open-marine environment. Fossils present include crinoids, algal laminae, solitary corals, fusulinids (including *Triticites*), bryozoans, brachiopods, mollusks, and ostracods (Maulsby, 1981; Lucas et al., 2009a). Based on conodonts, the age of the Moya Member is Virgilian (Lucas et al., 2009a, 2022a; Barrick et al., 2013).

Figure 9. Upper Atrasado Formation in the eastern Loma de las Cañas quadrangle (view is to the northeast from 338050E, 3771858N, zone 13, NAD 27). The lower limestone is part of the Story Member; the middle, recessive interval is the Del Cuerto Member; and the upper limestone is the Moya Member.

Bursum Formation

Wilpolt et al. (1946) proposed the term Bursum Formation for the transitional beds between the underlying Pennsylvanian marine strata and the overlying continental red beds of the Permian Abo Formation in central New Mexico. They designated the type section in SE1/4 sec. 1, T. 6 S., R. 4 E., about 30 km southeast of the study area. I follow Wilpolt and Wanek (1951) and most subsequent workers in excluding the Bursum Formation from the Madera Group (cf., Kues, 2001). The following discussion is modified from Cather (2018).

Lucas and Krainer (2004) and Krainer and Lucas (2009, 2013) subdivided the Bursum into four lateral members (Oso Ridge, Bruton, Red Tanks, and Laborcita Members; note that the last three have at times been considered formations). Not strictly lithostratigraphic in nature, these members are based on the ratio of marine to continental beds, overall thickness, and grain size. The lithologic characteristics for individual members have not been quantitatively defined, and member names have not been applied in a systematic fashion. For example, Bursum strata of the Tinajas Arroyo section of Krainer and Lucas (2009) were classified as the Bruton Member (i.e., containing >50% marine strata; Lucas and Krainer, 2004, p. 44), despite containing only around 38% marine beds by their own estimation. The Bursum Formation was not subdivided during the present study.

The Bursum Formation consists of 25 m to possibly as much as 120 m of variegated greenish-gray and purplish-red beds of mudstone, marine limestone, sandstone, conglomerate, and calcic pedogenic horizons (Fig. 10). The Bursum typically exhibits cyclic alternation of marine and continental beds. These beds define transgressive–regressive sequences that generally range from about 10–50 m thick and reflect both eustatic and tectonic processes (Krainer and Lucas, 2009). Bedding in the Bursum Formation is laterally discontinuous. The basal parts of aggradational sequences were commonly confined within shallow paleovalleys 0.1–1.5 km wide (Fig. 11). Beds in the Bursum cannot be easily traced for more than a kilometer or two, making correlation among discontinuous exposures difficult. Although Krainer and Lucas (2009) attempted to correlate depositional sequences between Bursum outcrops, they noted such correlations are difficult due to structure, facies changes, and discontinuous exposure. The correlation of Bursum depositional sequences across the Joyita Uplift (Krainer and Lucas, 2009, fig. 3) seems particularly problematic.

The Bursum Formation is regionally somewhat time-transgressive in central New Mexico, ranging in age from late Virgilian to early Wolfcampian (Lucas and Krainer, 2004; Krainer and Lucas, 2009, 2013). In the study area, the Bursum is likely early Wolfcampian in age based on fusulinids in the lower part of the formation (Lucas and Krainer, 2017). In the northern part of the study area near Cibola Spring, however, Allen et al. (2013a) reported late Virgilian(?) fusulinids (*Triticites*) in the lower part of the Bursum and early Wolfcampian fusulinids (*Schwagerina* and *Triticites*) in its middle part. From the same area near Cibola Spring, Kottlowski and Stewart (1970; their Palo Duro Canyon section in sec. 13, T. 1 S., R. 2 E., projected) reported *Schwagerina emaciata, S. jewetti, S. grandensis, S.* cf. *pinosensis, Stewartina* spp., *Triticites hugensis, T. ventricosus, T.* n. sp., and *Oketaella*(?) from the lower and middle Bursum, indicating a Wolfcampian age. Maulsby (1981) collected the Wolfcampian fusulinid *Triticites creekensis* from the central part of the study area. In a study of several Bursum outcrops throughout the Quebradas area, Altares (1990) reported the Wolfcampian fusulinids *Schwagerina pinosensis, Triticites* aff. *T. creekensis, T.* cf. *Triticites directus*, and *Leptotriticites* sp. Except for *S. pinosensis*, all were collected within 10 m of the base of the Bursum Formation. The Pennsylvanian–Permian boundary, as construed by Davydov et al. (1998), closely corresponds to the contact between the Bursum and the overlying Abo Formation (see summary in Lucas et al. [2002]). In a subsequent paper, Lucas et al. (2022b) regarded the Bursum Formation as lower Permian.

The Bursum Formation consists of marine beds and intercalated continental red beds that are transitional between the marine limestone of the upper Atrasado Formation and the fluvial Abo Formation (see Nelson et al. [2017] for a detailed description of Bursum lithofacies). The base of the Bursum is defined by the lowermost reddish continental deposits above the marine Moya Member of the Atrasado Formation. The Bursum Formation disconformably overlies Virgilian upper Atrasado strata throughout the study area (Krainer and Lucas, 2009; Allen et al., 2013a).

Figure 10. Interbedded fluvial sandstone and marine limestone in the lower part of the Bursum Formation. Hammer rests on arkosic, pebbly, fluvial sandstone, which is overlain by a transgressive succession of ~1.5 m of gray marine(?) siltstone and ~0.3 m of gray marine limestone (upper ledge). View is to the east from 336949E, 3760462N (zone 13, NAD 27), San Antonio quadrangle, ~1.3 km north of the Cerro del Viboro measured section of Krainer and Lucas (2009).

Figure 11. Shallow paleovalley or paleochannel fills containing arkosic, pebbly sandstone in the lower part of the Bursum Formation. The channel-fill deposit in the foreground (with hammer for scale) is ~0.5 m thick and 2 m wide. Larger valley-fill above and to the right (above gray bushes) is ~1.5 m thick and 10 m wide. Generally, paleovalley fills in the Bursum are thicker and wider than these but are more difficult to photograph. View is to the east (subparallel to the paleoflow direction) from near 337000E, 3760410N (zone 13, NAD 27), ~1.3 km north of the Cerro del Viboro measured section of Krainer and Lucas (2009), San Antonio quadrangle.

The associated lacuna appears to encompass part or all of late Virgilian time, representing perhaps a few million years or less. The late Virgilian was a time of eustatic sea-level fall (e.g., Montañez and Poulsen, 2013, fig. 2g), which perhaps partly accounts for the sub-Bursum disconformity. Eustatic effects, however, are difficult to confirm given the clear evidence for tectonism in New Mexico at that time. For example, north of the study area along the western flank of the Pennsylvanian Joyita Uplift, the Bursum laps across tilted and beveled rocks of Missourian, Atokan, Desmoinesian, and Proterozoic age (Kottlowski and Stewart, 1970). This angular unconformity must be, at least in part, related to orogeny. The unconformity at the base of the Bursum Formation perhaps represents the only substantial regional lacuna during Pennsylvanian–Permian sedimentation in the study area.

The nature of the upper contact of the Bursum Formation in the Quebradas region is variable. I have seen evidence for both disconformable and conformable contacts with the overlying Abo Formation, as did Colpitts (1986), Altares (1990), and Nelson et al. (2017). Other workers interpreted the upper contact with the Abo to be gradational (Rejas, 1965; Kottlowski and Stewart, 1970; Arendt, 1971; Maulsby, 1981). I observed no evidence in the Quebradas region for substantial soil development or deep ravinement beneath the Abo Formation, which suggests the Bursum–Abo contact represents at most a short lacuna.

In contrast, Krainer and Lucas (2009) interpreted the Bursum–Abo contact to be disconformable everywhere in the Quebradas region. This interpretation is largely based on the anomalously thick measured section of the Bursum Formation at Gallina Well, which contains six disconformity-bounded depositional sequences. To explain the preservation of fewer sequences (three or fewer) in their other, thinner measured sections, Krainer and Lucas (2009) invoked the effects of widespread, deep pre-Abo erosion. The Gallina Well section, however, may be fault-repeated (see below). Even if it is not, the increased number of Bursum depositional cycles in the Gallina Well section may simply reflect increased syndepositional subsidence relative to adjacent areas rather than pre-Abo erosion. During my mapping of this region, I saw no evidence for more than a few meters of stratigraphic relief on the Bursum–Abo contact.

Ideally, the upper contact of the Bursum Formation is placed at the top of the stratigraphically highest marine limestone or marine mudstone beneath the Abo. In practice, however, the top of the Bursum is commonly placed within nonmarine sandstones and mudstones, at a color change from greenish-gray, grayish-red, or purplish-red in the Bursum Formation to red and reddish-brown in the Abo. For example, in the Loma de las Cañas and Mesa del Yeso measured sections of Krainer and Lucas (2009), the top of the Bursum consists of continental beds, and their Joyita Hills B section of the Bursum is entirely nonmarine. The uppermost parts of most Bursum Formation sections measured by Kottlowski and Stewart (1970) also consist of nonmarine strata.

Unlike most of the underlying Pennsylvanian succession, the Bursum Formation is widely exposed in the study area and contains coarse clastic deposits that are amenable to paleocurrent analysis. A paleocurrent study was therefore undertaken to provide insight into the latest Carboniferous paleogeography and sediment-dispersal systems. About 650 paleocurrent measurements were made in Bursum fluvial sandstones within and near the study area (Fig. 12). Nearly all measurements were derived from structurally restored, foreset dip-directions of tabular cross-bedding in sandstones. The remainder (about 7%) is from trough cross-bedding and pebble imbrication. Not incorporated into the present study are the few paleocurrent measurements by Altares (1990), some of which are based on features of dubious utility, such as ripple cross-laminations and the orientation of plant fragments. In the present study, paleocurrents for individual localities typically display unimodal or closely grouped polymodal distributions (Fig. 12). The lack of polar bimodality suggests little or no tidal or estuarine influence during deposition of Bursum sandstones.

Two broad, semiradial arrays of fluvial paleocurrent directions are present in the Bursum Formation within and north of the study area (Fig. 13). The southern array corresponds to notably arkosic Bursum exposures in the central and southern part of the study area where pebbles mostly consist of Proterozoic lithologies (granite, gneissic granite, and vein quartz, with minor schist and greenstone; Fig. 14) with subsidiary, mostly intraformational carbonate clasts. The semiradial easterly to northerly paleocurrents of this basement-derived petrofacies suggest Proterozoic exposures existed within what is now the Socorro Basin of the Rio Grande rift.

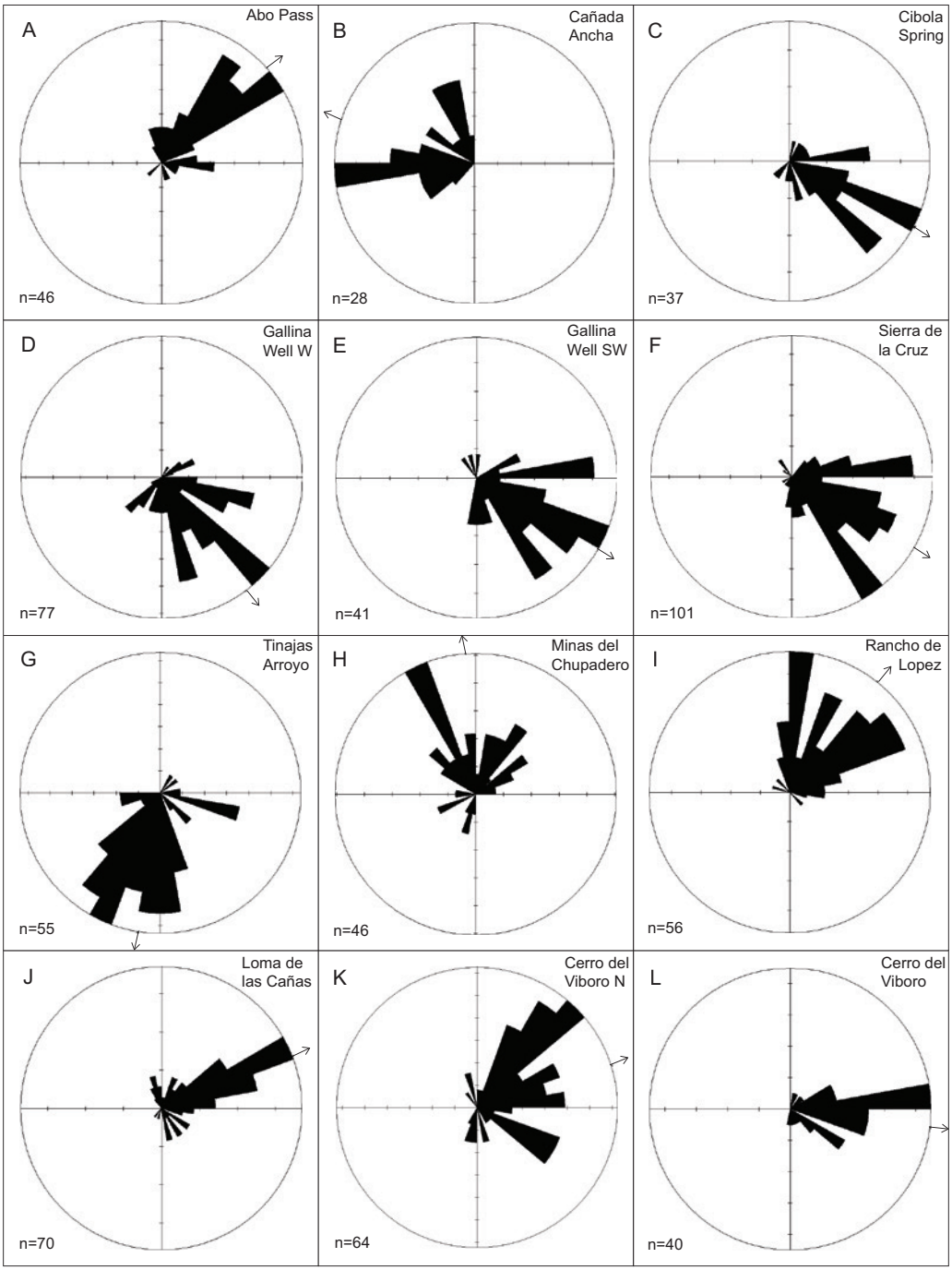

Figure 12. Paleocurrent data (north at top) and mean paleocurrent directions (arrows) for the Bursum Formation exposures in the study area and in surrounding areas. Localities within the study area are depicted in Figure 13. **A**—Middle part of Bursum Formation near Abo Pass in roadcuts along U.S. Route 60, measurements from 361994E, 3807769N (all UTM locations are zone 13, NAD 27) and westward for ~300 m; **B**—Upper part of Bursum Formation in the Los Cañoncitos area south of Cañada Ancha, near 333137E, 3796382N; **C**—Lower and middle parts of Bursum Formation ~1 km southwest of Cibola Spring, measurements from 345147E, 3788062N and westward for ~1 km; **D**—Lower part of Bursum Formation ~1.5 km west of Gallina Well, measurements from 341017E, 3779585N and north-northwestward for ~400 m; **E**—Lower part of Bursum Formation ~2 km southwest of Gallina Well, measurements from 340740E, 3778278N and southward for ~400 m; **F**—Middle and upper parts of Bursum Formation ~3.2 km south of Sierra de la Cruz, measurements from 343734E, 3780095N and southeastward for ~500 m; **G**—Lower and middle parts of Bursum Formation near Tinajas Arroyo section of Krainer and Lucas (2009), measurements from 340764E, 3775876N and southwestward for ~400 m; **H**—Lower and middle parts of Bursum Formation near Minas del Chupadero, measurements from 332266E, 3775595N and eastward for ~300 m; **I**—Lower, middle, and upper parts of Bursum Formation ~2.3 km south of Rancho de Lopez, measurements from 335787E, 3772676N and southward for ~1.7 km; **J**—Lower and middle parts of Bursum Formation near the Loma de las Cañas section of Krainer and Lucas (2009), measurements from 338387E, 3771413N and north-northeastward for ~300 m; **K**—Lower and middle parts of Bursum Formation ~1.3 km north of Cerro del Viboro section of Krainer and Lucas (2009), measurements from 337119E, 3760568N and southward for ~300 m; **L**—Lower and middle parts of Bursum Formation near the Cerro del Viboro section of Krainer and Lucas (2009), measurements from the area near 3337293E, 3759225N.

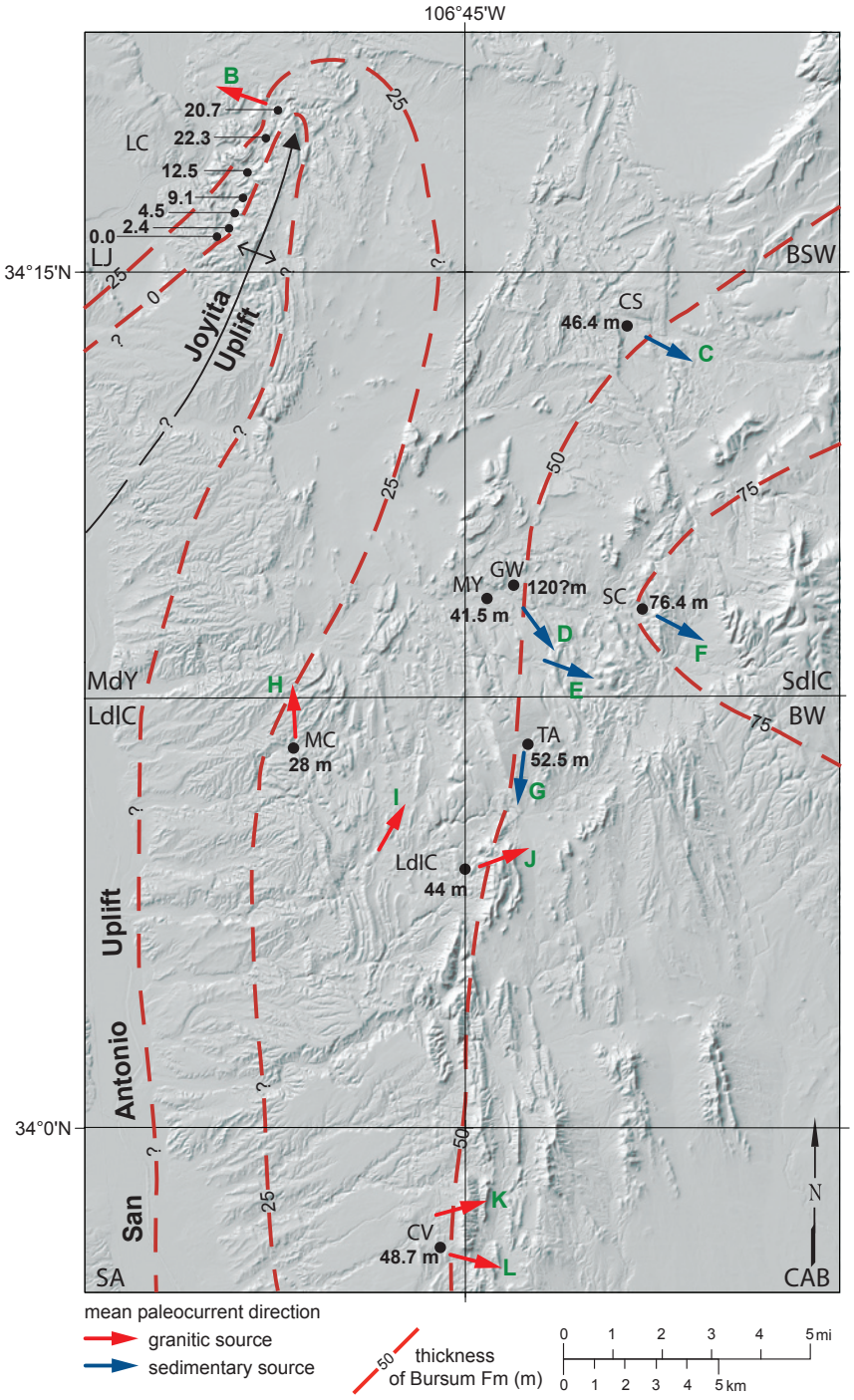

Figure 13. Map of the study area and adjacent regions to the north showing average paleocurrent directions (green letters are keyed to Fig. 12) and thickness for the Bursum Formation. Names of measured sections are modified from Krainer and Lucas (2009; note that several of their sections were incorrectly located on their maps and have been replotted here and on subsequent figures). **LC**—Los Cañoncitos (includes seven measured sections along the western flank of the Joyita Uplift), **CS**—Cibola Spring, **MY**—Mesa del Yeso, **GW**—Gallina Well, **SC**—Sierra de la Cruz, **MC**—Minas del Chupadero, **TA**—Tinajas Arroyo, **LdlC**—Loma de las Cañas, **CV**—Cerro del Viboro. Thicknesses are averaged for localities in which more than one section has been measured. These localities include Cibola Spring (average of 52.7 m measured by Altares [1990] and 40 m by Allen et al. [2013a]), Mesa del Yeso (average of 57.9 m maximum thickness measured by Kottlowski and Stewart [1970] and 25 m by Krainer and Lucas [2009], fig. 3]), Sierra de la Cruz (average of 88.1 m measured by Altares [1990], 78 m by Krainer and Lucas [2009], and 63.2 m by Colpitts [1986]), Tinajas Arroyo (average of 51.9 m measured by Altares [1990] and 53 m by Krainer and Lucas [2009]), Loma de las Cañas (average of 41.3 m measured by Altares [1990], 54 m by Krainer and Lucas [2009], and 36.7 m by Maulsby [1981]), and Cerro del Viboro (average of 41 m measured by Altares [1990], 46 m by Krainer and Lucas [2009], and 59 m by Fagrelius [1982]). Thicknesses at Los Cañoncitos (seven localities) are from Kottlowski and Stewart (1970), and those near Minas del Chupadero and Gallina Well are from Krainer and Lucas (2009, fig. 5). The anomalous 120 m thickness near Gallina Well was not contoured (see text). Quadrangle abbreviations are **BSW**—Becker SW, **BW**—Bustos Well, **CAB**—Cañon Agua Buena, **LJ**—La Joya, **LdlC**—Loma de las Cañas, **MdY**—Mesa del Yeso, **SA**—San Antonio, and **SdlC**—Sierra de la Cruz.

Herein, this source terrane is termed the San Antonio Uplift (Fig. 13).

The northern semiradial array of northeasterly (at Abo Pass), southeasterly, and southerly paleocurrents (Fig. 13) corresponds to dominantly subarkosic to calcarenitic fluvial sandstones (see point-count data in Colpitts [1986]). These sandstones locally contain pebbles of mostly limestone and siltstone (Fig. 15); basement-derived pebbles are a minor constituent. Northeast of the study area near Abo Pass, paleocurrent indicators in Bursum exposures along U.S. Route 60 show that paleoflow was toward the northeast (Fig. 12A), similar to the results of Krainer et al. (2009). The deposits at Abo Pass appear to have been derived from the Joyita Uplift based on their southwesterly derivation. Deposits of the northern semiradial array are interpreted to represent a distributive fluvial system (e.g., Weissmann et al., 2010) in which sand and gravel were primarily derived from recycling of Pennsylvanian rocks exposed in the Joyita Uplift, particularly the upper Madera Group. Reworking of upper Madera deposits may explain the compositional differences between conglomerate and sandstone of the Bursum in the northern part of the study area; pebbles were derived mostly from indurated Madera limestone and siltstone, but most sand was recycled from weakly indurated Madera subarkosic sandstone.

Figure 14. Coarse sandstone with basement-derived clasts of granite and vein quartz in the middle part of the Bursum Formation, typical of outcrops in the southern part of the study area (337232E, 3759058N, zone 13, NAD 27, San Antonio quadrangle).

Figure 15. Typical fluvial pebble suite of the Bursum Formation in the northern part of the study area. Note the predominance of clasts of Pennsylvanian limestone (gray) and siltstone (yellow-orange). The sandstone in the upper part of the photo is calcarenitic. Outcrop is in the lower part of the Bursum Formation near Cibola Spring (344943E, 3788457N, zone 13, NAD 27, Sierra de la Cruz quadrangle).

North of the study area, in the Los Cañoncitos area on the western flank of the Joyita Uplift, Bursum fluvial deposits mostly consist of arkosic sandstone and conglomerate that contain clasts of Proterozoic rocks and, less commonly, pebbles of Pennsylvanian limestone (Kottlowski and Stewart, 1970). Limited paleocurrent data from the upper part of the Bursum near section JH1 of Kottlowski and Stewart (1970) suggest paleoflow was toward the west-northwest (Figure 12B).

The thickness of the Bursum Formation in the study area, based on 15 sections measured by previous workers, ranges from approximately 25 m to possibly as much as 120 m. Because thicknesses measured in individual exposures varied among workers, the average measured thickness for each locality is presented in Figure 13, which also shows the contoured thickness of the Bursum Formation. Variability of thicknesses measured in local areas may reflect actual thickness differences, but more likely is related to differing placement of contacts and varying appreciation of structural complications among workers.

North of the study area, on the western flank of the Joyita Uplift, the Bursum ranges from 0 to 22 m thick at seven measured sections, rapidly thickening away from the uplift (Kottlowski and Stewart, 1970). Southeast of the uplift, the Bursum Formation thickens gradually and monotonically eastward. An exception is the anomalously thick (120 m) section measured by Krainer and Lucas (2009) near Gallina Well. This section likely represents a fault-repeated section (for a similar opinion, see R. Colpitts [2009], written communication, in Krainer and Lucas [2009],

p. 168). The anomalous thickness at the Gallina Well section is illustrated by comparison to nearby, thinner measured sections in the Bursum Formation. About 1.1 km west of the Gallina Well section, Krainer and Lucas (2009, fig. 3) measured only 25 m of Bursum in their Mesa del Yeso section (note that the Gallina Well and Mesa del Yeso measured section locations are transposed on their fig. 1). Kottlowski and Stewart (1970, p. 23) measured no more than 57.9 m nearby to the west. Not contoured in Figure 13, the 120 m thickness of the Gallina Well section, if correct, may require a local, deeply subsided subbasin within the study area.

Figure 16 shows the percentage of marine strata within 10 measured sections of the Bursum Formation based on the paleoenvironmental interpretations by Krainer and Lucas (2009). East of the Joyita and San Antonio Uplifts, the abundance of marine rocks in the Bursum increases rather systematically eastward. A westward embayment in the 25% contour, defined by the percentage of marine beds in the Minas de Chupadero and Tinajas Arroyo sections of Krainer and Lucas (2009), approximately coincides with the area between the two semiradial distributive fluvial systems described above. The increased percentage of marine strata in this area probably reflects a paleotopographic low area between the two constructional lobes, where marine flooding was more frequent or more persistent.

Maximum clast-size data, based on the average size of the 10 largest clasts observed at each locality, were collected from fluvial beds in the study area (Fig. 17). These data define a fine-grained area between the two distributive fluvial systems and suggest lower fluvial paleogradients existed in the intervening embayment. No systematic study of maximum clast size was attempted in the Los Cañoncitos area west of the Joyita Uplift, but Kottlowski and Stewart (1970) reported clasts as large as cobbles in that area. No pebbles other than intraformational rip-up clasts were observed in outcrops at Abo Pass.

Paleocurrent data and the dominance of north–south contours of thickness, percent marine strata, and maximum clast size in the Bursum Formation (Figs. 13, 16, and 17) are not compatible with derivation of sediments solely from the Joyita Uplift. They instead suggest that a late Paleozoic uplift (herein termed the San Antonio Uplift) occupied much of the Socorro Basin, in a fashion similar to the subsequent Laramide Sierra Uplift (see below). Although shown as being contiguous with the Joyita Uplift, available data also allow that the San Antonio Uplift was separated from the Joyita Uplift by a topographically low area near the town of Socorro.

Most workers depict the Joyita Uplift as a small positive feature with a paleogeographic extent similar to that of the present outcrops of Proterozoic rocks in the Joyita Hills. The geometry of much of the uplift, however, is obscure. The western flank of the uplift is well preserved in the Los Cañoncitos area, where Bursum and Abo beds lap onto the Proterozoic core of the uplift (Kottlowski and Stewart, 1970) and evidence of late Paleozoic sinistral-oblique normal growth faulting has been documented (Beck, 1993). The northern tip of the Pennsylvanian Joyita Uplift was located near the present northern extent of Proterozoic outcrops, where the tip plunges northward beneath antiformal beds of the Madera Group (Beck, 1993; de Moor et al., 2005). The locations of southern and eastern margins of the uplift, however, are poorly constrained. The eastern flank of the uplift was subsequently downdropped by Laramide and younger slip on the East Joyita fault (Beck and Chapin, 1994). The southern part of the Joyita Uplift lies concealed beneath the Neogene Santa Fe Group of the Socorro Basin (Plate 1).

The angular unconformity at the base of the Bursum Formation at Los Cañoncitos is indicative of a pulse of latest Pennsylvanian Ancestral Rocky Mountain deformation in the Joyita Uplift (Kottlowski and Stewart, 1970; Beck, 1993; Krainer and Lucas, 2009). Beneath the Bursum at Los Cañoncitos, Atokan through Missourian strata are anomalously thin, exhibit wedge shapes and local evidence for growth faulting, and contain numerous disconformities (Kottlowski and Stewart, 1970; Siemers, 1978, 1983; Beck and Chapin, 1994; Nelson et al., 2017), all of which suggest synsedimentary deformation on the western flank of the nascent uplift during the Pennsylvanian. Locally, the Bursum Formation contains clastic wedges of thinly bedded mudstone and fine-grained sandstone as much as 45 m thick. These clastic wedges were interpreted by Nelson et al. (2017) to have resulted from synsedimentary slip on Ancestral Rocky Mountain faults.

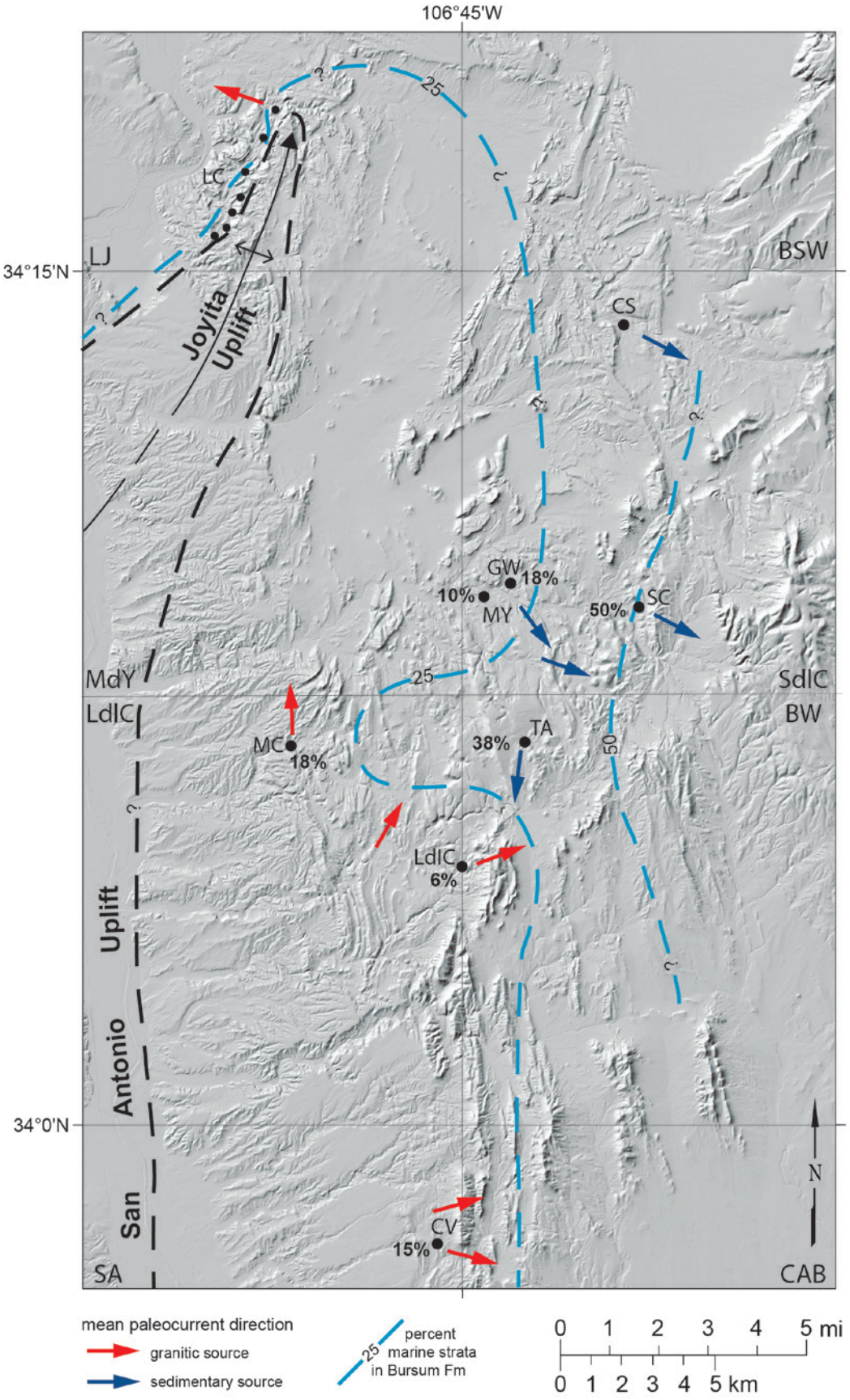

Figure 16. Map showing average paleocurrent directions (from Figs. 12 and 13) and percentage of marine strata in the Bursum Formation, compiled from the interpretations of Krainer and Lucas (2009, 2013). Percentage of marine strata in the Los Cañoncitos area west of Joyita Uplift is estimated from the lithologic descriptions of Kottlowski and Stewart (1970). Abbreviations are defined in Figure 13.

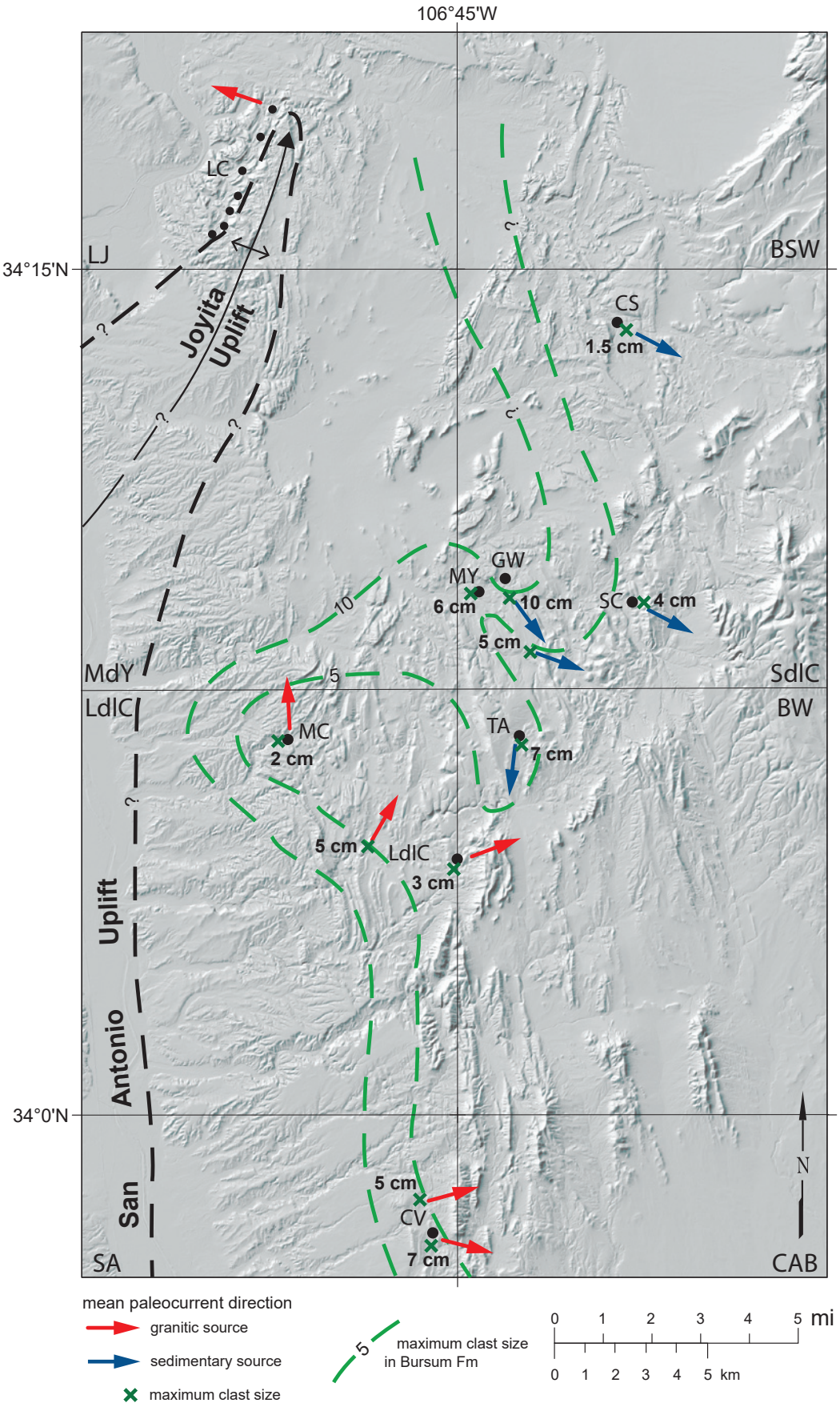

Figure 17. Map of average paleocurrent directions (from Figs. 12 and 13) and maximum clast size for the Bursum Formation. Maximum clast size is the average size of the 10 largest clasts encountered during collection of paleocurrent data at each locality. Abbreviations are defined in Figure 13.

In the Los Cañoncitos area, pebbles in the Bursum Formation consist of mostly Proterozoic lithologies with subordinate clasts derived from the Madera Group. These pebble types are consistent with the rock types exposed along the western flank of the Joyita Uplift during onlap of the Bursum Formation. In contrast, pebble compositions in Bursum deposits derived from the eastern flank of the Joyita Uplift are dominated by limestone and siltstone of the Madera Group. This suggests that extensive exposures of the Madera once existed on the eastern flank of the uplift, but were subsequently downfaulted and buried beneath younger strata east of the East Joyita fault.

Controls on Pennsylvanian Sedimentation

Pennsylvanian strata in the Quebradas region are crudely cyclical, with limestone-dominated successions (parts of the Sandia Formation; the Gray Mesa Formation; the Amado, Council Spring, upper Burrego, Story, and Moya Members of the Atrasado Formation; and parts of the Bursum Formation) alternating rather haphazardly with siliciclastic-dominated ones. Most limestones in the Gray Mesa and Atrasado Formations were deposited below wave base (Krainer et al., 2017). In the northern Oscura Mountains, members of the Atrasado Formation typically each consist of two to three depositional cycles, within which limestone marks episodes of maximum marine flooding (Lucas and Krainer, 2009).

There are only two examples within the study area in which lateral changes of lithofacies have created correlation problems at the member level (see above discussion of the Story Member of the Atrasado Formation). Significant lithologic and thickness variations within members (particularly the siliciclastic-dominated ones), however, are common. Most members vary in thickness by a factor of approximately 1.5–6 (Table 1) within the Quebradas region, but the Burrego Member varies in thickness by a factor of greater than 9. Only the Bartolo Member of the Atrasado Formation maintains a relatively even thickness.

In the Quebradas region, Krainer et al. (2017) interpreted that limestone-dominated parts of the Gray Mesa and Atrasado Formations were deposited during times of tectonic quiescence, but siliciclastic parts accumulated during times of tectonism. The diversity of allogenic factors that potentially influenced Pennsylvanian sedimentation in southwestern Laurentia, however, suggests this interpretation may be simplistic. For example, global glacioeustatic sea-level variations have been invoked to explain Pennsylvanian cyclic sedimentation in the mid-continent region (e.g., Heckel, 1990). Climate change unrelated to glacioeustacy also may influence sequence architecture over broad regions, principally through transgressions and regressions (progradations) that are driven by variation of siliciclastic sediment supply (e.g., Feldman et al., 2005). In New Mexico, where Pennsylvanian basins are flanked by Ancestral Rocky Mountain uplifts, the role of tectonism has been commonly emphasized (e.g., Krainer and Lucas, 2009; Lucas and Krainer, 2009; Krainer et al., 2017). A further, often unappreciated complication is that crustal deformation can be broadly divided into two types: orogeny (local subsidence or uplift caused by the flexural isostatic response to loading/unloading along crustal faults) and epeirogeny (regional uplift or subsidence driven by density changes or flow in the mantle).

The Bursum Formation is a Pennsylvanian unit for which a major orogenic influence (block faulting and tilting) can be confidently inferred. This is shown by variations in lithofacies and thickness within the Bursum, the unconformity (locally angular) at its base, and its well-exposed syntectonic relation to the Joyita Uplift (Kottlowski and Stewart, 1970; Siemers, 1978, 1983; Beck and Chapin, 1994; Nelson et al., 2017). Basinward thickening of Atokan through Missourian strata along the western flank of the Joyita Uplift (Kottlowski and Stewart, 1970; Nelson et al., 2017) is also suggestive of earlier orogenesis. Evidence for major orogenic influences on Pennsylvanian sedimentation elsewhere in central and southern New Mexico is less clear, except locally along the western margin of the Pedernal Uplift (Otte, 1959; Pray, 1961). Local variations of thickness in Pennsylvanian stratigraphic units of central and southern New Mexico are likely an intrabasinal response to orogeny.

In the Quebradas region, member-rank units of the Madera Group are typically around 10–100 m thick (Table 1). Despite their relative thinness, several members of the Gray Mesa and Atrasado Formations can be correlated over a broad region of central and southern New Mexico, at least from the Mud Springs Mountains on the south to the Manzanita Mountains

on the north, a distance of 220 km (Nelson et al., 2013). It seems unlikely that orogenic effects would produce a fine-scale, correlatable lithostratigraphy over such a broad region. For example, I know of no examples of synorogenic stratigraphic intervals of comparable thickness that can be correlated over similar distances within the fault-controlled basins of the Laramide Rocky Mountains or the Rio Grande rift. In contrast, thin stratigraphic units such as the Juana Lopez Beds and the Bridge Creek Limestone Beds (see below) were widespread over broad regions in the Cretaceous Western Interior Seaway, where epeiric subsidence was largely controlled by flow in the mantle (e.g., Heller and Liu, 2016; Chang and Liu, 2021).

In summary, at least four allogenic processes of differing geographic scales potentially influenced Pennsylvanian sedimentation in New Mexico: global glacioeustacy, regional climate change, regional epeirogeny, and local orogeny. Orogenic effects can be demonstrated near the Pedernal and Joyita Uplifts for some stratigraphic intervals. Orogeny also provides a plausible explanation for local variations of thickness and lithofacies *within* Pennsylvanian member-rank units (particularly the siliciclastic ones), although autocyclic processes such as avulsion and delta-lobe switching were also likely important contributors to lithologic variation at that scale. Lithologic differences *among* the members of the Gray Mesa and Atrasado Formations, however, are perhaps best explained by some combination of glacioeustatic, paleoclimatic, and epeirogenic processes because orogeny cannot easily explain the great lateral persistence of such thin lithostratigraphic units.

PERMIAN STRATA OF THE QUEBRADAS REGION

Steven M. Cather

Introduction

Permian strata in the study area are approximately 600–700 m thick and were deposited after Ancestral Rocky Mountain deformation ceased in central New Mexico. The middle Wolfcampian–lower Leonardian(?) Abo Formation filled relict Ancestral Rockies basins and buried parts of the Joyita Uplift (Kottlowski and Stewart, 1970) and the Pedernal Uplift to the east (Broadhead and Jones, 2004).

During early Leonardian through Guadalupian time, central New Mexico was part of a stable shelf northwest of the Delaware Basin. The Yeso Group, Glorieta Sandstone, San Andres Formation, and Artesia Group represent eolian, coastal-plain, sabkha, and restricted-marine deposits that accumulated during transgressive–regressive cycles in an arid, evaporitic environment (e.g., Stanesco, 1991; Mack and Dinterman, 2002; Kues and Giles, 2004; Lucas and Zeigler, 2004; Lucas and Krainer, 2017).

Abo Formation

The name Abo Formation was first applied by Lee (in Lee and Girty [1909]) to a continental red-bed succession of Permian mudstone, sandstone, and limestone exposed near Abo Pass, about 25 km northeast of the study area. Needham and Bates (1943) removed the basal limestone-bearing beds from the Abo. Near Mesa Lucero in western Valencia County, these limestone-bearing beds were subsequently termed the Red Tanks member of the Madera limestone by Kelley and Wood (1946). In central New Mexico, they were named the Bursum Formation (Wilpolt and Wanek, 1951), a separate unit above the Madera limestone. Kelley and Wood (1946) removed the upper sandstone- and siltstone-dominated interval from the Abo Formation and placed it in the overlying Yeso Formation as the Meseta Blanca Sandstone member. Following these excisions, the Abo Formation at its type locality is now around 300 m thick (Lucas et al., 2005).

Tonking (1957) divided the Abo Formation into a lower, mudstone-dominated member and an upper member characterized by greater sandstone

content. Lucas et al. (2005) named these units the Scholle Member and the Cañon de Espinoso Member, respectively. The Abo Formation was not subdivided during mapping for this report.

The Abo Formation is approximately 140–240 m thick in the study area. Thicknesses reported in theses (see Fig. 2 for locations) are, from north to south, 207.9 m (measured by Colpitts [1986]; republished by Lucas et al. [2005]), 200 m (estimated by Brown [1987]), >175.3 m (incomplete section measured by Cappa [1975]), 140 m (estimated by Rejas [1965]), 187 m (measured by Maulsby [1981]; note that Bauch [1982] considered this thickness too large due to faulting), >135.1 m (incomplete section measured by Bauch [1982]), 236 m (estimated by Craig [1992]), and >112.8 m (incomplete section measured by Fagrelius [1982]). Lucas and Krainer (2017) reported thicknesses of approximately 210 m near Minas del Chupadero, approximately 165 m at Loma de las Cañas, and approximately 98 m (possibly thinned by faulting) at Cañoncita de la Uva. Based on these sparse data, there are no obvious thickness trends for the Abo Formation in the study area. This differs from the underlying synorogenic Bursum Formation and suggests that deposition of the Abo largely postdated the Ancestral Rocky Mountain orogeny.

In the Quebradas region, the Abo Formation consists of 75–80% dark reddish-brown mudstone with subordinate sandstone and minor conglomerate (Colpitts, 1986; Brown, 1987). Abo mudstone contains clays of mostly kaolinitic and chloritic composition with minor (approximately 10%) illite and smectite (Cappa, 1975). Mudstones contain local horizons with scattered nodules of micritic limestone, which probably represent calcic paleosols. Local, gray reduction spots a few centimeters in diameter are common in the Abo Formation; some appear to have formed around carbonaceous plant fragments.

Abo sandstone mostly is arkosic to subarkosic in composition; fine sandstone and siltstone are considerably more quartzose (Cappa, 1975; Colpitts, 1986; Lucas and Krainer, 2017). At least locally, feldspar in Abo sandstone has been albitized diagenetically (Cappa, 1975). Bedding surfaces of fine sandstone and siltstone commonly display mud cracks and the impressions of plants or raindrops. Pebbles in Abo Formation sandstone and conglomerate are mostly micritic limestone and red siltstone; most appear to be intraformational. Micritic limestone pebbles are probably recycled from Abo calcic paleosols.

Invertebrate, vertebrate, and trace fossils (including tetrapod footprints) are present in the Abo Formation, as are impressions of plant fragments (DiMichele et al., 2007; Cantrell et al., 2013; Lucas et al., 2013a; DiMichele and Lucas, 2017; Voigt and Lucas, 2017). Plant varieties in the study area, mostly from the upper Abo Formation, include *Walchia* sp., *Brachyphyllum* sp., *Supaia* cf. *S. thinnfeldoides*, cf. *Glenopteris simplex*, and *Callipteris*(?) sp., all possibly of Leonardian age (Hunt, 1983). Throughout central New Mexico, the Abo Formation ranges in age from approximately middle Wolfcampian to late Wolfcampian or early Leonardian (Lucas et al., 2013a, 2022b).

The Abo Formation is largely fluvial in origin, although some mudstone in the lower Abo may have been deposited within floodplain lakes. Mudstone beds in the lower part of the Abo contain prominent upward-fining lenticular sandstones as much as 5 m thick that commonly display lateral accretion bedding (Fig. 18). These sandstones are interpreted to have been deposited on point-bars of paleorivers (e.g., Allen, 1970) that meandered on a muddy floodplain and imply that bankfull channel depth in Abo paleorivers was as much as around 5 m. Such paleorivers were too large to have only drained local uplifts but rather were probably sourced from relict Ancestral Rocky Mountain uplifts to the north. These paleorivers drained southward toward the Hueco seaway of southern New Mexico. There has been no systematic study of Abo paleoflow in the study area, except locally in the north-central part of the Loma de las Cañas quadrangle where Cappa (1975) and Cappa and McMillan (1983) documented diverse, but mostly southerly and westerly, paleocurrent directions.

Tabular sandstones in the lower Abo are generally less than 1 m thick and are interpreted as crevasse-splay deposits. Voluminous mudstones of the lower Abo Formation are suggestive of rapid sedimentary accommodation during deposition. This may have resulted from increased tectonic subsidence and/or rising sea level (i.e., rising base level), perhaps related to transgression of the Hueco seaway to the south (note that Lucas et al. [2013a] and Lucas et al. [2016a] interpreted falling base level during this interval).

Fluvial sandstones in the upper Abo are more sheetlike in geometry and are associated with less voluminous mudstone units. Sandstone is typically ripple-laminated and displays local climbing-ripple stratification. The scarcity of lateral accretion beds in the upper Abo is suggestive of lower sinuosities of paleorivers, and greater sandstone content perhaps is the result of lower rates of sedimentary accommodation during upper Abo deposition.

Yeso Group

The Permian Yeso Group (or Formation) is widely exposed in the Quebradas region, and its type locality lies within the study area. First named by Lee (in Lee and Girty [1909]), the lithologic content and nomenclatural subdivisions of the Yeso have evolved considerably. In the Mesa Lucero region of western Valencia County, Kelley and Wood (1946) removed the sandstone- and siltstone-dominated interval from the upper Abo Formation and included it in the lower Yeso Formation as the Meseta Blanca Sandstone member. They coined the term the Los Vallos member for the upper part of the Yeso.

In northern New Mexico near the Nacimiento Mountains, Wood and Northrop (1946) named the lower and upper parts of the Yeso Formation the Meseta Blanca Sandstone and San Ysidro members, respectively. This terminology was extended to the Hagan area north of the Sandia Mountains by Cather et al. (2002). Lucas et al. (2005) subsequently raised the San Ysidro to formation rank and abandoned the term Meseta Blanca (see discussion below).

In central Socorro County, Wilpolt et al. (1946) and Wilpolt and Wanek (1951) also applied the term Meseta Blanca to the lower part of the Yeso Formation but divided the upper Yeso into three members, in ascending order: the Torres member, the Cañas gypsum member, and the Joyita sandstone member (Fig. 19). Until recently, this nomenclature was applied by all workers in the study area. The tripartite Torres-Cañas-Joyita stratigraphy of the upper Yeso has since been recognized over a broad region of New Mexico, ranging from the Fra Cristobal Mountains on the south to Mesa Lucero and near Abo Pass on the north (Lucas et al., 2013b, 2016a). Because this three-part stratigraphy is also

Figure 18. Upward-fining clinoforms in an Abo Formation channel sandstone, interpreted as lateral accretion beds produced by point-bar migration. Exposure is in Tinajas Arroyo near 377539E, 3772963N (zone 13, NAD 27). Channel sandstone thickness (and minimum inferred paleochannel depth) is ~3 m.

apparent within Kelley and Wood's (1946) Los Vallos member, the Los Vallos has been raised to formation rank by Lucas et al. (2013b) and widely applied by them to upper Yeso beds in the region mentioned above.

In his assessment of the Permian stratigraphy of the Colorado Plateau region, Baars (1962) noted that the term Meseta Blanca Sandstone is a junior synonym of the De Chelly Sandstone of Gregory (1917). Baars therefore abandoned the term Meseta Blanca based on priority and replaced it with the De Chelly Sandstone, which he removed from the Yeso Formation. Nearly all geologists in New Mexico, however, continued to use the term Meseta Blanca and included it in the Yeso Formation. Dickinson (2018, p. 46) stated that the De Chelly Sandstone may be a lateral equivalent of the Yeso Formation, but he considered its principal homotaxial equivalent to be the Glorieta Sandstone (his fig. 29).

Lucas et al. (2005) again advocated adoption of the Arizona term De Chelly Sandstone in lieu of Meseta Blanca for northern New Mexico, while retaining the De Chelly Sandstone within the Yeso, now raised to group rank. To the south, in central and southern New Mexico, Lucas et al. (2005) replaced the Meseta Blanca Sandstone with the term Arroyo de Alamillo Formation, also part of the Yeso Group. The principal distinction between the De Chelly Sandstone and the laterally equivalent Arroyo de Alamillo Formation is the presence of mostly cross-bedded eolian dune deposits and eolian sand-sheet deposits in the former and mostly eolian sand-sheet, loess, and coastal-plain/sabkha deposits in the latter. These two lithofacies are intimately interfingered along the southwestern flank of the Albuquerque Basin. (Note that the original definition of the term Arroyo de Alamillo Formation is confusing: "We name this unit, which is correlative to the De Chelly Sandstone, the Arroyo de Amarillo [sic] Formation. The name is for Arroyo de Amarillo [sic], which flows westward in the southern part of T1S, R1-2E near the Yeso type section" [Lucas et al., 2005, p. 107]).

Principal problems with the nomenclatural scheme of Lucas et al. (2005) for the lower part of the Yeso are as follows. First, abandoning the term Meseta Blanca based on the priority of a unit in an adjacent state is inadvisable given its nearly ubiquitous use on maps, in theses, and in professional journals between 1946 and 2005. Second, the mappability of the proposed laterally equivalent formations in the lower Yeso Group (the De Chelly Sandstone and the Arroyo de Alamillo Formation) has not been demonstrated, as is required by the North American Stratigraphic Code (North American Commission on Stratigraphic Nomenclature, 2005). Indeed, the lithologic criteria by which such lateral contacts may be mapped remain undefined. In my experience, lateral lithofacies transitions within the lower Yeso are quite gradual and cannot be divided into mappable formations in a nonarbitrary, reproducible manner. Moreover, the type De Chelly of northeastern Arizona consists almost entirely of large-scale eolian dune deposits, whereas the Meseta Blanca of northern New Mexico contains mixed deposits of eolian dunes, eolian sand sheets, and subordinate loessic siltstone. It thus seems preferable to retain the term Meseta Blanca Sandstone as a formation-rank term and divide it into lithofacies or members (Fig. 19), for which mappability is not a requirement.

For these reasons, Cather et al. (2013) abandoned the Arroyo de Alamillo Formation and replaced it with the original term Meseta Blanca. In further advocacy of the term Arroyo de Alamillo Formation, Lucas et al. (2016a, p. 324) and Lucas and Krainer (2017, p. 238) incorrectly stated that Cather et al. (2013) did not acknowledge the existence of facies changes within the lower Yeso. In fact, Cather et al. (2013, p. 105) described such lateral facies changes. Lucas et al. (2016a), Lucas and Krainer (2017), and Lucas et al. (2022b) incorrectly claimed that Cather et al. (2013) did not recognize that Meseta Blanca is a junior synonym of the De Chelly Sandstone. Cather et al. (2013, p. 105 and 115) recognized this but stated that the priority does not warrant the disruption of long-established stratigraphic nomenclature.

I concur the Yeso may be considered a group where it is mappable as two superposed formations, such as in the study area. In other areas where such subdivision is not practical, the Yeso should be regarded as a formation or an undivided group. Where mappable, the lower, sandstone- and siltstone-dominated part of the Yeso Group should continue to be termed Meseta Blanca Formation (Cather et al., 2013). The upper, more lithologically diverse part of the Yeso Group is termed the San Ysidro Formation in northern New Mexico and the Los Vallos Formation in central New Mexico (see below).

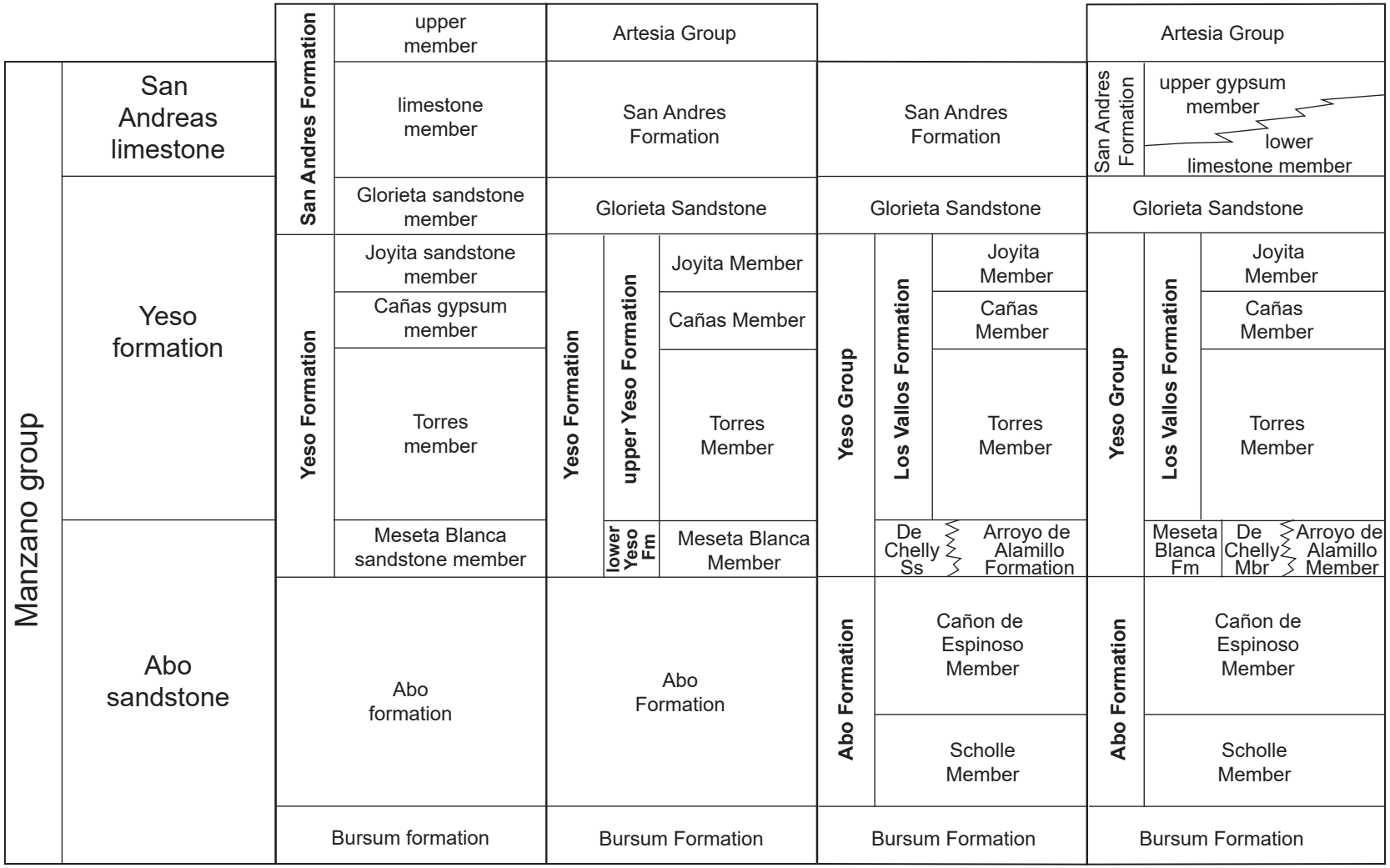

Figure 19. Correlation chart showing evolution of stratigraphic nomenclature for uppermost Pennsylvanian (Bursum Formation) and Permian strata in central Socorro County. Fm—Formation, Ss—Sandstone, Mbr—Member.

The type section of the Yeso Group is located in the west-central part of the Sierra de la Cruz quadrangle in sec. 33, T. 1 S., R. 2 E., and sec. 4 and 5, T. 2 S., R. 2 E., about 3 km southeast of Mesa del Yeso. The exposure there is probably the best in the region, but it is cut by two bedding-plane faults in its upper part (Plate 1; see also Colpitts [1986]). These faults do not appear to have significantly modified the thickness of the type Yeso, which is 331.6 m thick (Lucas et al., 2005). Colpitts (1986) measured a composite section 301.1 m thick in the Yeso Group at the type section (lower part) and at Sierra de la Cruz (upper part). Elsewhere in the study area, thicknesses reported for the Yeso in theses are 170.5 m (Maulsby, 1981), 214.4 m (Bauch, 1982), and 286.6 m (Fagrelius, 1982; see Fig. 2 for theses locations; all are minimum thicknesses due to detachment faulting in the upper part of the unit).

No age-diagnostic fossils have been collected from the Yeso Group in the study area, although trace fossils are present in the Meseta Blanca Formation (see Lucas et al. [2013b] and Voigt and Lucas [2017]). Regionally, the Yeso is early to middle Leonardian in age (Lucas et al., 2013b, 2022b; Vachard et al., 2015).

The **Meseta Blanca Formation** constitutes the basal sandstone- and siltstone-dominated part of the Yeso Group (Fig. 20). At the type section of the Yeso, reported thicknesses of the Meseta Blanca Formation are 91.5 m (Colpitts, 1986) and 106.6 m (Lucas et al., 2005, their Arroyo de Alamillo Formation). To the south, measured thicknesses of the Meseta Blanca in theses are 71.1 m (Maulsby, 1981) and 89.6 m (Fagrelius, 1982). Rejas (1965) estimated 97.5 m.

The contact between the Meseta Blanca Formation and the underlying Abo Formation is typically

Figure 20. Outcrop photo of red and gray sandstones and siltstones of the Meseta Blanca Formation of the Yeso Group. Upper sandstone bed is ~1.5 m thick. View is to the north from 338049E, 3759094N (zone 13, NAD 27), San Antonio quadrangle.

gradational and somewhat arbitrary. Placement of the contact commonly depends upon the nature and quality of exposure. Criteria used to define the contact during mapping in this study and in theses include (1) color change from red or reddish-brown in the Abo to grayish-orange, gray, or greenish-gray in the Meseta Blanca; (2) the first upsection occurrence of salt casts or thin dolomitic beds (note, however, that Bauch [1982, p. 42] included salt-cast-bearing gray siltstones in the upper Abo Formation); and (3) decrease in red mudstone and change to tabular bedding of sandstone in the basal Meseta Blanca Formation.

Because these criteria for the Abo–Yeso contact are not always stratigraphically coincident, placement of the contact is commonly somewhat arbitrary within a stratigraphic interval of a few tens of meters or less. Accordingly, the Abo–Yeso contact is generally marked by a dashed line on Plate 1. In my opinion, it would have been preferable to leave the Meseta Blanca beds within the Abo Formation, as originally envisaged by Lee in 1909. The basal limestone of the Torres Member would serve as a far more reproducible formation-rank contact for mapping in central New Mexico.

The Meseta Blanca Formation consists of variable proportions of sandstone and siltstone. Minor, thin beds of dolomite and claystone are also locally present. Colpitts (1986) estimated the sandstone content of the Meseta Blanca at the Yeso type section to be approximately 80%. In contrast, Lucas et al. (2005) estimated a content of sandstone and coarse siltstone of less than about one-third. The reason for this discrepancy is not known. Inspection of this interval by the author, using a hand lens and grain-size chart, suggests Colpitts' estimate is likely more realistic. To the south, percentages of sandstone in the Meseta Blanca were reported to be approximately 50% (Maulsby, 1981), approximately 90% (Bauch, 1982, based on a partial section), and approximately 43% (Fagrelius, 1982). Sandstone is medium grained to very fine grained and generally well sorted. The composition of Meseta Blanca siliciclastic rocks, particularly of fine sandstone and siltstone, is more quartzose than the underlying Abo and Bursum formations (Lucas and Krainer, 2017).

Most bedding in the Meseta Blanca Formation is tabular and less than around 2 m thick. Lenticular sandstone units are present but uncommon. Stratification is mostly horizontal but commonly includes ripple laminations and local climbing-ripple stratification. Bedding-plane features include symmetric and asymmetric ripples, salt casts and hoppers, and mud cracks. The Meseta Blanca is a fundamentally eolian unit deposited in low-relief coastal-plain and sabkha environments. It mostly consists of eolian sheet sands and loessic silts that were reworked to varying degrees by floods and marine inundations.

Here I adopt the term **Los Vallos Formation** (Lucas et al., 2005) for the upper part of the Yeso Group in the Quebradas region, consisting of the Torres, Cañas, and Joyita Members (Plate 1). The lateral contact between the Los Vallos Formation and the San Ysidro Formation of northern New Mexico occurs within an area of no exposure near the latitude of the northern Manzano Mountains, and thus does not present a mappability issue.

The **Torres Member** conformably overlies the Meseta Blanca Formation. The contact between them is placed at the base of the stratigraphically lowest bed of limestone that is greater than about 1 m thick (note, however, that the lower 26 m of the Torres Member as mapped by Fagrelius [1982] is sandstone). The thickness of the Torres Member at the type section of the Yeso Group was reported as 156 m (Colpitts, 1986; Lucas et al., 2013b) and about 146 m (Lucas and Krainer, 2017). It consists of grayish-red, grayish-yellow, and grayish-orange siltstone and sandstone, medium- to dark-gray limestone and dolomite, and, mostly in the northern part of the study area, light-gray gypsum. These lithologies commonly form cyclic successions 10–40 m thick (Bauch, 1982; Lucas et al., 2005; Lucas and Krainer, 2017). These cyclic successions, where complete, consist of limestone and dolomite overlain by siliciclastic deposits, with gypsum mostly occurring toward the top of each cycle. Lucas and Krainer (2017) interpreted the Torres Member to record the alternation of shallow-marine and coastal-sabkha environments.

Limestone and dolomitic limestone of the Torres Member typically occur as laterally continuous beds approximately 0.5–4 m thick. Most limestone is micrite or peloidal wackestone. Some limestones display a low-diversity assemblage of fossils, including crinoids, brachiopods, gastropods, and forams (Lucas et al., 2013b). Limestone is commonly fetid

and locally contains small vugs filled by asphaltic hydrocarbons (Bauch, 1982; Colpitts, 1986). Diagenesis of organics in Torres Member limestone commonly caused de-reddening of subjacent sandstone, producing a useful stratigraphic-up indicator in deformed successions (Fig. 21).

Sandstone and siltstone of the Torres Member are quartzose, typically horizontally laminated, and form thin, tabular bodies that can be laterally traced for hundreds of meters. Ripple laminations are locally present; trough cross-beds are rare.

Gypsum is preserved as beds approximately 0.5–8 m thick, and typically displays horizontal lamination or nodular mosaic textures. Gypsum beds commonly host low-angle faults within the Torres Member and overlying Cañas Member. Such faulting causes shear features and complex folding within gypsum beds and adjacent strata.

The **Cañas Member** conformably overlies the Torres Member. The lower contact is typically placed at the base of the first thick gypsum above siliciclastic beds in the Torres Member. At the Yeso Group type section, the measured thickness of the Cañas Member is 66.4 m (Lucas et al., 2005; Lucas and Krainer, 2017). At Sierra de la Cruz it is 24.2 m thick (Colpitts, 1986), near Arroyo de las Cañas it is at least 99.1 m thick (Bauch, 1982), and at Cerro del Viboro it is at least 10.7 m thick (Fagrelius, 1982). These measured sections, however, contain low-angle normal faults that have excised an unknown thickness of the Cañas Member (see Chapter 5).

The Cañas Member mostly consists of light-gray gypsum with subordinate buff to greenish-gray siltstone and gray dolomite and limestone that formed in a sabkha environment. Gypsum is thickly bedded and commonly displays nodular mosaic textures or dark-gray horizontal or wavy laminations a few millimeters thick. Siltstone and very fine sandstone occur as thin beds that display horizontal stratification. Carbonate beds are generally micritic and less than a few meters thick

Figure 21. View to the north across Quebradas road showing reddish-orange siltstone and fine sandstone interbedded with gray limestone in the Torres Member of the Los Vallos Formation. Note the common yellowish bleaching (de-reddening) of siliciclastic beds beneath the limestones, which provides a useful stratigraphic-up indicator in structurally complex areas. The Torres Member here lacks bedded gypsum (337286E, 3762552N, zone 13, NAD 27, northeastern San Antonio quadrangle).

(see Lucas et al. [2005] and Lucas and Krainer [2017] for petrographic analyses of these beds). Limestone in the middle part of the Cañas Member locally contains fossil algae, bivalves, gastropods, forams, and ostracods (Bauch, 1982).

The **Joyita Member** is the upper part of the Los Vallos Formation. It consists mostly of well-sorted, fine to very fine quartzose sandstone and subordinate siltstone. Bedded gypsum is absent, but siltstone is commonly gypsiferous. Coloration is pastel hues of red, yellow, orange, and pink. Sandstone displays horizontal lamination and low-angle cross-stratification. The well-sorted nature and fine grain size of sandstone in the Joyita Member suggest it was deposited as sheet sands by eolian processes, with modest reworking by streams.

The basal contact of the Joyita Member is conformable and placed at the top of the uppermost bedded gypsum of the Cañas Member. Reported thicknesses for the Joyita Member are 12.3 m at the Yeso Group type section (Lucas et al., 2005; Lucas and Krainer, 2017), 29.4 m at Sierra de la Cruz (Colpitts, 1986), approximately 18 m near Rancho de Lopez (Maulsby, 1981), at least 16.5 m near Arroyo de las Cañas (Bauch, 1982), and 47.5 m at Cerro del Viboro (Fagrelius, 1982).

Glorieta Sandstone

Along with the overlying San Andres Formation, the Permian Glorieta Sandstone holds up many of the high peaks and mesas in the study area. The term Glorieta was first applied to sandstones exposed near the southern terminus of the Sangre de Cristo Mountains in northern New Mexico by Keyes (1915), although he miscorrelated it with the Cretaceous Dakota Sandstone. Most early workers considered the Glorieta to be a member of either the Yeso Formation or the San Andres Formation (see history of Glorieta nomenclature in Lucas et al. [2013c]). In central New Mexico, most now regard the Glorieta as a distinct formation—a practice followed in this study. Needham and Bates (1943) designated the type section on Glorieta Mesa, southeast of Santa Fe (see Krainer and Lucas [2015]).

The Glorieta Sandstone consists largely of moderately sorted to well-sorted, very fine to medium quartzose sandstone (Fig. 22). A few thin beds of limestone commonly occur in its upper part, and siltstone is common, mostly in its lower part. Sandstone is typically light gray in color on fresh surfaces but weathers to pale shades of red, orange, brown, and yellow. Bedding in sandstone is massive (structureless), horizontally laminated, ripple-laminated, or cross-stratified (mostly low- to moderate-angle planar cross-beds). Some of the horizontally laminated sandstones exhibit upward-coarsening laminae diagnostic of migrating eolian ripples (Hunter, 1981; Mack and Bauer, 2014), indicating deposition on a rippled sand sheet. Cross-beds are typically less than 3 m thick. They commonly display subcritically climbing translatent stratification produced by eolian ripples migrating across avalanche faces. The cross-bedded sandstones appear to have been primarily deposited by eolian dunes (see also Lucas et al. [2013c], Krainer and Lucas [2015], and Lucas and Krainer [2017]).

Most recent studies of the Glorieta in central New Mexico have interpreted it as a fundamentally eolian sandstone, mostly deposited as eolian sheet sands and dunes that were reworked to varying degrees by marine incursions and fluvial processes (Lucas et al., 2013c; Mack and Bauer, 2014). Cross-bedding dip direction indicates winds were mostly from the northeast (Mack and Bauer, 2014).

Lucas et al. (2013c) measured 87 m of Glorieta Sandstone near the Yeso Group type section in the west-central part of the Sierra de la Cruz quadrangle. Measured thicknesses from theses (see Fig. 2 for locations) are, from north to south, 37.5 m (Arendt, 1971), 62.8 m (Colpitts, 1986), >41.2 m (Maulsby, 1981; this is an incomplete section), and 40.5 m (Fagrelius, 1982). Some exposures in the study area appear to have been thinned by stratal omission along low-angle normal faults at the base of the Glorieta Sandstone, but the amount of thinning is difficult to quantify.

In the study area, the basal contact of the Glorieta Sandstone with the underlying Joyita Member of the Los Vallos Formation ranges from conformable to mildly erosive (disconformable), but no evidence for deep ravinement or soil development was noted. The lower contact is placed at the base of the stratigraphically lowest, thick gray quartzose sandstone. Interbeds of Joyita-like siltstones, however, are locally present in the lower part of the Glorieta (Arendt, 1971). In many places, the basal contact of

Figure 22. View to the east of light-gray and yellowish-gray Glorieta Sandstone in the eastern part of the Loma de las Cañas quadrangle near 337300E, 3768300N (zone 13, NAD 27). The Glorieta is overlain by dark-gray limestone of the San Andres Formation and underlain by reddish-brown beds of the Joyita Member of the Los Vallos Formation.

the Glorieta is a low-angle normal fault, with much of the Los Vallos Formation missing in the footwall (Colpitts, 1986).

No age-diagnostic fossils have been reported from the Glorieta Sandstone. Based on regional correlations, it is probably late Leonardian in age (Lucas et al., 2013c). The Glorieta Sandstone represents the eastern, sand-sheet-dominated part of the Coconino/de Chelly erg of Arizona (Baars, 1962; Dickinson, 2018). The detrital zircon population of the Glorieta Sandstone was largely derived from the Appalachian region (Mack and Bauer, 2014). Zircon-bearing sands were carried westward, presumably by a major transcontinental river system that lay to the north of New Mexico, and then blown southwestward by prevailing trade winds (Mack and Bauer, 2014; Dickinson, 2018).

San Andres Formation

In the study area, the San Andres Formation can be divided into two informal members—a lower limestone member and an upper gypsum member (Fagrelius, 1982). The limestone member is widely exposed; the gypsum member mostly crops out in the north-central and east-central parts of the study area. No complete section of the San Andres Formation has been measured in the study area, but it appears to be approximately 100–150 m thick based on cross sections. Partial measured thicknesses from theses (Fig. 2) are 82.6 m (Fagrelius, 1982), 58.2 m (Colpitts, 1986), 21.7 m (Maulsby, 1981), and 71.6 m (Arendt, 1971). Colpitts (1986) estimated a possibly complete thickness of about 120 m for the San Andres Formation in the southeastern part of the Mesa del Yeso quadrangle. Lucas and Krainer (2017) measured an incomplete section of 90 m near

Figure 23. View to the northeast from 337293E, 3760331N (zone 13, NAD 27, San Antonio quadrangle) showing planar nature of basal contact of the dark-gray San Andres Formation (lower limestone member) with the underlying, yellowish-gray Glorieta Sandstone, the top of which is marked by the pinkish-gray bed. The Los Vallos Formation is exposed in the middle ground and at the base of the slope.

Gonzales Well in the northwestern part of the Cañon Agua Buena quadrangle.

The lower contact of the San Andres Formation is placed at the base of the first thick limestone above the Glorieta Sandstone. The lower contact of the San Andres Formation is widely exposed in the study area and appears sharp and planar when viewed from a distance (Fig. 23), but detailed inspection commonly reveals interbedding of sandstone and limestone. For example, two thin limestones occur in the upper part of the Glorieta at the measured section of Lucas et al. (2013c) near Mesa del Yeso, and similar limestones were noted by the author elsewhere in the study area. It is common to find a few horizontally stratified or structureless quartzose sandstone beds as much as around 4–6 m thick in the lower San Andres (e.g., Maulsby, 1981; Colpitts, 1986). These Glorieta-like sandstone beds typically lack eolian cross-bedding, but they also lack marine fossils, so it is unclear if they represent the last gasps of Glorieta eolian sheet-sand sedimentation or are simply Glorieta sands reworked during the San Andres transgression (e.g., Brose et al., 2013). The lack of evidence for soil development or ravinement at the Glorieta–San Andres contact indicates the contact is conformable or paraconformable (see similar interpretations by Colpitts [1986] and Fagrelius [1982]). This contrasts with Brose et al. (2013), who regarded the contact as a regional unconformity. Locally, such as in the southeastern part of the Loma de las Cañas quadrangle, the lower contact of the San Andres Formation is a low-angle fault (Plate 1).

The principal lithotypes present in the lower limestone member of the San Andres Formation are limestone (locally dolomitized), fine to medium quartzose sandstone, and mudstone (these and other lithofacies in the San Andres Formation were described and interpreted by Lucas and Krainer [2017]). Limestone is thin- to medium-bedded, yellowish-brown to black micrite, wackestone, and grainstone. Grain types include peloids and ooids. Fossil brachiopods, gastropods, pelecypods,

bryozoans, rugose corals, crinoids, and phylloid algae have been reported in the study area (Fagrelius, 1982; Colpitts, 1986). Freshly broken surfaces commonly exude a slightly fetid odor. The lower limestone member of the San Andres Formation locally contains a few meter-scale beds of quartzose sandstone and sparse, thin interbeds of buff-colored siliciclastic mudstone. Discontinuous tabular zones of brecciated limestone are common in the lower part of the formation. These breccias probably result from dissolution of evaporite beds.

Gypsum primarily occurs as thick beds in the upper San Andres Formation, but the former presence of scattered beds of gypsum in the lower part of the formation is suggested by local dissolution breccias and detachment horizons (see Chapter 5). The upper gypsum member is preserved primarily in the northern half of the study area, near Bordo Atravesado and northeast of Mesa del Yeso, where gypsum and gypsiferous mudstone dominate the upper one-third to one-half of the San Andres Formation. Gypsum is gray in color and generally poorly exposed, but in places displays alternating light- and dark-gray beds (these are thicker than the millimeter-scale, dark-and-light gypsum laminations seen in the Cañas Member of the Los Vallos Formation). Thin interbeds of dark-gray dolomitic limestone and gray to red siltstone are also present (Fig. 24) in the upper gypsum member.

Remnants of the upper gypsum member less than a few tens of meters thick are locally preserved beneath the Permian Artesia Group in the southern part of the study area, in the northwestern part of the Cañon Agua Buena quadrangle. One exposure (SE1/4 sec. 22, T. 4 S., R. 2 E.) was described by Fagrelius (1982) as 15 m of white bedded gypsum, tan siliciclastic mudstone, and karstic breccia disconformably overlain by the Permian Artesia

Figure 24. Outcrop image of gypsum beds, gypsiferous mudstone, and thin ledges of limestone that are typical of the upper San Andres Formation (upper gypsum member) in the east-central and north-central parts of the study area. View is to the north from 338155E, 3786813N (zone 13, NAD 27), Sevilleta National Wildlife Refuge, Mesa del Yeso quadrangle.

Group (his Bernal Formation). In other areas, the upper gypsum member is commonly eroded. The missing section beneath the Triassic seems to be greater in the southern part of the study area (see below). Further study will be necessary, however, to determine the relative importance of syndepositional facies changes versus postdepositional erosion in the observed northward increase in gypsum abundance in the upper San Andres Formation.

The San Andres Formation in central New Mexico is late Leonardian in age (Brose et al., 2013; Vachard et al., 2015), although no fossils have been recovered from the upper gypsum member. Limestones were deposited in various shallow-marine environments, including open-shelf, intertidal, and hypersaline lagoon settings. The upper gypsum member of the San Andres Formation records hypersaline paleoenvironments during the final withdrawal of the Permian sea from the region.

Artesia Group

The Artesia Group is the youngest Permian unit exposed in central New Mexico. Formerly known as the Bernal Formation (Bachman, 1953), here these beds are termed the Artesia Group following Tait et al. (1962; see also Lucas and Hayden [1991]). The Artesia Group mostly consists of tabular-bedded, calcareous and locally gypsiferous, pale-orange to reddish-orange siltstone and fine quartzose sandstone. It is 0–20 m thick. The Artesia Group is missing in most of the study area because of erosion prior to Triassic sedimentation; it was mapped separately only in the Mesa del Yeso, San Antonio, and Cañon Agua Buena quadrangles. A thin sequence of orange gypsiferous siltstone occurs locally at the top of the San Andres Formation in the Bustos Well quadrangle. These siltstones may pertain to the Artesia Group but were included in the San Andres Formation during mapping. The Artesia Group is also present north of the study area, in the Becker SW quadrangle (Allen et al., 2013b).

Fagrelius (1982) measured a 30.2-m section of Artesia Group (his Bernal Formation) in the southwestern part of the Cañon Agua Buena quadrangle in SW1/4, SW1/4 sec. 4, T. 5 S., R. 2 E. (note that Fagrelius incorrectly placed these exposures in T. 4. S.). By my interpretation, the upper two-thirds of this section (as well as much of what Fagrelius mapped elsewhere as Bernal Formation) pertains to the Triassic Moenkopi Formation—a unit not recognized by Fagrelius. The lower 11.7 m of Fagrelius' measured section appear to be true Artesia Group strata. He described these strata as mostly reddish-brown mudstone and minor fine to medium sandstone with local horizons of mud cracks and salt casts. Lucas and Krainer (2017) described an 11-m Artesia Group section of dominantly sandstone and siltstone in the west-central part of the Cañon Agua Buena quadrangle (their Gonzalez Well B section).

The contact of the Artesia Group with the underlying, upper gypsum member of the San Andres Formation is disconformable and is commonly marked by karstic brecciation of underlying beds. Because age constraints are poor, it is unclear if this disconformity represents a significant hiatus. Fagrelius (1982) reported areas where the Artesia Group unconformably overlies the lower limestone member of the San Andres Formation. The overlying strata in these areas, however, appear to belong to the Triassic Moenkopi Formation, not the Artesia Group.

The Artesia Group in the study area contains no age-diagnostic fossils, but it is Guadalupian in its type area in southeastern New Mexico. The Artesia Group in the study area represents deposition in the distal feather edge of the Northwest Shelf of the Delaware Basin. Depositional processes are unstudied but appear to have been fundamentally eolian (loess and eolian sheet sands), with occasional reworking by sheet floods.

CHAPTER 3: MESOZOIC ROCKS

TRIASSIC STRATA OF THE QUEBRADAS REGION

Steven M. Cather

Introduction

Triassic strata in central New Mexico were deposited within broad, regional basins by mostly fluvial processes. These strata are assigned to two formations: the Middle Triassic Moenkopi Formation and the Upper Triassic Chinle Formation. Moenkopi strata accumulated in the eastern part of the Sonoma proforeland basin (Lawton, 1994). This basin developed behind the East Mexico arc (e.g., Dickinson and Gehrels, 2008), although no genetic relation between the two features has been demonstrated.

Following an approximately 10 Myr lull in sedimentation, the Upper Triassic Chinle Formation began to accumulate behind the nascent Cordilleran arc within the vast Dockum–Chinle basin that extended from Texas to Nevada (Blakey and Gubitosa, 1983; Dubiel, 1994; Lawton, 1994). Both the Moenkopi and Dockum–Chinle basins drained northwestward to the sea (Dickinson, 2018).

Moenkopi Formation

The Moenkopi Formation in the study area disconformably overlies Permian beds, either the Artesia Group or the San Andres Formation. Early workers mapped the Moenkopi as part of the Dockum Formation (Wilpolt and Wanek, 1951) or as Bernal Formation (Fagrelius, 1982). Although first recognized in central New Mexico by Stewart et al. (1972), Moenkopi beds were first noted in the study area by Hunt and Lucas (1987a; see also Lucas [1991]). The best Moenkopi exposures in the study area are in the Cañon Agua Buena quadrangle, where several sections have been measured (Spielmann and Lucas, 2009). These strata correlate with the Anton Chico Member of the Moenkopi Formation in northeastern New Mexico and have yielded fossils of Middle Triassic (Anisian) age (Lucas, 1991; Spielmann and Lucas, 2009).

The Moenkopi in the Quebradas region typically consists of approximately 20–40 m of grayish-red and reddish-brown sandstone, mudstone, and minor, mostly intraformational conglomerate (Fig. 25). The ratio of sandstone to mudstone is locally variable but subequal in most exposures. The Moenkopi Formation can be difficult to distinguish from the overlying Chinle Formation where the pebbly Shinarump Member of the lower Chinle is absent or unexposed. Although Moenkopi sandstone tends to be less quartzose and somewhat more grayish-red in coloration than the main part of the Chinle (the San Pedro Arroyo Member), there is considerable overlap of petrology (at least as seen through a hand lens) and coloration between the two units. Consequently, in the Bustos Well quadrangle where the Shinarump Member is generally absent or unexposed, the Moenkopi was in most places mapped together with the Chinle as an undifferentiated Triassic unit (Plate 1). Both the Moenkopi and

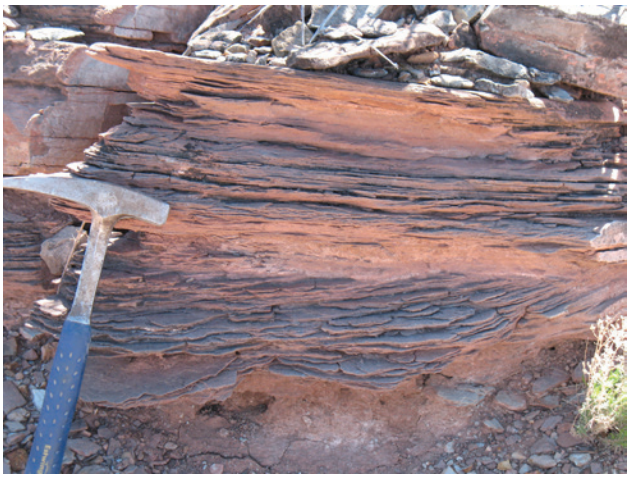

Figure 25. Moenkopi fluvial sandstone bed with cross-bedding, horizontal bedding, and low-angle cross-bedding. View is to the east from 341611E, 3756234N (zone 13, NAD 27), Cañon Agua Buena quadrangle.

Shinarump are eroded or covered in much of this quadrangle (Fig. 26).

In the study area, the Moenkopi Formation is largely fluvial in origin. Sandstone is medium grained to fine grained and appears to be subarkosic to sublitharenitic in composition, although no petrographic analyses were performed. Sandstone occurs as broad, tabular beds less than about 1 m thick that exhibit trough cross-bedding, low-angle cross-bedding, and horizontal stratification (Fig. 25), suggesting shallow paleoflow in broad channels. Paleocurrent analysis of the Moenkopi Formation in the study area has not been undertaken, but Lucas (1991) noted Moenkopi paleoflow in south-central New Mexico was toward the north or northwest.

Chinle Formation

Upper Triassic beds in the Quebradas region were mapped as Dockum Group (or Formation) by most early workers (Wilpolt et al., 1946; Wilpolt and Wanek, 1951; Tabet, 1979; Fagrelius, 1982; Smith, 1983; Colpitts, 1986) and in a recent study (de Moor et al., 2005). Fagrelius (1982) and Smith (1983) divided the Dockum Group in the study area into two map units: a lower unit of mostly sandstone and conglomerate (the Santa Rosa Sandstone) and an upper unit of mostly mudstone (the Chinle Formation).

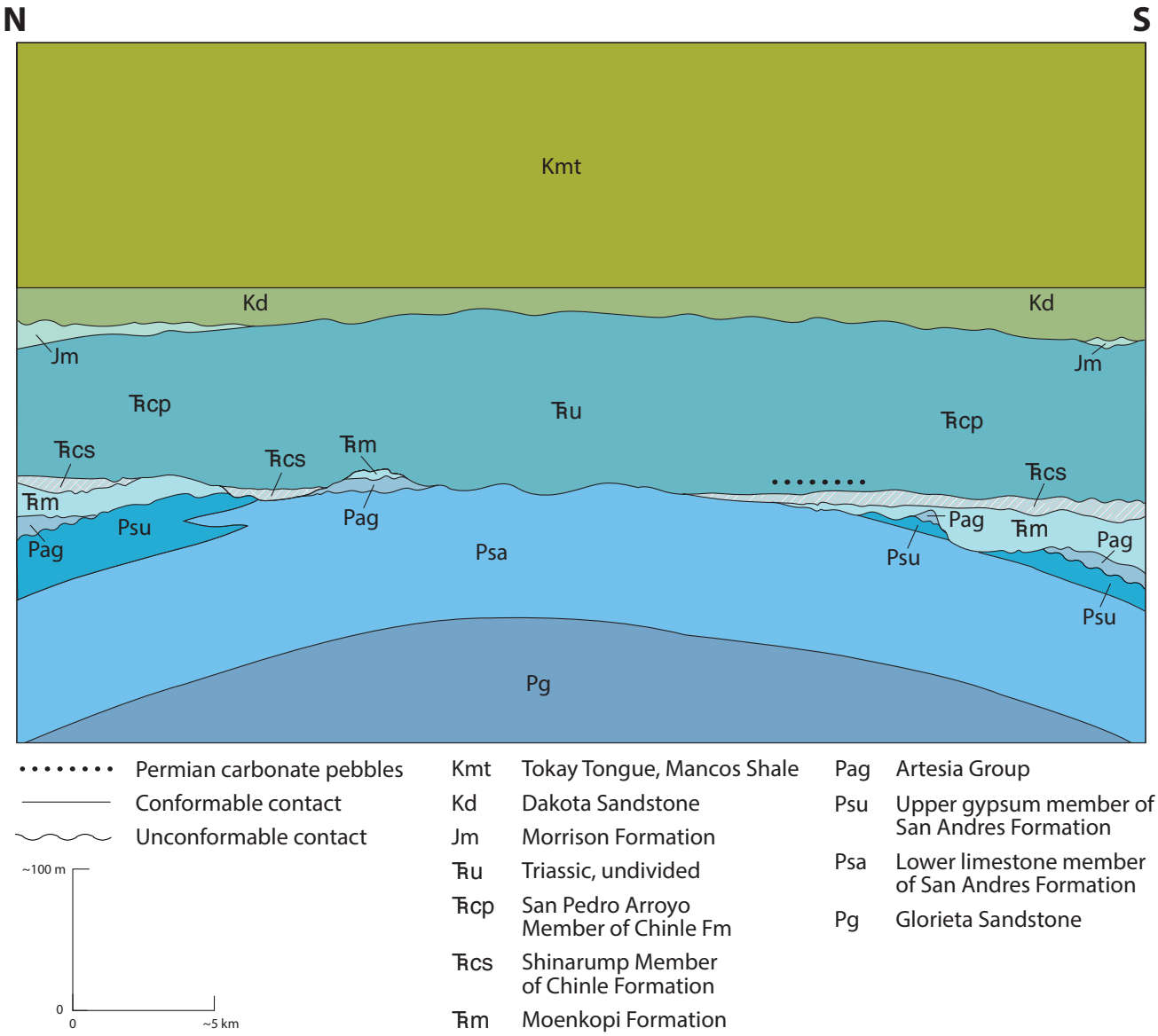

Figure 26. Schematic north–south cross section through the Quebradas region showing interpreted contact relations among Permian, Triassic, and Cretaceous strata.

Early workers (Darton, 1928; Smith, 1961; Hilpert, 1969) arbitrarily regarded the Rio Grande as the nomenclatural boundary between the Dockum Group and the correlative Chinle Formation to the west. Lucas (1993) raised the Chinle to group rank and extended it to encompass all Upper Triassic nonmarine strata (including the Dockum Group and Dolores Formation) in the southwestern United States. Although many workers disagree with the use of the term Chinle Group in Colorado, Texas, and eastern New Mexico (see discussion in Cather et al. [2013]), extension of the term Chinle to former Dockum beds on the eastern flank of the Rio Grande rift is justified because of the continuity of Upper Triassic beds across the rift in the subsurface of the Albuquerque Basin. Accordingly, I have adopted the term Chinle for Upper Triassic strata in the Quebradas region, although I regard it as a formation-rank term because its constituent parts are not mappable everywhere in the study area. I use the terminology of Lucas (1991) for subdivisions of the Chinle, but at member rank: the Shinarump Member and the San Pedro Arroyo Member.

The **Shinarump Member** constitutes the lower part of the Chinle Formation throughout much of the Quebradas region. No age-diagnostic fossils have been recovered in the study area. The age of the Shinarump is controversial. Regionally, Shinarump vertebrate faunas have been interpreted as late Carnian (Lucas, 2004; Spielmann and Lucas, 2009). Regional stratigraphic correlation, magnetostratigraphy, and U-Pb geochronology, however, favor a Norian age for the lower Chinle Formation (see discussion in Dickinson [2018], p. 63).

In most areas, the Shinarump disconformably overlies the Moenkopi Formation. It primarily occurs within shallow paleovalleys carved into the underlying Moenkopi (Fig. 26). The basal part of the Shinarump is in most places pebbly sandstone or conglomerate (Fig. 27), but locally it is sandstone that lacks pebbles. The Shinarump Member consists of reddish-brown to grayish-red fluvial sandstone, pebbly sandstone, conglomerate, and minor red mudstone. Pebbles are mostly quartzite, chert, and limestone. Sandstone is well cemented, medium to very coarse grained, and commonly cross-bedded, forming lenticular beds. Limited paleocurrent data from the Cañon Agua Buena quadrangle suggest paleoflow was toward the northwest (Plate 1).

The Shinarump Member ranges from 0–30 m thick in the study area by my estimation. Fagrelius (1982) measured a 72-m composite section (of his Santa Rosa Sandstone) in the Cañon Agua Buena quadrangle, a thickness significantly greater than seems reasonable based on my own observations and the 1.3–21.2 m range of thickness reported by Spielmann and Lucas (2009). The anomalous thickness reported by Fagrelius (1982) is possibly the result of miscorrelation because the two parts of his composite section are widely separated.

In the central part of the Cañon Agua Buena quadrangle (sec. 26 and 27, T. 4 S., R. 2 E.), prominent ridge-forming sandstone a few tens of meters thick were mapped as the Shinarump Member during this study and as Santa Rosa Sandstone by Fagrelius (1982). In contrast, at their Cañon Agua Buena 1 measured section, Spielmann and Lucas (2009) correlated these sandstones with the Moenkopi Formation. Through a hand lens, the lower part of these sandstones does indeed resemble the Moenkopi Formation, but the upper part is more quartzose, more like sandstones of the Chinle. It is thus unclear if the sandstones in question are actually part of the Moenkopi or were simply recycled from that unit. I favor the latter interpretation based on lateral lithofacies trends seen in other exposures of the Shinarump Member.

The **San Pedro Arroyo Member** constitutes the majority (around 90%) of the Chinle Formation in the study area. It conformably and transitionally

Figure 27. Unusually coarse conglomerate of the Shinarump Member of the Chinle Formation. View is to the west from 338504E, 3751991N (zone 13, NAD 27), Cañon Agua Buena quadrangle.

overlies the Shinarump Member. The lower contact of the San Pedro Arroyo Member is placed at the base of the lowermost thick mudstone in the Upper Triassic section. The San Pedro Arroyo Member is 165–210 m thick in the study area based on the measured sections of Fagrelius (1982) and Spielmann and Lucas (2009). Fossils suggest the San Pedro Arroyo Member is mostly upper Carnian, although the upper part is possibly lower Norian (Spielmann and Lucas, 2009). Dickinson (2018, and references therein), however, interpreted the entire Chinle Formation as Norian based on regional stratigraphic correlation, magnetostratigraphy, and U-Pb geochronology.

The San Pedro Arroyo Member mostly consists of mudstone (around 60–80%) with subordinate sandstone and minor conglomerate and limestone (Fig. 28). Siliciclastic beds of the San Pedro Arroyo Member are largely fluvial in origin, although some laminated mudstones may have accumulated in floodplain lakes and ponds. Mudstone, typically poorly exposed, is mostly red, red-brown, or maroon in color, but bluish-gray, brown, and gray intervals are not uncommon. Sandstone occurs as tabular beds and, less commonly, channel-form beds that exhibit trough cross-bedding, low-angle cross-stratification, and horizontal stratification. No petrographic analysis of sandstone of the San Pedro Arroyo Member has been attempted in the study area. Most sandstones appear to be sublitharenites or subarkoses when viewed through a hand lens.

Conglomerate occurs as scattered lenses within sandstone units and mostly consists of intraformational clasts of mudstone and calcareous nodules. In SW1/4 sec. 23, T. 4 S., R. 2 E., and in the northeastern part of the Mesa del Yeso quadrangle beneath the Jurassic Morrison Formation, however, local conglomeratic horizons occur in the upper part of the San Pedro Arroyo Member. These largely

Figure 28. Red mudstone and sandstone of the San Pedro Arroyo Member of the Chinle Formation. The gray bed below the hammer is a pebbly sandstone with clasts of reworked pedogenic carbonate and siltstone fragments. View is to the west from 338798E, 3751545N (zone 13, NAD 27), Cañon Agua Buena quadrangle.

consist of gray pebbles of nonfossiliferous, micritic limestone with subordinate clasts of indurated siltstone (Fig. 29), suggesting nearby exposures of Permian strata during deposition. North of the study area, in the Becker SW quadrangle (Allen et al., 2013b), the Morrison Formation locally overlies the lower part of the Chinle Formation (Lucas et al., 2016b), suggesting deep erosion prior to the Late Jurassic. The presence of probable Permian pebbles and the anomalous contact relations for Triassic and Jurassic strata (Fig. 26) suggest mild tectonic activity in central New Mexico during the Late Triassic, a possibility first pointed out to me by the late Clay T. Smith during the 1990s. If correct, this tectonism may be related to the only two known examples of Late Triassic deformation in New Mexico: an angular unconformity between the Dockum Group and overlying Jurassic strata near Battleship Rock in the Dry Cimarron Valley of northeastern New Mexico (Baldwin and Muehlberger, 1959) and an angular unconformity within the Chinle Group near Youngsville (Kelley et al., 2005). The structural controls for Late Triassic deformation in New Mexico are unclear.

Limestone is present as discrete beds in the lower part of the San Pedro Arroyo Member and as horizons of scattered nodules in the upper part. Nodules appear to be pedogenic in origin, suggesting seasonal semiaridity. The lower bedded limestones are of regional extent and have been variously interpreted as lacustrine deposits (Lucas, 1991), pedogenic carbonates (Spielmann and Lucas, 2009), or pond and spring deposits overprinted by pedogenesis (Tanner and Lucas, 2012). Termed the Ojo Huelos Member of the San Pedro Arroyo Formation by Lucas (1991), these limestones are given the rank of beds in this study.

Present in a fairly continuous interval approximately 10–30 m above the base of the San Pedro Arroyo Member, the **Ojo Huelos beds** consist of several limestones that occur as either closely stacked beds or ones separated by several meters of intervening siliciclastic deposits. Individual limestone beds typically can be traced laterally for several tens of meters to a few hundred meters. The Ojo Huelos beds exhibit coated grains, pisolites (Tanner and Lucas, 2013), breccias, bacterial(?) lamination, horizontal stratification, and cross-stratification (Fig. 30). Many beds are clastic in nature (they were termed limestone-clast conglomerates by Fagrelius [1982]), with calcareous grains ranging in size from coarse sand to pisolites as much as 4 cm in diameter. Calcareous laminations of probable biological origin coat grains and some bedding surfaces.

The bases of beds are sharp and locally appear erosional. In SE1/4 sec. 27, T. 4 S., R. 2 E., limestone beds are intercalated with fluvial sandstones. Cross-stratification in these sandstones indicates the paleoslope was toward the north or northwest during deposition. Siliciclastic beds associated with the Ojo Huelos tend to be grayer (less oxidized) than is typical of the rest of the San Pedro Arroyo Member. Regionally, the Ojo Huelos beds contain

Figure 29. Pebbles of probable Permian limestone and siltstone in a conglomerate of the San Pedro Arroyo Member of the Chinle Formation. Note reddish, concentric pisolite toward the top of image that is possibly recycled from the Ojo Huelos bed (342093E, 3756704N, zone 13, NAD 27, Cañon Agua Buena quadrangle).

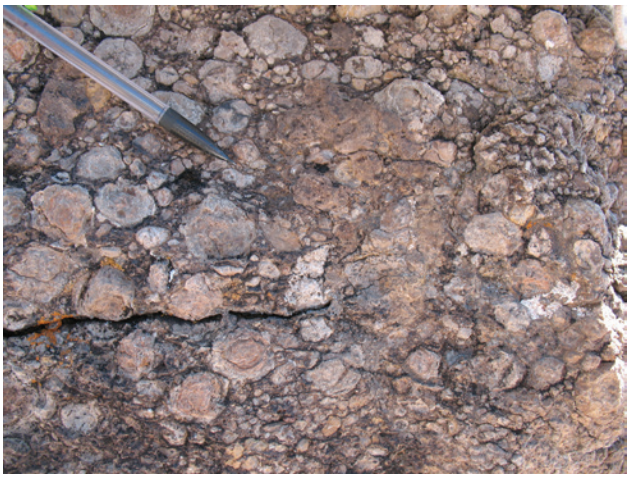

Figure 30. Pisolitic limestone of the Ojo Huelos bed, in the lower part of the San Pedro Arroyo Member of the Chinle Formation (341510E, 3755657N, zone 13, NAD 27, Cañon Agua Buena quadrangle).

fossils of fish, gastropods, ostracods, a hybodont shark, amphibians, reptiles (including phytosaurs), and abundant silicified wood (Spielmann and Lucas, 2009; see also Heckert and Lucas, 2002).

Based on the above observations, limestone of the Ojo Huelos beds was likely deposited in spring-fed ponds, streams, and wetlands, similar to the interpretation of Tanner and Lucas (2012). Given the widespread occurrence of the Ojo Huelos in Socorro and Valencia counties (Lucas, 1991), these beds probably reflect an interval of moist paleoclimate and high water tables during the early stages of deposition of the San Pedro Arroyo Member. I have seen no evidence to support a calcic paleosol origin for these beds (e.g., Spielmann and Lucas, 2009), although modest overprinting by pedogenic processes is possible. In particular, the fossil content, sharp bases of the limestone beds, and lack of other, noncalcic soil horizons argue against a purely pedogenic origin. Breccias within the limestones suggest bioturbation or perhaps episodes of exposure during deposition of the Ojo Huelos beds.

Spielmann and Lucas (2009) named the strata below and above the Ojo Huelos beds the Araya Well and Cañon Agua Buena members, respectively. Where the Ojo Huelos is absent or not exposed, however, the lithologic characteristics of these members are not sufficiently distinct to warrant separate nomenclatures. I consider the upper Chinle Formation in the study area to consist solely of the San Pedro Arroyo Member, within which the limestones of the Ojo Huelos beds are intercalated.

JURASSIC STRATA OF THE QUEBRADAS REGION

Steven M. Cather

Introduction

Thin, discontinuous strata of probable Jurassic age are locally present in the study area. These beds are assigned to the Morrison Formation, which accumulated in a huge, mostly nonmarine, retroarc basin that extended from central New Mexico to southern Saskatchewan (Turner and Peterson, 2004).

Morrison Formation

Nonfossiliferous beds probably correlative to the Upper Jurassic Morrison Formation crop out in the northern and southern parts of the study area but are missing beneath the Upper Cretaceous Dakota Sandstone in the central part (Fig. 26, Plate 1). In the northeastern part of the Mesa del Yeso quadrangle, the Morrison Formation consists of kaolinitic, cross-bedded sandstone, pebbly sandstone, and greenish-gray mudstone that disconformably overlie the upper part of the Chinle Formation (Fig. 31). There, the Morrison is approximately 16 m thick (Lucas et al., 2016b). Nearby to the north of the study area, in the Becker SW quadrangle (Allen et al., 2013b), the Morrison Formation overlies the lower part of the Chinle Formation (Lucas et al., 2016b). As noted above, these contact relations may provide evidence for pre-Morrison (Late Triassic and/or Early Jurassic) mild tectonism and erosion in the Quebradas region. Renewed weak arching in the central part of the study area prior to deposition of the Dakota Sandstone may explain the absence of the Morrison Formation there.

Near Carthage in the southern part of the study area, discontinuous exposures of probable Morrison Formation locally overlie the Chinle Formation. These Morrison outcrops consist of light-gray kaolinitic sandstone and greenish-gray to grayish-purple mudstone 0–3 m thick (Hunt and Lucas, 1987b). Because of its thinness, the Morrison Formation near Carthage was not separately mapped, but was included in the underlying Chinle Formation (Plate 1).

It is unclear how the beds in the study area correlate to the Morrison Formation of northern New Mexico. Hunt and Lucas (1987b) argued that Jurassic beds near Carthage likely represent a condensed section within the lower part of the Morrison Formation, whereas Lucas et al. (2016b) suggested all Jurassic beds in the Quebradas region correlate to the Brushy Basin or Jackpile Sandstone Members of the upper Morrison. If correlation to the Jackpile Sandstone is correct, however, these beds may not be Jurassic. Stratigraphic and detrital zircon studies have shown that the Jackpile Sandstone is possibly correlative with the Lower Cretaceous Burro Canyon Formation of northern New Mexico and Colorado (Aubrey, 1992; Dickinson and Gehrels, 2010; Cather et al., 2013; Dickinson, 2018).

Outcrops of the Morrison Formation in the Quebradas region and near Capitan 120 km to the east (Lucas, 1991) represent the erosionally discontinuous, southern feather-edge of the Morrison depositional basin in central New Mexico. This southern limit steps to the right about 90 km across the Rio Grande rift and supports the concept of Laramide dextral faulting along the eastern Colorado Plateau boundary (Cather, 1999).

Figure 31. View to the northwest from 338797E, 3790340N (zone 13, NAD 27), Mesa del Yeso quadrangle, showing brownish-gray, pebbly sandstone of the upper Chinle Formation (Trc, with hammer) overlain by light-gray sandstone and greenish-gray mudstone (mostly covered on slope above light-gray sandstone) of the Jurassic Morrison Formation (Jm). Golden-brown Dakota Sandstone (Kd) is on the skyline.

CRETACEOUS STRATA OF THE QUEBRADAS REGION

S.C. Hook and W.A. Cobban*
*deceased April 21, 2015

Introduction

The predominantly marine Upper Cretaceous strata of the Quebradas area were deposited during the first three of five major transgressive–regressive (T-R) cycles of the western shoreline of the Late Cretaceous Western Interior Seaway (WIS) across New Mexico (Fig. 32). These five cycles, defined by Molenaar (1983a), are designated T-1/R-1 through T-5/R-5, from oldest to youngest. The general positions of the western shoreline in New Mexico at maximum transgressions (T-1, T-2, and T-3) and maximum regressions (R-1, R-2, and R-3) are shown in Figure 32.

Positions of the shorelines in Figure 32 applicable to the Upper Cretaceous framework of the Quebradas area are based primarily on the geographic distribution of fossils from the following ammonite zones: SB ("Thatcher fauna," *Conlinoceras tarrantense* Zone), T-1 (*Euomphaloceras septemseriatum* Zone), R-1 (*Prionocyclus hyatti* Zone), T-2 (*Prionocyclus novimexicanus* Zone), and R-2 (*Cremnoceramus deformis erectus* Zone) (Fig. 33). The maximum inland position of the T-2 shoreline, which occurred during *P. quadratus* time, is estimated on the geographic distribution of *P. novimexicanus* because *P. quadratus* is uncommon in New Mexico (Fig. 33). Raw data for these distributions are in Hook and Cobban (1979), Cobban and Hook (1984), and Kennedy et al. (2001).

The approximate beginnings and ends of the initial three cycles are plotted in Figure 33 against (1) the stratigraphic framework for the study area, (2) middle Cenomanian through lower Coniacian faunal zones for New Mexico, and (3) radiometric age dates from these zones. (Bold age dates in Fig. 33 are from bentonites within a fossil zone [Cobban et al., 2006]; others are interpolated.)

Although the western shoreline of the Late Cretaceous WIS transgressed and regressed three times across the southern two-thirds of New Mexico during the middle Cenomanian through the early Coniacian (Fig. 32), it was in continuous transgression in central and northern Utah (Hook, 1983, fig. 2; Aubrey, 1991). The transgressions and regressions in the south led to a complex intertonguing of marine and continental deposits that created a stratigraphic framework of offshore shale, nearshore sandstone, and continental strata unique to New Mexico and Arizona (see Pike, 1947, fig. 7). Therefore, a stratigraphic nomenclature that applies only to this region was developed. Rock units unique to New Mexico and Arizona include the intertongued Dakota–Mancos succession (Landis et al., 1973; Hook et al., 1983; Hook and Cobban, 2015), a transgressive–regressive wedge called the Tres Hermanos Formation (Hook et al., 1983), the Pescado Tongue and D-Cross Tongue of the Mancos Shale (Pike, 1947; Dane et al., 1957), and the regressive Gallup Sandstone (Molenaar, 1974, 1983a). Great Plains rock units such as the Graneros Shale, Greenhorn Limestone, and Carlile Shale, which formed farther offshore from the influence of the western shoreline, generally cannot be lithologically differentiated in southern New Mexico. An exception to the exclusion of Great Plains stratigraphic units in southern New Mexico is the Bridge Creek Limestone, the uppermost member of the Greenhorn Limestone (Cobban and Scott, 1972).

The Bridge Creek Limestone Member is a succession of thin limestone beds separated by thicker beds of calcareous shale deposited during maximum transgression of the T-1 shoreline over a wide swath of the southern Western Interior region of the United States that includes New Mexico. According to Elder (1989, p. 300), limestones of this section "…appear to represent cyclic, near isochronal, basinwide changes in benthic oxygenation and substrate composition…" Elder (1989) correlated 11 marker limestones and four bentonites from the basal one-third of the Bridge Creek Limestone Member from its principal reference section near Pueblo, Colorado, as far south as Carthage, New Mexico, at the southern end of the Quebradas region. Thus, the Bridge Creek Limestone is the only Great Plains stratigraphic name used in this memoir, where it is a formal bed-rank unit in the Tokay Tongue of the Mancos Shale (Hook and Cobban, 2015).

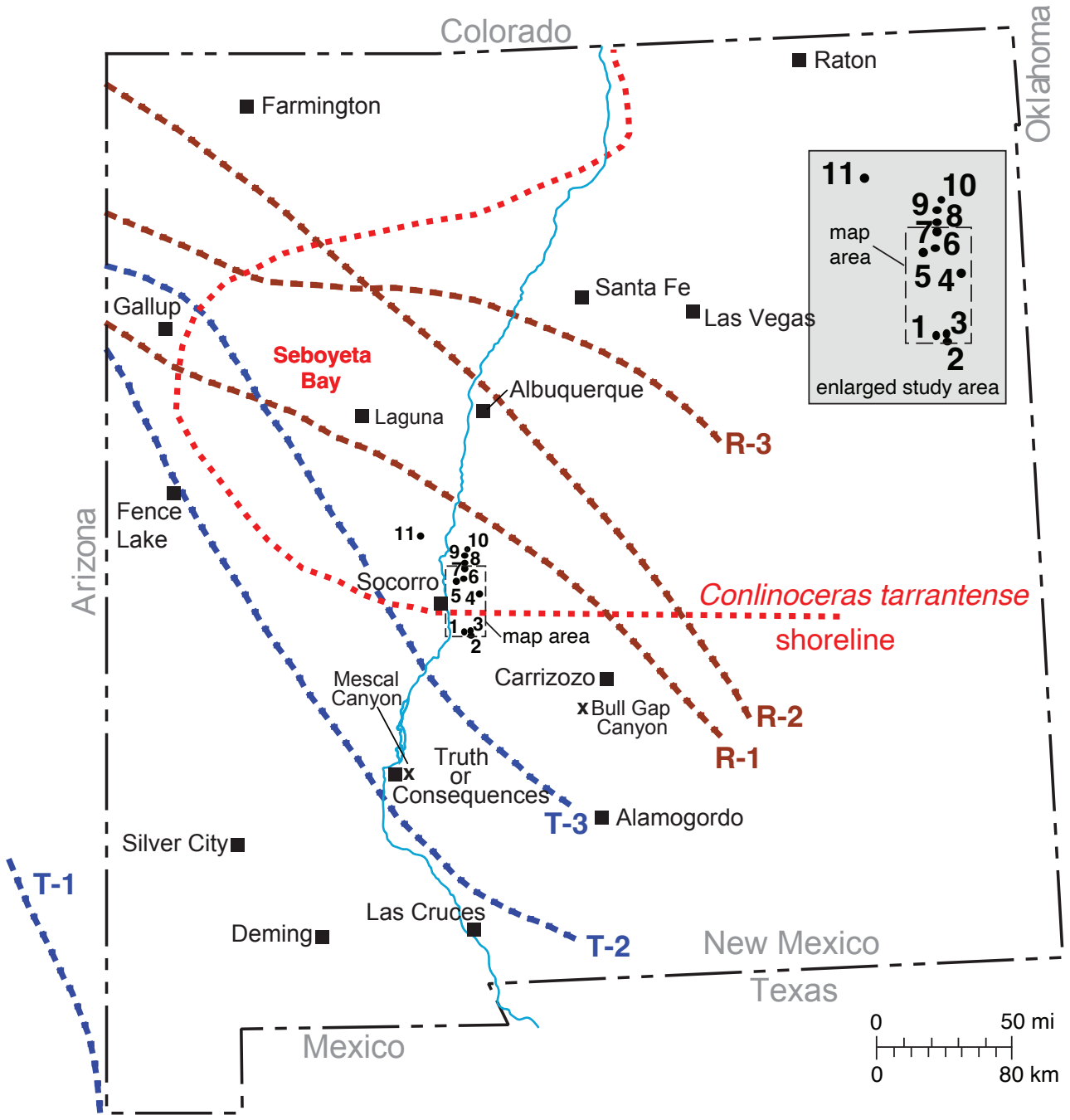

Figure 32. Map of New Mexico showing the locations of the 11 control points for Upper Cretaceous measured sections in the Quebradas area and approximate positions of the Late Cretaceous WIS shoreline at selected times. The dashed rectangle east of Socorro and in the inset is the map area. Approximate shoreline positions are shown for Seboyeta Bay (SB; red), which is the earliest shoreline that can be drawn, and the maximum landward (T-1, T-2, and T-3) positions (blue) and seaward (R-1, R-2, and R-3) positions (brown) of the western shoreline for the three earliest cycles of transgression–regression. Control points with UTM coordinates (zone 13, NAD 27) are (1) Carthage measured section—**CMS** (338281E, 3751223N), (2) Old Carthage section—**OCS** (340213E, 3749640N), (3) Carthage rift section—**CRS** (339042E, 3750833N), (4) Jornada del Muerto coal field section—**JdM** (347167E, 3775871N), (5) Old Stapleton Ranch section—**OSR** (334033E, 3782188N), (6) Mesa del Yeso section—**MdY** (338131E, 3783965N), (7) principal reference section—**PRS** (338702E, 3790369N), (8) Two Butte section—**TBS** (339239E, 3791943N), (9) Cibola Canyon section—**CCS** (338676E, 3797050N), (10) Palo Duro Canyon section—**PDCS** (339870E, 3799648N), and (11) Ladron Peak section—**LPS** (313478E, 3807242N).

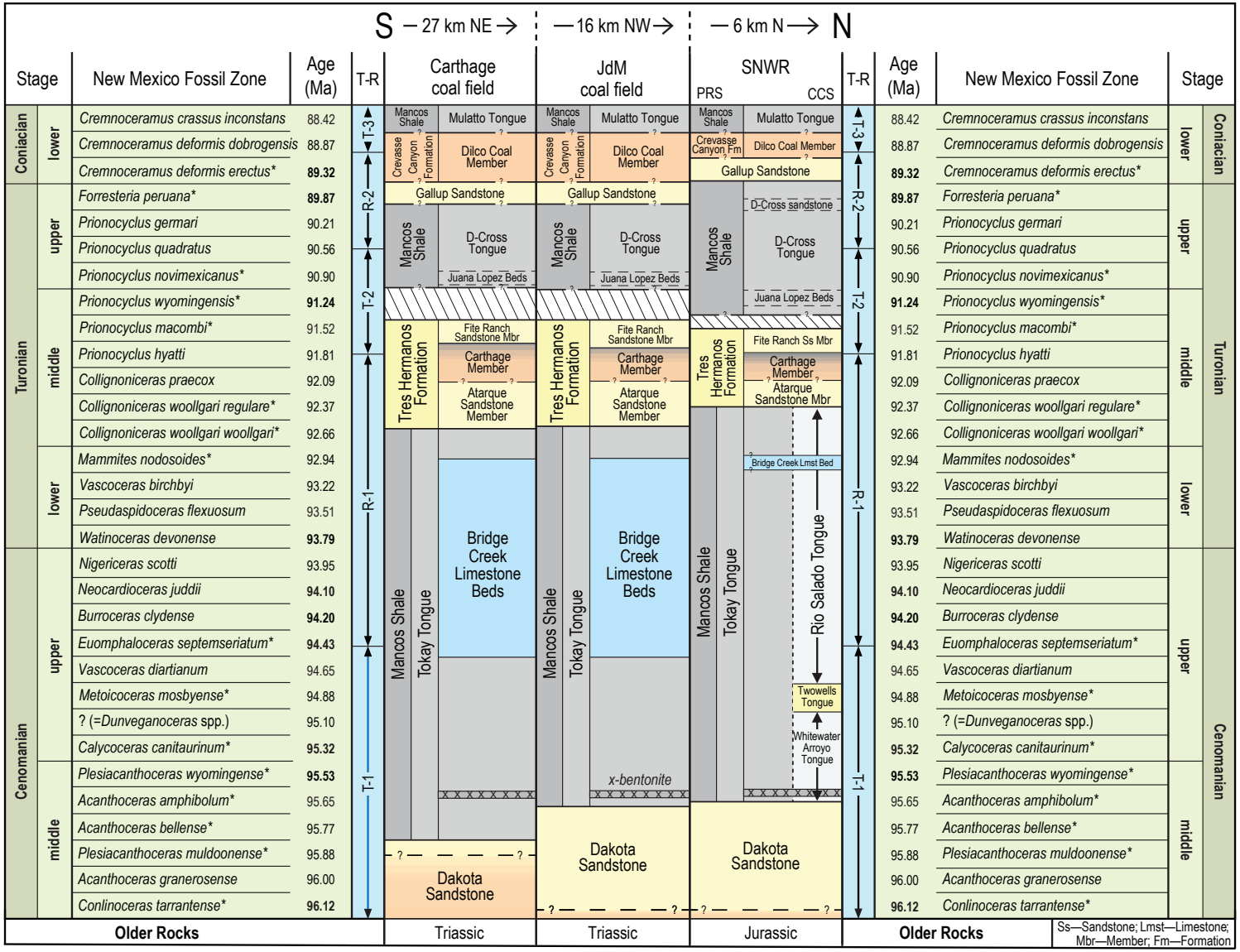

Figure 33. Correlation chart for the Upper Cretaceous strata of the Quebradas region. Stratigraphic units from the Carthage coal field, Jornada del Muerto (**JdM**) coal field, and Sevilleta National Wildlife Refuge (**SNWR**) are plotted against the standard New Mexico fossil zones for the middle Cenomanian through the lower Coniacian. Approximate beginning and ending points for the first three major transgressive–regressive cycles (**T-R**) of the western shoreline of the Late Cretaceous WIS are plotted against the standard zonation. Color code for the stratigraphic units: brown (nonmarine rocks), gray (marine shale), blue (marine limestone), and yellow (marine sandstone). An asterisk following a fossil name indicates that species was collected from the study area. A bold age date is based on a dated bentonite (Lynds and Slattery, 2017); all other age dates are interpolated. Other abbreviations: **PRS** = principal reference section, **CCS** = Cibola Canyon section.

Major stratigraphic names applied to the intertongued marine and continental rock record of these three cycles of deposition in the study area are, in ascending order, Dakota Sandstone (T-1), Tokay Tongue of the Mancos Shale (T-1/R-1), Tres Hermanos Formation (R-1/T-2), D-Cross Tongue of the Mancos Shale (T-2/R-2), Gallup Sandstone (R-2), Dilco Coal Member of the Crevasse Canyon Formation (R-2/T-3), Mulatto Tongue of the Mancos Shale (T-3/R-3), and Gibson Coal Member of the Crevasse Canyon Formation (R-3/?). About 6 km north of the mapped area, the thick Tokay Tongue of the Mancos Shale is divided into two thinner, formally named tongues of Mancos Shale by a marine sandstone, the Twowells Tongue of the Dakota Sandstone (T-1). These two thinner tongues of Mancos Shale are the Whitewater Arroyo Tongue (T-1) below the Twowells and the Rio Salado Tongue (T-1/R-1) above (Fig. 33). The last three stratigraphic names—Whitewater Arroyo, Twowells, and Rio Salado—are not used on the geologic map accompanying this memoir (Plate 1) because the Twowells Tongue is not present in the map area.

The initial three cycles of transgression and regression of the Late Cretaceous WIS across New Mexico created a set of time-transgressive, fossiliferous shoreline units that are well developed in the Quebradas area. These geographically isolated, fossiliferous outcrops allow detailed correlation with other areas in New Mexico. During the Late Cretaceous, New Mexico was at the transition between colder-water boreal faunas to the north and warmer-water Tethyan faunas to the south. This paleogeography created the ideal setting for mingling of faunas that allows for international correlation of faunas indigenous to the Western Interior. Three of the nominative ammonite species in Figure 33 were originally described from Tethyan faunas in Europe.

The authors have published more than 20 papers that deal with the stratigraphy and paleontology of the Quebradas area and have made more than 270 fossil collections from the area that are tied to detailed measured sections. The discussion that follows is a synthesis of more than 50 years of analyzing the Upper Cretaceous of this strategically important area. New and previously unpublished research is included.

Lucas et al. (2019), working on the Cretaceous strata to the south of the Quebradas area near Truth or Consequences (Fig. 32), proposed abandoning several well-established stratigraphic names used in this memoir and replacing them with either new names or those in use to the north. The authors object to their proposed changes and continue to use the regionally established stratigraphic names. Formal names used in this memoir conform to the North American Stratigraphic Code.

Stratigraphic names Lucas et al. (2019) abandoned affecting the Quebradas area are Tokay Tongue of the Mancos Shale, Bridge Creek Limestone Beds of the Tokay Tongue, and Carthage Member of the Tres Hermanos Formation. Lucas et al. (2019) replaced Tokay Tongue of the Mancos Shale with Graneros, Greenhorn, and Carlile Members. Objections to these changes are discussed in the appropriate sections below.

Transgressive–Regressive Cycles

The best-constrained of the three T-R cycles in the Quebradas area on both faunal and lithologic evidence is the first. The initial transgression, T-1, started during the time represented by the middle Cenomanian *Conlinoceras tarrantense* Zone, when strata that became the upper part of the Dakota Sandstone were deposited in the area of the Sevilleta National Wildlife Refuge (Fig. 33). T-1 ended during the time represented by the upper Cenomanian *Euomphaloceras septemseriatum* Zone, when the thin limy beds at the base of the Bridge Creek Limestone Beds of the Tokay Tongue of the Mancos Shale were deposited. The initial regression, R-1, lasted until the middle of the *Prionocyclus hyatti* Zone (Hook and Cobban, 2011a), when the middle part of the Carthage Member of the Tres Hermanos Formation was deposited. The second transgression, T-2, ended near the middle of the *Prionocyclus quadratus* Zone, about the time the middle part of the D-Cross Tongue of the Mancos Shale was deposited. R-2 ended during the middle of the *Cremnoceramus deformis* Zone, when the middle part of the Dilco Coal Member of the Crevasse Canyon Formation was deposited. The end of T-3 and beginning of R-3 are unconstrained in the study area (Fig. 33).

Peterson and Kirk (1977) previously recognized nine T-R cycles in the southern Colorado Plateau area; all their cycles are included in Molenaar's (1983a) five major cycles. Their first four cycles are included in T-1/R-1, their fifth cycle is equivalent to T-2/R-2, and their sixth cycle is the same as T-3/R-3 (Molenaar, 1983a, p. 212).

Other workers in the Western Interior referred to these T-R cycles as cyclothems (e.g., Hattin, 1962; Kauffman, 1969; Kirkland, 1996). The T-R cycles recognized in New Mexico, and the timing of their maxima, only correspond in part with cyclothems recognized elsewhere in the Western Interior because of differences in tectonic patterns in major source areas (Molenaar, 1983a). For example, the Gallup regression (R-2) is unique to New Mexico and northeastern Arizona (Molenaar 1983a, p. 212).

Two small-scale shoreline maps reflect the variation in T-R cycles within the Western Interior (Hook and Cobban, 1981, fig. 2; Hook, 1983, fig. 2). These maps show that while the early Coniacian shoreline was retreating seaward (regressing) in New Mexico, it was advancing landward (transgressing) elsewhere in the Western Interior. Both maps are based on the geographic distribution of index fossils.

A map of the entire Western Interior of the United States depicts the geographic distribution of the late Turonian–early Coniacian oyster "*Lopha*" *sannionis,* whose geologic range closely coincides with the time of deposition of the Gallup Sandstone in New Mexico (Hook and Cobban, 1981, fig. 2). The early Coniacian shoreline was situated seaward of the late Turonian shoreline in New Mexico but landward of it north of northeastern Arizona.

The map of parts of the Four Corners states shows the positions of five shorelines, labeled from oldest (#1) to youngest (#5; Hook, 1983, fig. 2). These five numbered shorelines closely coincide with the shorelines labeled SB, T-1, R-1, T-2, and R-2 in Figure 32. Shoreline #5 (= R-2), the youngest, is seaward of shoreline #4 (= T-2) in New Mexico but landward of it in southern Utah. In central Utah, however, the five shorelines are part of a single transgression (i.e., each younger shoreline is landward of an older shoreline). Index species and geographic control points used to estimate positions of the shorelines are in Hook and Cobban (1981, fig. 2) and Cobban and Hook (1984, figs. 1, 4, and 6).

The Late Cretaceous WIS entered New Mexico from the east in the earliest middle Cenomanian during the *Conlinoceras tarrantense* Zone. By the end of *C. tarrantense* time, an embayment called **Seboyeta Bay** covered most of the northern half of the state and extended almost to Gallup on the west (Fig. 32; Hook and Cobban, 2015, fig. 1A). Seboyeta Bay was defined by the geographic distribution of the middle Cenomanian Thatcher fauna in New Mexico (Hook et al., 1980). This fauna is characteristic of the Thatcher Limestone Member of the Graneros Shale in the Pueblo, Colorado, area (Cobban and Scott, 1972). It attains its greatest diversity in the Western Interior in west-central New Mexico, where it is preserved in the Oak Canyon and Cubero Members of the Dakota Sandstone. There, it includes 34 species of bivalves, 11 species of gastropods, and 5 species of ammonites (Cobban, 1977a, 1977b). *Conlinoceras tarrantense*, the most common of the Thatcher ammonites (Cobban and Hook, 1984, p. 260), gives its name to the lowest middle Cenomanian zone (Fig. 33).

Strata deposited in Seboyeta Bay during the time represented by the *C. tarrantense* Zone occupy an area of northern New Mexico roughly centered on Laguna that extends 338 km from east to west and 237 km from north to south (Fig. 32, SB shoreline). Subsequent shorelines in Figure 32 indicate the bay did not persist after the culmination of T-1. At the end of T-1 in the late Cenomanian, all of New Mexico was covered by seawater, and the shoreline was located in eastern Arizona to the west (Hook and Cobban, 2015, fig. 1B) and somewhere in Mexico to the south (Fig. 32, T-1 shoreline).

By the latest Cenomanian, when the regressing western shoreline reentered southwestern New Mexico during R-1, it had assumed its characteristic NW–SE trend across the state (Hook and Cobban, 2015, fig. 1E). Thereafter, it transgressed to the southwest and regressed to the northeast. At the end of R-1 in the middle Turonian, the shoreline was midway between Socorro and Albuquerque (Fig. 32, shoreline R-1). Each successive transgression progressed less far to the southwest than the previous, and each regression reached farther northeast than the previous—until the western shoreline eventually retreated from New Mexico and, ultimately, the North American continent in the Maastrichtian. The result of the three major (and some minor) cycles of shoreline translation across the study area is a complex record of intertongued marine and continental rock (Fig. 33). The causes of shoreline migrations recorded in the intertongued marine and nonmarine rocks in Quebradas are, however, beyond the scope of this paper.

Marine deposition in the study area began in the earliest middle Cenomanian about 96.1 Ma during T-1 and probably ended in the latest early Coniacian around 88 Ma during R-3, resulting in a stratigraphic record spanning approximately 8.1 Myr. The amount of time represented by each of the first four of these depositional half-cycles in New Mexico can be estimated from Figure 33 by assuming (1) each radiometrically dated bentonite, shown in bold in the "Age" column, is at the base of its zone; (2) zones that occur between dated bentonites are of equal duration (i.e., the interpolated, nonbold dates); and (3) half-cycles terminate at the midpoint of the zone. These assumptions are generally not true or cannot be tested, but provide a consistent way to make gross estimates for shoreline movements and compacted sedimentation rates. Using these assumptions, the initial transgression, T-1, lasted about 1.81 Myr (including the time it took to form Seboyeta Bay); the first regression, R-1, lasted about 2.65 Myr; the second transgression, T-2, lasted about 1.28 Myr; and the second regression, R-2, lasted about 2.41 Myr (Table 2).

Rates of Transgression, Regression, and Sedimentation

The formation of Seboyeta Bay appears to have occurred rapidly during the time represented by the entire *Conlinoceras tarrantense* Zone, about 0.12 Myr (Table 2, Fig. 33). Using the east–west dimension of the embayment (338 km) results in a maximum transgression rate of 2,817 km/Myr, or around 2.82 m/yr. After the formation of Seboyeta Bay, rates of shoreline movement decreased to <20 cm/yr. Note that in calculating T-0, the initial rate of transgression of the bay, two key variables are not known: (1) the position of the shoreline to the east before the formation of the bay and (2) the time the bay began to form. Although the lowest dated bentonite in Figure 33 is in the *C. tarrantense* Zone, there are at least 7 m of unfossiliferous marine strata below the first occurrence of the Thatcher fauna at the type section of the Oak Canyon Tongue of the Dakota Sandstone near Laguna (Landis et al., 1973). These strata may be older than the *C. tarrantense* Zone.

Hook and Cobban (2007, p. 91) estimated the expansion rate of Seboyeta Bay to the south from the end of *Conlinoceras tarrantense* time to the end of *Acanthoceras amphibolum* time to be 194 km/Myr, or less than 20 cm of net transgression per year (Fig. 33). Estimates based on the approximate positions of the shoreline at the ends of T-1, R-1, T-2, and R-2, with distances measured on a NE–SW line passing through the center of the mapped area, yield similar rates that range from 189 km/Myr for T-1 to 83 km/Myr for R-2 (Table 2, Fig. 32). Absolute values of these estimated rates are not as important as their relations because of assumptions used in calculating the duration of ammonite zones and uncertainty in locating shoreline positions. The paucity of Upper Cretaceous outcrops in the southern part of the state probably provides the greatest uncertainty. Hook and Cobban (2007) used radiometric dates from Cobban et al. (2006); the radiometric dates in Table 2 and Figure 33 are from Lynds and Slattery (2017).

Table 2. Approximate rates of Late Cretaceous shoreline movements across New Mexico, beginning with the initial entry (T-0) of marine water and ending with the third regression (R-3). Approximate compacted sedimentation rates during the same depositional half-cycles are based on rock thicknesses from the Carthage coal field.

From	To	Start (Ma)	End (Ma)	Dur (Myr)	D (km)	T-R (km/Myr)	T-R (m/yr)	ThCar (m)	Sed (m/Myr)	Sed (cm/yr)
T-0	SB	96.12	96.00	0.12	338	2,817	2.82	---	---	---
SB	T-1	96.00	94.31	1.69	319	189	0.19	96	57	0.0057
T-1	R-1	94.31	91.66	2.65	375	142	0.14	144	54	0.0054
R-1	T-2	91.66	90.38	1.28	154	120	0.12	85	66	0.0066
T-2	R-2	90.38	87.97	2.41	201	83	0.08	80	33	0.0033
R-2	T-3	87.97	---	---	138	---	---	33	---	---
T-3	R-3	---	---	---	217	---	---	---	---	---

See Figure 32 for the geographic positions of the shoreline at the end of each half-cycle and Figure 33 for the radiometric dates and rock units used in these calculations. T-0 represents the starting time for the initial shoreline's incursion into New Mexico at the beginning of *Conlinoceras tarrantense* time until the formation of Seboyeta Bay (SB) at the end of *C. tarrantense* time. Abbreviations: Dur = duration, D = distance, T-R = transgression-regression, ThCar = thickness of strata at Carthage, and Sed = compacted sedimentation rate. Radiometric dates are from Lynds and Slattery (2017).

After the formation of Seboyeta Bay, shoreline movements were much slower and ranged from 189 km/Myr for T-1 to 83 km/Myr for R-2. Shoreline movement was greater during T-1 (189 km/Myr) and R-1(142 km/Myr) than during T-2 (120 km/Myr) and R-2 (83 km/Myr). The landward advances (transgressions) in each full cycle were faster than the seaward retreats (regressions) for both full cycles recorded in the study area.

Using the thickness of strata at Carthage as a proxy for the compacted sediment thickness for each half-cycle, compacted sedimentation rates ranged from 33 m/Myr for R-2 to 66 m/Myr for T-2. The R-2 regression, also called the Gallup regression by Molenaar (1983a), is unique to New Mexico and eastern Arizona. If the uncompacted sedimentation rates are an order of magnitude greater than the compacted rates, the rates are still low, less than 0.066 cm/yr. These long-term averages, however, are similar to those obtained by Hook and Cobban (2015) for shorter-term, bed-rank averages for the Tokay Tongue of the Mancos Shale at Carthage and by Cather (2003, p. 121) for the Mancos Shale, Point Lookout Sandstone, and Menefee Formation in the San Juan Basin.

These low sedimentation rates suggest that deposition during the Late Cretaceous in the Quebradas area was episodic. For example, volcanic ash beds, which accumulated instantaneously in a geologic sense, are common in the Mancos Shale in the Quebradas area. Hook and Cobban (2015) measured 77 bentonites in the Tokay Tongue of the Mancos Shale at Carthage. Thirteen of the 77 bentonites are at least 10 cm thick, and two are 30 cm or thicker. The x-bentonite, at 30.5 cm thick, would represent 6,100 years of deposition if it accumulated at the compacted sedimentation rate and 610 years at the uncompacted sedimentation rate. The 64 bentonites in the Tokay Tongue at Carthage below the Bridge Creek Limestone Beds, with a cumulative thickness of 3.6 m, would represent 72,000 years of deposition if the average compacted rate of 0.005 cm/yr applied to volcanic ash beds and 7,200 years if the uncompacted rate applied. To compensate for the instantaneously rapid sedimentation rates during bentonite deposition, extremely low sedimentation rates, along with nondepositional and erosional intervals, must be present elsewhere in the section as well.

Stratigraphy and Biostratigraphy

The predominantly marine rocks from the base of the Dakota Sandstone to the top of the Mulatto Tongue of the Mancos Shale are up to 433 m thick in the study area. A substantial but unmeasured thickness of continental rock above the Mulatto Tongue is present at the southern end of the study area in the Carthage coal field. There, Gardner (1910, p. 455) estimated 183 m of tan sandstone and drab shale with traces of coal above the uppermost fossil-bearing rock in the Mulatto. These units are now assigned to the upper part of the Crevasse Canyon Formation. Commercial quantities of coal were mined from a 1.5-m-thick seam of bituminous coal near the base of the Crevasse Canyon Formation in the Carthage and Jornada del Muerto coal fields during the late 1800s and early 1900s (Chapter 7).

The middle Cenomanian through the lower Coniacian in New Mexico has been divided into 30 fossil zones (Fig. 33). Ammonites are used for the lower 27 zones and inoceramids for the upper three. The words “ammonite” and “inoceramid” are used as both nouns and adjectives in this report.

Biostratigraphically significant marine fossils are preserved throughout the study area from the top of the Dakota Sandstone into the Mulatto Tongue of the Mancos Shale. The zonal index species marked with asterisks in Figure 33 were collected in the area. These zonal indices (also called nominative species elsewhere in this chapter) and an oyster restricted to the early Coniacian indicate that the marine section ranges in age from earliest middle Cenomanian to latest early Coniacian, a span of around 8.1 Myr. The abundance of fossils in the isolated exposures of the Upper Cretaceous of the Quebradas area makes it an important area for correlation to the better-studied and more continuous outcrops to the north and northwest, especially in the San Juan Basin.

Lower and upper contacts of most of the major stratigraphic units are at least slightly diachronous across the study area because of the paleoshoreline movements. The oldest invertebrate fossils are present near the top of the Dakota Sandstone on Sevilleta National Wildlife Refuge (SNWR) and in the Jornada del Muerto (JdM) coal field. The youngest invertebrate fossils are preserved in the Mulatto Tongue at Carthage and on SNWR and JdM. Fourteen of the nominative species of this zonal

scheme have been collected within the mapped area or, in the case of *Metoicoceras mosbyense*, 6 km north (Fig. 32).

A small-scale graphic section (stratigraphic column) extending from the Dakota Sandstone through the Mulatto Tongue is presented for each of the three areas discussed in this chapter. From south to north, these areas are the Carthage coal field, Jornada del Muerto coal field (JdM), and Sevilleta National Wildlife Refuge (SNWR). In addition, at least one larger-scale graphic section of an important or unique section of the column for each area is presented. Many of the primary lithostratigraphic units (e.g., the Tres Hermanos Formation) are similar among areas and are only described in detail in the section on the Carthage coal field. Secondary lithostratigraphic units (e.g., the Juana Lopez Beds of the D-Cross Tongue of the Mancos Shale) vary in age and thickness and are discussed as encountered. The middle Cenomanian ammonite succession on SNWR, which is one of the most complete in the Western Interior, is discussed in detail. Two unconformities on SNWR, both marked by phosphatic nodules or pebbles, are also discussed in detail. For the history of the stratigraphic nomenclature of the Upper Cretaceous section and correlations used in Socorro County from 1900 to 1984, refer to summary articles by Hook (1983, 1984).

Carthage Coal Field

Upper Cretaceous rocks of the Carthage coal field are the best exposed, most easily accessed, most fossiliferous, and most studied in the study area. These rocks crop out in the Cañon Agua Buena, San Antonio, and Cerro de la Campana 7.5-minute quadrangles. The Carthage coal field has been used as a natural laboratory by the students, faculty, and staff of the New Mexico Institute of Mining and Technology, in Socorro, almost since its founding in 1889. Commercial quantities of coal at Carthage made understanding its complexly faulted geology an economic necessity (Gardner, 1910). Lee (1916), Rankin (1944), Pike (1947), and Molenaar (1974, 1983a), among others, recognized the importance of the isolated exposure at Carthage in understanding the Upper Cretaceous geology of the southern Western Interior. Of earlier workers in the study area, only Gardner (1910), working in the Carthage coal field, and Darton (1928), working on SNWR, recognized the marine units now assigned to the Mulatto Tongue of the Mancos Shale. Before the detailed mapping of the Mesa del Yeso, Bustos Well, Cañon Agua Buena, and San Antonio 7.5-minute quadrangles for this memoir, strata deposited during this third cycle of transgression–regression (T-3/R-3) had been overlooked (e.g., Hook et al., 1983). A detailed discussion of this omission in the geologic literature can be found in Hook (2010).

In addition, the Carthage coal field contains the type sections of the Tokay Tongue of the Mancos Shale (Hook and Cobban, 2015) and the Carthage and Fite Ranch Sandstone Members of the Tres Hermanos Formation (Hook et al., 1983). These member-rank units are recognized over a wide swath of west-central and southwestern New Mexico (see Hook et al. [1983, chart 1] and Hook and Cobban [2015, fig. 1]). Carthage was also designated as the principal reference section for the Tres Hermanos Formation by Hook et al. (1983).

Hook (2009, p. 25) reported that the Tokay Tongue of the Mancos Shale at Carthage contains more discrete ash beds of middle to late Cenomanian age than any other published section in the Western Interior, thus providing a potential means for detailed correlation among widespread sections. The Tokay Tongue at both Carthage and JdM contains the Cenomanian–Turonian boundary limestone, which can be correlated to its global boundary stratotype at Pueblo, Colorado (Kennedy et al., 2000, 2005).

The Upper Cretaceous succession at Carthage is fossiliferous from near the base of the Tokay Tongue to the middle of the Mulatto Tongue, and ranges in age from late middle Cenomanian to latest early Coniacian (Fig. 33). There are 154 distinct USGS Mesozoic invertebrate fossil localities (Denver, Colorado) from the Carthage coal field. Denver locality numbers are preceded by the letter D. The earliest numbered USGS collection (Washington, D.C.) from Carthage was made in 1905 by Willis Lee (Kauffman, 1965, p. 76). (Washington locality numbers are preceded by the letter W in this chapter.) Hyatt (1903) named the ammonite *Coilopoceras colleti* from specimens in his personal collection from Carthage.

Cretaceous rocks from the Carthage coal field are assigned to the following major stratigraphic units, in ascending order: Dakota Sandstone, Tokay Tongue of the Mancos Shale, Tres Hermanos

Formation, D-Cross Tongue of the Mancos Shale, Gallup Sandstone, Dilco Coal Member of the Crevasse Canyon Formation, Mulatto Tongue of the Mancos Shale, and Gibson Coal Member of the Crevasse Canyon Formation. All units, with the exception of the Gibson Coal Member, which was not measured for this study, are discussed in detail in the sections below.

The **Dakota Sandstone** is 24 m thick at the Carthage measured section (CMS; Fig. 32, control point #1) and consists of resistant, dark-brown-weathering, ridge-forming quartzite (Figs. 34A and 35). The upper 5 cm of the Dakota are burrowed and of marine origin; the remainder is mostly shorezone and fluvial deposits. The Dakota rests with pronounced unconformity on the Triassic Chinle Formation and locally on the Jurassic Morrison Formation. Its upper contact is conformable with the overlying Tokay Tongue of the Mancos Shale. No body fossils have been reported from the Dakota at Carthage. The upper, marine part of the Dakota was deposited in the middle Cenomanian during the early part of T-1 (Fig. 34A).

The **Tokay Tongue of the Mancos Shale** was named by Hook and Cobban (2015) for exposures in the Carthage coal field about 2 km north of the ruins of the ghost town of Tokay. Hook and Cobban (2015, p. 27) defined it as "that portion of the Mancos Shale lying between the undifferentiated or main body of the Dakota Sandstone and the Tres Hermanos Formation (or offshore equivalent)." At its type section in the Carthage coal field, the Tokay Tongue of the Mancos Shale is 175 m thick and ranges in age from middle Cenomanian to middle Turonian (Fig. 34A). It consists of five bed-rank lithologic units, in ascending order: (1) shale and sandstone beds, 55 m thick; (2) calcareous shale and bentonite beds, 36 m thick, containing 40 discrete bentonites; (3) the Bridge Creek Limestone Beds, 22 m thick; (4) calcareous shale beds, 34 m thick; and (5) noncalcareous shale beds, 27 m thick. Only the Bridge Creek Limestone Beds is a formally named stratigraphic unit; the other four are used informally and denoted with lowercase letters. The overall pattern of lithologies within the Tokay Tongue is of noncalcareous shale that gradually becomes more calcareous upsection until limestone appears near the middle of the tongue, followed by calcareous shale that becomes successively less calcareous upsection, succeeded by noncalcareous shale. Thus, noncalcareous and calcareous shale units are arranged symmetrically about the limestone beds. Calcareous shale represents deeper-water deposition farther from the shoreline. Noncalcareous shale represents shallower-water deposition closer to shore, where there was a greater influx of fresh water. The Tokay Tongue was deposited during T-1 from the middle through the late Cenomanian and during the first two-thirds of R-1 into the middle Turonian (Fig. 33).

The lower contact of the Tokay Tongue is sharp and conformable with the Dakota Sandstone (Fig. 35, inset); the upper 5 cm of the Dakota are burrowed above a chert-pebble conglomerate, which could indicate an intraformational unconformity within the Dakota or simply a transgressive lag associated with the initial transgression. Mack et al. (2016, p. 794) interpreted it as a transgressive lag, representing "…a non-Waltherian, landward shift in lithofacies, in that lower offshore shale overlies either fluvial or paralic lithofacies." The upper contact of the Tokay Tongue is fairly abrupt but conformable with the overlying Atarque Sandstone Member of the Tres Hermanos Formation.

Ash beds (bentonites) are abundant in the lower two-thirds of the Tokay Tongue at Carthage (Figs. 34A and 36). The 77 ash beds measured in the Tokay Tongue are unevenly distributed through the five bed-rank units of the tongue. There are 24 bentonites in the shale and sandstone beds, 40 in the calcareous shale and bentonite beds (Fig. 36), 10 in the Bridge Creek, 3 in the calcareous shale beds, and none in the uppermost noncalcareous shale beds.

These 77 bentonites range in thickness from 0.6 to 35.6 cm; most are white but weather orange. Based on thickness, stratigraphic position, and underlying fauna, a 30.5-cm-thick bentonite, 12.2 m above the Dakota Sandstone, is correlated with the widespread x-bentonite (Fig. 34A). The x-bentonite is present throughout the Western Interior and is always in the *Acanthoceras amphibolum* Zone (Cobban and Scott, 1972). Elder (1988) used four bentonites above or just below the base of the Bridge Creek Limestone Beds to make high-precision correlations between the Carthage coal field and sections elsewhere in the Western Interior. The thickest ash bed in the Tokay Tongue is a 36-cm-thick, white-weathering bentonite within the upper one-third of the calcareous shale and bentonite beds, 11 m below the base of the Bridge

Creek Limestone Beds (Fig. 36, CS-143). This bed shows up well on satellite images of the coal field as a white band offset by small-displacement, north–south trending normal faults.

The lower four bed-rank units of the Tokay Tongue (i.e., those with observed bentonites) record one ash fall approximately every 47 kyr. The lower two bed-rank units have frequencies of 28 and 20 kyr/ash fall, respectively, indicating that the middle to earliest late Cenomanian was a time of increased volcanic activity in the southern Western Interior. In the overlying Bridge Creek Limestone Beds and calcareous shale beds, the average frequency of eruptions decreased to one eruption every 198 kyr and 57 kyr, respectively (Hook and Cobban, 2015). There are no ash beds recorded in the noncalcareous shale beds, the uppermost unit of the tongue.

There are more bentonites of middle to late Cenomanian age in the Tokay Tongue at Carthage than in temporal equivalents to the north. There are 62 bentonite beds in the Tokay Tongue at Carthage from the x-bentonite to the base of the Turonian Stage (Fig. 34A, D10128 level to D14702 level). In contrast, the well-exposed and well-documented principal reference section of the Greenhorn Limestone at Rock Canyon anticline near Pueblo, Colorado, contains only 27 bentonite beds in the same stratigraphic interval from the x-bentonite to the base of the Turonian Stage (Cobban and Scott, 1972).

Fossils from the Tokay Tongue in the Carthage coal field range in age from late middle Cenomanian to earliest middle Turonian, spanning the approximately 3.46 Myr from 95.15 Ma to 91.69 Ma (Fig. 33). The nominative species for 6 of the first 19 standard Upper Cretaceous fossil zones for New Mexico have been collected from the Tokay Tongue at Carthage; an asterisk follows the name of each of these species in Figure 33. Included are three ammonites from the shale and sandstone beds, two from the Bridge Creek Limestone Beds, and one from the calcareous shale beds. The calcareous shale and bentonite beds and noncalcareous shale beds are unfossiliferous, at least at the macrofossil level.

The lowest collection from 2.4 m above the base of the shale and sandstone beds includes *Acanthoceras bellense* Adkins, *Inoceramus arvanus* Stephenson, and *Ostrea beloiti* Logan, all indicative of the middle Cenomanian *Acanthoceras bellense* Zone (Fig. 34A, D14726 level). All fossil collections utilized in this study are assigned USGS Mesozoic locality numbers that begin with the prefix "D" for Denver and were housed at the Federal Center in Denver, Colorado, but now have been transferred to the Smithsonian Institution, Washington, D.C. The highest collection in the Tokay Tongue, at the contact between the calcareous and noncalcareous shale beds, consists of only the bivalve *Mytiloides subhercynicus* (Seitz), indicative of the middle Turonian *Collignoniceras woollgari woollgari* Subzone (Fig. 34A, D10129 level). *Collignoniceras woollgari woollgari* is also present below this collection in the calcareous shale beds (Fig. 34A, D14708 level) and above it in the base of the Atarque Sandstone Member of the Tres Hermanos Formation (Fig. 34A, D10241 level). A description of each of the five bed-rank units of the Tokay Tongue follows.

The **shale and sandstone beds**, the lowest bed-rank unit in the Tokay Tongue, consist of 55 m of interbedded shale, siltstone, bentonite, and sandstone. The base of the unit is a 64-cm-thick, dark-gray, noncalcareous shale that lies on the Dakota dipslope (Fig. 35, inset). Shale beds become progressively more calcareous upsection, reflecting the increasing distance between Carthage and the advancing T-1 shoreline to the southwest. Its upper contact is an 8-cm-thick, tan-weathering, very fine-grained sandstone that creates an impressive dipslope (Fig. 34A, D14757 level). There are at least 24 ash beds in the unit, including the 30.5-cm-thick x-bentonite.

This basal bed-rank unit is fossiliferous from bottom to top (Fig. 34A), but contains low-diversity faunas. Despite this low diversity, the rare ammonite *Metengonoceras acutum* Hyatt? was collected just below the middle of the unit (Fig. 34A, D5777 level). Engonoceratids like *M. acutum* have a typically Tethyan distribution; before the discovery of *M. acutum*? at Carthage, they were known from only a few localities in the Western Interior (Cobban and Kennedy, 1989).

The lowest fossils (Fig. 34A, D14726 level) from the unit come from a 2.1-m-thick, thin-bedded, fine-grained sandstone that is 64 cm above the base of the tongue. Fossils collected from this ledge-forming sandstone include the ammonite *Acanthoceras bellense* Adkins, the clam *Inoceramus arvanus* Stephenson, and the oyster *Ostrea beloiti* Logan. Together, this fauna represents the middle Cenomanian *Acanthoceras bellense* Zone (Fig. 33).

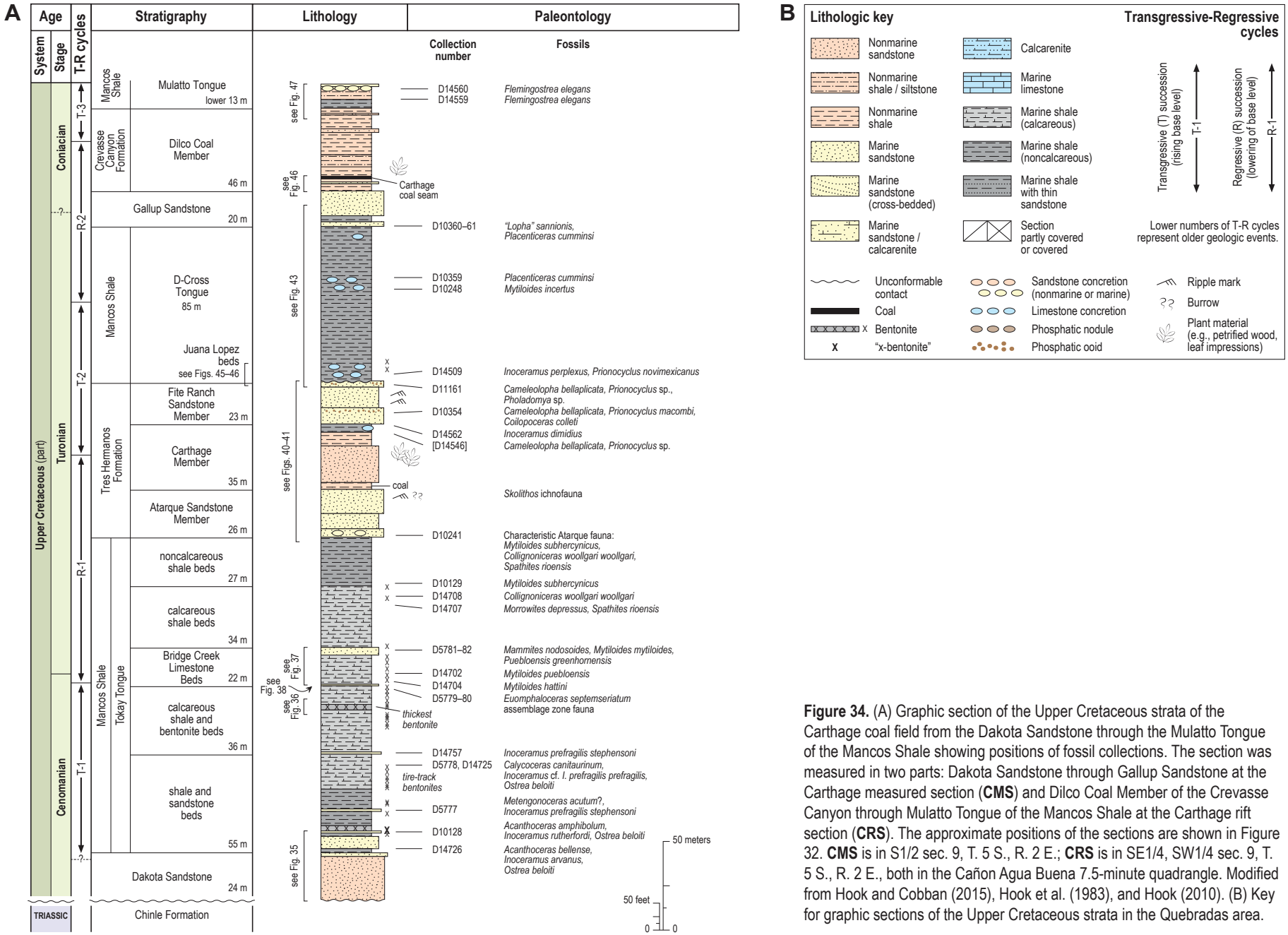

Figure 34. (A) Graphic section of the Upper Cretaceous strata of the Carthage coal field from the Dakota Sandstone through the Mulatto Tongue of the Mancos Shale showing positions of fossil collections. The section was measured in two parts: Dakota Sandstone through Gallup Sandstone at the Carthage measured section (**CMS**) and Dilco Coal Member of the Crevasse Canyon through Mulatto Tongue of the Mancos Shale at the Carthage rift section (**CRS**). The approximate positions of the sections are shown in Figure 32. **CMS** is in S1/2 sec. 9, T. 5 S., R. 2 E.; **CRS** is in SE1/4, SW1/4 sec. 9, T. 5 S., R. 2 E., both in the Cañon Agua Buena 7.5-minute quadrangle. Modified from Hook and Cobban (2015), Hook et al. (1983), and Hook (2010). (B) Key for graphic sections of the Upper Cretaceous strata in the Quebradas area.

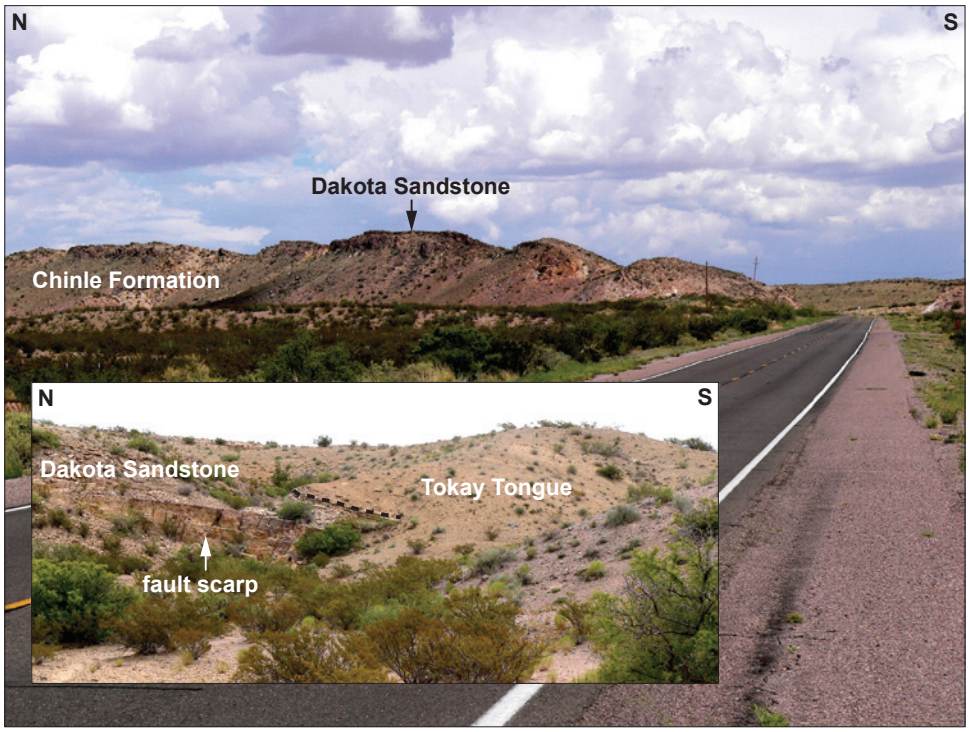

Figure 35. Hogback of south-dipping Dakota Sandstone on the west side of the Carthage coal field. View is to the east from the intersection of U.S. Route 380 and Fite Ranch Road. Outcrops of Dakota in the Carthage coal field are the best in the Quebradas area. The contact of the Dakota with the underlying Triassic Chinle Formation is sharp and disconformable; the contact with the overlying Tokay Tongue of the Mancos Shale is sharp and conformable (inset). Inset photograph is to the east from the Fite Ranch Road at a cross-sectional view of the Dakota-Mancos contact along a north-striking normal fault with the east side up.

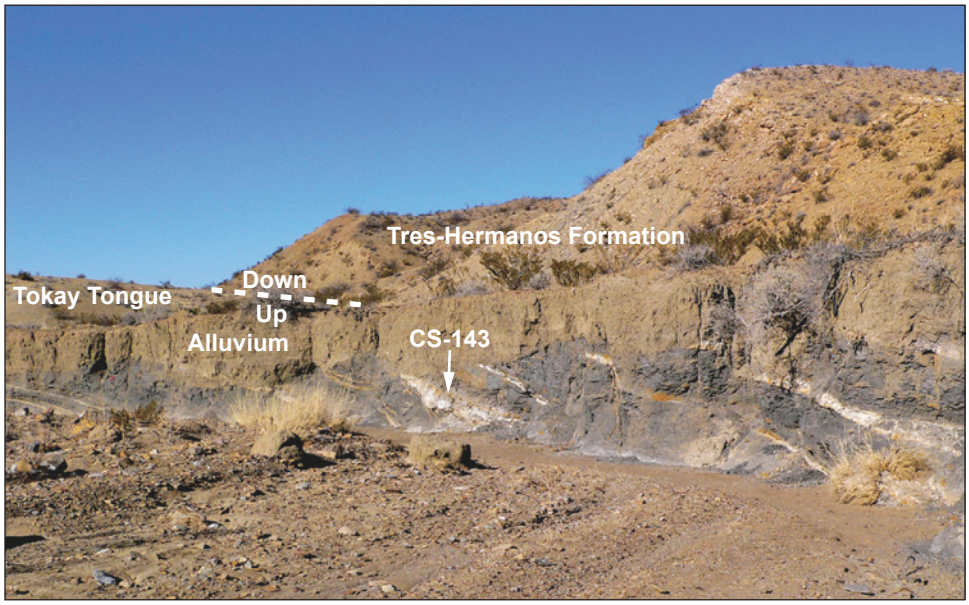

Figure 36. The upper part of the calcareous shale and bentonite beds of the Tokay Tongue of the Mancos Shale in an arroyo in the SE1/4, NE1/4, SE1/4 sec. 8, T. 5 S., R. 2 E., Cañon Agua Buena 7.5-minute quadrangle. Nine white bentonites, including the thickest bentonite measured in the Carthage coal field (unit CS-143) at 36 cm, are visible below an angular unconformity. See Hook and Cobban (2015, fig. 4) for details on Carthage section (**CS**) stratigraphic unit numbers.

Although the fauna is of low diversity, the clam and especially the oyster occur in abundance, often as fragments on bedding planes. The ammonite, of which there are only three specimens, is preserved as impressions (bounce marks?) on bedding surfaces (Hook and Cobban, 2015, fig. 7G). *Acanthoceras bellense* is an uncommon ammonite in New Mexico, but is also known from the Dakota Sandstone elsewhere in the Quebradas area (Hook and Cobban, 2007, p. 94).

Acanthoceras bellense gave rise to the morphologically similar *A. amphibolum* Morrow, which occurs stratigraphically higher, about 11 m above the Dakota, in siltstone ledges just beneath the x-bentonite (Fig. 34A, D10128/D14728 level). Associated fauna include the clam *Inoceramus rutherfordi* Warren and the oyster *Ostrea beloiti*. These fossils represent the next-higher middle Cenomanian *Acanthoceras amphibolum* Zone (Fig. 33). This assemblage is common in the Paguate Sandstone Tongue of the Dakota Sandstone in the San Juan Basin to the northwest (Cobban, 1977a, table 1). The x-bentonite is used to mark the boundary between the Graneros Shale (below) and the Greenhorn Limestone (above) at the principal reference section of the Graneros Shale and Greenhorn Limestone near Pueblo, Colorado (Cobban and Scott, 1972).

The 12 m of slightly calcareous shale with interbedded thin sandstones above the x-bentonite are almost barren of megafauna. A thin sandstone 1.5 m above the x-bentonite yielded a complete right valve of a large *Ostrea beloiti* (Fig. 34A, D15042 level) that has a height of 4.0 cm and a length of 2.4 cm. The rare ammonite *Metengonoceras acutum*? (Fig. 34A, D5777 level), mentioned above, occurs as an internal mold 25 m above the Dakota, along with the bivalve *Inoceramus prefragilis stephensoni* Kauffman and Powell. The presence of *Inoceramus prefragilis stephensoni* in this collection indicates it is from the upper Cenomanian *Calycoceras canitaurinum* Zone.

Calycoceras canitaurinum, the name-bearer for the lowest upper Cenomanian ammonite zone (Fig. 33), occurs as poorly preserved internal molds in sandy limestone concretions in calcareous shale about 6.1 m below the top of the unit (Fig. 34A, D5778 level). Occasional fragments of *Inoceramus* sp. occur in the concretions as well.

The uppermost bed of the shale and sandstone beds has produced only one fossil, but with a height of 21 cm and an estimated length of 18 cm, it is the largest inoceramid collected in the Carthage area (Hook and Cobban, 2015, fig. 7E). This giant *Inoceramus prefragilis stephensoni* (Fig. 34A, D14757), which is preserved as an impression on the dipslope, was collected as a peel.

The 55-m-thick shale and sandstone beds at Carthage are the temporal equivalent of the upper part of the Graneros Shale and the entire Lincoln Limestone Member of the Greenhorn Limestone, which are around 15 m thick at the principal reference section of the Graneros Shale and Greenhorn Limestone near Pueblo, Colorado (Cobban and Scott, 1972). The shale and sandstone beds are also the temporal equivalent of the upper third of the Cubero Tongue through the lower part of the Twowells Tongue of the Dakota Sandstone at the Laguna, New Mexico, measured section (Landis et al., 1973, p. J4–J8). The Clay Mesa, Paguate, and Whitewater Arroyo Tongues are included within this stratigraphic interval (Hook and Cobban, 2015, fig. 5). Together, the correlative portions of these tongues of Dakota Sandstone and Mancos Shale are approximately 76 m thick. (Elsewhere in this discussion of the Tokay Tongue, the Graneros/Greenhorn principal reference section will be shortened to the "Pueblo section.")

The **calcareous shale and bentonite beds,** 36 m thick, are the second-thickest subdivision of the Tokay Tongue (Fig. 34A). Sedimentation occurred entirely in offshore environments as the T-1 shoreline transgressed southwestward across New Mexico. New Mexico was completely covered by marine water at the end of its deposition as the T-1 shoreline reached maximum transgression (Fig. 32). The unit is composed almost entirely of medium- to dark-gray, calcareous shale (94%) and white bentonite beds (6%). Both its lower and upper contacts are conformable. The unit is one of the easiest to differentiate in the Carthage coal field; it is the soft, slope-forming, partially to completely covered shale between the highest ridge of the shale and sandstone unit (Fig. 32, D14757 level) and the lowest ridge of the Bridge Creek Limestone Beds (Fig. 34A, D5779-80 level).

There are 40 ash beds in the calcareous shale and bentonite beds, more than in any other unit of the Tokay Tongue (Fig. 34A). These 40 ash beds have an aggregate compacted thickness of 203 cm and account for almost 6% of the unit's thickness. Five of these 40 bentonites are at least 10 cm thick, including the thickest bentonite in the tongue, which is 35.6 cm thick. Figure 36 shows the middle part of the calcareous shale and bentonite beds at the type section of the Tokay Tongue, where they crop out beneath the angular unconformity with the Quaternary alluvium. There are nine white bentonite beds visible in this image (Fig. 36).

Megafossils have been collected from only one interval in the calcareous shale and bentonite beds: a thin shale 30 cm below the top of the unit contains original shells of the oyster *Pycnodonte newberryi* (Stanton) (Fig. 37, D14728 level). This first occurrence of *P. newberryi* is probably from the top of the *Vascoceras diartianum* Zone (Fig. 33). Otherwise, the unit is unfossiliferous in terms of megafaunal body fossils. Therefore, it has to be dated indirectly using the highest datable fossil in the underlying unit (*Inoceramus prefragilis stephensoni*) and the lowest datable fossil in the overlying unit (*Euomphaloceras septemseriatum*) to bracket its age (Fig. 34A, D14757 and D5779-80 levels). This bracket places the calcareous shale and bentonite unit entirely in the upper Cenomanian between the basal upper Cenomanian *Calycoceras canitaurinum* Zone and the middle upper Cenomanian *Euomphaloceras septemseriatum* Zone (Fig. 33). Assuming that the inoceramid at the top of the lower unit represents the top of the *Calycoceras canitaurinum* Zone and that *Euomphaloceras septemseriatum* at the base of the Bridge Creek represents the base of the zone, then the calcareous shale and bentonite unit was deposited over approximately 790 kyr (Fig. 33), and ash falls occurred about every 20 kyr.

Hook et al. (2012, p. 131) thought the lack of fossils in this unit could have been a result of the extensive volcanic activity that fouled the water with ash, thus inhibiting bottom-dwelling, filter-feeding organisms such as clams and oysters. The approximately 20 kyr between recorded ashes suggest that this hypothesis is not tenable over the entire unit. Nektonic organisms, especially ones that could have floated for some time after death like the ammonites, would not have been affected by the ash in the water. The lack of concretions and/or hard beds may be a better explanation for the absence of megafossils. A few thin, resistant beds of very fine-grained calcarenite are present near the top of the unit. These calcarenites are composed almost entirely of the tests of globigerinid foraminifera.

In terms of the Pueblo section, the 36-m-thick calcareous shale and bentonite unit at Carthage is the temporal equivalent of the entire 18-m-thick Hartland Shale Member of the Greenhorn Limestone (Hook and Cobban, 2015, fig. 5). It is also the temporal equivalent of the upper part (approximately 12 m) of the Twowells Tongue of the Dakota Sandstone and the basal 7 m of the overlying Rio Salado Tongue of the Mancos Shale at the Laguna, New Mexico, section (Landis et al., 1973, p. J4–J8).

In the study area, the **Bridge Creek Limestone Beds** are best developed and best exposed at Carthage, where they contain the most diverse fauna in the Tokay Tongue. Consequently, this unit is discussed in detail with a large-scale graphic section (Fig. 37).

At Carthage, the Bridge Creek Limestone Beds of the Tokay Tongue of the Mancos Shale are a formally named bed-rank unit that is 22 m thick and lies 91 m above the top of the Dakota Sandstone. The Bridge Creek Limestone Beds are composed primarily of medium-gray, blocky- to chippy-weathering calcareous shale (77%) with subsidiary amounts of calcarenite (16%), limestone (5%), and bentonite (3%). The resistant limestones and calcarenites, which are concentrated at the bottom and top of the unit, respectively, form persistent ridges in the shale valley between the underlying Dakota Sandstone and the overlying Atarque Sandstone Member of the Tres Hermanos Formation. Both the lower and upper contacts of the Bridge Creek are conformable.

In southern and west-central New Mexico, the one to six thin (generally less than 18 cm thick) concretionary to nodular limestones at or near the base of the Bridge Creek Limestone Beds are easily recognized because of their nodular appearance and distinctive golden-brown weathering (Fig. 38). These limestones contain the most diverse fauna in the Tokay Tongue, with six ammonite, two oyster, two clam, one echinoid, one brachiopod, and several gastropod species (Figs. 37 and 39).

The straight ammonite *Sciponoceras gracile* (Shumard) is so abundant in the basal limestones that they are referred to (informally) as the "scip zone" limestones and are numbered from #1 at the bottom to #4 at the top at Carthage. For many years, *S. gracile* was the nominative species for an upper Cenomanian ammonite zone used in the same context that the *Euomphaloceras septemseriatum* Zone is used today (Fig. 33). Cobban et al. (1989) showed that *Sciponoceras gracile* ranged upward two range zones into the *Neocardioceras juddii* Zone. Consequently, *Euomphaloceras septemseriatum*, which does not range upward, was chosen as the new zonal index.

The four scip zone limestones at Carthage are lithologically distinct (Figs. 37 and 38). Limestone #1 (CS-174) is concretionary and laterally discontinuous; limestone #2 (CS-176) is bedded and persistent; limestone #3 (CS-179) is a dense, black limestone that breaks with a conchoidal fracture, pinches and swells, and is as much as 33 cm thick; and limestone #4 (CS-181) is concretionary but generally present. Thin-section analyses of these limestones reveal that they are foraminiferal wackestones (Mack et al., 2016).

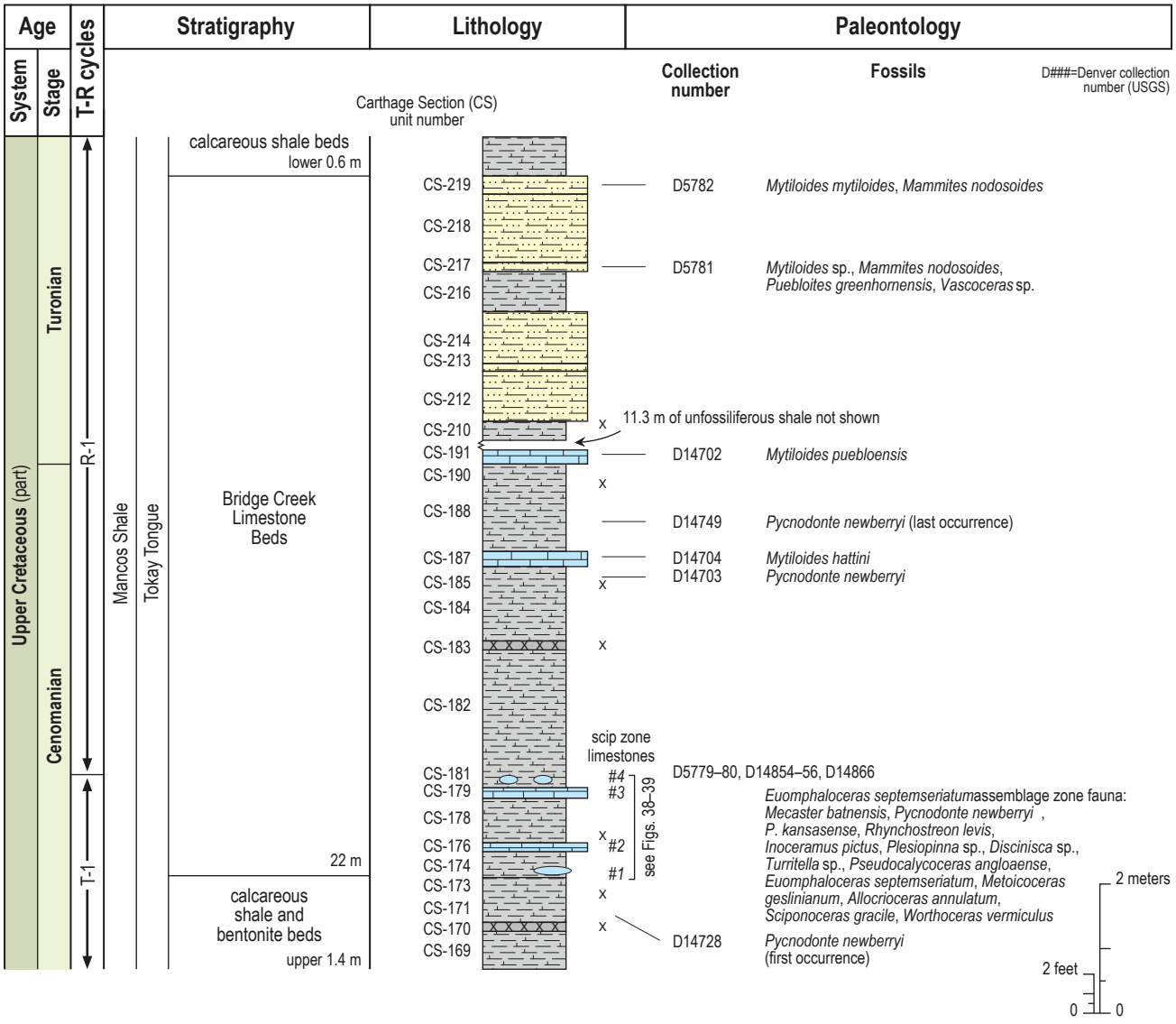

Figure 37. Graphic section of the Bridge Creek Limestone Beds of the Tokay Tongue of the Mancos Shale in the Carthage coal field showing positions of fossil collections. The section was measured in SE1/4, SE1/4 sec. 8, T. 5 S., R. 2 E., Cañon Agua Buena 7.5-minute quadrangle. Modified from Hook and Cobban (2017, fig. 6). See Figure 34B for key.

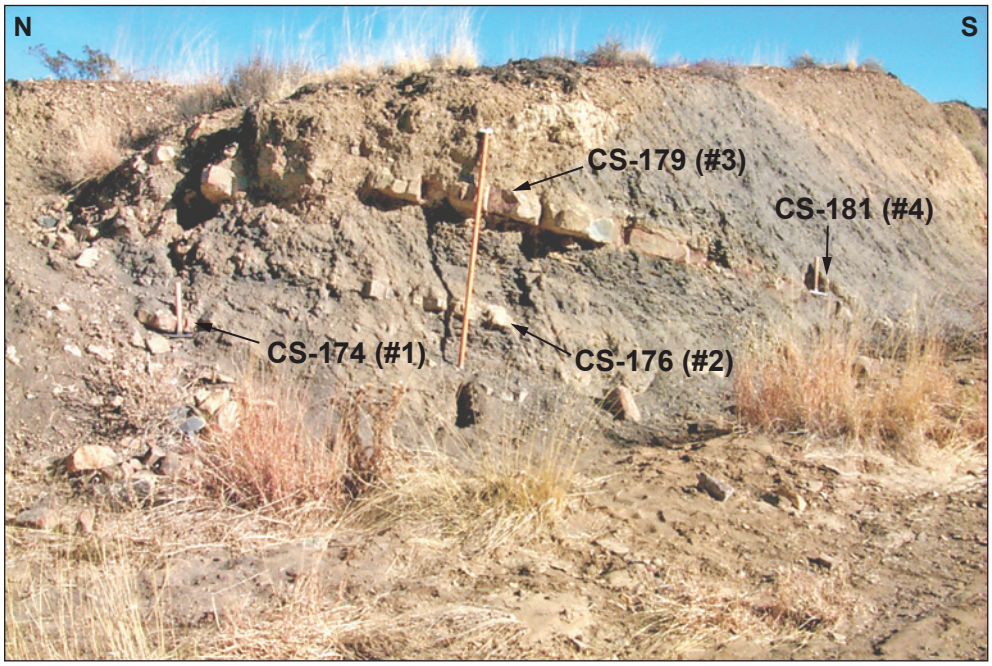

Figure 38. The four scip zone limestone beds (CS-174, 176, 179, and 181) at the base of the Bridge Creek Limestone Beds of the Tokay Tongue of the Mancos Shale are exposed farther south in the arroyo shown in Figure 36. Modified from Hook and Cobban (2015, fig. 8B). The Jacob staff is 1.5 m long.

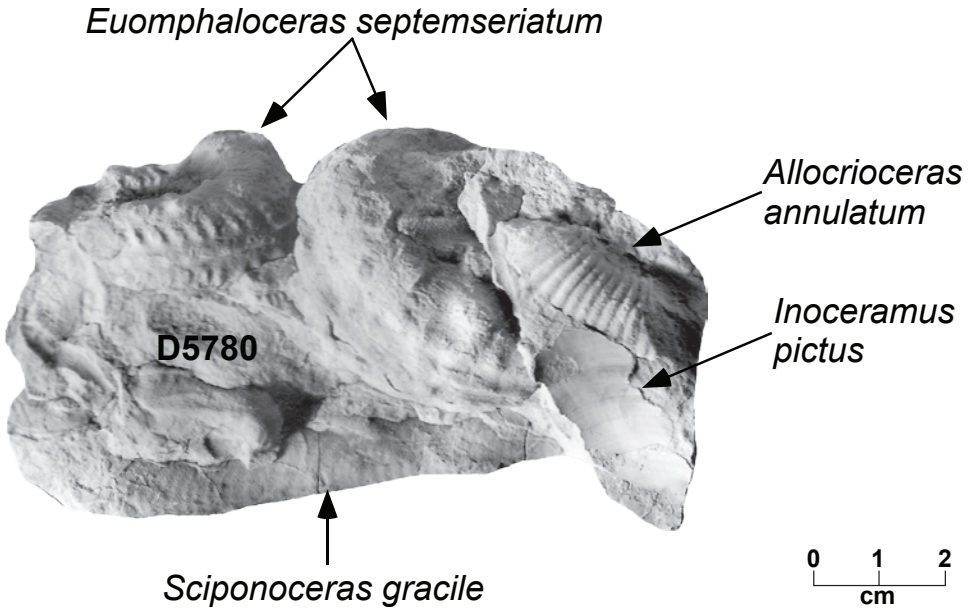

Figure 39. Hand sample (USNM 616439) from the basal part of the Bridge Creek Limestone Beds of the Tokay Tongue of the Mancos Shale at USGS Mesozoic invertebrate locality D5780 in NE1/4, SE1/4 sec. 8, T. 5 S., R. 2 E., Cañon Agua Buena 7.5-minute quadrangle. The upper surface of this slab of bed CS-179 (Fig. 37) preserves two specimens of the index ammonite *Euomphaloceras septemseriatum* (Cragin) (the larger has a diameter of 4.0 cm), one specimen of the straight ammonite *Sciponoceras gracile* (Shumard) that extends the entire length of the hand sample, one specimen of the irregularly coiled ammonite *Allocrioceras annulatum* (Shumard), and a fragment of the index inoceramid *Inoceramus pictus* Sowerby. This dense occurrence of fossils is from scip zone limestone #3 and is indicative of the upper Cenomanian *Euomphaloceras septemseriatum* Zone (Fig. 33).

Each of these four limestones at Carthage contains the late Cenomanian *Euomphaloceras septemseriatum* assemblage zone fauna that is listed in Figure 37. This assemblage includes abundant oyster shells along with an unusual faunal element—an echinoid. Echinoids are rare in the Upper Cretaceous of the Western Interior, where fewer than 60 occurrences are known to date, with most represented by only a few tests or isolated spines (Hook and Cobban, 2017). A notable exception is Carthage, where more than 200 specimens of the echinoid *Mecaster batnensis* (Coquand), previously referred to *Hemiaster jacksoni* Maury, were collected from the basal Bridge Creek Limestone Beds (Fig. 37). Prolific occurrences from the same beds are known elsewhere in west-central and southwestern New Mexico (Hook and Cobban, 2017).

The abundant oyster, *Pycnodonte newberryi* (Stanton), a common and easily recognized guide fossil known only from the Four Corners states (Hook and Cobban, 1977), is present at or near the base of the Bridge Creek Limestone Beds in the study area. At Carthage, it has a stratigraphic range of 5.6 m, from the shale just below the base of the Bridge Creek Limestone Beds (Fig. 37, D14728 level) to the shale just below the Cenomanian–Turonian boundary limestone (Fig. 37, D14749 level). Biostratigraphically, this interval ranges from the top of the *Vascoceras diartianum* Zone to the top of the *Nigericeras scotti* Zone (Fig. 33), all in the upper Cenomanian. Elsewhere in the Four Corners states, *Pycnodonte newberryi* has been reported from the lower Turonian *Pseudaspidoceras flexuosum* Zone (Hook and Cobban, 2016, fig. 7). In an unpublished collection (D6817) from Mescal Canyon east of Truth or Consequences (Fig. 32), *Pycnodonte newberryi* occurs with *Mammites nodosoides*.

Hook and Cobban (2015, p. 41) collected corroded, oyster-encrusted internal molds of the ammonite *Metoicoceras geslinianum* (d'Orbigny) from the scip zone limestones at Carthage, which they interpreted as hiatus concretions in which corrosion and encrustation occurred on the seafloor after the "prefossilized" molds were eroded out of the sediment. Similar internal molds have been reported from the Bridge Creek elsewhere in New Mexico and near Mesa Verde, Colorado (Hook and Cobban, 1981, 2017), indicating that the erosive conditions that prevailed at Carthage were widespread. The T-1 shoreline was at or near maximum transgression at this time (Fig. 32), suggesting that the erosion was caused by currents rather than by wave action.

The 20-cm-thick, white-weathering limestone bed (Fig. 37, CS-191) that is 6.3 m above the base of the Bridge Creek contains the inoceramid bivalve *Mytiloides puebloensis* Walaszczyk and Cobban (D14702), a taxon used to define the base of the Turonian Stage in the Western Interior and throughout the world (Kennedy et al., 2000, 2005). *Mytiloides hattini* Elder (Fig. 37, D14704 level), the youngest Cenomanian inoceramid, was collected from a 25-cm-thick limestone (Fig. 37, CS-187), 1.5 m below the bed containing *M. puebloensis*.

Internal molds and the comminuted remains of the inoceramid bivalve *Mytiloides mytiloides* (Mantell) (Fig. 37, D5781-82 level), with occasional internal molds of the early Turonian ammonite *Mammites nodosoides* (Schlüter), compose the resistant, brown-weathering, thinly bedded calcarenites at the top of the Bridge Creek Limestone Beds (Fig. 37, CS-217 through CS-219).

Murphy et al. (2007, p. 63) asserted that the calcarenite at the top of the Bridge Creek Member "…yields numerous shells of the bivalves *Ostrea beloiti* and *Mytiloides mytiloides*…" and that "…this assemblage occurs within the *Sciponoceras gracile* ammonite zone." Both statements are incorrect and biostratigraphically impossible. Within the Western Interior, the oyster *Ostrea beloiti* has a known range of middle to upper Cenomanian (Cobban and Hook, 1980), ranging from the *Conlinoceras tarrantense* Zone through the *Calycoceras canitaurinum* Zone. The inoceramid bivalve *Mytiloides mytiloides* is present in lower Turonian rocks in the *Mammites nodosoides* Zone (Cobban 1984b, p. 35). Therefore, *Ostrea beloiti* and *Mytiloides mytiloides* cannot co-occur.

At the type section of the Tokay Tongue (Fig. 34A), the stratigraphically highest occurrence of *Ostrea beloiti* is in sandy limestone concretions near the top of the shale and sandstone beds (Fig. 34A, D5778 level), 49 m above the top of the Dakota Sandstone. The first occurrence of *Mytiloides mytiloides* (Fig. 34A, D5781-82 level) is in a calcarenite near the top of the Bridge Creek Limestone Beds, 113 m above the top of the Dakota

Sandstone. *Sciponoceras gracile* is a late Cenomanian ammonite that is present in limestones at the base of the Bridge Creek in the *Euomphaloceras septemseriatum* Zone (Fig. 34A, D5779-80 level). *Sciponoceras gracile* does not range into the Turonian (Cobban et al., 1989, p. 62–64) and, therefore, cannot occur with *Mytiloides mytiloides*. The well-documented, Western-Interior-wide biostratigraphy of both *Ostrea beloiti* and *Mytiloides mytiloides* indicates that the two species do not co-occur, suggesting that at least one species was misidentified by Murphy et al. (2007).

The shale above the Bridge Creek Limestone Beds is calcareous for another 34 m. This slope-forming, medium-gray, blocky to chippy shale makes up the **calcareous shale beds**. An 18-cm-thick bentonite separates the calcareous shale beds (below) from the 27-m-thick **noncalcareous shale beds** (above). This bentonite is the uppermost ash bed in the Tokay Tongue at Carthage (Fig. 34A). Concretions developed in, on, and just below the bentonite preserve a middle Turonian *Collignoniceras woollgari woollgari* fauna (Fig. 34A, D14707-08 and D10129 levels). The overlying Atarque Sandstone Member of the Tres Hermanos Formation also contains a *Collignoniceras woollgari woollgari* fauna (Fig. 34A, D10241 level).

Rocks of *Collignoniceras woollgari woollgari* age at Truth or Consequences, 96 km to the south (Fig. 32), are continental (Mack et al., 2016). The absence of this thick bentonite in the upper part of the Tokay Tongue in Mescal Canyon indicates that the upper part of the Tokay Tongue at Truth or Consequences is in the *Mammites nodosoides* Zone.

As the R-1 shoreline retreated to the northeast from Truth or Consequences, noncalcareous marine muds were deposited at Carthage. The change from calcareous shale below to noncalcareous shale above is interpreted to represent a change in the chemistry of the seawater caused by the influx of more fresh water into the depositional system because of the encroaching R-1 shoreline (Fig. 32). This contact, which is diachronous, has been verified at outcrops of the Rio Salado Tongue at Puertecito and the Tokay Tongue at the Jornada del Muerto coal field, the Carthage coal field, and Mescal Canyon east of Truth or Consequences. The noncalcareous shale beds of the Tokay Tongue at Carthage are 27 m thick and are macroscopically unfossiliferous.

The 61-m-thick combined calcareous and noncalcareous shale beds of the Tokay Tongue at Carthage are the temporal equivalent of most of the upper 7 m of the 18-m-thick Bridge Creek Member of the Greenhorn Limestone at the Pueblo section (Hook and Cobban, 2015, fig. 5).

Hook and Cobban (2015, table 1) estimated the compacted sedimentation rate for the entire Tokay Tongue at Carthage at 0.0046 cm/yr. They also estimated compacted sedimentation rates for each of the bed-rank units in the Tokay Tongue at Carthage. They found the compacted sedimentation rates decreased from 0.0082 cm/yr in the shale and sandstone beds to 0.0046 cm/yr in the calcareous shale and bentonite beds to 0.0011 cm/yr in the Bridge Creek Limestone Beds. These decreases reflect the increasing distance from Carthage to the T-1 shoreline, which advanced toward the southwest and was at its maximum at the time of deposition of the basal Bridge Creek (Fig. 32).

The compacted sedimentation rates then increased to 0.0203 cm/yr in the calcareous shale beds before decreasing to 0.0168 cm/yr in the noncalcareous shale beds. These higher rates reflect the decreasing distance from Carthage to the R-1 shoreline as it retreated to the northeast from Mexico, eventually leaving the Carthage area during *Collignoniceras praecox* time, when the nonmarine strata near the base of the Carthage Member of the Tres Hermanos Formation were deposited (Fig. 33). The R-1 shoreline reached its maximum position northeast of Carthage during early *Prionocyclus hyatti* time (Fig. 33).

A sequence-stratigraphic analysis of the Tokay Tongue of the Mancos Shale and the overlying Atarque Sandstone Member of the Tres Hermanos Formation at Carthage can be found in Mack et al. (2016).

Rejected Lower Mancos Terminology

We reject the following stratigraphic terminology proposed for the lower tongue of the Mancos Shale by Lucas et al. (2019): Graneros, Greenhorn, and Carlile Members of the Mancos Formation. These terms were specifically applied to the Upper Cretaceous outcrops in Sierra and Socorro Counties but were intended for use throughout New Mexico.

Lucas et al. (2019, p. 10–11) abandoned the name Tokay Tongue of the Mancos Shale because they believed it to be a synonym of the older term Colorado

Formation as used in New Mexico (Gardner, 1910; Darton, 1928; Rankin, 1944). To support the claimed synonymy of Colorado Formation and Tokay Tongue at Carthage, Lucas et al. (2019, fig. 6, right stratigraphic column) labeled the stratigraphic unit between the Dakota Sandstone and the Tres Hermanos Formation as the "Tokay Tongue or Colorado Formation," an equivalence they stated "… is the nomenclature of Hook and Cobban (2015)." Nowhere did Hook and Cobban (2015) state that the two names are equivalent. Gardner (1910, p. 455), Darton (1928, p. 74–75), and Rankin (1944, fig. 5) applied the name Colorado (in the group sense) in the Carthage coal field to all strata between the Dakota Sandstone and the Gallup Sandstone, not just to the thick shale between the Dakota Sandstone and the Tres Hermanos Formation. Thus, their usage of the Colorado (group) at Carthage included strata now referred to the Tokay Tongue of the Mancos Shale, the Tres Hermanos Formation, and the D-Cross Tongue of the Mancos Shale.

Lucas et al. (2019, p 10) justified abandoning the Tokay Tongue at Carthage, its type area, because "the lower Mancos can be readily divided into Graneros, Greenhorn and Carlile intervals, as was first done by Rankin (1944, p. 21–22, fig. 6)." Ready division of a stratigraphic succession into intervals is not a criterion for correlating rock units.

Rankin's (1944, p. 21–22, fig. 6, section 8) Colorado group at Carthage encompassed all strata between the Dakota Sandstone and the Gallup Sandstone, not just the Tokay Tongue of the Mancos Shale as asserted by Lucas et al. (2019). Rankin (1944) subdivided his Colorado group, in ascending order, into Graneros, Greenhorn, and Carlile formations. He used the Greenhorn formation in the same sense that we use Bridge Creek Limestone Beds of the Tokay Tongue. His Carlile formation, unlike that of Lucas et al. (2019), extended from the top of his Greenhorn formation to the base of the D-Cross Tongue of the Mancos Shale. Thus, Rankin's (1944) Carlile formation included the upper part of the Tokay Tongue and all of the Tres Hermanos Formation, which includes a continental core.

Rankin's (1944) use of Graneros, Greenhorn, and Carlile at Carthage conformed to the stratigraphic usage of the 1940s but does not conform to present-day stratigraphic nomenclature. Cobban and Scott (1972, p. 14)—in a paper not cited by Lucas et al. (2019)—established the principal reference section for the Greenhorn Limestone at the Rock Canyon anticline in the Pueblo, Colorado, area, where "[t]he Greenhorn Limestone, of Cenomanian and Turonian age, contains three members—in ascending order, the Lincoln Limestone, Hartland Shale, and Bridge Creek Limestone—all originally named for exposures in Kansas. Together, these make up a unit 153 feet thick, which consists of a lower calcareous shale containing calcarenite beds, a middle calcareous shale, and an upper limestone and shale. The Greenhorn was named by Gilbert (1896, p. 570) for exposures near Greenhorn Station, which is 28 miles south of Pueblo, and along Greenhorn Creek. The name originally was applied only to the 57-foot-thick Bridge Creek Limestone Member, but as used here, includes all three members. Because no type section was published by Gilbert, we measured a section at Rock Canyon anticline where the entire Greenhorn is well exposed and here designate it the principal reference section."

Cobban and Scott (1972, p. 7–9) also established the principal reference section for the Graneros Shale at the Rock Canyon anticline. Regarding the contact between the Graneros and Greenhorn, Cobban and Scott (1972, p. 6) stated "the boundary established by Gilbert (1896, p. 564) was nearly 100 feet higher than the currently used boundary. In the upper part of the type Graneros, Gilbert included calcareous shale and calcarenite beds that are now assigned to the Lincoln Limestone and Hartland Shale Members of the Greenhorn Limestone. In the type Greenhorn, Gilbert included only the thin hard beds of limestone now called the Bridge Creek Member. We are here redefining the Greenhorn so that it includes all the calcareous beds of the Lincoln, Hartland, and Bridge Creek. We are further redefining the Graneros so that it contains only the generally noncalcareous beds below the marker bentonite bed." Hook and Cobban's (2015) usage of Bridge Creek Limestone Beds of the Tokay Tongue of the Mancos Shale conforms to the redefined Greenhorn Limestone of Cobban and Scott (1972). Hook and Cobban's (2015, fig. 5) correlation diagram showed that only the basal 12 m of the Tokay Tongue below the x-bentonite correlates with the Graneros Shale; the remaining 163 m of the tongue correlate with the Greenhorn Limestone, as does the overlying Atarque Sandstone Member of the Tres Hermanos Formation (Hook and Cobban, 2015, fig. 5).

Lucas et al. (2019, p. 11–12) also abandoned the term Bridge Creek Limestone Beds at Carthage, because "…this stratigraphic interval correlates to part of the Bridge Creek Member of the Greenhorn Formation on the High Plains, but is not the same unit lithologically … (cf. Hattin, 1975, 1987)." Their explanation, however, fails to adequately justify using the more inclusive term "Greenhorn," which comprises three members, for exactly the same interval that Hook and Cobban (2015) called Bridge Creek Limestone Beds, correlating it with only the lower part of the upper member. In addition, Hattin (1987, fig. 2) and Lucas et al. (1987, fig. 1) showed that the Greenhorn Limestone (or Formation) of northeastern New Mexico consists of three members, in ascending order, the Lincoln, Hartland, and Bridge Creek Members. Hattin (1987, fig. 2) showed that the stratigraphic unit called the Greenhorn Limestone Member of the Mancos Shale in the San Juan Basin is equivalent to only the Bridge Creek Member of the Greenhorn Limestone in central and southern Colorado and northeastern New Mexico.

Elder (1989) correlated a package of 11 marker limestones and 4 bentonites from the basal one-third of the Bridge Creek Limestone Member of the Greenhorn Limestone near Pueblo, Colorado, to the Bridge Creek Limestone Beds at Carthage, New Mexico, thereby demonstrating they are the same section of rock and that any differences are due to lateral facies variations. Among the eight limestone beds that Elder (1989, fig. 24) identified at Carthage, four are equivalent to limestones that Hattin (1987) traced from the Greenhorn Limestone of Kansas into the Bridge Creek Member of the Greenhorn Limestone in northeastern New Mexico.

Moreover, the term Bridge Creek Limestone Member of the Mancos Shale is widely used in the subsurface in the San Juan Basin (see Molenaar et al. [2002]). Molenaar and Baird (1991, p. C7) stated the Bridge Creek is "…a widespread unit throughout the area, and its contacts are well defined on geophysical logs … This unit was formerly known as the Greenhorn Limestone Member; the name Bridge Creek Limestone Member was recently applied because it more accurately relates the unit to the Bridge Creek Member of the Greenhorn Limestone near Pueblo, Colo. (Huffman, 1987; Kirk et al., 1988)."

Additionally, Lucas et al. (2019) published two radically different interpretations of the lithosomes that constitute their Graneros and Greenhorn Members in Sierra County. The top of the Greenhorn Member in their surface section is approximately 30 m above the Dakota Sandstone (fig. A3.3); in their well section, it is approximately 62 m above the Dakota Sandstone in the Sun #2 (fig. A7.1). The combined Graneros/Greenhorn interval encompassed the lower 19% of the Mancos Formation in their surface section, and the Carlile encompassed the remaining 81%. In the well section, the combined Graneros/Greenhorn interval represented 48% of the Mancos Formation, and the Carlile represented 52%. Based on these positional and proportional differences, the lithosome that Lucas et al. (2019) identified as the Greenhorn Member in their surface section is not the same lithosome they correlated as the Greenhorn Member in their well cross section, which in turn is correlated with the Bridge Creek Limestone Beds of Hook et al. (1983).

Based on these considerations, we reject all the stratigraphic terminology that Lucas et al. (2019) applied to the lower Mancos Shale. In the sections that follow, the Tokay Tongue of the Mancos Shale is used for the lower part of the Mancos Shale in the Quebradas area, where it is generally subdivided into five bed-rank units, of which four are informal and one, the Bridge Creek Limestone Beds, is formal. The informal names are primarily used for discussion purposes, but they also refer to separate lithologic bed-rank units.

The **Tres Hermanos Formation,** which conformably overlies the Tokay Tongue of the Mancos Shale, is arguably the most important Upper Cretaceous stratigraphic unit in the Quebradas area with respect to correlation. The depositional and biostratigraphic frameworks of this unit provide the key for correlating the Upper Cretaceous at Carthage and other isolated exposures in southern New Mexico to the better-studied rocks to the northwest in the San Juan Basin (Hook et al., 1983). Before 1983, the rock unit now called the Tres Hermanos Formation had been miscorrelated with the stratigraphically higher Gallup Sandstone (Pike, 1947; Molenaar, 1974, 1983a).

The Tres Hermanos sandstone was named by Herrick (1900), and simultaneously by Herrick

and Johnson (1900), for a band of sandstone with "enormous" concretions just east of Tres Hermanos Peaks—three basaltic necks in the Rio Salado Valley in northwestern Socorro County. Herrick, who worked long before the complex intertonguing of the Mancos Shale and Dakota Sandstone was understood, also misapplied the formation name to an older sandstone in the Rio Puerco Valley east of Laguna, New Mexico (Fig. 32). This misapplication of the name Tres Hermanos resulted in more than 80 years of confusion surrounding the stratigraphic identity of the Tres Hermanos sandstone. Hook et al. (1983), working in the type area of the Tres Hermanos sandstone, redefined the unit as the Tres Hermanos Formation. The revision of Hook et al. (1983) has been applied on geologic maps of the southern half of New Mexico (e.g., Anderson and Osburn, 1983; Seager and Mack, 1998, 2003) and on the latest version of the Geologic Map of New Mexico (New Mexico Bureau of Geology and Mineral Resources [NMBGMR], 2003). Hook et al. (1983) designated exposures in the Carthage coal field as the principal reference sections for the Tres Hermanos Formation and the Atarque Sandstone Member and as the type sections for the Carthage and Fite Ranch Sandstone Members.

As revised by Hook et al. (1983), the Tres Hermanos Formation is a middle Turonian, regressive–transgressive wedge of nearshore marine and continental sandstone, shale, and coaly beds that separates the lower part of the Mancos Shale into two parts in west-central New Mexico. In its type area in the Rio Salado Valley, the Tres Hermanos Formation separates the Mancos Shale into the Rio Salado Tongue below and the D-Cross Tongue above. At its reference section in the Rio Salado Valley (Hook et al., 1983, table 3), the Tres Hermanos Formation is 72 m thick and divided into three members, in ascending order: the Atarque Sandstone Member (20 m thick), the Carthage Member (37 m thick), and the Fite Ranch Sandstone Member (15 m thick).

At Carthage, the Tres Hermanos Formation separates the lower part of the Mancos Shale into the Tokay Tongue below and the D-Cross Tongue above (Fig. 34A). The Tres Hermanos Formation at its principal reference section at Carthage is 84 m thick and divided into three members, in ascending order: the Atarque Sandstone Member (26 m thick), the Carthage Member (35 m thick), and the Fite Ranch Sandstone Member (23 m thick).

The Tres Hermanos was deposited during the last part of R-1 and the first part of T-2, all during the middle Turonian (Figs. 33 and 34A). Its lower contact is conformable and its upper contact is disconformable.

The **Atarque Sandstone Member** is a regressive coastal-barrier sandstone or shoreface complex that prograded northeastward into the R-1 seaway. At its principal reference section near Carthage, it is 26 m thick and dominantly sandstone (Fig. 34A). These regressive sandstones are gray on fresh surfaces but weather brown or buff (Figs. 40 and 41). Fossiliferous sandstone concretions near the base are dark brown. The coarsening-upward member ranges from very fine to fine grained and contains abundant interstitial clay. Bedding is generally planar, but minor, medium-scale cross-beds are present. Burrows are common, especially near the top of the member.

Body fossils are present only in the basal part of the Atarque. Fossiliferous, dark-brown, calcareous sandstone concretions contain a diverse molluscan fauna from the *Collignoniceras woollgari woollgari* Subzone (Fig. 33). This fauna is so abundant, widespread, diverse, and generally well preserved that Hook et al. (1983, p. 22) regarded it as the characteristic fauna of the Tres Hermanos Formation throughout west-central New Mexico, although it is more appropriately referred to as the characteristic Atarque fauna.

The non-cephalopod portion of this fauna was facies controlled and followed the retreating R-2 shoreline. Fossils occur in great numbers in the nearshore, high-energy sandstone concretions at or near the base of the regressive Atarque in west-central and southwestern New Mexico. The fossils, preserved as internal molds, are mixed together in coquina-like masses in the concretions. Infaunal and epifaunal species occur jumbled together, with the bivalves arranged in every orientation. Hook et al. (1983, p. 22) recognized 4 species of ammonites, 22 species of bivalves, and 9 species of gastropods at Carthage. Four of these species, including the ammonite *Spathites rioensis* Powell and the clam *Mytiloides subhercynicus* (Seitz), are shown in a coquina-like accumulation of bivalve internal molds in Figure 42.

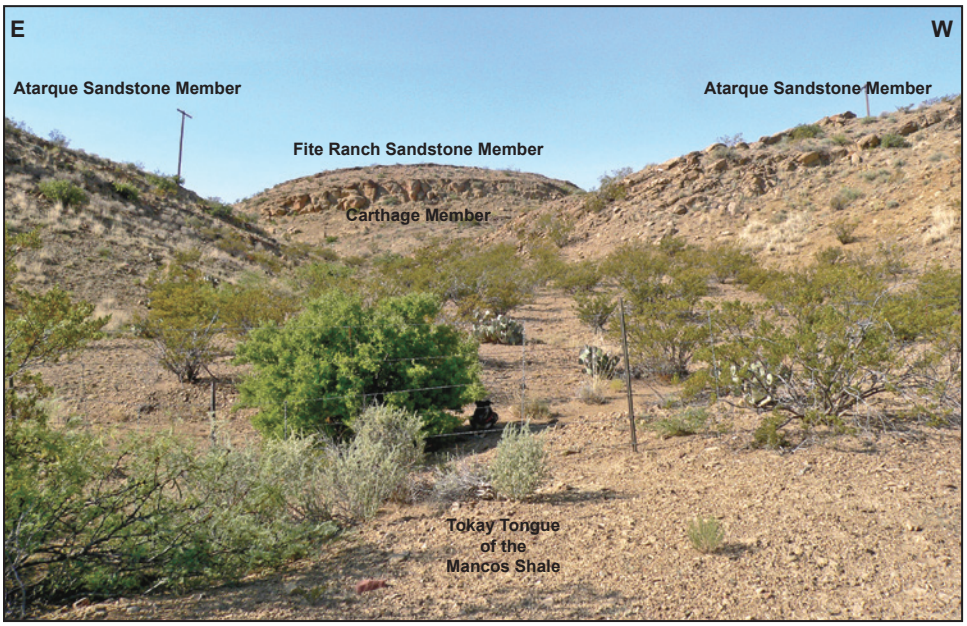

Figure 40. View to the south from U.S. Route 380 of the Tres Hermanos Formation through a fault gap where two normal faults with opposite displacements converge near the center of sec. 9, T. 5 S., R. 2 E., Cañon Agua Buena 7.5-minute quadrangle. The Tokay Tongue of the Mancos Shale in the foreground gives way to resistant ridges of the conformable Atarque Sandstone Member. Massive cliffs of the Fite Ranch Sandstone Member rise above the soft, mostly continental shales of the Carthage Member in the center of this small graben.

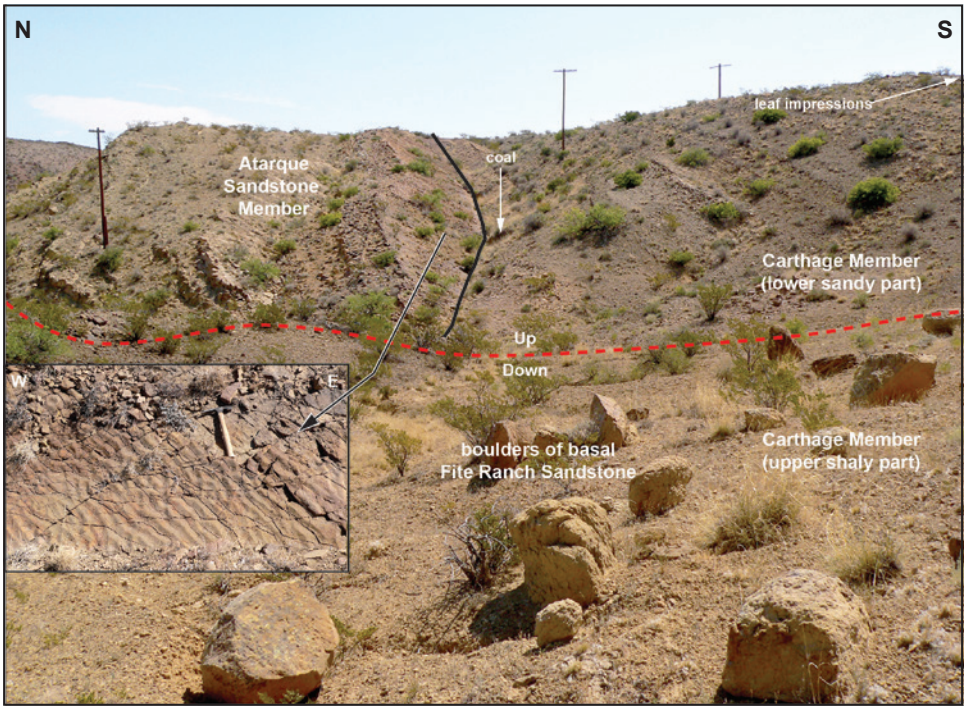

Figure 41. View to the east from the upper part of the Carthage Member of the Tres Hermanos Formation across the eastern normal fault (dashed red line) that forms the fault gap in Figure 40, showing the sharp contact (solid black line) of the uppermost ridge of the marine Atarque Sandstone Member with the continental lower part of the Carthage Member. Inset photograph shows the burrowed, ripple-marked quartzose sandstone that marks the top of the Atarque Sandstone Member throughout the Carthage coal field. Boulders in the foreground on the upper part of the Carthage Member weathered from the overlying Fite Ranch Sandstone Member. Inset photograph is in SE1/4, SE1/4, NW1/4 sec. 10, T. 5 S., R. 2 E., Cañon Agua Buena 7.5-minute quadrangle.

Only the biostratigraphically important species in this characteristic fauna are listed in Figure 34A (D10241 level).

The 35 invertebrate species recorded from the characteristic Atarque fauna in the *Collignoniceras woollgari woollgari* Subzone at Carthage make it the most diverse invertebrate fauna from the Upper Cretaceous in the Quebradas area and the second most diverse in New Mexico. Only the Thatcher fauna from the Laguna area with 50 species of invertebrates exceeds it (Cobban, 1977a).

The uppermost 1 m of the Atarque Sandstone Member at Carthage, and only at Carthage, consists of oscillation-ripple-marked, burrowed quartzites that contain a *Skolithos* ichnofacies, including the vertical, U-shaped burrows of *Diplocraterion* sp. and the horizontal burrows of *Thalassinoides* sp. (Fig. 41, inset; Hook and Cobban, 2011a). It was the last marine bed deposited during R-1 at Carthage (Fig. 41, inset). Mack et al. (2016, p. 19) interpreted the contact between the Atarque Sandstone and overlying Carthage Member as a sequence boundary in which fluvial strata overlie lower shoreface sandstone. Root traces extend downward from the sequence boundary into the sandstone.

We assume that the Atarque Sandstone Member was deposited until the middle of the time represented by the *Collignoniceras praecox* Zone, although there are no body fossils in the upper part of the member. Fossils from the base of the member lie in the older *Collignoniceras woollgari woollgari* Subzone (Fig. 33). The basal part of the Atarque at Carthage is the temporal equivalent of the uppermost part of the Bridge Creek Member of the Greenhorn Limestone at the principal reference section of the Greenhorn Limestone at Rock Canyon anticline, Colorado (Cobban and Scott, 1972). Cobban and Hook (1979)

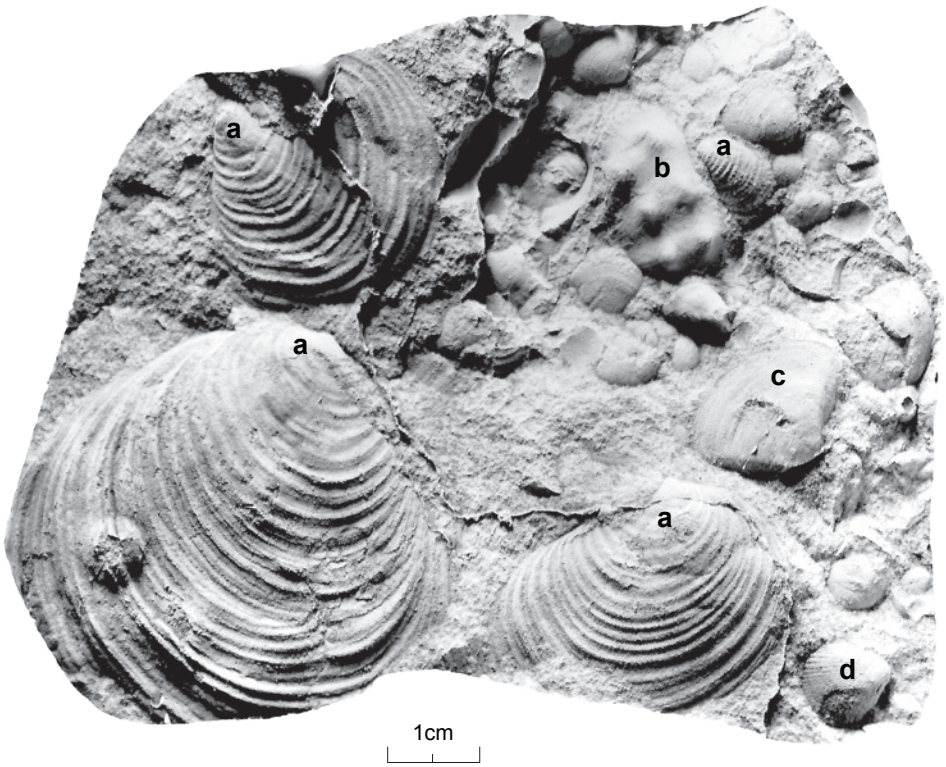

Figure 42. Several members of the characteristic Atarque fauna are preserved on this slab of fine-grained sandstone concretion (USNM 720106) from the basal part of the Atarque Sandstone Member of the Tres Hermanos Formation at USGS Mesozoic invertebrate locality D10242 in NW1/4, SW1/4 sec. 9, T. 5 S., R. 2 E., Cañon Agua Buena 7.5-minute quadrangle. Internal molds of (a) *Inoceramus subhercynicus* (Seitz) and (b) *Spathites rioensis* Powell are preserved in a coquina-like accumulation of the bivalves (c) *Cymbophora emmonsi* (Meek) and (d) *Pleuriocardia pauperculum* (Meek). These species are indicative of the middle Turonian *Collignoniceras woollgari woollgari* Subzone (see Fig. 33).

figured several specimens of *Collignoniceras woollgari woollgari* (Mantell) and *Spathites rioensis* Powell from the Atarque at Carthage.

The **Carthage Member** is the medial, mostly continental part of the Tres Hermanos Formation. At its type section in the Carthage coal field, it is 35 m thick (Fig. 34A). The lower part of the Carthage Member is sandy and the upper part is predominantly shale (Figs. 40 and 41). The sandstones are generally thin, discontinuous, fine-grained, cross-bedded, fluvial-channel deposits. A thin coal is present near the base of the member, and petrified wood, logs, and leaves are preserved near the top of the sandy unit (Fig. 34A). The continental shale above the sandy unit probably represents a marsh.

The uppermost part of the Carthage Member is gray marine shale approximately 5 m thick that contains fossiliferous limestone concretions. These concretions contain the middle Turonian oyster *Cameleolopha bellaplicata* (Shumard) and fragments of an adult prionocyclid ammonite with an arched venter that is probably the early form of *Prionocyclus macombi* Meek (Fig. 34A, D14546 level), but could be the older *P. hyatti* (Stanton). C.M. Molenaar (personal communication, 1982) referred to the marine part of the Carthage Member as a "brackish transgression."

The Carthage Member was deposited in the middle Turonian during the waning stage of R-1 and the beginning of T-2 (Figs. 33 and 34A). Deposition was probably on a broad, low-relief coastal or deltaic plain. Both upper and lower contacts are conformable.

We reject Lucas et al.'s (2019, p. 14) suggestion that the name Carthage Member (of the Tres Hermanos Formation) be abandoned and replaced by a new term, the Campaña Member. They point out that the name Carthage was used first for a Pennsylvanian limestone in Kentucky in 1856 and is, therefore, a preoccupied name. Article 7c of the North American Stratigraphic Code (North American Commission on Stratigraphic Nomenclature, 2005, p. 1562), however, states that "[p]riority in publication is to be respected, but priority alone does not justify displacing a well-established name by one neither well-known nor commonly used." Since its publication (Hook et al., 1983), the name Carthage Member of the Tres Hermanos Formation has become well established in the geologic literature of central New Mexico. It has appeared on numerous cross sections (e.g., Nummedal and Molenaar, 1995; Molenaar et al., 2002; Mack et al., 2016), on numerous geologic quadrangle maps (e.g., Osburn, 1984; Anderson, 1987; Zeigler and Allen, 2010), and on the Geologic Map of New Mexico (NMBGMR, 2003). We note that the name Carthage Member of the Tres Hermanos Formation was approved for use by the USGS Geologic Names Committee as part of the formal USGS manuscript-review process in 1983. There is no potential for confusion in using the term Carthage for both an Upper Cretaceous sandstone in New Mexico and a Pennsylvanian limestone in Kentucky.

At its type section at Carthage, the **Fite Ranch Sandstone Member** of the Tres Hermanos Formation is a well-developed, coastal-barrier sandstone that is 23 m thick (Fig. 34A). The sandstones are light gray but weather to medium brown; they consist of a coarsening-upward succession generally ranging from very fine to fine grained. Upper-fine to medium-size grains occur in the distinctive 1-m-thick, dark-brown, hematite-cemented sandstone that caps the member (Fig. 43). Planar bedding predominates but is obscured by bioturbation, especially in the lower one-third of the member. Ripple marks, cross-beds, and impressions of rip-up clasts are present at two levels, near the middle and just below the top of the member (Fig. 34A). The rip-up clasts, which are thin (<2 mm thick), irregularly shaped fragments a few centimeters across, weather light brown. G.H. Mack (personal communication, 2018) interprets them to be microbial mat chips. Microbial mats are especially common in tidal flats. The mats and ripple marks are unique to the Fite Ranch Sandstone at Carthage and suggest that the seaway shallowed at least twice during deposition of the Fite Ranch strata. This, in turn, suggests minor regressions in the T-2 shoreline. Hook et al. (1983, p. 21) also thought that the basal part of the Fite Ranch Sandstone represented "a transgression followed by an offlap or regression during which the major part of the Fite Ranch was deposited."

The middle Turonian oyster *Cameleolopha bellaplicata* (Shumard) and ammonites *Prionocyclus macombi* Meek and *Coilopoceras colleti* Hyatt are abundant throughout the basal 9 m of the member (Fig. 34A, D10354 level). This occurrence places

the basal part of the Fite Ranch in the lower part of the *P. macombi* Zone (Fig. 33). A few specimens of the middle Turonian clam *Inoceramus dimidius* White were collected from concretions at the base of the member (Fig. 34A, D14562 level). In addition, Schweitzer et al. (2017) reported a decapod crustacean fauna from rubbly sandstone 9 m above the base of the member. *Cameleolopha bellaplicata* and a single, poorly preserved prionocyclid, *Prionocyclus* sp., are preserved in the uppermost bed of the member (Fig. 34A, D11161 level). The presence of *C. bellaplicata* in the D11161 collection indicates that the prionocyclid is *P. macombi*, not the younger *P. wyomingensis* Meek. Hook et al. (1983, chart 1, section 59, D11161 level) erred in showing that *P. macombi*, *Coilopoceras inflatum*, and "*Lopha*" *sannionis* were present in the uppermost bed. Reexamination of the D11161 collection revealed that (a) the only prionocyclid in the collection is too poorly preserved to be specifically determined, (b) there is no coilopocerid in the collection, and (c) the oyster is a fragment of *Cameleolopha bellaplicata*. No specimens of the ammonite *Coilopoceras inflatum* Cobban and Hook have been found in the Quebradas area. Elsewhere in New Mexico (e.g., at Bull Gap Canyon, Fig. 32), *Coilopoceras inflatum* occurs in the upper part of the *Prionocyclus macombi* Zone in association with the younger oyster *Cameleolopha lugubris* (Conrad).

Within the Quebradas area, exposures of the Fite Ranch Sandstone at Carthage are the most fossiliferous and best age-constrained. Both the lowermost and uppermost beds are fossiliferous and contain age-diagnostic fossils that constrain the member to the lower part of the *Prionocyclus macombi* Zone. By contrast, there are no macrofossils known from the Fite Ranch Sandstone on SNWR and only a few, non-age-diagnostic fossils from the member at JdM. Two collections from near the base of the member at an outcrop 1.6 km south of SNWR contained only a few specimens of *Cameleolopha bellaplicata*. The upper collection (D15243) is a single fragment of a disarticulated valve. The lower collection (D14471) consists of a few internal molds and impressions but no shell material; at Carthage, the oysters are preserved as original shells.

Phosphatic ooids are sporadically present in the sandstone matrix and abundant in the internal molds of the infaunal bivalve *Pholadomya* sp. in the dark-brown, hematite-cemented sandstone at the top of the Fite Ranch Sandstone (Fig. 34A, D11161 level). Similar ooids are present in the uppermost, dark-brown, hematite-cemented bed of the Fite Ranch Sandstone north of Bull Gap Canyon, 77 km southeast of Carthage (Fig. 32). At Bull Gap Canyon, Hook and Cobban (2012) interpreted a submarine, erosional unconformity that removed the upper portion of the Fite Ranch Sandstone. North of Bull Gap Canyon, the top of the Fite Ranch Sandstone lies in the middle Turonian *Prionocyclus macombi* Zone; south of the canyon, 2.3 km to the southwest, the top of the Fite Ranch is one faunal zone lower and lies in the *Prionocyclus hyatti* Zone. A minimum of 8 m of section is missing at the southern outcrop.

The ooids at Carthage formed penecontemporaneously with those at Bull Gap Canyon. These ooids are interpreted to have formed on an erosional surface under conditions of low sedimentation rates and/or sediment bypass. Similar phosphatic ooids are also present lower in the Fite Ranch in dark-brown sandstone concretions at approximately the D10354 level in Figure 34A, suggesting there may be other erosional intervals within the Fite Ranch Sandstone.

The Fite Ranch Sandstone at Carthage was deposited during the early part of the T-2 transgression (Figs. 33 and 34A) in the middle Turonian during the time represented by the *Prionocyclus macombi* Zone. Its lower contact is gradational and conformable and its upper contact is sharp and unconformable (Figs. 33, 34A, 44, and 45). The ammonites *P. macombi* and *Coilopoceras colleti* Hyatt from Carthage were figured in Hook and Cobban (2011a) and Cobban and Hook (1980), respectively. The earliest figured fossil from the Fite Ranch Sandstone at Carthage is the ammonite *C. colleti* in Hyatt (1903).

The **D-Cross Tongue of the Mancos Shale**, 85 m thick (Fig. 34A), is a mostly covered, poorly fossiliferous, noncalcareous, gray marine shale that forms valleys between the resistant ridges of the Fite Ranch Sandstone Member below and the Gallup Sandstone above (Fig. 43). Its base probably lies in the upper Turonian *Prionocyclus novimexicanus* Zone; its top is undetermined but lies below an occurrence of the early form of the late Turonian oyster "*Lopha*" *sannionis* (White) in the overlying Gallup Sandstone (Fig. 34A, D10360-61 level). This

occurrence probably places the top of the D-Cross in the uppermost Turonian *Forresteria peruana* Zone (Fig. 33). The upper contact of the D-Cross with the Gallup Sandstone is gradational and conformable; its lower contact with the Tres Hermanos is sharp and disconformable. The D-Cross Tongue was deposited during the last part of the T-2 transgression and the first part of the R-2 regression during the latest Turonian (Figs. 33 and 34A).

An 8-m-thick zone of large, septarian, cone-in-cone concretions 52 m above its base forms a distinct ridge in the valley developed in the poorly resistant D-Cross Tongue (Fig. 43). These concretions are sparsely fossiliferous but yield the late Turonian bivalve *Mytiloides incertus* (Jimbo) (Fig. 34A, D10248 level), probably indicative of the *Prionocyclus quadratus* Zone (Fig. 33). The long-ranging, late-Turonian ammonite *Placenticeras cumminsi* Cragin was collected from the top of the concretion zone (Fig. 34A, D10359 level). This thick zone of ridge-forming concretions is unique to the Carthage coal field in the Quebradas area.

A 1.3-m-thick interval near the base of the D-Cross is correlated with the **Juana Lopez Beds of the D-Cross Tongue** that were previously recognized farther to the north in the study area at JdM and SNWR (Hook and Cobban, 2013). This interval is composed primarily of shale and sandy shale but is bounded by thin calcarenites. The base of the Juana Lopez at Carthage is at a 2.5-cm-thick calcarenite (Fig. 44, unit 3), 1.6 m above the base of the tongue; its top, 1.3 m higher, is at a 3-cm-thick calcarenitic sandstone (unit 6). Fossils from the base of the Juana Lopez (Fig. 44, D14549 level) and from concretions just above the unit (Fig. 44, D14509/D14511 level) place it entirely in the upper Turonian *Prionocyclus novimexicanus* Zone (Fig. 33).

Hook and Cobban (2013) overlooked the Juana Lopez Beds in the Carthage coal field in their regional study of the Juana Lopez. Exposures of the Juana Lopez are limited at Carthage to two small localities, where the beds are preserved in shale hummocks on and just above the dip slope of Fite Ranch Sandstone (Fig. 45). These gray hummocks contrast sharply

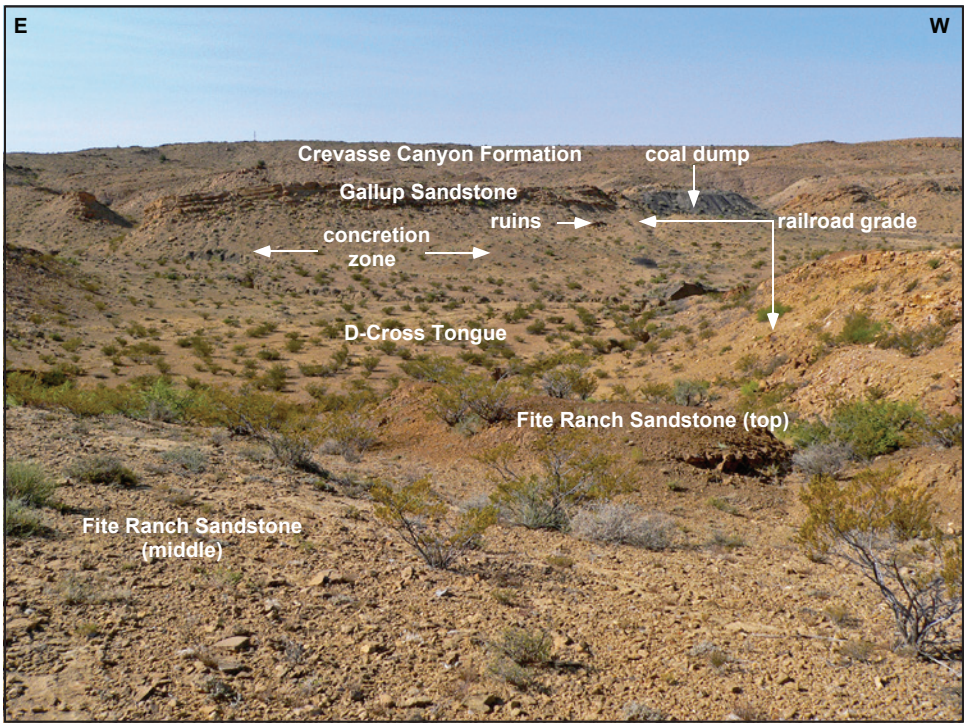

Figure 43. Typical, mostly covered valley developed in the D-Cross Tongue of the Mancos Shale between the resistant Fite Ranch Sandstone Member at the top of the Tres Hermanos Formation and the base of the Gallup Sandstone. This view, looking south in NE1/4, SW1/4 sec. 9, T. 5 S., R. 2 E., Cañon Agua Buena 7.5-minute quadrangle, shows that the resistant zone of large concretions, which developed just above the middle of the D-Cross, forms a persistent ridge. The abandoned railway line brought coal from the Emersion-Allaire mine to the New Mexico Midland Railway, which transported it 16 km east to San Antonio, New Mexico (Eveleth, 2015).

with the dark brown sandstone at the top of the Fite Ranch Sandstone. Figure 44 is the graphic section of the hummock shown as Figure 45.

The basal 1.5 m of the D-Cross is a noncalcareous, gray shale devoid of concretions, bentonites, and fossils (Fig. 44, unit 1). Fossils collected from the dark-brown sandstone at the top of the Fite Ranch Sandstone contain numerous phosphatic ooids, suggesting there is an unconformity between the Fite Ranch and the D-Cross (Fig. 44, D11161 and D14385 levels).

This noncalcareous shale (Fig. 44, unit 1) is succeeded by a 3-cm-thick bentonite (unit 2), capped by a 2.5-cm-thick interval of interbedded thin calcarenites and quartzose sandstones (unit 3) that marks the base of the Juana Lopez. The basal 1 cm of unit 3 is a thin-bedded, dark-brown calcarenite that contains abundant shell fragments of an inoceramid that is probably *Inoceramus perplexus* Whitfield (Fig. 44, D14549 level); these fragments have finer ornamentation and lack the geniculation of the older *I. dimidius* White (Fig. 34A, D14562 level). (Note: Geniculation involves an abrupt change in slope

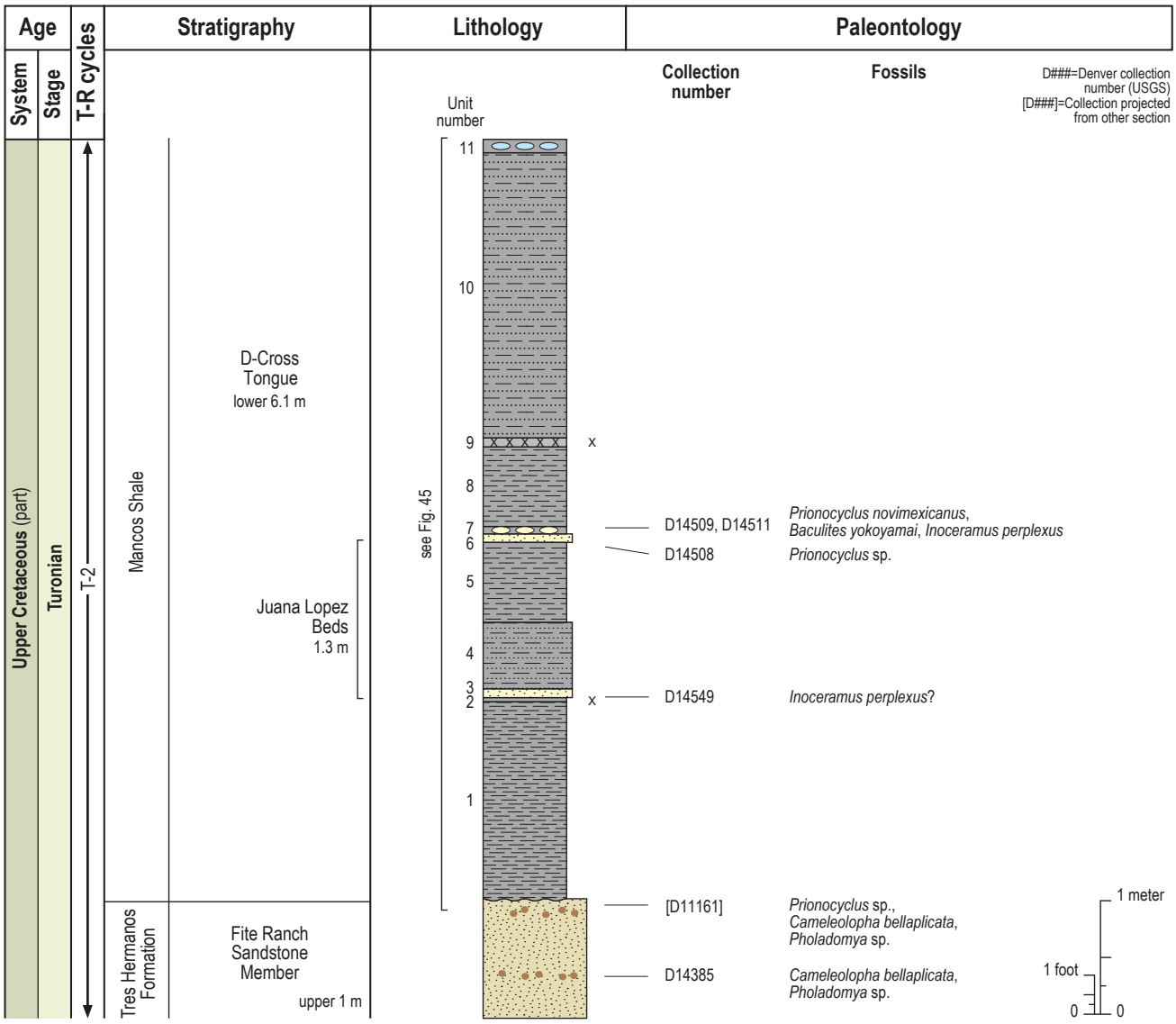

Figure 44. Graphic section of the basal part of the D-Cross Tongue of the Mancos Shale in the Carthage coal field showing positions of fossil collections and the Juana Lopez Beds. The section was measured in SW1/4, NW1/4, SW1/4 sec. 9, T. 5 S., R. 2 E., Cañon Agua Buena 7.5-minute quadrangle. See Figure 45 for a picture of this outcrop. See Figure 34B for key.

of the bivalve shell at maturity and, in the case of *I. dimidius*, a loss of or reduction in ornamentation.) The basal calcarenitic beds of the Juana Lopez are succeeded by 1.2 m of unfossiliferous shaly beds (units 4 and 5).

The sixth unit (Fig. 44, unit 6), a 3-cm-thick, very thin-bedded, calcarenitic sandstone, marks the top of the Juana Lopez and contains fragments of a large prionocyclid, *Prionocyclus* sp. Pancake-shaped limestone concretions (unit 7) in the shale just above this sandstone preserve numerous internal molds of *Prionocyclus novimexicanus* (Marcou) and *Inoceramus perplexus* (Fig. 44, D14509/14511 level). Many specimens of *P. novimexicanus* are body chambers of large individuals filled with the aligned internal molds of the straight ammonite *Baculites yokoyamai* Tokunaga and Shimizu, apparently washed in by currents. A 10-cm-thick bentonite (unit 9) is present 0.6 m above the concretions and is followed by 2 m of unfossiliferous, sandy shale. The hummock is capped by a 15-cm-thick bed of unfossiliferous limestone concretions (unit 11).

The top of the Tres Hermanos Formation at Carthage is probably in the upper part of the *Prionocyclus macombi* Zone, whereas the entire Juana Lopez is in the *P. novimexicanus* Zone (Fig. 33). The 1.5 m of unfossiliferous shale separating these two units could represent the entire *P. wyomingensis* Zone or could include portions of the underlying *P. macombi* Zone or the overlying *P. novimexicanus* Zone, or both. At a minimum, this interval of shale records a condensed succession. However, an erosional unconformity is interpreted at the top of the Fite Ranch Sandstone in Figures 33, 34A, and 44 because of evidence for erosion at this level to the north (discussed in detail in the next sections on JdM and SNWR) and the presence of phosphatic ooids in the uppermost Fite Ranch Sandstone at Carthage.

The **Gallup Sandstone** at Carthage is a coarsening-upward, coastal barrier sandstone that is 20 m thick (Fig. 34A). The Gallup was deposited near the middle of the R-2 regression during the latest Turonian (Figs. 33 and 34A). The R-2 regression, according to Molenaar (1983a, p. 201) "…appears to be unique to New Mexico and northeastern Arizona."

Both the base and top of the Gallup Sandstone at Carthage are conformable contacts. Its lower contact is gradational and its upper contact is sharp (Fig. 46). The only datable fossil collected from the Gallup at Carthage came from its base, where the small, finely ribbed form of the oyster "*Lopha*" *sannionis* (White) was collected (Fig. 34A, D10361 level). This finely ribbed, small form of *L. sannionis* appears to be confined to the late Turonian. The base of the Gallup Sandstone at Carthage is placed in the uppermost upper Turonian *Forresteria peruana* Zone (Fig. 33) because of this collection and an occurrence of the bivalve *Mytiloides incertus* (Jimbo) from the *Prionocyclus quadratus* Zone in the upper one-third of the underlying D-Cross Tongue (Fig. 34A, D10248 level). The upper part of the Gallup is placed in the lower Coniacian (Figs. 33 and 34A).

This age interpretation is consistent with fossils collected to the south and north of Carthage. To the south, the youngest fossils collected from the top of the Gallup at Mescal Canyon near Truth or Consequences (Fig. 32) are from the upper Turonian *Prionocyclus germari* Zone (Hook et al., 2012); to the north, fossils from the Gallup on SNWR are from the basal Coniacian *Cremnoceramus deformis erectus* Zone (Hook et al., 2012).

The **Dilco Coal Member of the Crevasse Canyon Formation** at Carthage is 46 m thick and consists of continental shale, fluvial sandstone, and coal (Fig. 34A and 47). It was deposited in the earliest Coniacian, near the end of R-2 and the beginning of T-3. Both its base and top are conformable and sharp. There are no datable fossils in the continental Dilco Member, although petrified logs up to 10 m long are preserved 12 m above the base. The Carthage coal seam, up to 1.5 m thick, lies 7.3 m above the Gallup (Figs. 34A and 46); a second, much thinner coal bed is present near the contact with the overlying Mulatto Tongue of the Mancos Shale (Figs. 34A and 47).

The **Mulatto Tongue of the Mancos Shale** is a minimum of 13 m thick at the continuous Carthage "rift section" (Fig. 32, control point #3), where its upper contact is not exposed (Fig. 34A). The Mulatto was deposited at the end of the T-3 transgression and the beginning of the R-3 regression in the early Coniacian. Its basal contact is conformable with the underlying Dilco Member, above a thin carbonaceous shale to coaly bed. The only datable fossil from the Mulatto Tongue is the oyster *Flemingostrea elegans* Hook (Fig. 34A, D14559-60 levels), which is confined to the lower Coniacian and ranges from the *Cremnoceramus deformis erectus* Zone into the *Cremnoceramus crassus inconstans* Zone (Fig. 33).

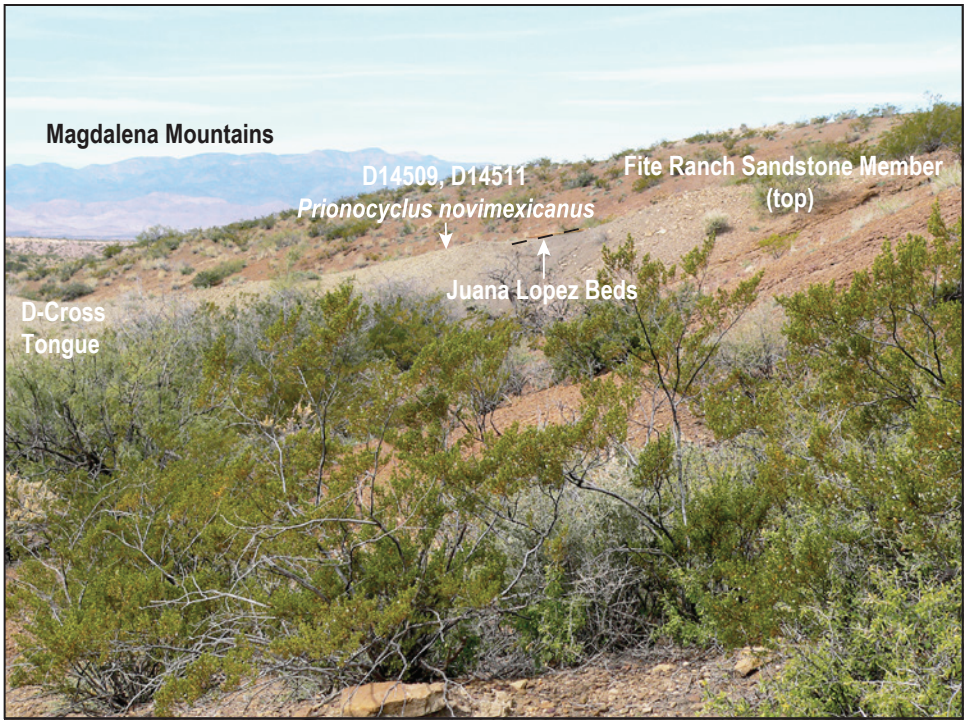

Figure 45. One of only two small exposures of the basal part of the D-Cross Tongue of the Mancos Shale in which the Juana Lopez Beds crop out in the Carthage coal field. View is to the west in SW1/4, NW1/4, SW1/4 sec. 9, T. 5 S., R. 2 E., Cañon Agua Buena 7.5-minute quadrangle. The contact with the underlying Fite Ranch Sandstone Member of the Tres Hermanos Formation is sharp and disconformable. The Juana Lopez Beds (dashed line) are poorly developed in the Carthage coal field, consisting of millimeter-thick beds of calcarenite at the base and the top that are separated by 1.3 m of gray, noncalcareous shale. See Figure 44 for graphic section. The Jacob staff is 1.5 m long.

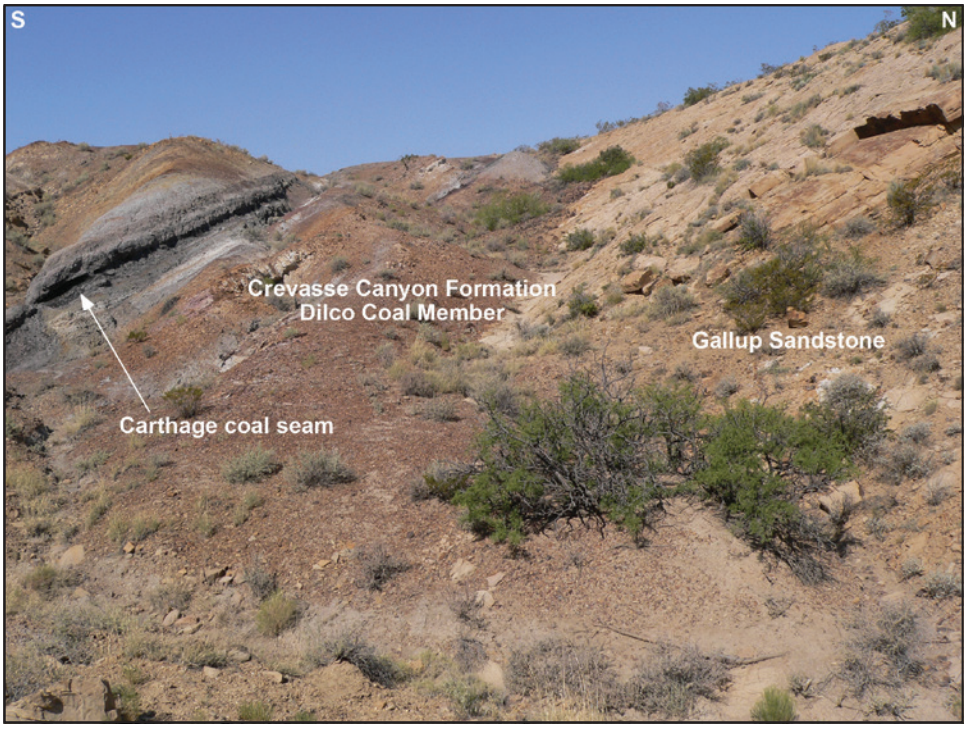

Figure 46. The only unmined outcrop of the Carthage coal seam, the Dilco Coal Member of the Crevasse Canyon Formation. The coal seam, which is 46 cm thick, is present 7.3 m above the sharp, conformable contact of the Dilco with the Gallup Sandstone. View is to the west in NE1/4, SW1/4 sec. 9, T. 5 S., R. 2 E., Cañon Agua Buena 7.5-minute quadrangle.

Near the ruins of old Carthage (Fig. 32, control point #2), a 1.3-m-thick marine sandstone is present 25 m below the *Flemingostrea*-bearing concretions near the base of the Mulatto Tongue (Fig. 47, D14480 level). This sandstone has been observed only at this stratigraphically "floating" section; i.e., it is an indeterminate distance above the Gallup Sandstone. However, this sandstone contains only Coniacian fossils, including the bivalve *Pleuriocardia curtum* (Meek) and the oysters "*Lopha*" *sannionis* and *Flemingostrea elegans*. This locality (D14857) is the only known occurrence of "*Lopha*" *sannionis* with *F. elegans* in the area and the only occurrence of *F. elegans* that is below the D14480 concretions and a coal bed, suggesting there was an earlier, minor incursion of the shoreline into the Carthage area before deposition of the Mulatto Tongue (see Hook [2010] for more detail).

Fossils from this third cycle of transgression–regression (T-3/R-3) at Carthage were recognized more than a century ago by Gardner (1910), then seemingly forgotten or ignored by later workers (including the present authors) until Hook (2010) rediscovered them in the field. Unfortunately, exposures of the Mulatto Tongue in the study area are so thin and discontinuous that they cannot be shown at the scale of the geologic map of the area. Instead, they were mapped with the Crevasse Canyon Formation (Plate 1, map unit Kcc). This omission in no way diminishes the importance of these rocks in deciphering the Late Cretaceous

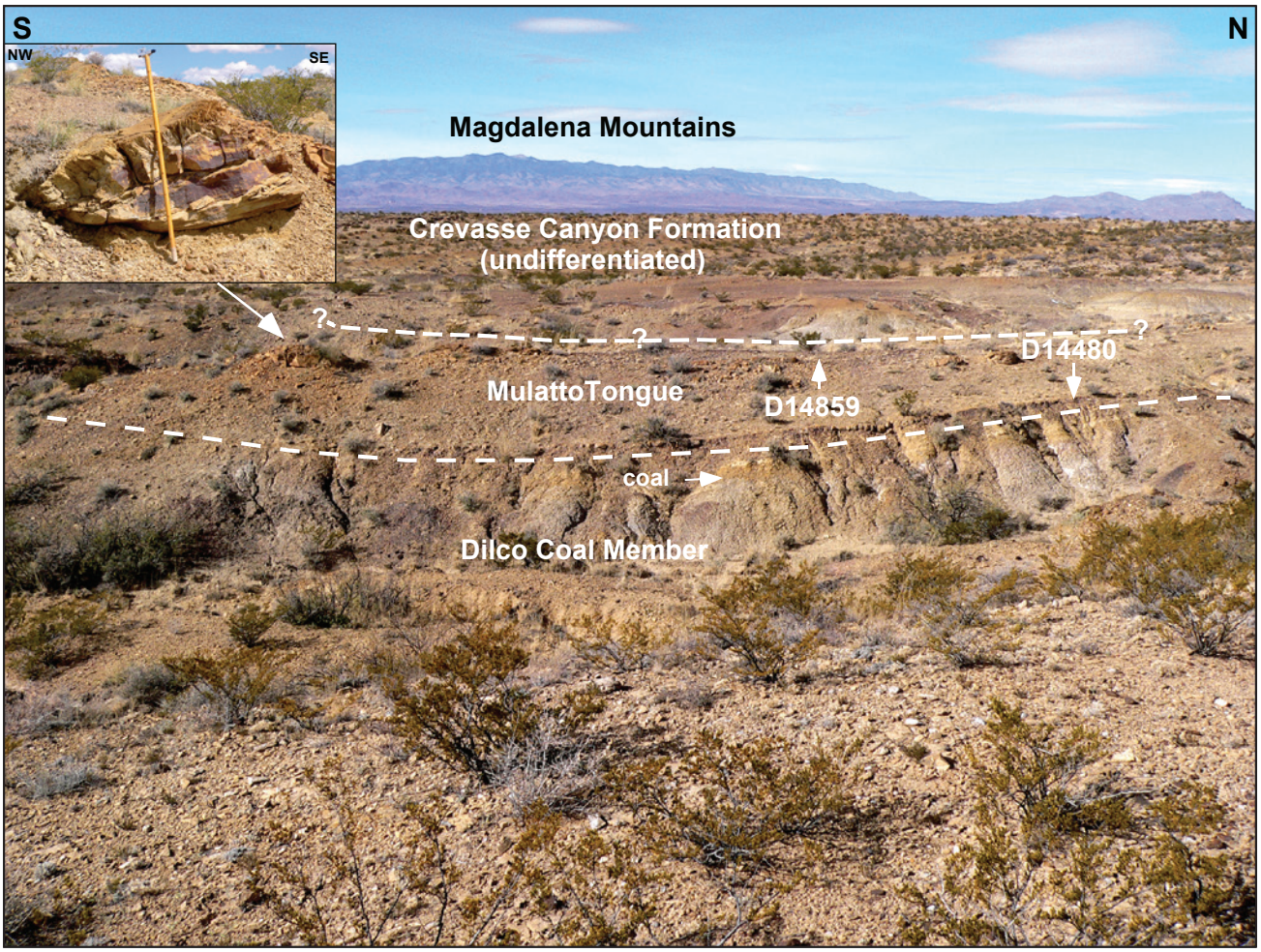

Figure 47. Panoramic view of the Mulatto Tongue of the Mancos Shale looking west from the ruins of the superintendent's house, Old Carthage, in SE1/4, NW1/4, NW1/4 sec. 15, T. 5 S., R. 2 E., Cañon Agua Buena 7.5-minute quadrangle. The base of the Mulatto is just below the D14480 collection that contains *Flemingostrea elegans* Hook; the top of the Mulatto is unconstrained lithologically but lies above the D14859 collection, which contains small marine bivalves. Inset photograph shows a large cone-in-cone concretion at the far left of the larger photo. The Jacob staff is 1.5 m long. These concretions are bedded in the lower part, with the cone-in-cone structures confined to the upper one-third (see Hook and Cobban [2010], fig. 8c, for a larger image).

history of west-central New Mexico. Age-equivalent rocks to the south in the Caballo Mountains near Truth or Consequences are continental (Seager and Mack, 2003), suggesting that the T-3 shoreline did not transgress that far to the south, making Carthage the southernmost known exposure of the Mulatto Tongue.

A lithologic aid to help distinguish the Mulatto Tongue from the D-Cross Tongue in stratigraphically isolated sections at Carthage and throughout the study area is a zone of large, cone-in-cone limestone concretions that developed in the lower portion of the Mulatto. However, the cone-in-cone structures are developed only in the upper part of the concretions; the lower one-half to one-third of the concretion is usually bedded (Fig. 47, inset). Concretions from lower in the succession in the D-Cross Tongue tend to be smaller and more regular in shape. The more spherical of the D-Cross concretions develop cone-in-cone structures throughout the concretion. Hook (2010, figs. 8C and 8D) illustrated both types of these cone-in-cone concretions.

A substantial (but unmeasured by us) thickness of continental, Upper Cretaceous rocks that are probably assignable to the **Gibson Coal Member of the Crevasse Canyon Formation** is present above the Mulatto Tongue at Carthage. Gardner (1910, p. 455) estimated that 183 m of tan sandstone and drab shale with traces of coal are present above what is now called the Mulatto Tongue at Carthage. Wilpolt and Wanek (1951, fig. 5, section 22) showed 302 m of Mesaverde Formation at Carthage. The Mesaverde part of their graphic section is the lithologic log from the Stackhouse No. 3 well in sec. 1, T. 5 S., R. 2 E., Cañon Agua Buena 7.5-minute quadrangle. Subtracting the thicknesses of the Gallup Sandstone, the Dilco Coal Member, and the Mulatto Tongue, which Wilpolt and Wanek (1951) included in the Mesaverde, yields a minimum thickness of 237 m for the Gibson. The only fossils known from the Gibson Member at Carthage are petrified wood, impressions of leaves and horsetails, and in situ petrified stumps from the upper one-third of the unit.

Note: Lucas et al. (2019, p. 19) proposed the Flying Eagle Canyon Formation for use in Sierra County, New Mexico, for the continental strata lying between the top of the Gallup Sandstone and the base of the Ash Canyon Formation. We had not planned to discuss the Flying Eagle Canyon Formation in this memoir because Lucas et al. (2019) applied it only to Sierra County. Therefore, their usage in Sierra County does not affect nomenclature used in Socorro County. If anything, usage in Socorro County should affect Sierra County. However, at the suggestion of memoir editor D. Koning, we are including a brief summary of our thoughts on that name as a formal, formational-rank unit.

The Flying Eagle Canyon Formation as defined encompasses continental strata that were deposited behind the retreating R-2 shoreline and, therefore, above the uppermost sandstone in the Gallup Sandstone. At Carthage, strata above the Gallup and below the base of the Mulatto Tongue of the Mancos Shale (Fig. 34A) have been assigned to the Dilco Coal Member of the Crevasse Canyon Formation. This is the accepted stratigraphic usage in the area (Molenaar, 1983a; Molenaar et al., 2002).

The contact between the Gallup Sandstone and the overlying continental rocks is diachronous: older to the south in Sierra County and younger in the north in Socorro County. Therefore, there could be differences in the architecture and composition of strata in the two areas, but that does not mean a new stratigraphic name is needed. In addition, Lucas et al. (2019, fig. A3.5) reported finding "oyster shells" at around 339 m above the top of the Gallup Sandstone at Mescal Canyon. This find is significant because it indicates that brackish water conditions, at a minimum, existed in Sierra County and that a shoreline was nearby to the north. The question of whether this oyster bed represents the T-3 transgression is unresolved according to Lucas et al. (2019, p. 21), but the presence of the oysters suggests marine influence. The T-3 transgression is the most likely choice among the younger shorelines.

Lucas et al.'s (2019) oyster bed is considerably higher in the stratigraphic section in Mescal Canyon than the Mulatto Tongue is at Carthage, where it is 46 m above the Gallup. However, the upper contact of the Flying Eagle Canyon Formation would also be diachronous if the oyster bed represents the T-3 transgression: older to the north and younger to the south. The two diachronous contacts could account for the thickness difference. We believe there is enough evidence that the oyster bed represents the T-3 transgression that it would have been prudent to use the name Crevasse Canyon Formation in Sierra County or, at the very least, to use Flying Eagle Canyon formation as an informal unit.

Jornada del Muerto Coal Field

Cretaceous rocks in the Jornada del Muerto coal field (JdM) lie approximately 30 km northeast of Carthage (Tabet, 1979). Only the northwestern part of the field is included in the study area, in the eastern part of the Bustos Well 7.5-minute quadrangle (Fig. 32, control point #4). Strata there are similar to those at Carthage and are assigned to the same major stratigraphic units, in ascending order: Dakota Sandstone, Tokay Tongue of the Mancos Shale, Tres Hermanos Formation, D-Cross Tongue of the Mancos Shale, Gallup Sandstone, Dilco Coal Member of the Crevasse Canyon Formation, Mulatto Tongue of the Mancos Shale, and Gibson Coal Member of the Crevasse Canyon Formation (Fig. 33). All strata above the D-Cross Tongue were mapped into a single undivided unit (Plate 1, map unit Kuu). Tabet (1979) mapped these Kuu strata as Mesaverde Group. The Cretaceous rocks on JdM from the base of the Dakota Sandstone to the top of the measured Mulatto Tongue of the Mancos Shale are 407 m thick (Fig. 48).

Although the rocks on the JdM are similar to those at Carthage, the ages of some of the units differ; e.g., the age of the basal marine section is older at JdM than at Carthage. In addition, calcarenites assigned to the Juana Lopez Beds are well developed at JdM at the base of the D-Cross Tongue but are poorly developed at Carthage.

The graphic section of the Upper Cretaceous at JdM (Fig. 48), from the upper part of the Dakota Sandstone through the lower part of the Mulatto Tongue of the Mancos Shale, is based on the section described by Tabet (1979, appendix 1). Stratigraphic units measured or remeasured for this memoir include (1) the upper part of the Dakota Sandstone, (2) the Tokay Tongue of the Mancos Shale, (3) the Juana Lopez Beds of the D-Cross Tongue of the Mancos Shale, (4) the Dilco Coal Member of the Crevasse Canyon Formation, and (5) the Mulatto Tongue of the Mancos Shale. The stratigraphic units present at JdM are discussed briefly below; see discussions of these units in the section on the Carthage coal field for lithologic detail. There are 28 USGS Mesozoic invertebrate fossil localities (Denver) from JdM. Darton (1928, p. 76) made the first recorded fossil collection (USGS W9764) from JdM in 1916.

The **Dakota Sandstone** attains a maximum thickness of 23 m at the north end of the Upper Cretaceous outcrop. To the south, the Dakota is generally less than 3 m thick and consists of a medium-brown, ridge-forming quartzite. A 10-cm-thick phosphatic nodule-bed (Fig. 48, D14472 level), 3.4 m below the top of the unit, preserved a single, flattened, internal mold of the earliest middle Cenomanian ammonite *Conlinoceras tarrantense* (Adkins). This occurrence marks the farthest south that *C. tarrantense* has been found in New Mexico and constrains the southern shoreline of Seboyeta Bay (Fig. 32) to a position between JdM and Carthage, where the oldest fossils are from the lower middle Cenomanian zone of *Acanthoceras bellense* (Fig. 34A, D14726 level).

A 5-cm-thick sandstone that is 1.1 m higher in the section yielded the ammonite *Plesiacanthoceras muldoonense* (Cobban and Scott) (Fig. 48, D14469-70 level), only the fourth known occurrence of the species outside its type locality near Pueblo, Colorado (Cobban and Scott, 1972). This species is indicative of the middle Cenomanian *Plesiacanthoceras muldoonense* Zone. The helically coiled ammonite *Turrilites scheuchzerianus* Bosc (Fig. 48, D14470 level) is present in the sandstone immediately above and is probably from the same zone.

A 1-m-thick sandstone just below the top of the Dakota preserved abundant, disarticulated valves of the oyster *Ostrea beloiti* Logan and the helical ammonite *Turrilites acutus* Passy, marking the beginning of the *Acanthoceras amphibolum* Zone (Figs. 33 and 48, D14384 level).

The upper contact of the Dakota Sandstone with the Tokay Tongue of the Mancos Shale is sharp but conformable. Its lower contact with the Triassic Chinle Formation is sharp and disconformable. Marine units in the upper Dakota Sandstone at JdM were deposited during the early part of T-1 (Figs. 33 and 48).

The **Tokay Tongue of the Mancos Shale** is best exposed near the north end of the JdM outcrop belt, where it is 155 m thick (Fig. 32, control point #4). There (Fig. 48), the tongue is subdivided into five bed-rank units that are similar lithologically to those at Carthage (Fig. 34A), although generally of different proportions and ages. These bed-rank units are, in ascending order, (1) noncalcareous shale and sandstone beds, 11 m thick; (2) shale and bentonite beds, 45 m thick; (3) Bridge Creek Limestone Beds,

19 m thick; (4) calcareous shale beds, 32 m thick; and (5) noncalcareous shale beds, 48 m thick. Only the Bridge Creek Limestone is a formally named stratigraphic unit.

The 11-m-thick **noncalcareous shale and sandstone beds** contain two bentonites and are capped by 3 m of sandy beds that contain the bivalve *Inoceramus arvanus* Stephenson and the oyster *Ostrea beloiti* Logan (Fig. 48, D14732 level), indicative of the *Acanthoceras amphibolum* Zone. This unit was deposited during the early part of T-1.

The 41-cm-thick bentonite at the base of the 45-m-thick **shale and bentonite beds** correlates with the x-bentonite because of its thickness and stratigraphic position in the *Acanthoceras amphibolum* Zone. This bentonite is the thickest in the study area and the lowest of the 12 bentonites measured in this bed-rank unit. Many more bentonites in this unit are exposed in arroyos, but they cannot be tied into the measured section with precision because this all-shale unit lacks other stratigraphic markers. The basal one-third of this unit is noncalcareous shale and the upper two-thirds are calcareous. No fossils were observed in this unit. It was deposited during the last part of T-1 (Fig. 48).

The distinctive nodular limestones of the 19-m-thick **Bridge Creek Limestone Beds** begin 56 m above the Dakota Sandstone. Although not as fossiliferous as those at Carthage, the three thin limestones at the base of the Bridge Creek at JdM contain the baculite *Sciponoceras gracile* (Fig. 48, D14733 level) and the echinoid *Mecaster batnensis* (Fig. 48, D10130 level), indicative of the upper Cenomanian *Euomphaloceras septemseriatum* Zone (Fig. 33). The oyster *Pycnodonte newberryi* (Fig. 48, D14734-35 level) is common in shales between the limestones. A 10-cm-thick, white, thin-bedded limestone, 5 m above the base of the Bridge Creek, contains the bivalve *Mytiloides puebloensis* (Fig. 48, D14736 level) and marks the Cenomanian–Turonian boundary. Calcarenites at the top of Bridge Creek Limestone contain the bivalve *M. mytiloides* (Fig. 48, D14737 level), just as they do at Carthage. No bentonites were observed in the Bridge Creek on JdM. The basal limestones in the unit were deposited at maximum transgression of T-1; the rest of the unit was deposited during the early part of R-1 (Fig. 48).

The 32-m-thick **calcareous shale beds** are macroscopically unfossiliferous and extend to a 5-cm-thick, white bentonite, similar to the same bed-rank contact at Carthage. Weakly calcareous shale extends about 1.5 m above the bentonite. This unit was deposited during R-1.

The 48-m-thick **noncalcareous shale beds** are only slightly more fossiliferous than the calcareous shale beds. Concretions near the base (Fig. 48, D14738 and D10260 levels) preserve internal molds of the large ammonites *Morrowites depressus* (Powell) and *Hoplitoides* cf. *H. koeneni* Solger, together indicative of the middle Turonian *Collignoniceras woollgari woollgari* Subzone. Concretions near the top preserve a coquina of the oyster *Crassostrea* aff. *C. subtrigonalis* (Evans and Shumard) (Fig. 48, D14739 level). The contact with the overlying Atarque Sandstone Member of the Tres Hermanos Formation is abrupt but conformable. This unit was deposited about midway through R-1.

The **Tres Hermanos Formation** at JdM is similar to that at Carthage. It is 75 m thick and comprises three members, in ascending order: the Atarque Sandstone Member, 24 m thick; the Carthage Member, 38 m thick; and the Fite Ranch Sandstone Member, 13 m thick (Fig. 48). The base of the Tres Hermanos is in the *Collignoniceras woollgari woollgari* Subzone (Fig. 48, D10254 level); the top is probably in the *Prionocyclus macombi* Zone (Fig. 33). The Tres Hermanos Formation was deposited during the last part of R-1 and the first part of T-2. Its contact with the underlying Tokay Tongue is sharp and conformable; its contact with overlying D-Cross Tongue is sharp and probably disconformable.

Sandstone concretions from near the base of the **Atarque Sandstone Member** contain *Collignoniceras woollgari woollgari* (Fig. 48, D10254 level), just as they do at Carthage. The D11603 collection made in 1978 from the upper part of the **Carthage Member** contains the marine oyster *Cameleolopha bellaplicata* (Fig. 48, D11603 level). This collection was the first evidence that the upper part of the Carthage Member was deposited in brackish to marine water. Later collections from about this level at Carthage and near SNWR contain ammonites and confirm a marine origin for the uppermost Carthage Member.

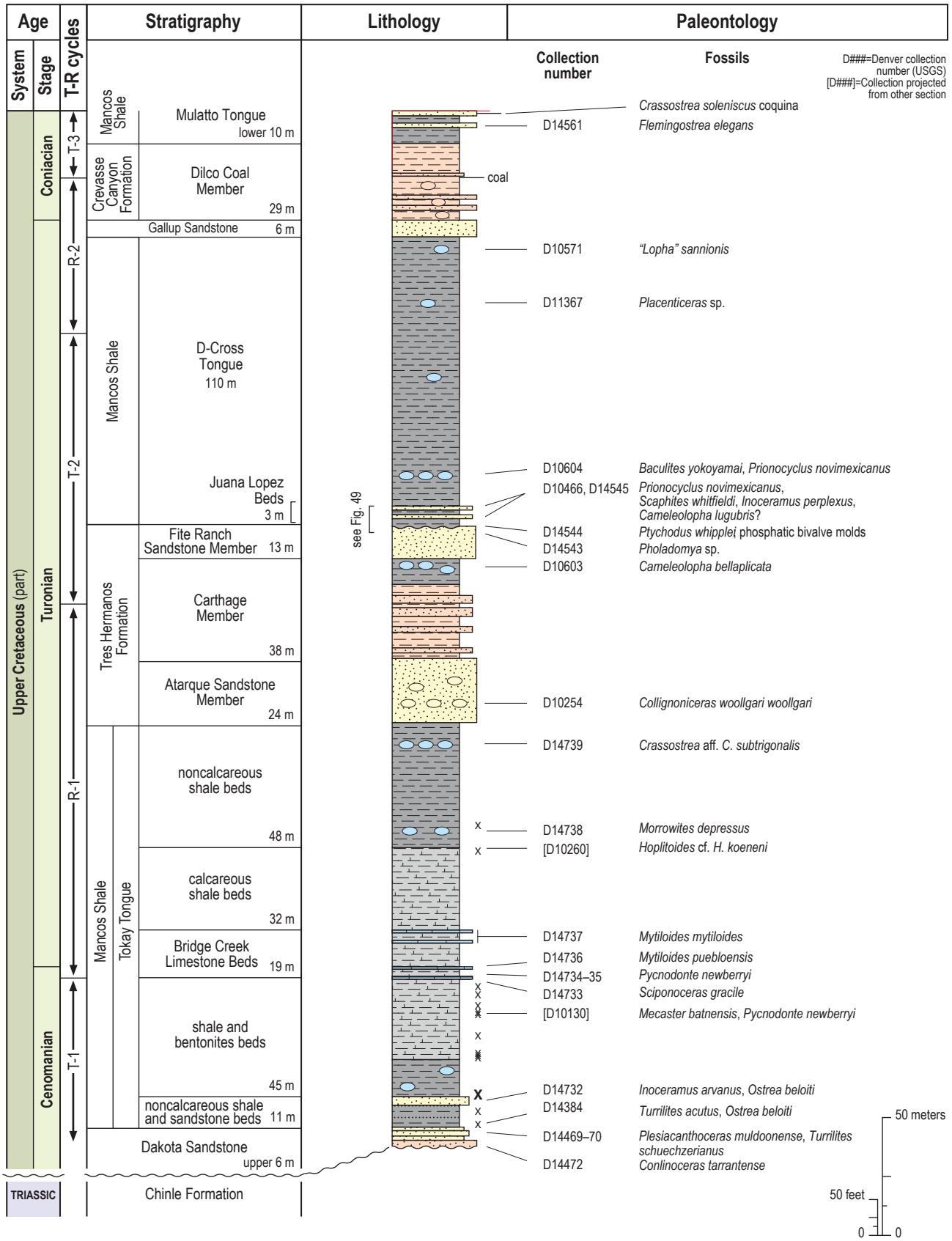

Figure 48. Graphic section of Upper Cretaceous strata of the Jornada del Muerto coal field (**JdM**) from the Dakota Sandstone through the Mulatto Tongue of the Mancos Shale showing positions of fossil collections. The section (Fig. 32, control point #4) was measured in SE1/4 sec. 19 and NE1/4 sec. 30, T. 2 S., R. 3 E., Bustos Well 7.5-minute quadrangle. The section is modified from Tabet (1979). See Figure 34B for key.

The **Fite Ranch Sandstone Member** on JdM is poorly fossiliferous, in contrast to Carthage. No impressions or shells of the oyster *Cameleolopha bellaplicata* were observed in the Fite Ranch. Only a single internal mold of the infaunal bivalve *Pholadomya* sp. (Fig. 48, D14543 level) was collected from the uppermost bed of the member. At Carthage, internal molds of this bivalve, in association with *Prionocyclus macombi*, litter the outcrop. Placement of the Fite Ranch in the *Prionocyclus macombi* Zone is based on collections of *Cameleolopha bellaplicata* below the member and the specimen of *Pholadomya* sp. at its top (Fig. 48, D14543 level).

The **D-Cross Tongue of the Mancos Shale** is 110 m thick and is composed primarily of noncalcareous, gray shale with subsidiary thin calcarenites at the base and limestone concretions scattered near the base and top (Fig. 48). The calcarenites are correlated with the Juana Lopez Beds; the rest of the tongue is not subdivided. The base of the tongue probably lies in the middle Turonian *Prionocyclus macombi* Zone, and the top is close to the Turonian–Coniacian boundary. The stratigraphically highest datable fossil is *P. novimexicanus* (Fig. 48, D10604 level) from limestone concretions 19 m above the base of the tongue. The oyster "*Lopha*" *sannionis* (Fig. 48, D10571 level) is present in limestone concretions about 5 m below the top, implying that the tongue at that level is still in the upper Turonian. The D-Cross was deposited during the last part of T-2 and the first part of R-2. Its contact with the underlying Tres Hermanos is sharp and disconformable; its contact with overlying Gallup Sandstone is sharp but conformable.

Worn internal molds of small bivalves—some phosphatized, others of sandstone composition—and numerous teeth of the shark *Ptychodus whipplei* at the base of the tongue suggest an unconformity (Fig. 48, D14544 level, and Fig. 49, D14544 level). The matrix-free bivalve molds required erosion from the underlying sandstone before phosphatization on the seafloor. The base of the Juana Lopez Beds, 2.6 m higher stratigraphically, carries a *Prionocyclus novimexicanus* fauna (Fig. 49, D10466 and D14545 levels). The absence of fossils representing the *Prionocyclus wyomingensis* Zone, which is present to the north on SNWR at the base of the Juana Lopez Beds, also indicates a loss of section. Hence, an erosional unconformity is shown in Figures 48 and 49.

The presence of relatively thick, ledge-forming calcarenites near the base of the D-Cross on JdM differentiates it lithologically from the D-Cross at Carthage (Figs. 34 and 45). The **Juana Lopez Beds of the D-Cross Tongue of the Mancos Shale** at JdM (Figs. 48 and 49) are 3.1 m thick and begin 2.6 m above the top of the Tres Hermanos Formation. They comprise two sets of thin-bedded calcarenites separated by up to 3 m of noncalcareous, gray shale. The lower calcarenite at the measured section is 10 cm thick, weathers rusty brown, and is fossiliferous. The upper calcarenite is also 10 cm thick, but it weathers brownish-orange and is less fossiliferous. Both calcarenites preserve a *Prionocyclus novimexicanus* Zone fauna (Fig. 49, D10466 and D14545 levels).

Both the basal and upper calcarenites of the Juana Lopez Beds contain impressions of the ammonites *Prionocyclus novimexicanus* (Marcou) and *Scaphites whitfieldi* Cobban along with internal molds and impressions of the bivalve *Inoceramus perplexus* Whitfield (Fig. 49, D10466 and D14545 levels)—all indicative of the upper Turonian *Prionocyclus novimexicanus* Zone (Fig. 33). In addition, the lower calcarenite yielded one left valve of a small, coarsely ribbed oyster with a large attachment scar. This specimen is referred questionably to *Cameleolopha lugubris* (Conrad) (D14545 level). The presence of this single specimen of *C. lugubris*? indicates that the base of the lower calcarenite was deposited at or very near the end of the time represented by the underlying middle Turonian *Prionocyclus wyomingensis* Zone, which is the upper limit of the known stratigraphic range of *Cameleolopha lugubris*.

This 3.1-m-thick section of the Juana Lopez Beds on JdM contrasts with the thick sections of Juana Lopez in the San Juan Basin. At its reference section in the San Juan Basin, 192 km to the northwest of JdM, the Juana Lopez is 33 m thick and spans the upper part of the middle Turonian *Prionocyclus macombi* Zone through the lower part of the upper Turonian *P. novimexicanus* Zone (Hook and Cobban, 2013; Fig. 33). Faunally, the entire Juana Lopez at JdM correlates with only the upper 1.5 m of the Juana Lopez at its reference section.

The calcarenites in the Juana Lopez on JdM vary laterally over short distances. The thickness of the lower ledge-forming calcarenite varies along strike from 10 to 46 cm. The composition of this ledge-forming unit varies from 100% calcarenite to two thin calcarenites separated by up to 30 cm of shale. The upper calcarenite varies from 5 to 20 cm in thickness. The base of the upper calcarenite appears to be an erosion surface; in places, it rests directly on the lower calcarenite. Where the upper ledge-forming calcarenite crops out, it varies from 0 to 3 m above the lower calcarenite. This variation suggests that the upper calcarenite was deposited on an erosion surface. The interval between the two calcarenites is generally covered.

The 2.6 m of shale separating the Juana Lopez from the Tres Hermanos on JdM represents the upper part of the *Prionocyclus macombi* Zone and all or most of the *P. wyomingensis* Zone. How much of those zones is represented by the erosional unconformity between the Tres Hermanos and the D-Cross cannot be determined (Fig. 33). However, fossils from the *P. wyomingensis* Zone are present in the Juana Lopez Beds of the D-Cross Tongue on SNWR, 16 km to the northwest (Fig. 32, control point #7).

The Juana Lopez Beds crop out only locally in JdM, primarily because the D-Cross Tongue is mostly covered by colluvium. Generally, only the basal calcarenite is exposed. Occasionally, both the upper and lower calcarenites are exposed by channeled erosion along the traces of small displacement, east–west, normal faults that form (dry) water gaps through the lower D-Cross Tongue into the upper part of the Tres Hermanos Formation. Outcrop photographs of the Juana Lopez on JdM can be found in Hook and Cobban (2013).

The **Gallup Sandstone** on JdM is a yellow-weathering, fine-grained, coarsening upward, unfossiliferous, 6-m-thick sandstone that forms a minor ridge at the top of the D-Cross Tongue. C.M. Molenaar (personal communication, 1982) described the Gallup on JdM as a "regressive sandstone, not well developed." The age of the Gallup is bracketed by the late Turonian fossil "*Lopha*" *sannionis* in the upper part of the underlying D-Cross Tongue and the early Coniacian fossil *Flemingostrea elegans* from the Mulatto Tongue, 29 m higher (Fig. 48, D10571 and D14561 levels). Based on regional considerations in the study area, the Turonian–Coniacian boundary is assumed to fall near the top of the Gallup (Fig. 48).

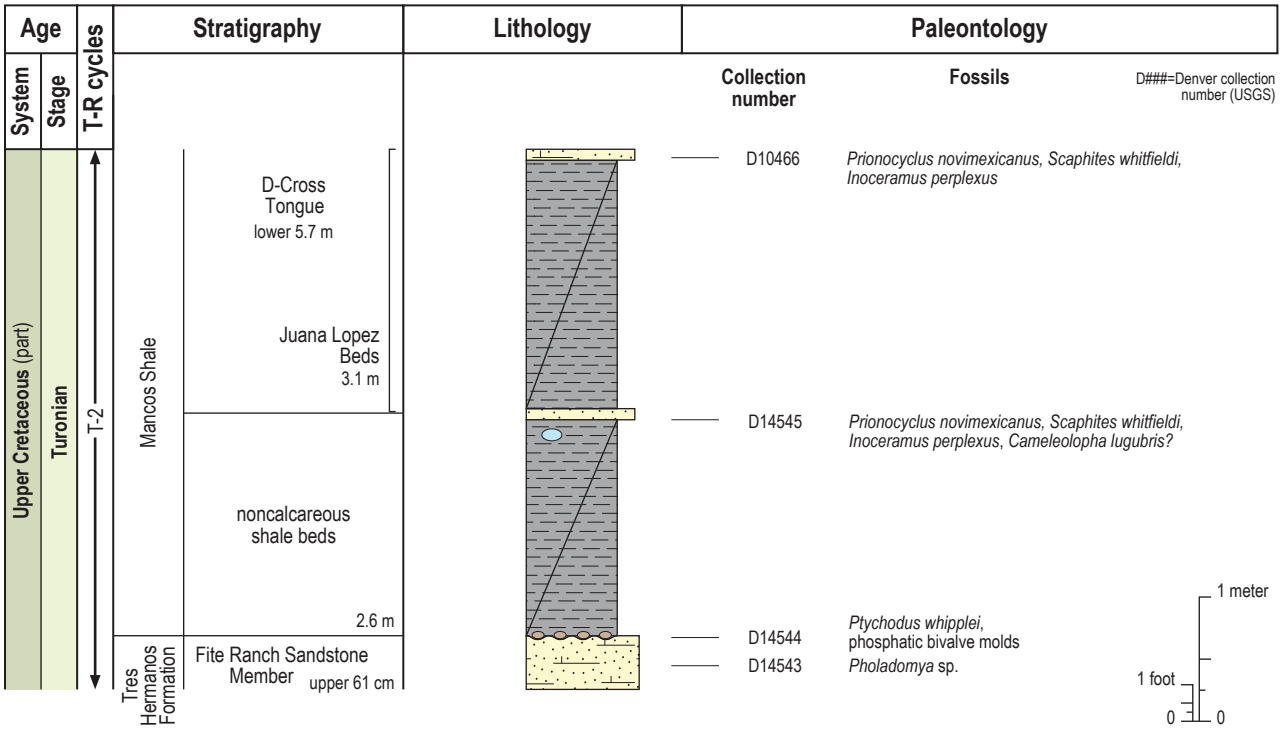

Figure 49. Graphic section of the basal part of the D-Cross Tongue of the Mancos Shale in the Jornada del Muerto coal field (**JdM**) showing positions of fossil collections and the Juana Lopez Beds. The section was measured in N1/4, SW1/4 sec. 5, T. 3 S., R. 3 E., Bustos Well 7.5-minute quadrangle. Modified from Hook and Cobban (2013). See Figure 34B for key.

The Gallup was deposited during the waning part of R-2. Both its base and top are sharp and conformable.

The **Dilco Coal Member of the Crevasse Canyon Formation** is 29 m thick and composed of continental sandstone, shale, and coal. The main coal seam is present 16 m above the base of the Dilco and is 60 cm thick at the measured section (Fig. 48). The Dilco Coal Member was deposited during the waning phase of R-2 and the early part of T-3; both upper and lower contacts are conformable.

The **Mulatto Tongue of the Mancos Shale** is a minimum of 10 m thick on JdM (Fig. 48). It is composed primarily of gray, noncalcareous shale that is generally concealed. A thin sandstone, 3 m below the measured top of the tongue, contains the early Coniacian oyster *Flemingostrea elegans* (Fig. 48, D14561 level). A thin, sandy coquina of the brackish-water oyster *Crassostrea soleniscus* (Meek) is the last unit exposed in the area of the measured section. The Mulatto Tongue was deposited during the last part of T-3 and the first part of R-3. The base of the Mulatto is a conformable shale-on-shale contact; its upper contact is covered.

Sevilleta National Wildlife Refuge

Within the mapped area, the Upper Cretaceous rocks on and south of the Sevilleta National Wildlife Refuge (SNWR) are identical in terms of stratigraphic nomenclature to those at Carthage and JdM. They consist of, in ascending order, the Dakota Sandstone, the Tokay Tongue of the Mancos Shale, the Tres Hermanos Formation, the D-Cross Tongue of the Mancos Shale, the Gallup Sandstone, the Dilco Coal Member of the Crevasse Canyon Formation, the Mulatto Tongue of the Mancos Shale, and the Gibson Coal Member of the Crevasse Canyon Formation. Cretaceous rocks on SNWR, from the base of the Dakota Sandstone to the top of the measured part of the Mulatto Tongue of the Mancos Shale, are an estimated 448 m thick (Fig. 50).

Many differences are present between the stratigraphic section on SNWR and those to the south. The base of the Dakota Sandstone on SNWR is lower by three zones than at Carthage, the regressive Atarque Sandstone Member of the Tres Hermanos Formation is higher by a subzone than at Carthage and JdM, and the transgressive Fite Ranch Sandstone Member is lower by a zone, as are the Juana Lopez Beds of the D-Cross Tongue of the Mancos Shale. The Dakota Sandstone on SNWR contains one of the most complete middle Cenomanian ammonite successions in the Western Interior region. Phosphatic beds are developed at three stratigraphic levels on SNWR and are important in decoding the geologic history of the area, especially the ages of the Dakota Sandstone and the Fite Ranch Sandstone Member.

There are 38 USGS Mesozoic invertebrate fossil localities from the mapped Mesa del Yeso quadrangle and an additional 58 from three nearby quadrangles on SNWR. Darton (1928, p. 76) made the first fossil collection (USGS W8312) from SNWR in 1913. The last fossil collection (D15604) was made in 2019, although fossils continue to be collected from previously measured sections.

Normal faults are so extensive on SNWR that assembling a composite Upper Cretaceous section for SNWR with adequate biostratigraphic control required examination of rocks in three additional 7.5-minute quadrangles. These quadrangles are La Joya (de Moor et al., 2005), Becker SW (Allen et al., 2013b), and Ladron Peak (Read et al., 2007). In addition, 6 km north of the mapped area in the adjacent La Joya quadrangle, the Twowells Tongue of the Dakota Sandstone splits the Tokay Tongue of the Mancos Shale into two formally named tongues, the Whitewater Arroyo Tongue, below, and the Rio Salado Tongue, above (Fig. 50, right side of column).

The small-scale graphic section for SNWR (Fig. 50) is a composite. The Dakota Sandstone and lower part of the Tokay Tongue of the Mancos Shale were measured at the principal reference section (PRS) in the Mesa del Yeso quadrangle (Fig. 32, control point #7), and the upper part of the Whitewater Arroyo Tongue through the Mulatto Tongue was measured at the Cibola Canyon section (CCS) in the Becker SW quadrangle (Fig. 32, control point #9).

The Bridge Creek Limestone Beds of the Tokay Tongue, which are well developed and stand in topographic relief at Carthage and JdM, are poorly developed on SNWR. Only a single calcarenite bed, 15 cm thick, is present at CCS. However, it contains fauna indicative of the lower Turonian *Mammites nodosoides* Zone (Fig. 50, D10974 and D14590 levels), similar to the uppermost calcarenites at Carthage (Fig. 34A, D5781-82 level) and JdM (Fig. 48, D14737 level). This single bed is labeled the Bridge Creek Limestone Bed in Figure 50.

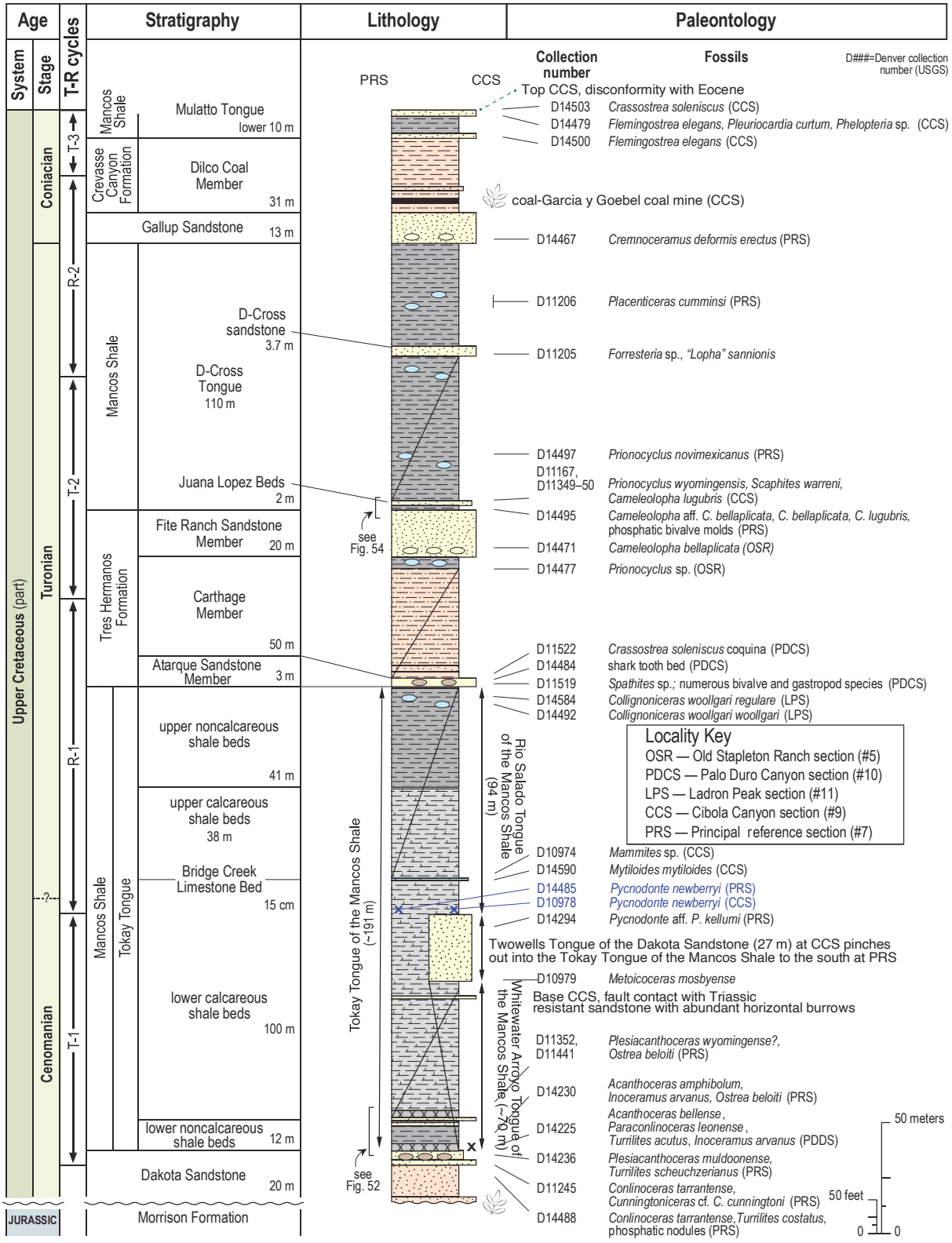

Figure 50. Graphic section of Upper Cretaceous strata on the Sevilleta National Wildlife Refuge (**SNWR**) from the Dakota Sandstone through the Mulatto Tongue of the Mancos Shale showing positions of fossil collections. The section is a composite of the principal reference section (**PRS**) and the Cibola Canyon measured section (**CCS**). The **PRS** extends from the base of the Dakota Sandstone to the middle of the Tokay Tongue and is modified from Hook and Cobban (2007). The **CCS** extends from the top of the Whitewater Arroyo Tongue to the top of the Dilco Coal Member and is modified from Hook (1983, 1984). The approximate positions of the two partial measured sections are shown in Figure 32; **PRS** is control point #7 and **CCS** is control point #9. The two measured sections are joined at the D14485 and D10978 levels (shown in blue), with the **PRS** below and the **CCS** above. See Figure 34B for key.

The scip zone limestones at the base of the Bridge Creek Limestone Beds, which are so conspicuous at Carthage and JdM, are not present in the Tokay Tongue in the Mesa del Yeso quadrangle. These limestones are also not present in the correlative part of the Rio Salado Tongue in the La Joya quadrangle, even though they appear prominently northwest of SNWR in the Acoma Basin in the type section of the Rio Salado Tongue about 10 m above the top of the Twowells Tongue (Hook et al., 1983, table 5). There are no thin nodular to concretionary limestones developed in this stratigraphic interval on SNWR to aid correlation. The oyster *Pycnodonte newberryi*, which is common at the base of the Bridge Creek at Carthage and JdM and in the basal part of the Rio Salado Tongue at its type section, is abundant in a thin zone at both PRS and CCS. The measured sections from these two localities were combined at the position of the first occurrence of *Pycnodonte newberryi* in each section (shown in blue in Fig. 50) to produce the composite section for SNWR.

The presence of abundant disarticulated shells of *P*. aff. *P. kellumi* (Fig. 50, D14294 level) in an interval 4 m below the first occurrence of *P. newberryi* (Fig. 50, D14485 level) at PRS indicates that this portion of the Tokay Tongue is stratigraphically complete (i.e., not faulted) and that the nodular limestones are simply not developed here. *Pycnodonte* aff. *P. kellumi* is the immediate ancestor of *P. newberryi* (Cobban, 1977a). At the "type" section of the intertongued Dakota/Mancos succession at Laguna, New Mexico (Fig. 32), *P.* aff. *P. kellumi* ranges from the top of the Twowells Tongue into the overlying calcareous shales but not into the Bridge Creek Limestone Beds, which contain abundant *P. newberryi* (Landis et al., 1973).

The **Dakota Sandstone** on SNWR is one of the more interesting and important units in the study area. The Dakota Sandstone was measured at three localities on SNWR (Fig. 32): the principal reference section (PRS; control point #7), the Two Butte section (TBS; control point #8), and the Palo Duro Canyon section (PDCS; control point #10). The Dakota Sandstone on SNWR preserves one of the most biostratigraphically complete successions of middle Cenomanian ammonites in the Western Interior (Hook and Cobban, 2007). In addition, the middle Cenomanian ammonite succession from *Conlinoceras tarrantense* through *Acanthoceras amphibolum* on SNWR is indicative of a condensed succession relative to that of better-known, coeval strata near Laguna, New Mexico, and near Pueblo, Colorado. At Laguna, 113 km to the northwest (Fig. 32), time-equivalent units in a section of intertongued Dakota Sandstone and Mancos Shale are 13 times thicker than at PRS. Near Pueblo, 418 km northeast and much farther offshore—where the strata should be thinner—they are five times thicker (Hook and Cobban 2007, fig. 9).

The ammonite succession within the Dakota Sandstone on SNWR was instrumental in firmly establishing the position of the *Acanthoceras bellense* Zone in the middle Cenomanian (Fig. 33). It took all three measured Dakota localities on SNWR to do this, however, because each locality lacked at least one of the zonal indices present at the other two (Fig. 51). In addition, fossils restricted to the *Acanthoceras granerosense* Zone, the second-oldest zone, have never been found outside the Pueblo, Colorado, area (Cobban and Scott, 1972), and *Plesiacanthoceras wyomingense*, guide to the uppermost middle Cenomanian zone, is a rare fossil in New Mexico and only questionably present in the Tokay Tongue of the Mancos Shale at PRS (Figs. 50 and 51).

The ammonites *Conlinoceras tarrantense*, *Acanthoceras granerosense*, *Plesiacanthoceras muldoonense*, and *Acanthoceras amphibolum* have been used as guides to the middle Cenomanian since

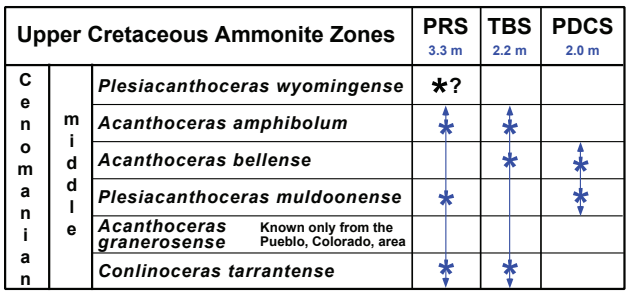

Figure 51. Distribution of middle Cenomanian index ammonite species collected from the Dakota Sandstone (arrowed lines) on Sevilleta National Wildlife Refuge (**SNWR**). Localities, from south to north on the east side of SNWR, are the principal reference section (**PRS**; Fig. 32, control point #7), Two Butte section (**TBS**; Fig. 32, control point #8), and Palo Duro Canyon section (**PDCS**; Fig. 32, control point #10). Index ammonites collected from each measured section are indicated by blue asterisks. The total thickness of the arrowed zones in the Dakota Sandstone at each measured section is indicated. (*Plesiacanthoceras wyomingense*[?] was collected from the Tokay Tongue of the Mancos Shale.) Modified from Hook (2016).

Cobban and Scott (1972, table 4). *Acanthoceras bellense* was inserted just above *Plesiacanthoceras muldoonense* by Cobban (1987a). Cobban (1987a, p. 24) qualified the addition of *Acanthoceras bellense* by saying that "…the position of this fossil in the middle Cenomanian acanthocerid sequence is not clear. … It seems likely that *A. bellense* lies some place between the zones of *[P.] muldoonense* and *[A.] amphibolum*."

The ammonite species collected at the three localities on SNWR are plotted against the middle Cenomanian ammonite zonation shown in Figure 33. PRS, which lies at the north end of the mapped area and is discussed in detail below, preserves the most complete section, with four nominative species, but it lacks *Acanthoceras bellense* (Fig. 51). TBS, 1.6 km to the north, has three species, with *Acanthoceras bellense* bracketed below by *Conlinoceras tarrantense* and above by *A. amphibolum*, but it lacks *Plesiacanthoceras muldoonense* to constrain it below. PDCS, 4.8 km farther north, has two species, with *A. bellense* underlain by *P. muldoonense*, but it lacks *A. amphibolum* to bracket it above. The positions of all four ammonite species from the three sections reveal that *A. bellense* clearly falls between *P. muldoonense* below and *A. amphibolum* above.

A large-scale graphic section of the Dakota Sandstone at PRS, the most faunally complete on SNWR, is shown in Figure 52. Graphic sections of the Dakota Sandstone at TBS and PDCS can be found in Hook and Cobban (2007, figs. 6 and 8) along with photographs from all three outcrops.

The Dakota Sandstone at PRS is approximately 20 m thick (Fig. 50). It consists of unit 1, a lower, ridge-forming quartzite, 2 m thick; unit 2, a middle, valley-forming sandstone and carbonaceous shale unit, 13 m thick; unit 3, an upper, ridge-forming, extensively burrowed and bioturbated sandstone, 2 m thick; and unit 4, an upper unit of interbedded, thin, resistant and nonresistant sandstones, 3.4 m thick.

The lower two units are continental and the upper two are marine. Impressions of plant debris and seeds in unit 1 (Fig. 50) are followed by carbonaceous shale and siltstone in unit 2. *Thalassinoides* burrows are common on the upper surface of unit 3, which forms a prominent dip slope. Internal molds of ammonites are present at the base of unit 4. The ammonite fossils from all beds in the Dakota Sandstone at PRS consist of internal molds of outer whorls that often show effects of erosion; usually at least one side is corroded. These internal molds have not been colonized by oysters or other encrusting organisms, as occurs in the basal Bridge Creek Limestone Beds at Carthage.

Conlinoceras tarrantense, the lowest middle Turonian index ammonite, is present in two thin, resistant sandstones in the basal 1.5 m of unit 4. The lower occurrence is in a 5- to 8-cm-thick, gray-weathering sandstone and sandstone breccia (Fig. 52, D14488 level). The breccia is a fine-grained sandstone that contains rip-up clasts up to 10 cm across composed of a similar sandstone. Reworked internal molds of *C. tarrantense* are common and often cut across bedding. White- to dark-gray-weathering, irregularly spherical to cylindrical phosphatic nodules up to 2.5 cm in diameter and 5 cm long are abundant in the bed and litter the ground where they have weathered free of matrix (Fig. 53). The body chamber of an internal mold of *C. tarrantense* from this level contains one of these nodules as well.

The upper bed containing *Conlinoceras tarrantense* is an 8-cm-thick, brown-weathering, fine-grained, resistant sandstone that crops out continuously along the Dakota outcrop at PRS (Fig. 52, D11245 level). The preservation of ammonites from this bed is much better than in the lower bed, although only incomplete internal molds have been found. A well-preserved specimen of *C. tarrantense* from this level was figured by Hook and Cobban (2007, figs. 13A and 13B).

Plesiacanthoceras muldoonense is present in a 5- to 8-cm-thick sandstone that is 76 cm higher in the section (Fig. 52, D14236 level). *Acanthoceras amphibolum* appears more abundantly in a 15-cm-thick, dark-brown weathering, limy sandstone with small ironstone concretions that marks the top of the Dakota Sandstone (Fig. 52, D14230 level). The stratigraphic intervals that could contain *A. granerosense* Cobban and Scott and *A. bellense* Adkins at PRS are covered (Fig. 52). *Acanthoceras granerosense* has never been found outside the Pueblo, Colorado, area, but *A. bellense* has been projected into PRS (Figure 50, D14225 level) from PDCS, 10 km to the northeast (Fig. 32). A single specimen of *A. bellense* (D14466) was collected 1.6 km northeast of PRS at TBS.

The invertebrate faunas of the Dakota Sandstone on SNWR are dominated by ammonites and oysters. An undescribed oyster along with one specimen of *Turrilites costatus* Lamarck, two specimens of *Cunningtoniceras* cf. *C. cunningtoni* (Sharpe), and a few gastropods occur with abundant *Conlinoceras tarrantense* (Fig. 52, D14488 and D11245 levels). The turrilitid and gastropods are preserved in phosphatic nodules, as are a crab claw and *Teredo* tubes. A single specimen of *Turrilites* (*Euturrilites*) *scheuchzerianus* and numerous oyster fragments are present with *Plesiacanthoceras muldoonense* (Fig. 52, D14236 level). *Ostrea beloiti* and *Inoceramus arvanus* are common in the *Acanthoceras amphibolum* bed (Fig. 52, D14230 level). *Ostrea beloiti* is also abundant in the *Plesiacanthoceras wyomingense*? bed in the overlying Tokay Tongue of the Mancos Shale, primarily as broken, abraded valves (Fig. 52, D11352/ D11441 level).

Three of the Dakota ammonite species were unknown in New Mexico before their discovery on SNWR (Hook and Cobban, 2007). Previously, *Plesiacanthoceras muldoonense* had been reported from north-central Wyoming (Cobban, 1987a) and its type locality in southern Colorado (Cobban and Scott, 1972). *Turrilites* (*Euturrilites*) *scheuchzerianus* was known previously only from southern Colorado in association with *Plesiacanthoceras muldoonense* (Cobban and Scott, 1972). Specimens attributed to *Cunningtoniceras* cf. *C. cunningtoni* were collected from the Pueblo, Colorado, area (Cobban and Scott, 1972) and central Texas (Stephenson, 1952).

The phosphatic nodules present near the top of the Dakota Sandstone are unique to the northern part of the Quebradas area. They are present on SNWR at PRS and TBS and at JdM (Figs. 48 and 52) in the *Conlinoceras tarrantense* Zone (Hook and Cobban, 2007). At PRS, these white nodules lie on the bedding surface of the upper ridge-forming sandstone and occur in a 2.5-cm-thick breccia of rip-up clasts of sandstone and corroded internal molds of *C. tarrantense* that is directly above that

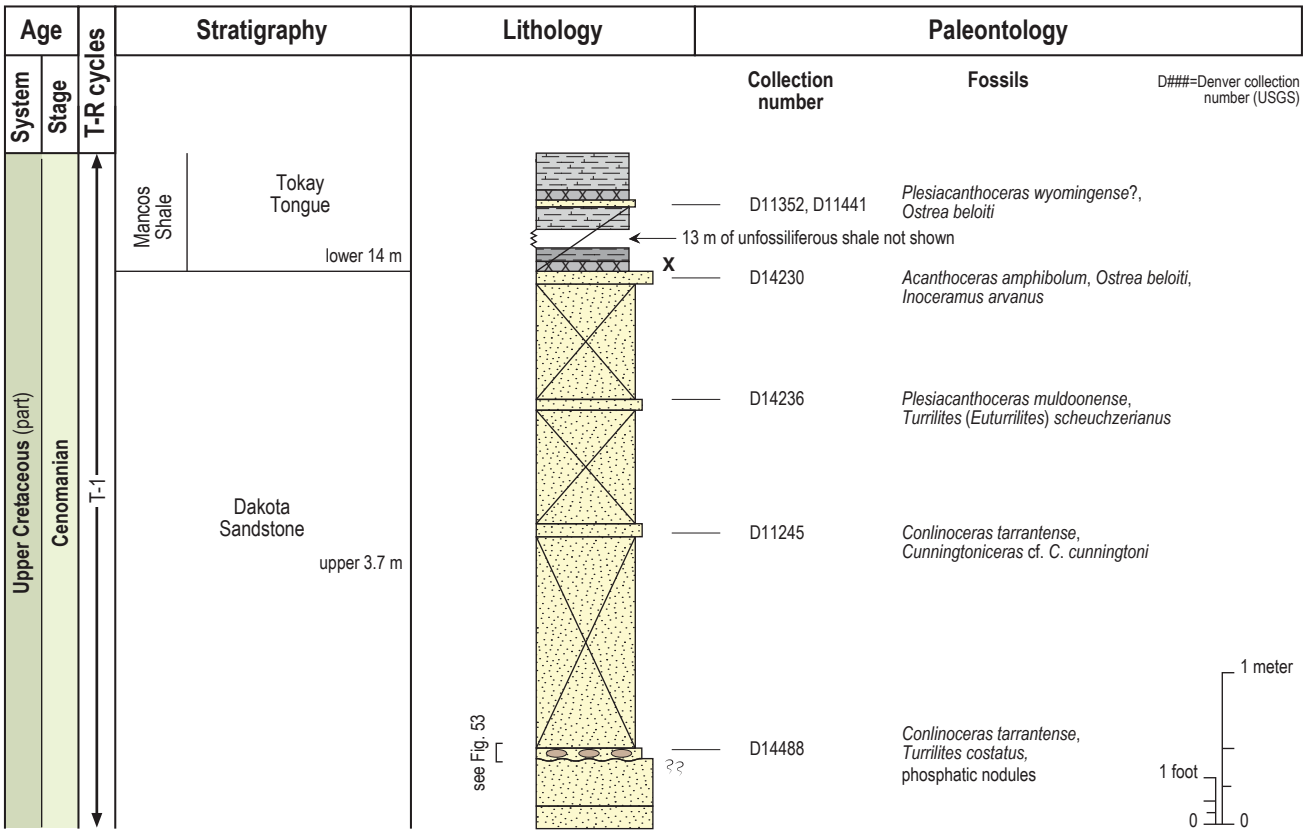

Figure 52. Graphic section of the upper part of the Dakota Sandstone and the basal part of the Tokay Tongue of the Mancos Shale at the principal reference section (**PRS**; Fig. 32, control point #7) showing positions of fossil collections. Modified from Hook and Cobban (2007). See Figure 34B for key.

sandstone (Fig. 52). They often weather free and litter the ground. They range in shape from almost perfect spheres and cylinders to highly irregular variants of these end members; the cylindrical ones commonly occur as fragments (Fig. 53). Most of the elongate nodules contain a cylindrical cavity oriented along the long axis of the nodule. These longitudinal cavities are usually circular in cross section and about 5 mm in diameter, although the axial cavities of the longer nodules taper slightly. These axial cavities are lined with either a single or double layer of well-sorted, fine quartz grains. The outer surfaces of the nodules are typically rough and knobby, coated with fine detrital quartz grains, but are not encrusted by organisms. A few nodules are recognizable as phosphatized internal molds of fossils or have nucleated around fossils. The fossils include gastropods (Fig. 53), arthropods, bored wood, and a single ammonite. One nodule had a shark tooth attached to it. The genesis of these nodules is unknown. Hook and Cobban (2007) speculated on their origin as coprolites but rejected this hypothesis because of the internal molds of fossils, which represent less than 1% of the nodules. The abundance of these nodules on SNWR makes them an excellent lithologic guide to the upper Dakota Sandstone, especially in the small, isolated exposures of sandstone just north of TBS.

The rip-up clasts and phosphatic nodules near the top of the Dakota suggest an erosional unconformity (Fig. 52). At PRS, the phosphatic nodules lie on burrowed but otherwise unfossiliferous sandstone and are present in the overlying breccia in association with sandstone internal molds of *Conlinoceras tarrantense*. The only datable phosphatic fossil is *Turrilites costatus* Lamarck, which has a range of upper lower Cenomanian through upper middle Cenomanian in New Mexico. The magnitude of the disconformity associated with the exhumation of the internal mold of *T. costatus*, its subsequent phosphatization, and the erosion that produced the breccia containing *C. tarrantense* could be (1) the entire rock record associated with the uppermost lower Cenomanian ammonite zone of *Forbesiceras brundrettei,* which is one zone lower than *C. tarrantense* (Cobban et al., 2008, fig. 1) and missing in the study area, or (2) only a portion of the rock record associated with the middle Cenomanian *C. tarrantense* Zone, which

Figure 53. Phosphatic nodules from the Dakota Sandstone, D14488 level, at the principal reference section (**PRS**; Fig. 32, control point #7). The nodule in the center contains the internal mold of a gastropod. The nodule in the lower right is spherical; the others are cylindrical. Four of the cylindrical nodules have axial cavities lined with one or two layers of fine quartz grains; the amorphous phosphate around the cavity and on the outsides of the nodules contains numerous individual quartz grains. Modified from Hook and Cobban (2007).

continues above the breccia. The larger-magnitude unconformity is common in Texas and the Gulf Coast, where it is referred to as the Gulfian–Comanchean unconformity. In New Mexico, the Gulfian–Comanchean unconformity has been documented only in the southern part of the state in the Cookes Range (Cobban, 1987b; Cobban et al., 1989) and at Cerro de Cristo Rey, near El Paso, Texas (Lovejoy, 1976; Kennedy et al., 1988). The rock record and ammonites preserved at PRS (Fig. 52) indicate the disconformity is confined to the *Conlinoceras tarrantense* Zone. The phosphatic nodule preserved in the body cavity of an internal mold of *C. tarrantense* in the breccia also supports this interpretation.

The basal contact of the Dakota Sandstone at PRS is disconformable with the underlying Jurassic Morrison Formation; its upper contact is conformable with the overlying tongue of Mancos Shale. The marine portion of the Dakota was deposited during the initial transgression (T-1) of the Western Interior Seaway into New Mexico. Outcrop photographs of the Dakota Sandstone on SNWR are in Hook and Cobban (2007).

The **Tokay Tongue of the Mancos Shale** on SNWR is estimated to be 191 m thick (Fig. 50). Its thickness, which is the greatest in the study area, was estimated by combining PRS with CCS 6 km to the north (Fig. 32, control points #7 and #9, respectively).

At PRS, the Tokay Tongue and Tres Hermanos Formation are in fault contact. The upper one-third of the Tokay is not present. At CCS, the Upper Cretaceous is in fault contact with the Triassic and begins in the Whitewater Arroyo Tongue of the Mancos Shale, about 3 m below the base of the Twowells Tongue of the Dakota Sandstone.

The composite section of the Tokay Tongue on SNWR (Fig. 50, left side of column), which is generally partly concealed, can be subdivided lithologically into five bed-rank units: (1) lower noncalcareous shale beds, 12 m thick; (2) lower calcareous shale beds, 100 m thick; (3) the Bridge Creek Limestone Bed, 15 cm thick; (4) upper calcareous shale beds, 38 m thick; and (5) upper noncalcareous shale beds, 41 m thick.

Judging by the numerous thin, white clay beds exposed in shale outcrops in small arroyos, there may be as many bentonites in the Tokay Tongue on SNWR as there are elsewhere in the study area. These beds can only be traced a short distance along strike before becoming covered.

The basal 15 m of the Tokay Tongue at PRS was trenched to a depth of 15 cm in an effort to locate the x-bentonite that is so prominent at Carthage and JdM (Figs. 34A and 48). Two 20-cm-thick bentonites in the trenched part of the Tokay Tongue were viable candidates to be the x-bentonite (Figs. 50 and 52). The lower one lies on the uppermost bed of the Dakota Sandstone at the base of the lower noncalcareous shale beds. *Acanthoceras amphibolum* is present in this sandstone bed (Fig. 52, D14230 level). The upper bentonite is 13.5 m above the Dakota at the base of the lower calcareous shale beds, just above a thin sandstone containing impressions of an ammonite identified as *Plesiacanthoceras wyomingense*? (Fig. 52, D11352/D11441 level). The specimens of *P. wyomingense*? are poorly preserved and could possibly be its ancestor, *A. amphibolum*. Therefore, a criterion other than biostratigraphy had to be used to determine which ash bed was more likely to be the x-bentonite. The lower bentonite correlates with the x-bentonite because of its stratigraphic position within noncalcareous shale and above a bed containing undoubted *A. amphibolum*, which is also the case at Carthage (Fig. 34A). The upper bentonite at PRS, which is present in calcareous shale, may be equivalent to one or both of the 15-cm-thick "tire track" bentonites within calcareous shale about two-thirds of the way through the shale and sandstone beds at Carthage (Fig. 34A).

The only other fossils found in the Tokay Tongue at PRS are the oysters *Pycnodonte* aff. *P. kellumi* (Fig. 50, D14294 level) and *P. newberryi* (Fig. 50, D14485 level), 98 m and 102 m above the base, respectively. Each species is preserved in a discrete, nonoverlapping zone at least 1 m thick.

Fossils collected from concretions in the Tokay Tongue below the Tres Hermanos Formation in the Ladron Peak quadrangle, 30 km to the northwest of PRS (Fig. 32, control point #11), indicate that the top of the Tokay lies within the *Collignoniceras woollgari regulare* Subzone (Fig. 50, D14584 level), one subzone higher than at Carthage and JdM. Lack of exposures lower in the section makes it impossible to determine whether these Ladron Peak concretions are from the Rio Salado Tongue, which

requires the Twowells Tongue at its base (Hook et al., 1983, p. 24–26), or the Tokay Tongue, which does not (Hook and Cobban, 2015).

The position of the Cenomanian–Turonian boundary, defined on the first occurrence of the bivalve *Mytiloides puebloensis*, cannot be located precisely at PRS. The limestone from the middle part of the Bridge Creek Limestone Beds at Carthage and JdM, where *M. puebloensis* is present, is not developed here or faulted out. This stage boundary is questionably located on SNWR just below the Bridge Creek Limestone Bed (Fig. 50).

At CCS, 6 km to the north of PRS, the Twowells Tongue of the Dakota Sandstone subdivides the Tokay Tongue of the Mancos Shale into two formally named parts—the Whitewater Arroyo Tongue below and the Rio Salado Tongue above (Fig. 50, right side of column). Only the upper 3 m of the Whitewater Arroyo are exposed above a fault contact with Triassic rocks (Hook, 1983, fig. 3). The thickness of the Whitewater Arroyo could not be measured on SNWR because of lack of exposure but is estimated to be 70 m, as inferred from the thickness of the Tokay Tongue at PRS below the base of the projected Twowells Tongue (Fig. 50).

The Twowells Tongue of the Dakota Sandstone at CCS is a 27-m-thick, ridge-forming, coarsening-upward, fine-grained, bioturbated sandstone (Hook, 1983, fig. 3). It has a sharp but conformable contact with the overlying shale and a gradational contact with the underlying shale. A single, internal mold of *Metoicoceras mosbyense* Cobban is the only body fossil recovered from the Twowells Tongue (Fig. 50, D10979 level). *Metoicoceras mosbyense* is the index ammonite for an upper Cenomanian zone in New Mexico (Fig. 33), where it is common in the Twowells Tongue in the San Juan Basin (Cobban, 1977a).

The Rio Salado Tongue of the Mancos Shale, which extends from the top of the Twowells to the base of the Tres Hermanos Formation, is 94 m thick at CCS (Fig. 32, control point #9). It consists of calcareous shale in the lower part and noncalcareous shale in the upper part. The exact position of calcareous–noncalcareous shale is undetermined because of extensive cover. The oyster *Pycnodonte newberryi* (Fig. 50, D10978 level) is abundant in the basal 1.5 m of the Rio Salado Tongue. Fragments of the early Turonian bivalve *Mytiloides mytiloides* (Fig. 50, D14590 level) are preserved in a thin, light-brown-weathering calcarenite 15 m above the Twowells. The early Turonian ammonite *Mammites* sp. (Fig. 50, D10974 level) was collected from a thin, white limestone from about the same level. The upper part of the Bridge Creek Limestone Beds at Carthage (Figs. 34A and 37) and JdM (Fig. 48) is similar to this occurrence in both lithology and fauna. Therefore, this bed at CCS is correlated with the uppermost part of the Bridge Creek Limestone Beds. Although exposures of the lower 15 m of the Rio Salado are generally good at CCS, no nodular limestones similar to those usually found at the base of the Bridge Creek were observed. Therefore, these nodular limestones, referred to as the scip zone limestones at Carthage and JdM, are either not developed at CCS or are replaced by the upper part of the Twowells Tongue.

The two collections from the Ladron Peak section (LPS; Fig. 32, control point #11) are probably from the upper part of the Rio Salado Tongue, as opposed to the upper part of the Tokay Tongue (Fig. 50, D14492 and D14584 levels). Normal faults in the Ladron Peak quadrangle produced Upper Cretaceous outcrops that are stratigraphically higher than the Twowells Tongue. The Twowells, however, is present in outcrops farther to the west in the Acoma Basin (Hook et al., 1983). The higher collection of *Collignoniceras woollgari regulare* (Fig. 50, D14584 level) indicates that the upper part of the Rio Salado Tongue and, by extension, the upper part of the Tokay Tongue on SNWR lie in the *Collignoniceras woollgari regulare* Subzone (Fig. 33), one subzone higher than at Carthage and JdM. This determination is consistent with the northeasterly retreating R-1 shoreline arriving at Carthage and JdM earlier than at SNWR.

We reject Lucas et al.'s (2019, p. 10, fig. 6) redefinition of the Rio Salado Tongue of the Mancos Shale. Hook et al. (1983, p. 24) defined the Rio Salado Tongue as "the shale tongue between the Twowells Tongue of the Dakota Sandstone and the Tres Hermanos Formation (or Atarque Sandstone)." They did not define the Rio Salado Tongue as "…the shale-dominated stratigraphic unit between the Twowells Tongue of the Dakota Sandstone (below) and the Tres Hermanos Formation or equivalent strata of the Juana Lopez Member of the Mancos Formation (above)…," as stated by Lucas et al. (2019,

p. 10), but erroneously attributed to Hook et al. (1983). The Tres Hermanos Formation and the Juana Lopez Member are disparate stratigraphic units. In central New Mexico, where the two units locally occur in the same stratigraphic sequence, the base of the Juana Lopez is always above the top of the Tres Hermanos Formation or its offshore equivalent, the Semilla Sandstone Member of the Mancos Shale (Hook and Cobban, 2013). In addition, the two units are in different biostratigraphic zones or subzones; the base of the Juana Lopez is always in a higher zone or subzone than the top of the Tres Hermanos, and the base of the Tres Hermanos is several zones lower than the base of the Juana Lopez. These relationships are well established and have been known since Hook et al. (1983). On SNWR, for example, the base of the Juana Lopez Beds of the D-Cross Tongue of the Mancos Shale is 75 m above the base of the Tres Hermanos Formation and is three biostratigraphic zones higher (Fig. 50).

The Tokay Tongue and its time-equivalent units (the Whitewater Arroyo Tongue, Twowells Tongue, and Rio Salado Tongue) were deposited during T-1 and the first half of R-1. All contacts are conformable.

The **Tres Hermanos Formation** is 73 m thick at CCS (Fig. 50). It consists of three members: (1) the marine Atarque Sandstone Member, 3 m thick; (2) the mostly continental Carthage Member, 50 m thick; and (3) the marine Fite Ranch Sandstone Member, 20 m thick. The Tres Hermanos Formation was deposited in the middle Turonian during the last part of R-1 and the first part of T-2. The regressive base of the Tres Hermanos is in the *Collignoniceras woollgari regulare* Subzone; its eroded, transgressive top is interpreted to be in the *Prionocyclus macombi* Zone (Fig. 33). The contact with the underlying Tokay Tongue of the Mancos Shale is sharp and conformable, whereas the contact with the overlying D-Cross Tongue of the Mancos Shale is sharp and disconformable.

The **Atarque Sandstone Member** varies in thickness from 3 m at CCS (Fig. 50) to 11 m at PDCS (Fig. 32, control point #10). Sandstone concretions near the base of the Atarque contain numerous species of bivalves and gastropods (referred to earlier as the characteristic Atarque fauna). Many specimens retain patches of replaced shell on the internal molds. Only one ammonite specimen was recovered from this member on SNWR—an internal mold of *Spathites* sp. (Fig. 50, D11519 level) from PDCS. This specifically indeterminate ammonite is probably *S. coahuilaensis* (Jones), which is restricted to the *Collignoniceras woollgari regulare* Subzone (Cobban, 1988).

A phosphatic pebble bed comprising abraded fish bones and teeth, about 15 cm thick, is present near the top of the Atarque at PDCS (Fig. 50, D14484 level). Wolberg (1985) listed 19 taxa of selachians (sharks and rays) from this bed. Spielmann et al. (2009) restudied the fauna and listed 17 taxa of chondricthys (cartilaginous fish, i.e., sharks and rays), 4 taxa of osteicthyes (bony fish), and 2 taxa of reptiles (one turtle and one dinosaur). The D14484 collection from this bed also includes broken shells of *Crassostrea soleniscus* and a well-preserved internal mold of the brackish-water gastropod *Craginia coalvillensis* (Meek). This carbonate internal mold has five whorls and is approximately 8 cm high. The shark tooth bed is unique to SNWR, where it is present at PDCS and PRS.

The Atarque on SNWR is usually capped by a 30-cm-thick oyster coquina of broken shells of the brackish-water oyster *Crassostrea soleniscus* (Fig. 50, D11522 level). The Atarque was deposited near the end of R-1 in the middle Turonian.

The **Carthage Member**, 50 m thick at CCS (Fig. 50), is primarily continental shale. Minor carbonaceous to coaly beds are present in the lower third of the member. The upper 10 m of the member are gray marine shale with sparsely fossiliferous limestone concretions. Concretions from the upper part of the Carthage Member at the Old Stapleton Ranch section (OSR; Fig. 32, control point #5) preserved two 25-cm-diameter internal molds of adult, robust prionocyclids. These two specimens, originally determined as *Prionocyclus macombi* in Hook et al. (2012, p. 132, fig. 6), are identified as *Prionocyclus* sp. in Figure 50 (D14477 level). Both specimens are completely septate and have adult whorl sections that are slightly broader than high. Ventrolateral tubercles have enlarged into horns on the outer whorls of both, making it impossible to determine whether the specimens had single or double ventrolateral tubercles. Double ventrolateral tubercles would indicate the older *P. hyatti*, while single ventrolateral tubercles would indicate the younger *P. macombi*. The early (inner) whorls, where it would be possible to see the tuberculation, are not visible on either specimen and may not be preserved.

Comparison with large collections of adults of both prionocyclid species housed in the Denver Federal Center suggests that the specimens are a slightly better fit qualitatively with *P. hyatti*. A single specimen of the oyster *Cameleolopha* aff. *bellaplicata* at the base of the D-Cross Tongue at PRC, 9 km northeast of OSR (Fig. 50, D14495 level), also suggests that these two ammonites are *P. hyatti*. *Cameleolopha* aff. *bellaplicata* is known from only the *P. hyatti* Zone at Bull Gap Canyon, New Mexico (Fig. 32; Hook and Cobban, 2011a).

The correlation of the upper part of the Tres Hermanos Formation shown in Figure 33 for SNWR reflects the importance of the single specimen of *Cameleolopha* aff. *bellaplicata* (D14495) from the base of the D-Cross Tongue and the uncertainty surrounding the specific identification of the ammonites from the D14477 collection from near the top of the Carthage Member. For a more detailed explanation, see the discussion of the D14495 collection in the section on the D-Cross Tongue below.

The Carthage Member on SNWR was deposited during the end of R-1 and the beginning of T-2 in the middle Turonian. The continental base of the member probably lies in the lower middle Turonian *Collignoniceras praecox* Zone; fossils from near the top of the member are probably from the upper middle Turonian *Prionocyclus hyatti* Zone (Fig. 33). The lower contact is sharp and conformable and the upper contact is gradational and conformable.

The **Fite Ranch Sandstone Member** on SNWR is a coarsening-upward, poorly fossiliferous, bioturbated sandstone that is 20 m thick (Fig. 50). C.M. Molenaar (personal communication, 1981) described the Fite Ranch Sandstone in the Quebradas area as regressive, marine sandstone deposited in a brackish setting during transgression.

Dark-brown, unfossiliferous, spherical sandstone concretions up to 1.2 m in diameter are present just above its base. The only fossils collected directly from the Fite Ranch Sandstone Member are a few impressions, broken valves, and internal molds of the oyster *Cameleolopha bellaplicata* (Fig. 50, D14471 level) from OSR (Fig. 32, control point #5), which is 1.6 km south of SNWR. Fossils that weathered from and accumulated as a lag deposit on the Fite Ranch Sandstone on SNWR are interpreted to be from the *Prionocyclus macombi* Zone (see discussion below for details). The Fite Ranch was deposited in the middle Turonian during T-2. The lower contact of the Fite Ranch is gradational and conformable and its upper contact is sharp and unconformable.

The **D-Cross Tongue of the Mancos Shale** is 110 m thick and comprises primarily noncalcareous shale at CCS (Fig. 32, control point #9), where it is divided into two parts by a 3.7-m-thick sandstone that is 63 m above its base (Fig. 50). Baker (1981) and Hook (1983, fig. 3) regarded this unit as a sandstone in the D-Cross, and Hook et al. (2012) regarded it as the base of the Gallup Sandstone. However, C.M. Molenaar (personal communication, 1982), who spent many years studying the Gallup Sandstone (Molenaar, 1974, 1983a, 1983b), did not assign this sandstone on SNWR to any of his informal Gallup Sandstone tongues; instead he showed it as a sandstone in the D-Cross (Hook, 1983, fig. 3). In this report, this sandstone is mapped as part of the D-Cross Tongue.

Fossils from the base of the D-Cross Tongue occur in a lag deposit on top of the underlying Fite Ranch Sandstone Member and are probably from the middle Turonian *Prionocyclus macombi* Zone (Fig. 33). Fossils from near the top of the D-Cross are probably from the upper Turonian *Forresteria peruana* Zone (Fig. 33; Fig. 50, D11205 and D11206 levels). The D-Cross Tongue was deposited during the last part of T-2 and the first part of R-3.

Loose phosphatic pebbles composed primarily of shark teeth and internal molds of small bivalves (with less common gastropods and ammonite chamber fillings), along with broken and abraded oyster shells, are present at the base of the D-Cross (Fig. 54, D15027/D14495 level; Fig. 55). The oysters from the D14495 collection are assigned to three species: *Cameleolopha* aff. *C. bellaplicata* (Fig. 55A), *C. bellaplicata* (Figs. 55B and 55C), and *C. lugubris* (Fig. 55D). Elsewhere in New Mexico, these three oyster species are part of an evolutionary sequence that begins in the *Prionocyclus hyatti* Zone and extends through the *P. wyomingensis* Zone (Hook and Cobban, 2012). The combined ranges of the oysters span three ammonite zones and encompass at least 500 kyr (Fig. 33). These three oyster species do not co-occur in a normal depositional sequence.

At Bull Gap Canyon (BGC), Lincoln County, New Mexico, 100 km southeast of PRS (Fig. 32), Hook and Cobban (2012) described four morphologically distinct, stratigraphically non-overlapping species of ribbed oysters that they assigned to an evolutionary sequence of the genus *Cameleolopha*. The oldest species, *C.* aff. *C. bellaplicata* (Fig. 55A), which is preserved with an undoubted specimen of *Prionocyclus hyatti* (Cobban, 1986, fig. 3Q), is a small, equivalved, densely ribbed, nearly flat oyster with an attachment scar that is small or absent. This oyster extends through 0.3 m of the section near the base of the Fite Ranch Sandstone at BGC. The second species in the succession at BGC, *C.* aff. *C. bellaplicata,* is missing on SNWR. The third species at BGC, *C. bellaplicata* (Figs. 55B and 55C), is present there with undoubted specimens of *Prionocyclus macombi* in the dark-brown, hematite-cemented sandstone at the top of the Fite Ranch Sandstone; it is a medium-sized, inequivalved, less densely ribbed, planoconvex oyster with little to no attachment scar. At BGC, *C. bellaplicata* is present 7.7 m stratigraphically above *C.* aff. *C. bellaplicata*. The fourth species in the succession at BGC, *C. lugubris* (Fig. 55D), is a small, slightly planoconvex, inequivalved species with a large attachment area fringed by fine to coarse ribs. Its first occurrence at BGC is at the top of the range of *P. macombi* in the base of the Juana Lopez Beds of the D-Cross Tongue of the Mancos Shale, 1.8 m above the Fite Ranch Sandstone. Prior to its discovery on SNWR, *C.* aff. *C. bellaplicata* had been known only from the Fite Ranch Sandstone at BGC. The other two species, *C. bellaplicata* and *C. lugubris,* are widely distributed in the Western Interior (Hook and Cobban, 2012).

The discovery of *Cameleolopha* aff. *C. bellaplicata* at the base of the D-Cross Tongue on SNWR (Fig. 54, D14495 level; Fig. 55A) suggests that a substantial thickness of Fite Ranch Sandstone down to that level had been eroded, allowing valves of *C.* aff. *C. bellaplicata* to be mixed with *C. bellaplicata* and *C. lugubris* within a lag deposit. By this interpretation and the known biostratigraphy of the oysters, the top of the Fite Ranch Sandstone on SNWR would be in the *Prionocyclus hyatti* Zone, not in the next higher *P. macombi* Zone as previously interpreted (Hook et al., 2012, fig. 6).

However, other direct evidence suggests that this zonal interpretation of the Fite Ranch Sandstone Member based on the presence of the single specimen of *Cameleolopha* cf. *C. bellaplicata* is incorrect. The most compelling evidence is that *C. bellaplicata* occurs sparingly in the basal part of the Fite Ranch Sandstone at

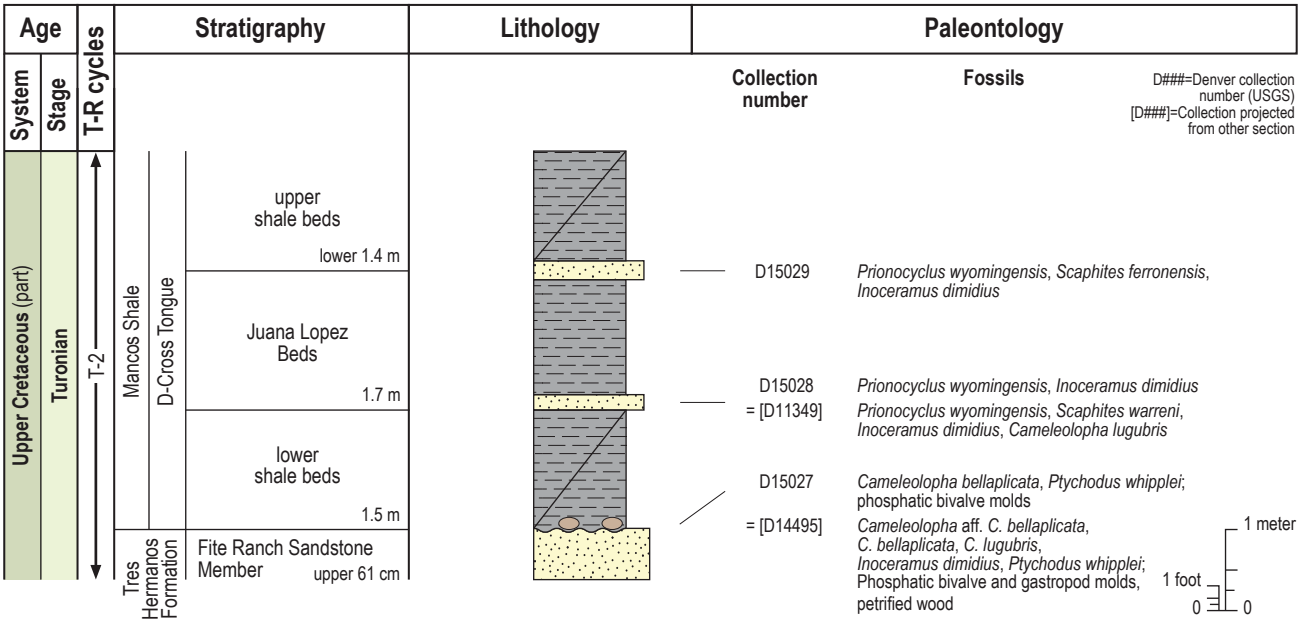

Figure 54. Graphic section of the basal part of the D-Cross Tongue of the Mancos Shale on Sevilleta National Wildlife Refuge (**SNWR**) at the principal reference section (**PRS**) showing positions of fossil collections and the Juana Lopez Beds. Modified from Hook and Cobban (2013). See Figure 34B for key.

the Old Stapleton Ranch (OSR) measured section (Fig. 56, D14471 and D15243 levels); OSR is 11 km south of PRS (Fig. 32, control points #5 and #7, respectively). That stratigraphic occurrence turns the biostratigraphy upside down, with the descendent (*C. bellaplicata*) appearing in the stratigraphic section almost 20 m below its ancestor (*C.* aff. *C. bellaplicata*). In addition, it is highly unlikely that valves of the younger two species (*C. lugubris* and *C. bellaplicata*), which would have undergone a longer period of exposure on the seafloor, would be as well preserved as they are (Figs. 55B–D).

There are additional caveats about this zonal interpretation. The D14495 specimen of *Cameleolopha* aff. *C. bellaplicata* (Fig. 55A) is larger than any specimen recorded from BGC, but its rib count, thickness, and key morphometric ratios lie within the ranges reported by Hook and Cobban (2012, appendix 1, table 1). Attempts to find more specimens of *C.* aff. *C. bellaplicata* or ammonites at or below the D14495 level on SNWR and JdM were unsuccessful. Therefore, the Fite Ranch Sandstone Member on SNWR is assumed to have been deposited primarily during the time represented by the *Prionocyclus macombi* Zone (Fig. 33). This interpretation means that the depositional history of the Fite Ranch Sandstone Member of the Tres Hermanos Formation is similar throughout the Quebradas area (Fig. 33).

The geographic distribution of fossils from the *P. macombi* Zone in New Mexico indicates the shoreline was at least 120 km southwest of PRS (Fig. 32, control point #7) at the time the lag deposit formed there (Hook and Cobban, 2011a, fig. 3). The cause(s) of the erosive and/or nondepositional periods that produced the lag deposit are unknown but had to involve high-energy conditions, perhaps related to storms. Phosphatization of internal molds of mollusks involved an extended interval of nondeposition or sediment bypass after exposure on the seafloor.

In order to be phosphatized, internal molds of bivalves, gastropods, and ammonites—which were originally of carbonate composition—were eroded from the Fite Ranch Sandstone and then concentrated on the seafloor, where they became phosphatized during a nondepositional interval. In addition, most of the bivalve internal molds have a groove worn into them along the commissure (join line) of the two valves (Figs. 55G and 55K–M). The origin of this groove is unknown. This small bivalve species, which is undetermined, has not been found outside the JdM and SNWR areas.

Sandstone in the spaces between the ribs of the oysters originated in the sandy deposits of the Fite Ranch Sandstone, not in the clayey deposits that would become the D-Cross. The internal surface of one broken, upper valve of *C. bellaplicata* has a phosphatic ooid attached to it (not shown in Fig. 55). This ooid is similar to those found at BGC and Carthage. Phosphatic ooids were observed first in the internal molds of *Pholadomya* sp. from the top of the Fite Ranch at BGC, then at Carthage (Fig. 34A, D10354 and D11161 levels), and later at SNWR.

The single specimen of *Inoceramus dimidius* White (Fig. 55H) recovered from the D14495 level is an internal mold of sandstone composition with a thin coating of white phosphate on its underside. The only other occurrence of *I. dimidius* from the Quebradas area is from the base of the Fite Ranch Sandstone at Carthage (Fig. 34A, D14562 level). The large, smooth bivalve (Fig. 55F) is probably a worn internal mold of an adult inoceramid. The lack of ornamentation makes it difficult to determine a species. The specimen is not geniculated, so it is not *I. dimidius* White; it lacks a fold, so it cannot be *I. howelli* White. It has the general outline of *I. cuvieri* Sowerby, which is known from the lower part of the *Prionocyclus hyatti* Zone (Dane et al., 1968, p. F9).

Internal molds of the bivalves and gastropods and the shells of all three oyster species are interpreted to have been eroded—albeit at different times—in a submarine environment from the Fite Ranch Sandstone, where they accumulated as lag deposits on the erosional surface at the top of the Tres Hermanos Formation (Fig. 54).

The phosphatic pebbles from the base of the D-Cross Tongue (Figs. 55E–L) differ from the phosphatic nodules near the top of the Dakota Sandstone (Fig. 53) in that they are smaller and consist of phosphatized internal molds of small bivalves with an occasional phosphatized internal mold of a gastropod or ammonite chamber. By contrast, <1% of the Dakota nodules are recognizable as fossils, and <1% of the D-Cross pebbles are recognizable as irregular cylinders with longitudinal tubes, which are abundant in the Dakota collections.

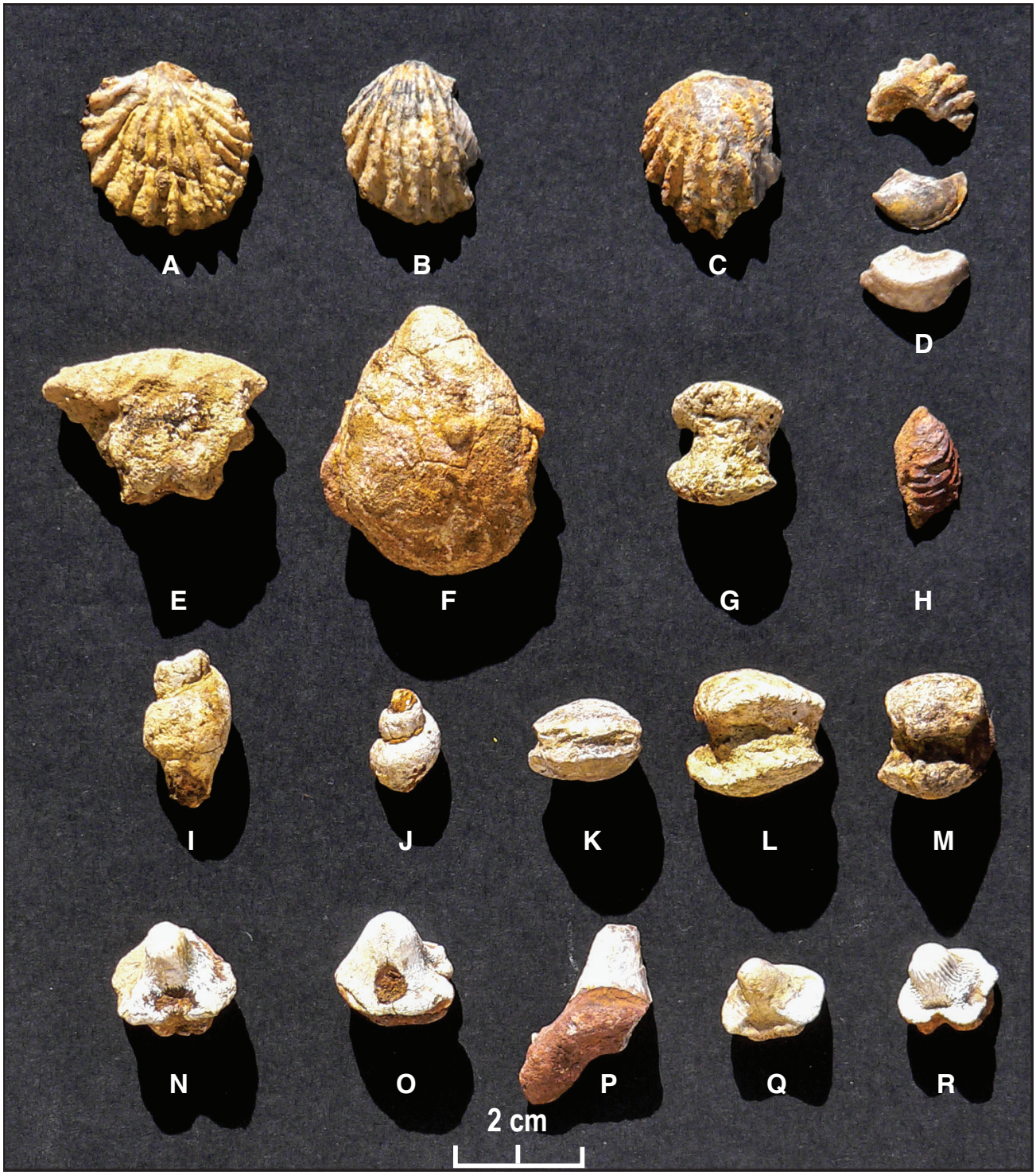

Figure 55. Oysters (**A-D**), phosphatic pebbles (**E-M**), and shark teeth (**N-R**) from the base of the D-Cross Tongue of the Mancos Shale at USGS Mesozoic locality D14495. **A**—*Cameleolopha* aff. *C. bellaplicata* (Shumard); USNM 720107. **B–C**—*Cameleolopha bellaplicata* (Shumard); USNM 720108 and 720109, respectively. **D**—*Cameleolopha lugubris* (Conrad); USNM 720110, 720111, and 720112, from top to bottom. **E**—*Prionocyclus* sp.; USNM 720113. **F—***Inoceramus* sp.; USNM 720114. **G, K–M**—phosphatic internal molds of bivalves; USNM 720115, 720116, 720117, and 720118, respectively. **H**—*Inoceramus dimidius* White; USNM 720119. **I–J**—phosphatic internal molds of gastropods; USNM 720120 and 720121, respectively. **N–O, Q–R**—*Ptychodus whipplei* (Marcou); USNM 720122, 720123, 720124, and 720125, respectively. **P**—*Cretolamna* cf. *C. appendiculata* Agassiz (identified by D.L. Wolberg); USNM 720126. The UTM coordinates for USGS Mesozoic Locality D14495 are 338298E and 3790453N (zone 13, NAD 27), Mesa del Yeso 7.5-minute quadrangle.

Higher in the D-Cross Tongue on SNWR but still near its base, an interval consisting of two thin calcarenites separated by noncalcareous shale is correlated with the **Juana Lopez Beds** (Fig. 50). Although these SNWR calcarenites are lithologically similar to those on JdM, they contain a *Prionocyclus wyomingensis* Zone fauna that is one faunal zone lower. A detailed section of the Juana Lopez Beds from 1.6 km north of PRS is shown in Figure 54. The two sets of rusty- to orange-brown-weathering calcarenites are composed primarily of comminuted *Inoceramus* prisms and oyster shells. The Juana Lopez Beds are 1.7 m thick, lie 1.5 m stratigraphically above the top of the Tres Hermanos Formation, and encompass only the *Prionocyclus wyomingensis* Zone (Fig. 33). The lower calcarenite is 17 cm thick and fossiliferous. The upper calcarenite is 5 cm thick and almost as fossiliferous. Both beds contain *Prionocyclus wyomingensis*, *Inoceramus dimidius,* and scaphites (Fig. 54). The lower bed preserves *Scaphites warreni* Meek and Hayden (Fig. 54, D15028 level) and the upper bed preserves *S. ferronensis* Cobban (Fig. 54, D15029 level). These two scaphite species are often used to define subzones within the *P. wyomingensis* Zone (e.g., Hook, 1983, fig. 1). The calcarenites are separated by 1.5 m of gray, noncalcareous shale.

The Juana Lopez Beds on SNWR (Fig. 54) are only about half as thick as those on JdM (Fig. 49) and one faunal zone lower. At Carthage, only poorly developed, very thin calcarenites are present in the Juana Lopez (Fig. 44), but they are the same age as those at JdM. Calcarenites within the Juana Lopez at Carthage, JdM, and SNWR indicate extensive shell beds had developed on the seafloor in the region and that energy conditions were great enough to reduce the shells to sand-size grains. High-energy conditions might suggest that the Quebradas area was near the western shoreline at the time the shells were comminuted, which would have been near the end of the time represented by the *Prionocyclus macombi* Zone during early T-2 (Fig. 33).

The oyster *Cameleolopha bellaplicata*, which is at the base of the D-Cross on SNWR (Fig. 54) and at the top of the Fite Ranch Sandstone on Carthage (Fig. 45), has also been collected from the base of the D-Cross in Mescal Canyon, 112 km south of Carthage (Fig. 32). The Mescal Canyon occurrence places the western shoreline of the seaway more than 100 km to the south of Carthage at the time the calcarenites formed (Hook and Cobban, 2013, fig. 1), close to the position of the shoreline at maximum transgression during T-2 (Fig. 32). The great distance to the shoreline suggests that currents, rather than waves, were the more likely cause of the high-energy environment. Cobban and Scott (1972) have also suggested that shell-crushing sharks and fish could have played a role in creating calcarenites.

For many years, the base of the Juana Lopez was regarded as a timeline, a chronostratigraphic surface thought to be essentially the same age everywhere (e.g., Molenaar, 1974, 1983a, 1983b). In their regional biostratigraphic study of the Juana Lopez from Mesa Verde National Park (Four Corners area, Colorado) to High Nogal Ranch (Otero County, New Mexico) 400 km to the southeast, Hook and Cobban (2013, fig. 14) showed that both the age of the base and the top of the Juana Lopez are variable but fall within three ammonite zones in the middle to upper Turonian: the *Prionocyclus macombi, P. wyomingensis,* and *P. novimexicanus* Zones. The Juana Lopez in the Quebradas area was shown by Hook and Cobban (2013) to be entirely in the *P. wyomingensis* Zone to the north on SNWR and entirely in the higher *P. novimexicanus* Zone to the south in JdM. The Juana Lopez at Carthage was not recognized by Hook and Cobban (2013). No section of Juana Lopez in the Quebradas area was known at that time to contain both zones. *Prionocyclus novimexicanus* (Fig. 56, D15244 and D15245 levels) was subsequently collected in the upper part of the Juana Lopez Beds at the Old Stapleton Ranch section (OSR), just south of the southern boundary of SNWR.

The Juana Lopez Beds at OSR (Fig. 32, control point #5; Fig. 56) are 3.5 m thick and consist of three, 5- to 10-cm-thick calcarenites that start 2.4 m stratigraphically above the top of the Tres Hermanos Formation. The basal calcarenite preserves a *Prionocyclus wyomingensis* Zone fauna (Fig. 56, D14478 level), whereas the upper two have a younger *P. novimexicanus* Zone fauna (Fig. 56, D15244 and D15245 levels). Thus, the Juana Lopez section at OSR is intermediate in age and geographic location between the section at PRS (Fig. 32, control point #6; Fig. 54), which lies entirely in the *P. wyomingensis* Zone, and the two sections to the south—JdM (Fig. 32, control point #4; Fig. 49) and Carthage

(Fig. 32, control point #1; Fig. 44)—which lie entirely in the *P. novimexicanus* Zone.

Evidence for high-energy conditions and erosion within the Juana Lopez at OSR (Fig. 56) includes the calcarenites and the preservation of a large internal mold of *Prionocyclus novimexicanus* (Fig. 56, D15245 level) and a smaller internal mold of *P. novimexicanus* (Fig. 56, D15244 level). The D15245 specimen is a body chamber, 11.4 cm × 7.6 cm × 3.8 cm, that is worn smooth on one side—presumably the stratigraphically up side on the seafloor—but is well preserved on the other side. The D15244 specimen is a phragmocone of a completely septate *P. novimexicanus*, 4.6 cm in diameter. One side is worn through past the siphuncle; the other side is well preserved and shows the ornamentation characteristic of the species, including fine ribs and single ventrolateral tubercles. The good side of the ammonite is interpreted to have been the stratigraphically down side of the internal mold, while the worn side was stratigraphically up and subject to corrosion by currents.

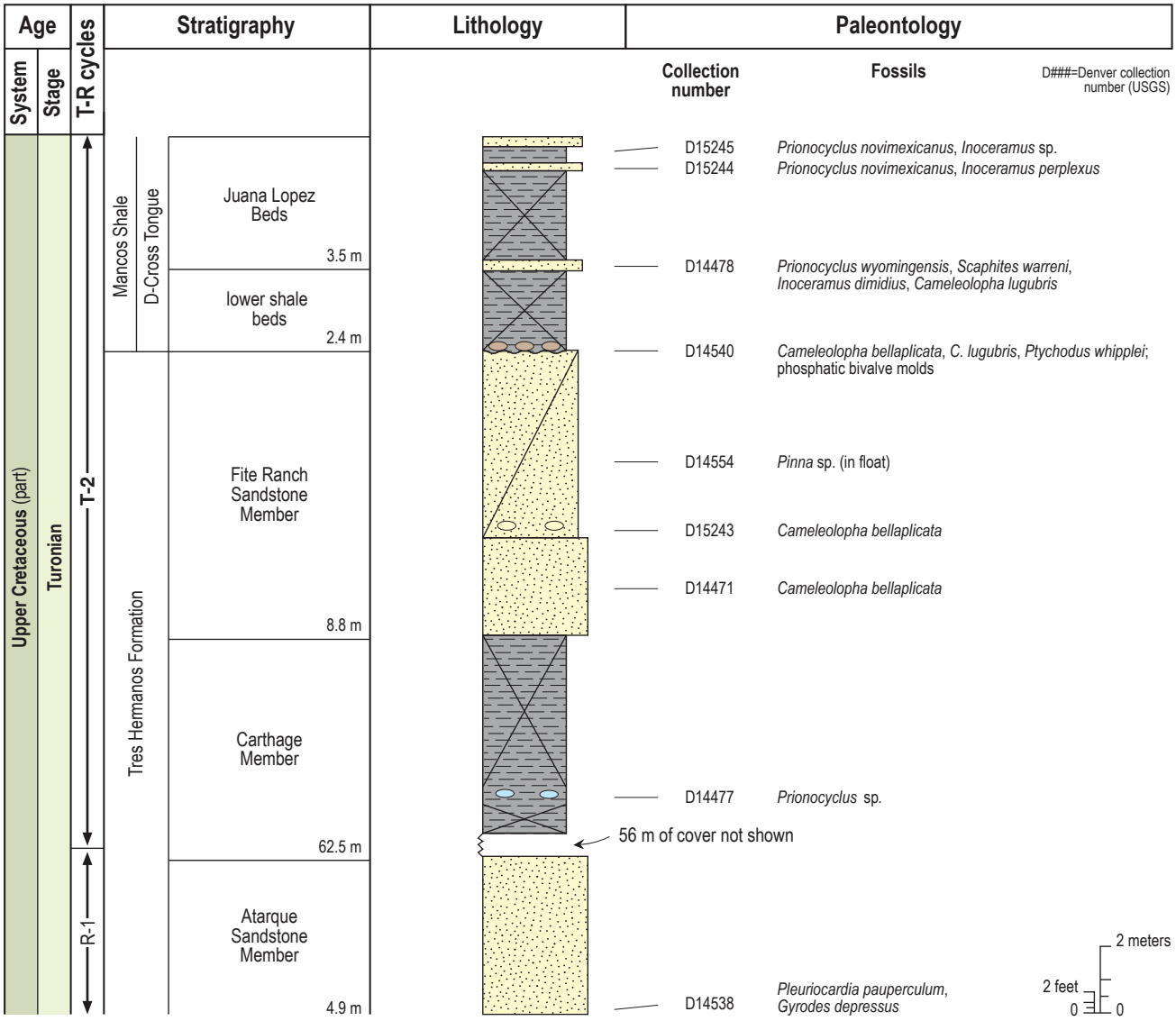

Figure 56. Graphic section of the Tres Hermanos Formation and the lower part of the D-Cross Tongue of the Mancos Shale at the Old Stapleton Ranch section (**OSR**; Fig. 32, control point #5), in NW1/4 sec. 1, T. 2 S., R. 1 E., Mesa del Yeso 7.5-minute quadrangle, showing positions of fossil collections. This is the only outcrop in the study area in which the Juana Lopez Beds of the D-Cross Tongue contain fossils from more than one ammonite zone. See Figure 34B for key.

Evidence for erosion at the base of the D-Cross Tongue from SNWR to JdM is the accumulation of phosphatic pebbles (shark teeth and internal molds of bivalves) and broken shells of the oyster *Cameleolopha*. At Carthage, the upper bed of the Fite Ranch Sandstone contains phosphatic ooids. In addition, the Fite Ranch Sandstone at OSR is only 8.8 m thick (Fig. 56), about half the thickness of the Fite Ranch Sandstone elsewhere in the Quebradas area (see Figs. 34, 48, and 50).

Erosive conditions could have swept to the south and southwest (landward) from OSR during *Prionocyclus novimexicanu*s time and produced the age difference at the base of the Juana Lopez from SNWR to Carthage. Thickness differences in the Fite Ranch would have to be partially the result of an earlier erosive interval during middle to late *P. macombi* time.

Higher in the section, the D-Cross sandstone (Fig. 50) divides the D-Cross Tongue into two parts on SNWR. This informally named sandstone is 3.7 m thick and is 63 m above the base of the D-Cross. It preserves the smaller, finely ribbed variety of "*Lopha*" *sannionis* (Fig. 50, D11205 level) that appears to be confined to the late Turonian (Fig. 56). A poorly preserved internal mold of the ammonite *Forresteria* that is probably the latest Turonian species *F. peruana* (Brüggen) is present with it. Cobban et al. (2008, p. 81) noted that *F. peruana* straddles the Turonian–Coniacian boundary. No other age-diagnostic fossils have been found in the D-Cross on SNWR.

The D-Cross Tongue on SNWR was deposited from the latest middle Turonian through at least the latest Turonian during the last half of T-2 and the first half of R-2.

The **Gallup Sandstone** at CCS (Fig. 32, control point #9) is a 13-m-thick, coarsening-upward, fine-grained, ridge-forming sandstone. No fossils were collected from the Gallup at CCS, but concretions near its base at PRS (Fig. 32, control point #7) yielded abundant specimens of the early Coniacian inoceramid *Cremnoceramus deformis erectus* (Fig. 50, D14467 level). The Gallup on SNWR was deposited during the late part of R-2 in the earliest Coniacian. Both upper and lower contacts are sharp and conformable. The Turonian–Coniacian boundary is probably near or at the boundary of the Gallup with the D-Cross.

The **Dilco Coal Member of the Crevasse Canyon Formation** is 31 m thick at CCS (Fig. 50). It consists primarily of paludal carbonaceous shale and siltstone with a few thin sandstone beds. A 1-m-thick bed of coal 5 m above the base was the site of the Garcia y Goebel coal mine. Petrified logs are preserved in the lower 3 m of the Dilco at PRS. The Dilco was deposited in the early Coniacian during the waning part of R-2 and the early part of T-3.

The **Mulatto Tongue of the Mancos Shale** is at least 10 m thick at CCS (Fig. 32, control point #9), where its upper contact is at an unconformity with the Eocene Baca Formation (Fig. 50). Its contact with the underlying Dilco is at the base of a 1.5-m-thick bed of friable sandstone that contains some of the best specimens in the area of the early Coniacian oyster *Flemingostrea elegans* (Fig. 50, D14500 level). The oysters are commonly preserved as fully articulated original shells. The presence of the brackish-water oyster *Crassostrea soleniscus* in a coquina (Fig. 50, D14503 level) directly on top of a sandstone containing *F. elegans* and marine bivalves (Fig. 50, D14479 level) suggests that the coquina is close to the top of the marine section at this location. However, an outcrop to the southeast of Mesa del Yeso and south of the southern boundary of SNWR indicates that the Mulatto could be thicker in the area. This outcrop, which lacks stratigraphic context, is discussed below.

The Mulatto Tongue of the Mancos Shale at the Mesa del Yeso measured section (MdY; Fig. 32, control point #6) was originally thought to be at least 37 m thick (Hook and Cobban, 2010, fig. 10). This exposure (Fig. 57) emerges from the late Quaternary alluvium and its top is covered. The lower 27 m of the outcrop consists of unfossiliferous sandstone and silty shale. Root casts and plant debris discovered in 2016 throughout the silty shale indicate that this part of the section is continental. A 3-m-thick, resistant bench of fine-grained, ripple-marked, cross-bedded sandstone 24 m above the base of the section is capped by a 61-cm-thick, fossiliferous sandstone concretion bed. Fossils from this bed (Fig. 57, D14482 level) consist of shells of the early Coniacian oyster *Flemingostrea elegans* and internal molds of the bivalve *Pleuriocardia subcurtum* (Meek). This sandstone rests on a thin bed containing chert pebbles interpreted as a transgressive lag (Fig. 57). A thin sandstone 5 m higher yields the bivalves *P. subcurtum* and *Crassostrea soleniscus* (Fig. 57, D14494 level).

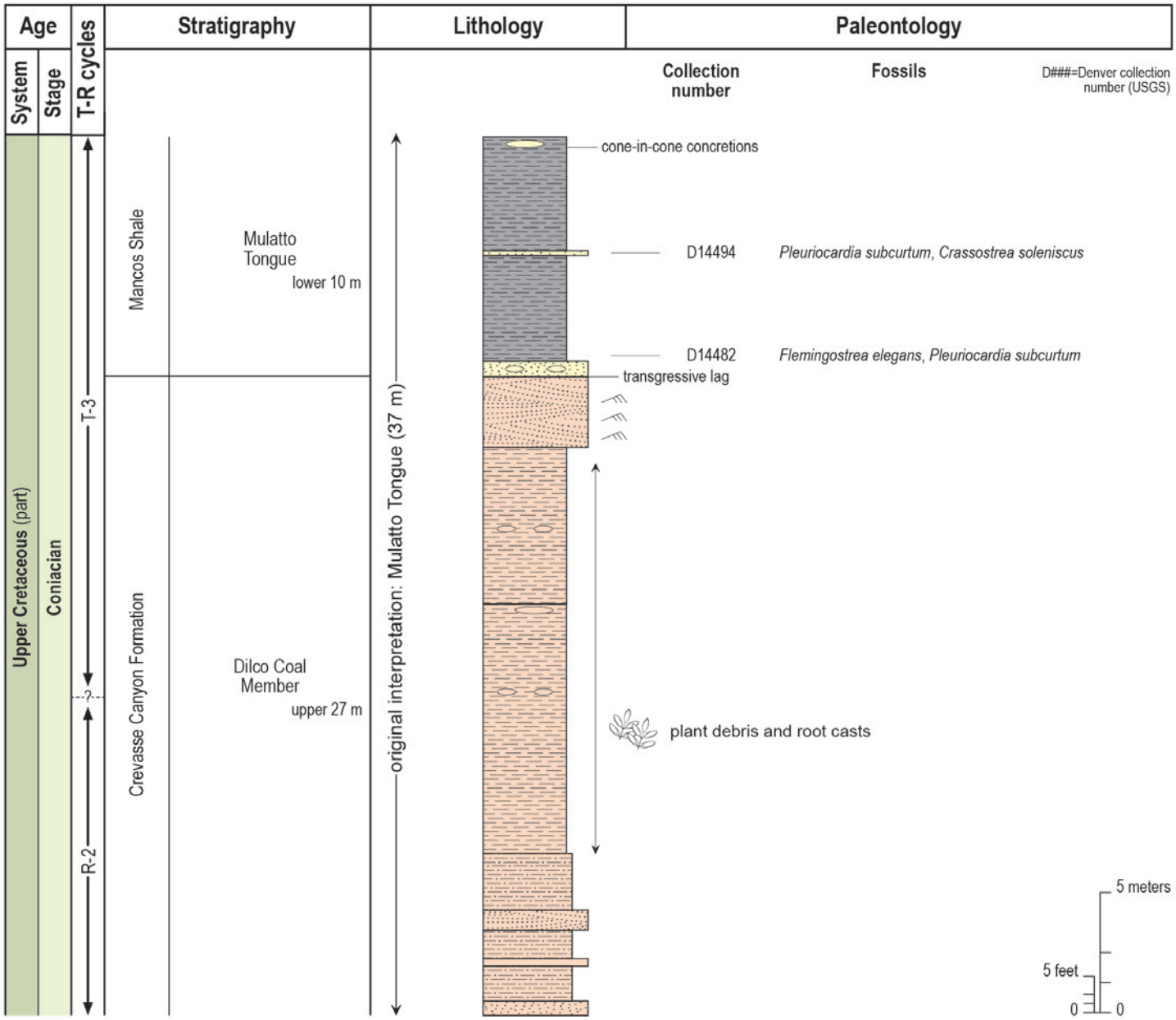

Figure 57. Graphic section of the Mulatto Tongue of the Mancos Shale at the Mesa del Yeso measured section (**MdY**; Figure 32, control point #6), in NW1/4 sec. 32, T. 1 S., R. 5 E., Mesa del Yeso 7.5-minute quadrangle, showing positions of fossil collections. Originally, this entire isolated exposure was interpreted as the Mulatto Tongue (Hook, 2010, fig. 10). Subsequent field work in 2016 with G.H. Mack revealed root casts and plant debris preserved in the shales in the lower 27 m. This lower interval is reassigned to the Dilco Coal Member of the Crevasse Canyon Formation. See Figure 34B for key.

A zone of cone-in-cone limestone concretions caps the section under a cover of colluvium. Outcrop photographs and a large-scale graphic section of MdY can be found in Hook and Cobban (2010, figs. 8E, 8F, and 10).

An isolated exposure consisting of approximately 20 m of carbonaceous shale and interbedded sandstone crops out in a structural saddle to the northeast and stratigraphically above MdY (Fig. 57). The stratigraphic interval separating this exposure from the top of the section shown in Figure 57 is undetermined because of cover and possible structural complications; however, it is less than 30 m thick if the section is simply covered. A 5-m-thick sandstone at the top of this exposure is capped by a 1-m-thick, dark-brown, burrowed sandstone that may be the Dalton Sandstone Member of the Crevasse Canyon Formation. No body fossils were collected from this sandstone, although bits of oyster shells were observed on its upper surface. Whether this sandstone represents a minor fluctuation of the R-3 shoreline or the incursion of the T-4 shoreline into the area cannot be determined because of the absence of identifiable body fossils.

The Mulatto Tongue of the Mancos Shale on SNWR was deposited during the last part of T-3 and early part of R-3 in early Coniacian time (Fig. 33). It is the youngest marine Upper Cretaceous unit known with certainty in the study area.

Summary

The Upper Cretaceous of the Quebradas area is a complex stratigraphic succession of intertongued marine and continental strata deposited during the first three transgressive–regressive (T–R) cycles of the western shoreline of the Late Cretaceous Western Interior Seaway across New Mexico (Table 2). The stratigraphic succession exceeds 610 m in thickness at the Carthage coal field (Fig. 34A). Strata discussed in this chapter are divided into seven major stratigraphic units, in ascending order: (1) Dakota Sandstone, (2) Tokay Tongue of the Mancos Shale, (3) Tres Hermanos Formation, (4) D-Cross Tongue of the Mancos Shale, (5) Gallup Sandstone, (6) Dilco Coal Member of the Crevasse Canyon Formation, and (7) Mulatto Tongue of the Mancos Shale. Each unit is recognized throughout the study area. The Gibson Coal Member of the Crevasse Canyon Formation lies above the Mulatto Tongue but was not measured and is not discussed in detail in this report. Just north of the mapped area, the Twowells Tongue of the Dakota Sandstone divides the Tokay Tongue of the Mancos Shale into two formally named, member-rank units of Mancos Shale—the Whitewater Arroyo Tongue below and the Rio Salado Tongue above—further complicating the Upper Cretaceous stratigraphy of the region.

Marine rocks in the area range in age from middle Cenomanian to early Coniacian, a time span of about 8.1 Myr. After the initial incursion of Seboyeta Bay into New Mexico in the earliest middle Cenomanian, the western shoreline of the seaway transgressed from northeast to southwest and regressed from southwest to northeast (Fig. 32). Therefore, the bases of transgressive strata in the study area are older in the north (SNWR) and regressive strata are older in the south (Carthage).

More bentonites of middle to late Cenomanian age are documented in the Tokay Tongue of the Mancos Shale at Carthage than in temporal equivalents elsewhere in the Western Interior, indicating that the middle to late Cenomanian was a time of relatively intense volcanic activity in the southern part of the Western Interior.

Using the better-exposed Upper Cretaceous strata at Carthage (Fig. 34A) as typical of the Quebradas area, the compacted sedimentation rates for the first four half depositional cycles are 57 m/Myr (0.0057 cm/yr) for T-1, 54 m/Myr (0.0054 cm/yr) for R-1, 66 m/Myr (0.0066 cm/yr) for T-2, and 33 m/Myr (0.0033 cm/yr) for R-2 (Table 2). If the uncompacted sedimentation rates were an order of magnitude greater than the compacted rates, the resulting rates are less than 660 m/Myr (0.066 cm/yr), suggesting that deposition during the Late Cretaceous in the Quebradas area was more episodic than continuous, perhaps driven in part by storms and erosion. Erosional disconformities are interpreted near the top of the Dakota Sandstone on JdM and SNWR, at the top of the Tres Hermanos Formation throughout the area, within the Tres Hermanos Formation at Carthage, and within the Juana Lopez Beds throughout the area. Most of these unconformities are identified by the presence of phosphatic deposits and missing faunal zones.

Changes in Upper Cretaceous stratigraphic terminology recommended by Lucas et al. (2019)

for use in Socorro and Sierra Counties are rejected. For example, their subdivision of the lower part of the Mancos Shale—the unit called the Tokay Tongue of the Mancos Shale in this report—into Graneros, Greenhorn, and Carlile Members is based on outdated and specifically superceded definitions; the pertinent literature for this newer research is not cited in their paper. Lucas et al. (2019) correlated these rock units into the area from a single section in the northern Raton Basin, Colorado, that is more than 250 km north of Socorro County.

The Upper Cretaceous in the Quebradas area is generally well exposed and fossiliferous but is complicated by faults. Quebradas outcrops are important in linking the better-studied, more-continuous exposures of the Upper Cretaceous in the San Juan Basin to geographically limited exposures to the south and southwest in New Mexico. Upper Cretaceous outcrops southwest of the Quebradas area contain marine strata that were deposited during only the first cycle of transgression–regression; those outcrops to the south contain marine strata deposited during the first two cycles. Without the understanding and insight provided by study of the Upper Cretaceous strata in the Quebradas area, especially the outcrops at Carthage, the isolated exposures in the southern part of the state would have been more difficult to interpret.

CHAPTER 4: CENOZOIC ROCKS

MIDDLE EOCENE BACA FORMATION OF THE QUEBRADAS REGION

Steven M. Cather

Introduction

The 75–35 Ma Laramide orogeny produced numerous intraforeland basins and uplifts in New Mexico (Cather, 2004). Deformation resulted from northeast–southwest contraction, which caused important dextral components of slip along north-trending faults in New Mexico and southern Colorado (Chapin and Cather, 1981, 1983; Dickinson et al., 1988; Cather, 1999, 2004; Cather et al., 2006). Synorogenic sedimentation in central New Mexico occurred in the middle Eocene, late in the Laramide episode.

In central and western New Mexico, fill of Laramide basins is termed the Baca Formation. The Baca Formation was named by Wilpolt et al. (1946) for siliciclastic red-bed exposures in Baca Canyon of the Bear Mountains, about 50 km northwest of Socorro. Their initial lithologic description of the unit, however, was for 25–45 m of conglomerate, sandstone, and mudstone exposed near the Joyita Hills.

Cather (1980) and Cather and Johnson (1984) recognized that the Baca Formation of central and western New Mexico accumulated within two late Laramide basins divided by an area of uplift (the Sierra Uplift) occupying what is now the Socorro Basin and possibly the La Jencia Basin of the Rio Grande rift, and the Chupadera, Socorro, and Lemitar Mountains. To the west of the Sierra Uplift lies the Baca Basin; to the east is the Carthage–La Joya Basin. Baca Formation exposures in the study area are within the latter basin.

Lucas and Williamson (1993) coined the term Hart Mine Formation for limestone- and granite-clast conglomerates and pebbly sandstones that dominate the fill of the Carthage–La Joya Basin. Cather et al. (1994a) pointed out, however, that the eastern Baca Basin contains strata with similar pebble compositions (granite and limestone clasts in both basins were derived from the intervening Sierra Uplift). Moreover, subsequent mapping in the Mesa del Yeso quadrangle demonstrated that strata exhibiting a variety of clast compositions exist in the northern Carthage–La Joya Basin and are intimately interfingered with the limestone/granite petrofacies. For these reasons, Cather et al. (2013) abandoned the term Hart Mine Formation and reinstated the term Baca Formation for all pre-volcanic Cenozoic red beds of central New Mexico.

The thickness of the Baca Formation varies considerably in the study area. In the southern part of the study area, Gardner (1910) described a 312-m section of Eocene red beds near Carthage that were subsequently assigned to the Baca Formation. East of the Blackington Hills, the Baca is approximately 300 m thick but thins rapidly as it onlaps older rocks to the west in the Loma de las Cañas quadrangle, where it is approximately 20–100 m thick. In the Valle del Ojo de la Parida area, the Baca Formation is at least 200 m thick, but its true thickness is indeterminate due to faulting and cover.

The Baca Formation disconformably overlies strata of various ages in the study area. In the southern and northern parts of the study area, the Baca overlies relatively young rocks—the Upper Cretaceous Crevasse Canyon Formation near Carthage and in the northern part of Valle del Ojo de la Parida. In the intervening, middle part of the study area, it overlies mostly older strata. In the Bustos Well quadrangle, the Baca Formation overlies the Upper Cretaceous Tres Hermanos Formation and the Tokay Tongue of the Mancos Shale. Near the southern part of the Valle del Ojo de la Parida, it locally rests on the D-Cross Tongue of the Mancos Shale, the Tres Hermanos Formation, the Crevasse Canyon

Formation, and the Triassic Chinle Formation. In the southeastern part of the Loma de las Cañas quadrangle, it appears to overlie the Pennsylvanian Atrasado Formation within the Cañas structural zone (see Chapter 5). The depth of pre-Baca erosion in the study area is related to the spatial distribution of Laramide structures. Within individual exposures, the basal contact of the Baca Formation commonly exhibits several meters of relief.

The Baca Formation in the Carthage–La Joya Basin is middle Eocene. Gardner (1910) collected a fossil tooth from the lower part of the Baca section near Carthage, identified by J.W. Gidley as possibly *Palaeosyops*, a brontothere of probable Bridgerian age. From the same area, about 130 m above the base of the Baca Formation, fossil remains of lizards, turtles, and mammals were collected. The latter includes the brontothere *Telmatherium* of late Bridgerian age (approximately 46.5–46 Ma; Morgan et al., 2009).

Clasts of Proterozoic and Permian rocks in the Baca Formation at Palo Duro Canyon about 10 km north of the study area yielded apatite fission-track ages of approximately 57–45 Ma, suggesting that source rocks in the Sierra Uplift cooled through the approximately 110°C isotherm (about 3–5 km paleodepth) during late Paleocene through middle Eocene time (Kelley et al., 2009).

Lithofacies

The Baca Formation in the Quebradas region is a fluvial succession of conglomerate, fine to very coarse arkosic to subarkosic sandstone, and red mudstone. For the purpose of mapping, the Baca was divided into four lithofacies (Plate 1) based on clast types within conglomerates, paleoflow, and the interpreted depositional paleoenvironment. In the northern Carthage–La Joya Basin (north of the Tajo structural zone), the Baca Formation was deposited by a relatively complex variety of depositional paleoenvironments, including a gravelly axial river and associated, opposing braided-stream piedmont systems (Cather, 2009a). Paleoenvironments of the southern Carthage–La Joya Basin mostly consist of a simple east-facing braided-stream piedmont system, as shown by paleocurrents and the eastward fining of Baca deposits (Cather and Johnson, 1984, 1986; Cather, 2009a; cf., Hashberger et al., 2024, who interpreted northwest paleoflow for Baca deposits near U.S. Route 380). The **basement-clast-dominated piedmont lithofacies** (Plate 1, map unit Tbpg) contains >50% Proterozoic clasts, mostly granite and granitic gneiss with subordinate quartzite, greenstone, schist, and Paleozoic sedimentary clasts. Paleocurrents in this lithofacies indicate derivation from the Sierra Uplift to the west (Plate 1). At one locality in the south-central part of sec. 26, T. 3 S., R. 2 E., granite boulders as large as 2.5 m are present in the lower part of the Baca Formation (Fig. 58). These are the largest clasts known anywhere in the Baca Formation. The boulders are interpreted to mark the downstream terminus of an east-draining paleovalley partly exposed to the west in the footwall of the Ranchito fault zone, a hanging-wall splay of the regional Quebradas detachment fault (see Chapter 5). The maximum size of clasts decreases away from this locality to the north, south, and east, suggesting the paleovalley was a point-source for an alluvial fan in this part of the Carthage–La Joya Basin. These relations indicate west-up normal faults of the Ranchito fault zone formed a local margin of a half graben within the southern Carthage–La Joya Basin during the middle Eocene. In contrast, structural controls on Laramide basin subsidence to the north in the Valle del Ojo de la Parida area remain obscure.

The **sedimentary-clast-dominated piedmont lithofacies** (Plate 1, map unit Tbps; Fig. 59) is the most voluminous part of the Baca Formation in the Carthage–La Joya Basin. Conglomerate within it contains >50% clasts of Paleozoic limestone, sandstone, and siltstone, with subordinate Mesozoic sandstone and Proterozoic lithotypes. Paleocurrent indicators suggest derivation primarily from the Sierra Uplift to the west, but in parts of Valle del Ojo de la Parida this lithofacies appears to have been derived from the Montosa Uplift to the northeast (Fig. 60; Cather, 2009a). As has been previously noted (Cather et al., 2007; Cather, 2009a), the Baca Formation in the southern Carthage–La Joya Basin exhibits an anomalous, inverted unroofing succession, where the basal Baca is nearly exclusively composed of Proterozoic clasts that give way upsection to increasing proportions of limestone, sandstone, and siltstone clasts. A hypothesis relating this inverted unroofing succession to detachment faulting is described in Chapter 5.

Figure 58. Large granite boulders in the lower part of the Baca Formation (Plate 1; cross section D–D´, Plate 2; map unit Tbpg). View is to the north from 342608E, 3764799N (zone 13, NAD 27), Bustos Well quadrangle.

Figure 59. Baca Formation conglomerate (sedimentary-clast-dominated piedmont lithofacies, Plate 1) containing mostly Paleozoic sedimentary clasts and a few granite and gneissic granite clasts. View is to the south from 337880E, 3783922N (zone 13, NAD 27), Mesa del Yeso quadrangle.

Exposures of the **volcaniclastic piedmont lithofacies** (Plate 1, map unit Tbpv) are restricted to the southern Valle del Ojo de la Parida. This lithofacies consists of volcaniclastic tongues a few meters to a few tens of meters thick within the middle and upper parts of the Baca Formation, beneath the transitional contact with the overlying Spears Group. Consisting of approximately 10–50% intermediate volcanic detritus, with the remainder a mixture of Proterozoic lithotypes and Paleozoic/Mesozoic sedimentary clasts, this lithofacies occupies an unusually thick stratigraphic interval; in most other areas, the transition to the dominantly volcaniclastic Spears Group occurs within a stratigraphic interval of only a few meters. No paleocurrents were measured in this lithofacies, but it was probably derived from the west, as were the volcaniclastics of the overlying Spears Group.

The **axial-fluvial lithofacies** (Plate 1, map unit Tbae) contains well-rounded clasts of multicolored quartzite with subordinate clasts of felsic metavolcanic rocks, chert, quartz, and petrified wood. Several clasts of gray porphyry were also noted, but these are too altered for radioisotopic dating. Less than about 20% of clasts consist of subangular to subrounded pebbles of Paleozoic lithotypes, similar to those in associated piedmont deposits. No clasts of granite were observed. The axial-fluvial lithofacies is restricted to Valle del Ojo de la Parida, the northernmost Baca exposures in the Bustos Well quadrangle (thin deposits there were mapped

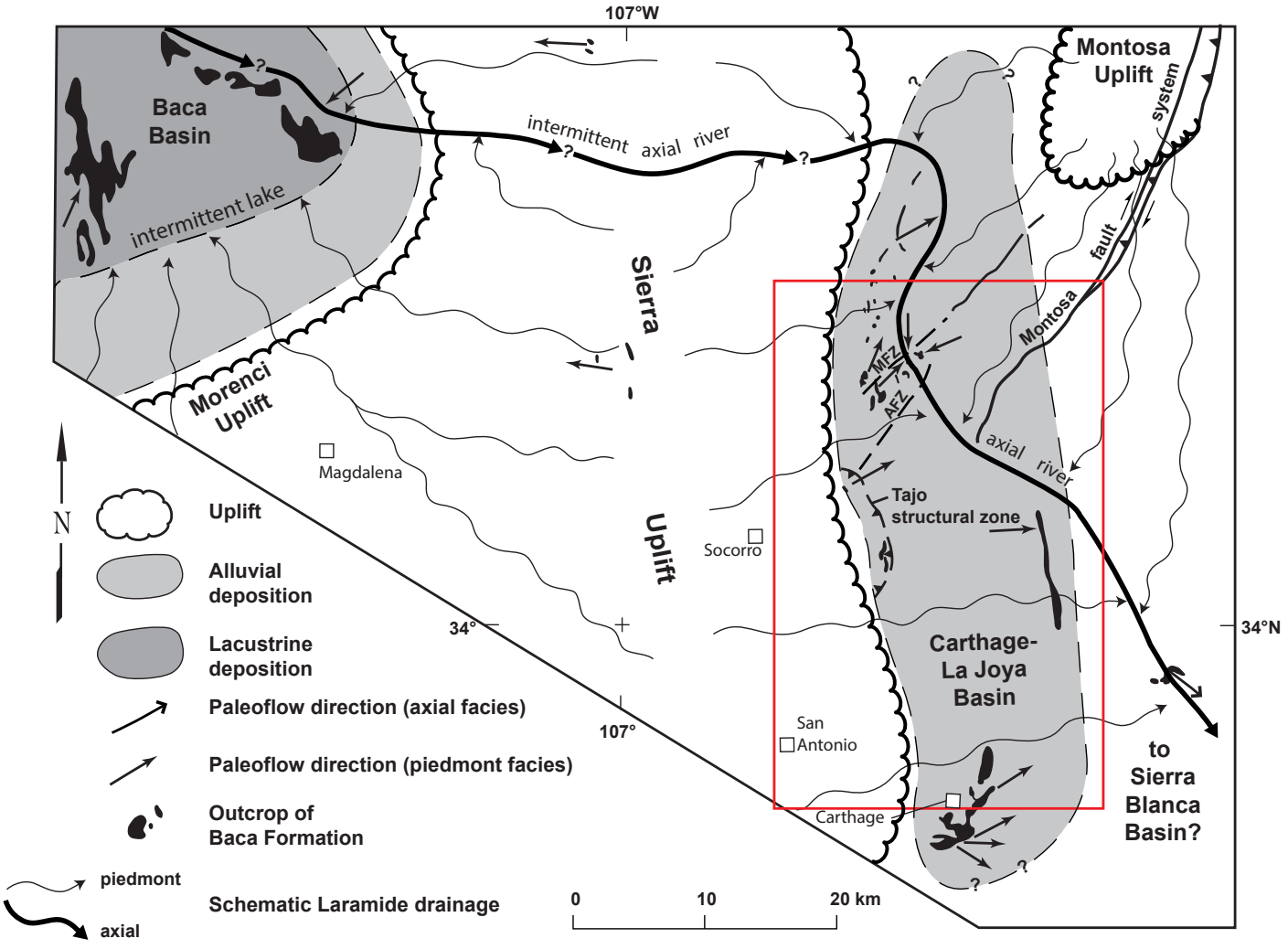

Figure 60. Late Laramide (middle Eocene) paleogeographic map of central New Mexico showing the study area (red rectangle), distribution of uplifts, basins, measured paleocurrents, and schematic Laramide paleodrainage relative to outcrops of the Eocene Baca Formation (modified from Cather [2009a]). Paleocurrent data are from Cather and Johnson (1984), Cather (2002), Cather et al. (2004, 2007), Cather and Colpitts (2005), and Read et al. (2007). Abbreviations: **MFZ**—Milagro fault zone, **AFZ**—Amado fault zone.

as part of the basement-clast-dominated piedmont lithofacies), and Rancho Ojo del Llano 6 km east of the Cañon Agua Buena quadrangle. In the northern Bustos Well quadrangle, pebble imbrication indicates paleoflow was eastward. At Rancho Ojo del Llano, paleoflow was southeasterly (Cather, 2009a). Due to poor exposure, no paleocurrent measurements were obtained from the axial-fluvial lithofacies in the Valle del Ojo de la Parida.

Clast lithologies present in the axial-fluvial lithofacies, with the exception of the Pennsylvanian and Permian types, are not well-matched to any known local source terrane. The clasts in these deposits are too coarse to have been recycled from local Mesozoic or Paleozoic conglomeratic strata. In central New Mexico, basement terranes are dominated by granitic gneiss, and quartzite is generally gray and not areally extensive. The lack of granite, preponderance of varicolored quartzite, and the notable roundness of the quartzite clasts suggest these deposits were derived from afar. Eocene conglomerate in the western part of the Baca Basin exhibits clast populations similar to those of the axial-fluvial lithofacies of the Carthage–La Joya Basin. The conglomerate of the Baca Basin was derived from the Mogollon Highlands of southern Arizona, which contained large exposures of varicolored Proterozoic Mazatzal Quartzite (Cather and Johnson, 1984, 1986). The age distribution of detrital zircons in Baca sandstone from Rancho Ojo del Llano contains a young mode at 74.4 ± 2.5 Ma (Donahue, 2016, her sample SCATH-2012-1), consistent with derivation from the porphyry copper province of central Arizona.

The exotic quartzite clasts and the approximately 74 Ma detrital zircons of the axial-fluvial lithofacies appear to have been derived from the Mogollon Highlands of southern Arizona, which implies that the eastward paleodrainage of the Baca Basin at times spilled eastward across the Sierra Uplift (Cather, 2009a). The Baca Basin was often hydrologically closed, as shown by the dominance of lake deposits in the Bear and Gallinas Mountains area (Cather and Johnson, 1984, 1986). The middle part of the formation (the middle sandstone member of Potter, 1970) in these areas, however, is fluviatile and may represent a time of throughgoing, extrabasinal drainage to the Carthage–La Joya Basin. The speculative course of this paleoriver is depicted in Figure 60.

MIDDLE EOCENE TO PLIOCENE VOLCANIC, VOLCANICLASTIC, AND INTRUSIVE ROCKS OF THE QUEBRADAS REGION

Steven M. Cather, Matthew T. Heizler, and William C. McIntosh

Introduction

Major regional volcanism began in the Mogollon–Datil volcanic field near the end of Laramide tectonism in New Mexico and continued during the initial stages of rifting, producing great volumes of volcanic and volcaniclastic rocks (Chamberlin, 1983; Cather, 1990; Chapin and Cather, 1994). Nomenclature for the volcanic and volcaniclastic rocks of the northeastern Mogollon–Datil volcanic field has evolved considerably since the early studies of Winchester (1920) and Loughlin and Koschmann (1942). In this report, we adopt the formation-rank terminology of Osburn and Chapin (1983) with minor modification, and we follow the usage of Cather et al. (1994a) for group-rank terms—the dominantly volcaniclastic Spears Group and the dominantly volcanic Datil and Mogollon Groups.

We report new $^{40}Ar/^{39}Ar$ ages from conglomerate clasts, lavas, and ignimbrites in the southern Joyita Hills and the Blackington Hills area (Table 3 and Appendix 1[1]). All of these ages are relative to Fish Canyon Tuff sanidine at 28.201 Ma (Kuiper et al., 2008). Previously published ages are corrected to this calibration. All errors reported here are 1σ.

Paleogene volcanic and volcaniclastic rocks crop out in three parts of the study area (Plate 1). The first is a swath of exposures in the southern Joyita Hills that bisect the Mesa del Yeso quadrangle (Spradlin, 1976) and extend discontinuously southward along the eastern margin of the Socorro Basin to Arroyo de las Cañas. The second is exposures near the Blackington Hills in the southern Bustos Well quadrangle and the northern Cañon Agua Buena quadrangle (Fig. 61). These exposures encompass the North Jornada del Muerto section of Osburn and Chapin (1983) and are cut by the Ranchito, Pinos, and Bustos normal faults (all hanging-wall splays associated with the Quebradas detachment fault),

1 Appendices can be downloaded at https://geoinfo.nmt.edu/publications/monographs/memoirs/51/

Table 3. $^{40}Ar/^{39}Ar$ ages for selected volcanic, volcaniclastic, and intrusive rocks in the Quebradas region.

Sample	Unit	Location (E, N) (zone 13, NAD 27)	L#	Irrad	Material	Age	Comments
Blackington Hills, east of Bustos fault							
BW-2014-12	South Canyon Tuff (upper)	0346161, 3764493	65579, 80	NM-289O	Sanidine	27.67 ± 0.01	TGA + SCLF; spectra steeply climbing to flat
BW-2014-11	South Canyon Tuff (lower)	0346246, 3764586	63296, 97	NM-272C	Sanidine	27.68 ± 0.02	Oldest steps from climbing spectra
BW-2014-10	Lemitar Tuff	0346318, 3764395	65590	NM-289O	Sanidine	28.25 ± 0.01	Oldest steps from climbing spectra
BW-2014-9	Vicks Peak Tuff	0346518, 3764289	65559, 60	NM-272C	Sanidine	28.77 ± 0.01	Plateau age plus some single step ages; spectra flat to climbing
BW-2014-8	La Jencia Tuff	0346586, 3764270	65581, 82; 63273, 74	NM-272A	Sanidine	29.00 ± 0.01	TGA + SCLF; spectra flat to climbing
BW-2014-6	Luis Lopez Formation fallout ash	0346703, 3764248	63265, 66, 67	NM-272A	Sanidine	29.00 ± 0.01	SCLF, omitted young grains
BW-2014-7	Luis Lopez Formation ignimbrite	0346704, 3764248	63269, 70, 72	NM-272A	Sanidine	29.02 ± 0.01	SCLF, omitted young grains
BW-2014-5	Unidentified ignimbrite	0346815, 3764397	63262	NM-272A	Sanidine	35.35 ± 0.02	SCLF
BW-102	Unidentified ignimbrite	0346815, 3764395 (approx.)	65584	NM-289O	Sanidine	35.35 ± 0.02	Oldest steps from climbing spectra
BW-102	Unidentified ignimbrite	0346815, 3764395 (approx.)	65766	NM-291A	Biotite	35.47 ± 0.08	Plateau ages for five replicate analyses
BW-2014-4	Rock House Canyon Tuff	0346897, 3764306	65551, 52, 53	NM-289N	Sanidine	34.78 ± 0.01	TGA + SCLF; spectra generally flat
BW-2014-3	Datil Well Tuff	0346958, 3764313	65449, 50	NM-289N	Sanidine	35.38 ± 0.01	Oldest ages from spectra plus SCLF; spectra generally rising
BW-2014-2	Clast from lower Spears Group	0347771, 3764128	63278	NM-272B	Hornblende	42.87 ± 0.03[1]	Complex spectrum
BW-2014-1	Clast from lower Spears Group	0347982, 3764122	63276	NM-272B	Hornblende	43.38 ± 0.04[1]	Complex spectrum
Blackington Hills area, west of Bustos fault							
BW-2014-22	La Jencia Tuff	0343854, 3763866	63305	NM-272C	Sanidine	29.00 ± 0.01	SCLF, omitted several young grains
BW-2014-23	Luis Lopez Formation	0343852, 3763977	63309, 10	NM-272C	Sanidine	29.01 ± 0.02	SCLF, omitted several young grains
BW-2014-21	Dacite lava	0344052, 3764493	63282	NM-272B	Hornblende	33.98 ± 0.05[2]	Flat age spectrum
BW-2014-13	Dacite lava	0343500, 3762200 (approx.)	63280	NM-272B	Hornblende	34.04 ± 0.02[2]	Flat age spectrum
BW-2014-20	Unidentified ignimbrite	0344192, 3763871	63302	NM-272C	Sanidine	35.38 ± 0.01	SCLF
BW-2014-24	Datil Well Tuff	0344334, 3764036	63313	NM-272C	Sanidine	35.32 ± 0.02	SCLF, omitted several young grains
Southern Joyita Hills							
NM-2607	South Canyon Tuff	0331482, 3780770	65573, 74, 75	NM-289M	Sanidine	27.65 ± 0.01	SCLF + TGA; spectra variable
NM-2605	Lemitar Tuff (lower)	0331908, 3780735	65576, 77	NM-289M	Sanidine	28.22 ± 0.01	SCLF + TGA; spectra mostly downward stepping
NM-2609	Vicks Peak Tuff	0332518, 3786079	65585	NM-289O	Sanidine	28.78 ± 0.01	TGA + plateau ages; spectra mostly flat
NM-2604	La Jencia Tuff	0332326, 3780820	65567, 68	NM-289M	Sanidine	28.98 ± 0.01	TGA + SCLF; spectra flat to climbing
NM-2602	Hells Mesa Tuff (upper)	0332423, 3780830	65569, 71, 72	NM-289M	Sanidine	32.35 ± 0.01	Oldest steps from climbing spectra
NM-2601	Hells Mesa Tuff (lower)	0332473, 3780793	65563, 64	NM-289M	Sanidine	32.35 ± 0.01	SCLF
Other areas							
SL-2	Andesite dike	0347200, 3780200 (approx.)	61128	NM-249B	Biotite	34.68 ± 0.11[1]	Complex spectrum; sampled by M. Green.
BLKMS-1	Black Mesa basalt (upper flow)	0350537, 3788168	58712	NM-221J	Groundmass	3.68 ± 0.34[3]	Complex spectrum; sampled by R.M. Chamberlin.

All ages reported at 1σ. Sanidine ages are weighted mean of selected analyses. L# = laboratory identifier, Irrad = irradiation identifier, SCLF = single-crystal laser fusion, TGA = total gas age, approx. = approximately located.

[1] Total gas age
[2] Plateau age
[3] Isochron age

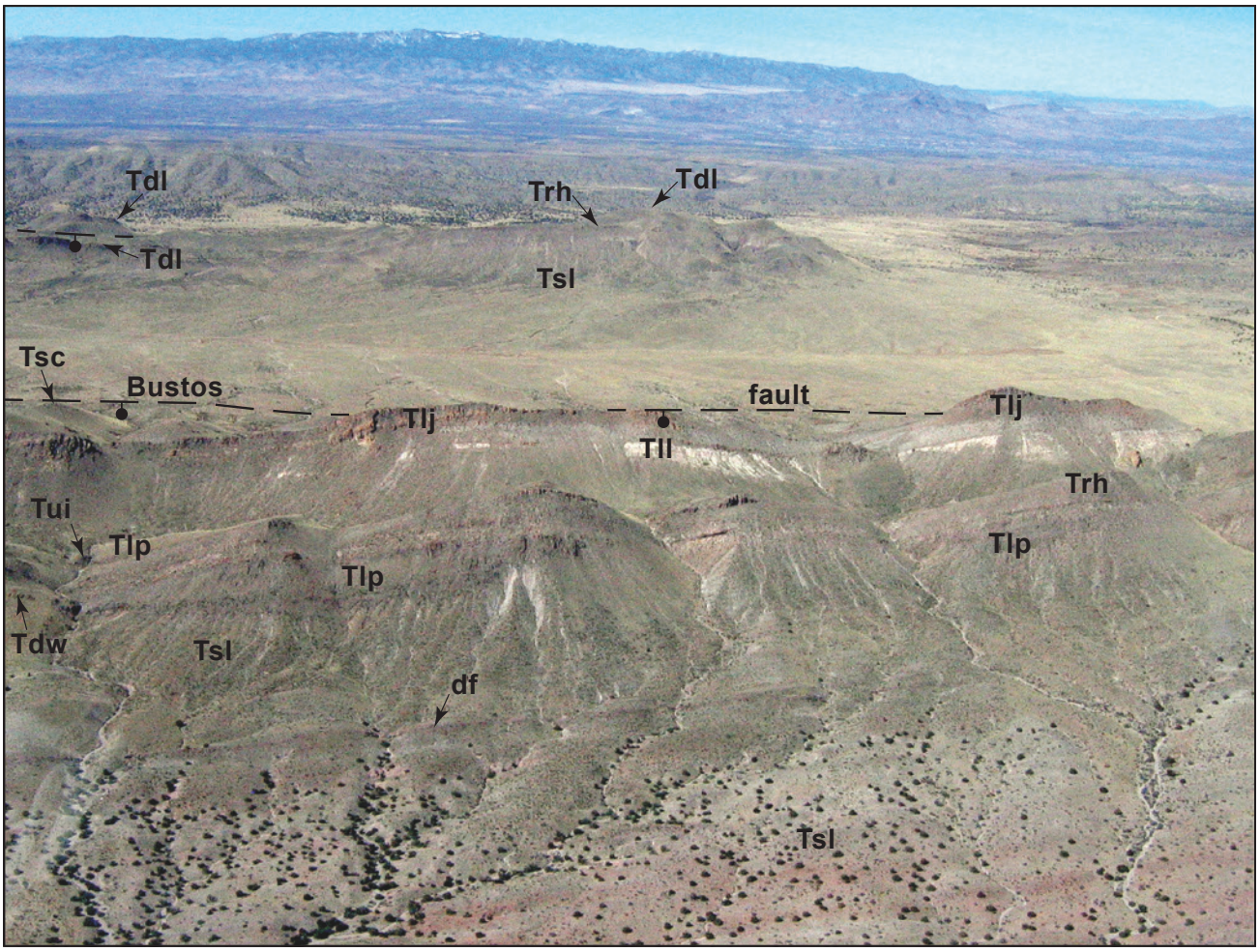

Figure 61. Aerial view of the Paleogene volcanic and volcaniclastic section exposed in the Blackington Hills (foreground) and the fault-repeated section in the footwall (west side) of the Bustos fault. The view is to the west above sec. 28, T. 3 S., R. 3 E., southern Bustos Well quadrangle; the Magdalena Mountains are on the skyline. Selected stratigraphic units: **Tsl**—lower Spears Group, **df**—debris-flow deposit in lower Spears Group, **Tdw**—Datil Well Tuff, **Tlp**—La Jara Peak Basaltic Andesite (lenticular fills in paleovalleys), **Trh**—Rock House Canyon Tuff, **Tui**—unidentified ignimbrite, **Tdl**—dacite lava flow, **Tll**—Luis Lopez Formation, **Tlj**—La Jencia Tuff, and **Tsc**—South Canyon Tuff.

producing three west-tilted fault blocks in which parts of the volcanic section are repeated. The third is a small exposure of the lower Spears Group near Carthage in the southern part of the Cañon Agua Buena quadrangle.

Intermediate to basaltic andesite intrusive rocks occur as sparse dikes and sills scattered widely throughout the study area. Most are probably upper Eocene–Oligocene, but only one was dated (at 34.7 Ma). Black Mesa, in the northeastern corner of the study area, is capped by Pliocene basalt flows.

Spears Group

In western New Mexico, the volcaniclastic strata that constitute the lower part of the Paleogene Mogollon–Datil volcanic field are apportioned among various formations of the middle Eocene to Oligocene Spears Group (Cather et al., 1994a; Chamberlin and Harris, 1994). Lithologic characteristics of these formations are related to their depositional paleoenvironment. In the northeastern part of the field near Socorro, the Spears Group is not easily divisible into formation-rank units, and no formation-rank terms have been applied to the Spears in the study area. Instead, we

have divided it into two informal parts, the lower and upper Spears Group, based on clast lithology.

The lower Spears Group mostly consists of compositionally monotonous clasts of intermediate volcanic rocks (light-gray porphyritic andesite and dacite with phenocrysts of plagioclase, hornblende, ± biotite; see Cather [1986] for detailed description of the petrology and chemistry of the Spears Group). The clast content of the upper Spears Group is more diverse, consisting of ignimbrite clasts, andesite–basaltic andesite clasts (dark-colored clasts with phenocrystic plagioclase and clinopyroxene or iddingsite; Cather, 1986), as well as clasts typical of the lower Spears. The upper Spears Group was mapped separately only where it forms tongues between volcanic units of the Datil Group. The transition from lower to upper Spears lithotypes, however, typically lies approximately 20–100 m stratigraphically below the base of the Datil Group (Cather, 1986). Because this contact is not readily mappable except in areas of good exposure, the pre-Datil parts of the upper Spears Group were mapped as lower Spears Group. We do not recommend elevating the lower and upper Spears Group to formation rank because their definitions are based on petrofacies (i.e., clast lithologies), not lithofacies (sandstone, conglomerate, and mudstone characteristics related to paleodepositional environment), as are the constituent formations of the Spears Group of western New Mexico.

Throughout the study area, the **lower Spears Group** transitionally overlies the Baca Formation. The base of the Spears is defined by the first upsection occurrence of >50% volcaniclastic detritus. Near the Blackington Hills, Cather (1986) measured 671 m of the lower Spears Group in N1/2 sec. 32, T. 3 S., R. 3 E.—the greatest thickness of any Phanerozoic unit in the study area. In the southern Joyita Hills (west of Valle del Ojo de la Parida), the estimated thickness is 200–400 m. A faulted, partial section of the lower Spears Group less than about 100 m thick crops out near Carthage. North of the study area in the Becker SW quadrangle, the Joyita Hills measured section of Cather (1986; N1/2 sec. 31, T. 1 N., R. 1 E., unsurveyed) is 533 m thick, and an exposure of the lower Spears 1.5 km to the south has an estimated thickness of 1,480 m (Cather, 1986, p. 334).

The lower Spears Group consists of gray to reddish-gray sandstone, pebbly sandstone, conglomerate, and minor mudstone. Above the transition with the Baca Formation, which typically occurs over a stratigraphic interval of a few meters, the lower Spears Group is exclusively volcaniclastic except for scattered clasts of mostly Permian sandstone, siltstone, and limestone (Fig. 62). The nonvolcanic clasts indicate the persistence of Laramide positive areas to the west during early Spears volcanism (Cather, 1986, 1990). Maximum clast size in the lower Spears Group is around 0.6 m.

Throughout the study area, the lower Spears Group largely consists of alluvial-apron deposits that give way upsection to increasingly abundant debris-flow deposits. Paleoflow during Spears Group deposition was toward the east (Plate 1; Cather, 1986). Volcanoes that erupted Spears andesite and dacite were located on the Sierra Uplift west of the Quebradas region (Cather, 1990).

Regionally, the age range of the lower Spears Group is approximately 39–36 Ma (Cather et al., 1987), but two clasts from the lower and middle parts of the lower Spears Group east of the Blackington Hills yielded imprecise $^{40}Ar/^{39}Ar$ hornblende ages of about 43 Ma (Table 3; Cather et al., 2014).

The **upper Spears Group** map unit consists of tongues of petrologically diverse volcaniclastic sedimentary rock (see above) intercalated with

Figure 62. Conglomeratic volcaniclastic deposits of the lower Spears Group with a boulder of yellow Permian sandstone. The view is to the north from 342864E, 3762061N (zone 13, NAD 27), Cañon Agua Buena quadrangle.

volcanic rocks of the lower part of the Datil Group. In the southern Joyita Hills, north of Puertecito of Bowling Green, conglomeratic upper Spears Group fills a paleovalley 30–60 m deep beneath the 32.4 Ma Hells Mesa Tuff. In the Blackington Hills area, the upper Spears is 0–120 m thick and fills paleovalleys above the 34.8 Ma Rock House Canyon Tuff and below the 29.0 Ma Luis Lopez Formation.

Throughout the study area, the upper Spears Group consists of gray sandstone and conglomerate, mostly of alluvial origin. Debris-flow deposits are less common than in the lower Spears Group. The upper Spears Group was probably derived from the west, although no paleocurrent data were collected. In the study area, the upper Spears Group is late Eocene to early Oligocene in age.

Datil Group

The Datil Group marks the beginning of peak Cenozoic ignimbrite volcanism in southwestern New Mexico (Chapin et al., 2004a, 2004b). The Datil Group consists of ignimbrites, lavas, and minor nonwelded pyroclastic deposits below a regional 31.4–29.0 Ma volcanic hiatus in the Mogollon–Datil volcanic field (Cather et al., 1994a). In the study area, this hiatus is marked by a disconformity at the base of the 29.0 Ma Luis Lopez Formation. The Datil Group in the Quebradas region consists of the Datil Well Tuff, Rock House Canyon Tuff, Blue Canyon Tuff, an unidentified ignimbrite, Hells Mesa Tuff, and an unnamed dacite lava flow in the western Blackington Hills area. Local tongues of the La Jara Peak Basaltic Andesite of the Mogollon Group are intercalated with the Datil Group. Interestingly, for unknown reasons, no ignimbrite of the Datil Group is present in both the southern Joyita Hills and Blackington Hills areas (Fig. 63). The thickness of the Datil Group is approximately 300–400 m, not including intercalated tongues of the upper Spears Group.

In the study area, the **Datil Well Tuff** crops out only in the Blackington Hills area. It is a medium-brownish-gray, moderately crystal-rich, lithic-rich, and pumice-poor welded rhyolitic ignimbrite probably erupted from the Emory caldera in the Black Range (Chapin et al., 2004a). Crystals constitute 15–25% of the ignimbrite and are mostly sanidine with minor clinopyroxene and biotite and traces of quartz and plagioclase (Osburn and Chapin, 1983). Thickness ranges from 0 to 50 m. $^{40}Ar/^{39}Ar$ sanidine ages are 35.32 ± 0.02 Ma (west of the Bustos fault) and 35.38 ± 0.01 Ma (east of the fault; Table 3).

The **Rock House Canyon Tuff** is a light-gray, crystal-poor rhyolitic ignimbrite possibly erupted from the Skeleton Ridge caldera in the San Mateo Mountains (Ferguson et al., 2012). Crystals (4–10% of rock volume) are mostly sanidine with minor plagioclase and biotite and trace amounts of quartz (Osburn and Chapin, 1983). It is poorly to moderately welded, with local zones of abundant flattened pumice. In the Blackington Hills, it is 90–150 m thick (Fig. 63). The Rock House Canyon Tuff is absent in the southern Joyita Hills except for just north of the study area, where it is thin (<5 m) and intercalated with the upper Spears Group (de Moor et al., 2005). The Rock House Canyon Tuff yielded an $^{40}Ar/^{39}Ar$ sanidine age of 34.78 ± 0.01 Ma in the Blackington Hills east of the Bustos fault (Table 3).

An **unidentified ignimbrite** (Fig. 61) of unknown correlation is present in the Blackington Hills area overlying the 34.8 Ma Rock House Canyon Tuff and stratigraphically beneath a 34.0 Ma dacite lava (described below). Outcrops are limited to two 0- to 10-m-thick erosional remnants within a fault-repeated paleovalley, one exposure on each side of the Bustos fault. The densely welded ignimbrite contains around 30% quartz, sanidine, and biotite and was initially thought to be Hells Mesa Tuff. The field relations and stratigraphic context of these outcrops, however, unambiguously bracket the age of the unit to between 34.8 Ma and 34.0 Ma—too old to be 32.4 Ma Hells Mesa Tuff.

Three samples (BW-2014-5, BW-2014-20, and BW-102; Table 3) from the unidentified ignimbrite yielded sanidine and biotite ages near 35.3 Ma (Table 3), similar to the age of the Datil Well Tuff and significantly older than the 34.8–34.0 Ma stratigraphic constraints. The K/Ca of sanidine crystals are unusually low (values near 10), also similar to Datil Well Tuff sanidine. We suggest that the dated crystals are xenocrysts swept up from exposed surfaces of the Datil Well Tuff during transport of the unidentified ignimbrite. Datable primary sanidine and biotite are either lacking in the unidentified ignimbrite or are sparse enough that none were recovered during the mineral separation process. More work is needed to address these issues.

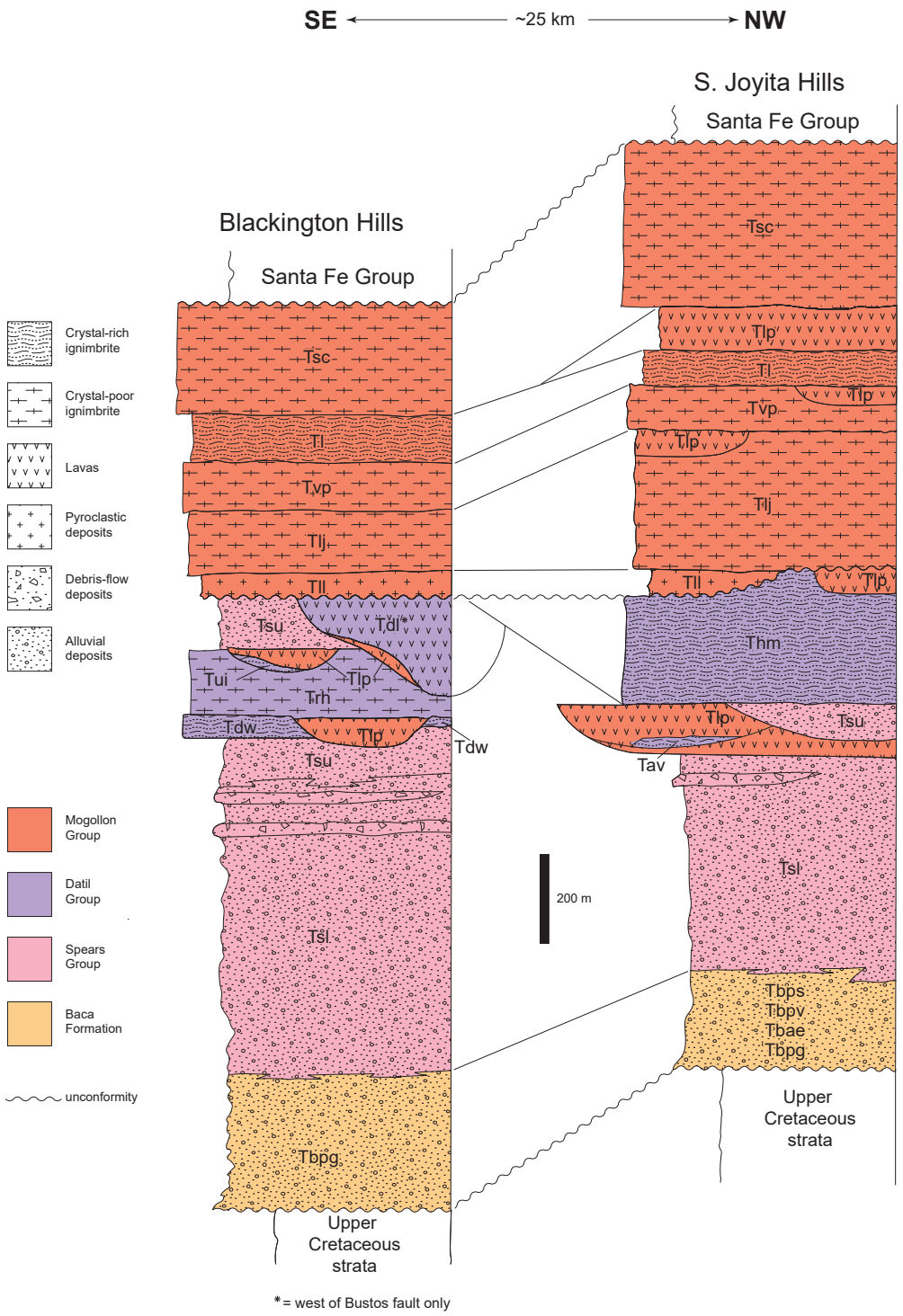

Figure 63. Schematic stratigraphic columns (each ~2 km thick) for Paleogene rocks in the Blackington Hills area (generalized to depict rocks both east and west of the Bustos fault) and southern Joyita Hills. Columns show nomenclature, lithologies, correlation, approximate thicknesses, and significant (> 2 Myr) disconformities. Datum is the base of the Luis Lopez Formation. Stratigraphic units are **Tbpg**—basement-clast-dominated piedmont deposits of the Baca Formation (middle Eocene), **Tbps**—sedimentary-clast-dominated piedmont deposits of the Baca Formation, **Tbpv**—volcanic-clast-bearing piedmont deposits of the Baca Formation, **Tbae**—extrabasinal axial-river deposits of the Baca Formation, **Tsl**—lower Spears Group (middle to upper Eocene), **Tsu**—upper Spears Group (upper Eocene–lower Oligocene; note that Tsu was only mapped where it intertongues with the Datil Group), **Tdw**—Datil Well Tuff (35.3 Ma), **Tlp**—La Jara Peak Basaltic Andesite (various tongues of late Eocene–late Oligocene age), **Trh**—Rock House Canyon Tuff (34.8 Ma), **Tav**—tuff of Arroyo Veranito (34.37 Ma), **Tdl**—unnamed dacite lava flow (34.0 Ma; note that this lava only crops out west of the Bustos fault in the Blackington Hills area), **Tui**—unidentified ignimbrite (see text), **Thm**—Hells Mesa Tuff (32.4 Ma), **Tll**—Luis Lopez Formation (29.0 Ma), **Tlj**—La Jencia Tuff (29.0 Ma), **Tvp**—Vicks Peak Tuff (28.8 Ma), **Tl**—Lemitar Tuff (28.2 Ma), and **Tsc**—South Canyon Tuff (27.7 Ma). Note that west of the Bustos fault in the Blackington Hills area, the Vicks Peak Tuff, Lemitar Tuff, and South Canyon Tuff are absent, probably due to erosion.

The unidentified 34.8–34.0 Ma welded ignimbrite may represent a previously unencountered local unit or the distal edge of a more regional unit, such as the 34.8 Ma tuff of Steins (McIntosh and Bryan, 2000). The distal edges of some ignimbrites are nearly crystal-free due to gravitational settling of crystals during transport; such ignimbrites would be ripe for contamination by crystals from underlying units. Most distal ignimbrites, however, are not welded. Alternatively, the unidentified ignimbrite could indeed be Hells Mesa Tuff, but this would require that the 34.0 Ma age for the overlying dacite lava is inaccurate by >1.5 Myr.

The **tuff of Arroyo Veranito** is approximately 20 m thick and crops out only in the southern Joyita Hills, where it corresponds to unit Tsp-af2 of Spradlin (1976). It is a pink, crystal- and lithic-rich, moderately welded ignimbrite. Crystals of plagioclase, sanidine, biotite, hornblende, and rare quartz constitute around 20–40% of the rock volume. Its $^{40}Ar/^{39}Ar$ age is 34.37 ± 0.06 Ma (Chamberlin et al., 2022). Smith et al. (1983, fig. 1-22.4a) described this ignimbrite as an "unnamed tuff" in the Datil Group.

Brownish-gray **dacite lava** crops out west of the Bustos fault in the Blackington Hills area (Fig. 64). Composed of a single flow as much as 90 m thick with an autobrecciated base, samples from this plagioclase- and amphibole-bearing flow have yielded $^{40}Ar/^{39}Ar$ hornblende ages of 34.04 ± 0.02 Ma (sample BW-2014-13) and 33.98 ± 0.05 Ma (sample BW-2014-21; Table 3). The dacite lava flow appears to have filled the area of maximum subsidence on the hanging wall of the east-down Pinos fault and has locally lapped westward onto its footwall (see Chapter 5). The eruptive center for the dacite is unknown.

The **Hells Mesa Tuff** is a brownish-pink, crystal-rich, densely welded rhyolitic ignimbrite. Crystals of sanidine, plagioclase, quartz, biotite, and opaque minerals constitute 30–45% of the rock (Spradlin, 1976). Quartz becomes more abundant upsection (Spradlin, 1976; Osburn and Chapin, 1983). Lithic

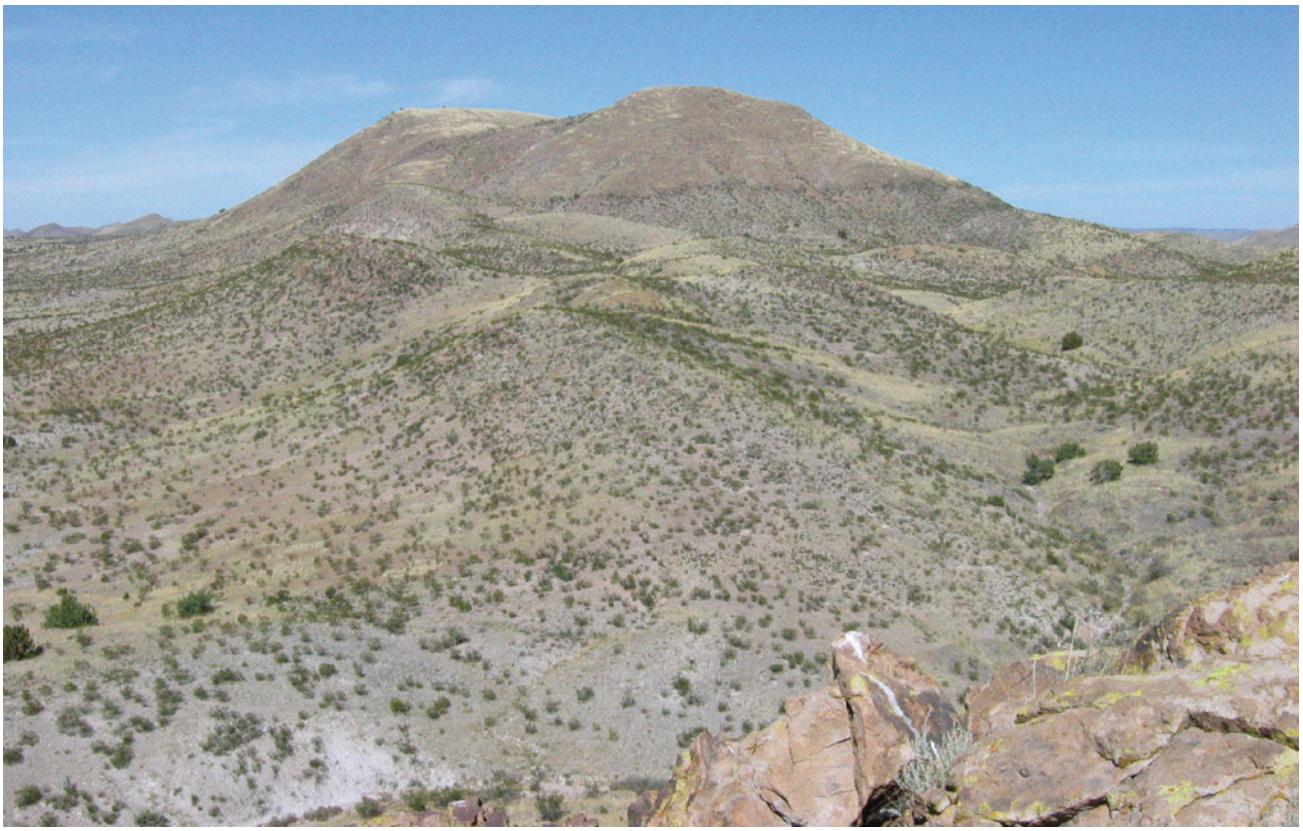

Figure 64. Thick dacite lava flow (light-brown rocks at the top of the hill on the skyline) seen in view to the north from 343576E, 3760981N (zone 13, NAD 27), Cañon Agua Buena quadrangle. The base of the flow is marked by the gently west-sloping line of bushes above the gray ignimbrites (Datil Well Tuff and Rock House Canyon Tuff).

fragments are sparse to abundant. Hells Mesa Tuff erupted from the nearby Socorro caldera (Chamberlin et al., 2004; Chapin et al., 2004a). In the southern Joyita Hills, the Hells Mesa Tuff is 150–300 m thick, but it is probably missing in the Blackington Hills area (see above discussion of unidentified ignimbrite). In the southern Joyita Hills, upper and lower samples of the tuff yielded identical $^{40}Ar/^{39}Ar$ sanidine ages of 32.35 ± 0.01 Ma (Table 3).

Mogollon Group

After a regional volcanic hiatus (Cather et al., 1994a), the Mogollon Group began to accumulate following resumption of major ignimbrite volcanism in the northern Mogollon–Datil volcanic field at around 29 Ma (note, however, that tongues of the La Jara Peak Basaltic Andesite span this hiatus and are intercalated with ignimbrites of both the Datil Group and the Mogollon Group). In the Quebradas region, this volcanic hiatus lasted approximately 3.3 Myr. The Mogollon Group is approximately 700–1,000 m thick in the study area. Unlike ignimbrites of the Datil Group, each ignimbrite of the Mogollon Group present in the southern Joyita Hills is also present in the Blackington Hills area and vice versa (Fig. 63).

The **La Jara Peak Basaltic Andesite** consists of medium- to dark-gray, aphanitic to slightly porphyritic lavas and associated autobreccias of basaltic andesite and andesite composition. Phenocrysts are plagioclase, clinopyroxene, iddingsite, and opaque minerals. We use the term La Jara Peak Basaltic Andesite in its original, broad sense of "lava flows and dikes ranging from alkali basalt to andesite but predominantly basaltic andesite" (Osburn and Chapin, 1983). The age range of the La Jara Peak Basaltic Andesite in the study area (approximately 35–28 Ma) is somewhat older than originally inferred by Osburn and Chapin (1983; approximately 31–24 Ma). Most dikes in the study area are lithologically similar to the La Jara Peak Basaltic Andesite and are probably intrusive equivalents.

The La Jara Peak Basaltic Andesite occurs as several paleovalley-filling tongues in the study area, ranging in stratigraphic position from below the 34.8 Ma Rock House Canyon Tuff to below the 27.7 Ma South Canyon Tuff (Fig. 63), thus spanning an age range of some 7 Myr. In the Blackington Hills, the La Jara Peak Basaltic Andesite occurs as several tongues as much as 80 m thick that fill paleovalleys low in the volcanic section, between the 35.3 Ma Datil Well Tuff and the 29.0 Ma Luis Lopez Formation. These lavas typically contain 5–20% phenocrysts of pyroxene and plagioclase (Osburn and Chapin, 1983, their North Jornada del Muerto section). Two prominent paleovalley-filling lavas are present in NW1/4 sec. 32, T. 3 S., R. 3 E. (Tlp units in the left part of Fig. 61). The stratigraphically lower lava fills a paleovalley below the Rock House Canyon Tuff and has an SiO_2 content (normalized to 100%, volatile free) of 62.2 wt.% (Cather, 1986; note that this flow is 775 m above the base of the measured section as shown on his p. 338, not 975 m as indicated on p. 363). The upper flow (above the Rock House Canyon Tuff and the unidentified ignimbrite) has a normalized SiO_2 content of 56.2 wt.% (Cather, 1986, p. 371).

In the southern Joyita Hills, the La Jara Peak Basaltic Andesite occurs as tongues as much as around 100 m thick intercalated with the Datil and Mogollon Groups. These lavas fill paleovalleys that are generally much broader than those of the Blackington Hills. Five La Jara Peak tongues are present in the southern Joyita Hills. These lavas are iddingsite bearing and correspond to units Tsp-a2, Thm-a, Talp-a, Taw-a, and Trdc-a of Spradlin (1976). They occur, respectively, below the 32.4 Ma Hells Mesa Tuff, the 29.0 Ma La Jencia Tuff, the 28.8 Ma Vicks Peak Tuff, the 28.2 Ma Lemitar Tuff, and the 27.7 Ma South Canyon Tuff (Fig. 63). Normalized chemical analyses of three of these lava flows average 51.7% SiO_2 (Spradlin, 1976).

A tongue of porphyritic andesite with phenocrysts of plagioclase and pyroxene, herein considered part of the La Jara Peak Basaltic Andesite, is intercalated with the Spears Group about 4 km north of the study area. This lava was termed Tsp-a1 by Spradlin (1976) and the andesite flow at El Valle de la Joya by de Moor et al. (2005).

The 29.0 Ma **Luis Lopez Formation** is the basal unit of the Mogollon Group in the Quebradas region. It consists of light-gray, moderately crystal-poor, pumiceous pyroclastic deposits of rhyolitic composition, primarily fallout tephras and poorly welded ignimbrites. Crystals (about 10% of rock volume; Osburn and Chapin, 1983) are mostly sanidine, quartz, and plagioclase. Lithic fragments range from sparse to abundant. These deposits are distal age-equivalents of the upper part of the Luis

Lopez Formation in the Chupadera Mountains (e.g., Chamberlin et al., 2002, 2004) and are probably associated with emplacement of pre-La Jencia Tuff rhyolitic domes in areas to the west. In the Blackington Hills area, $^{40}Ar/^{39}Ar$ sanidine ages are 29.01 ± 0.03 Ma (west of Bustos fault) and 29.02 ± 0.01 Ma and 29.00 ± 0.01 Ma (east of Bustos fault; Table 3). In the southern Joyita Hills, the Luis Lopez Formation was termed the tuff of South Crosby Peak by Beck (1993). The unit is 0–60 m thick in the study area.

The **La Jencia Tuff** forms thick outcrops in the Blackington Hills and southern Joyita Hills. It consists of pink to gray, moderately to densely welded, crystal-poor rhyolitic ignimbrite erupted from the Sawmill caldera in the Magdalena Mountains (Chapin et al., 2004a). The unit exhibits evidence for compound cooling, and its upper part is prominently flow banded. Crystals of sanidine and minor quartz, biotite, and opaque minerals constitute around 5–10% of the rock (Spradlin, 1976). Lithic fragments are sparse. Thickness is approximately 140–320 m. In the Blackington Hills east of the Bustos fault, the La Jencia Tuff yielded an $^{40}Ar/^{39}Ar$ sanidine age of 29.00 ± 0.01 Ma and an identical age for a sample west of the fault (Table 3). In the southern Joyita Hills, Spradlin (1976) mapped it as the lower part of A-L Peak Tuff (units Talp1, Talp2, Talp3A, Talp3, and Talp-af). The $^{40}Ar/^{39}Ar$ sanidine age for the La Jencia Tuff in the southern Joyita Hills is 28.98 ± 0.01 Ma (Table 3).

The **Vicks Peak Tuff** is a light-gray, moderately welded, crystal-poor rhyolitic ignimbrite approximately 100–110 m thick. Crystals (less than 5% of the rock) are mostly sanidine with sparse quartz, biotite, plagioclase, and opaque minerals. The Vicks Peak Tuff was erupted from the Nogal Canyon caldera in the San Mateo Mountains (Chapin et al., 2004a). In the Blackington Hills, the tuff has an $^{40}Ar/^{39}Ar$ sanidine age of 28.77 ± 0.01 Ma (Table 3; Cather et al., 2014). The Vicks Peak Tuff was mapped as the upper part of A-L Peak Tuff (unit Talp4) by Spradlin (1976) in the southern Joyita Hills. The $^{40}Ar/^{39}Ar$ sanidine age in the southern Joyita Hills is 28.78 ± 0.01 Ma (Table 3).

The **Lemitar Tuff** is approximately 75–110 m thick in the study area. It is a pink, densely welded, compositionally zoned, crystal-poor to crystal-rich rhyolitic ignimbrite. Crystals of sanidine, plagioclase, quartz, biotite, pyroxene, and opaque minerals constitute as much as 35% of the rock (Spradlin, 1976). Lithic fragments are minor. An $^{40}Ar/^{39}Ar$ sanidine age of 28.25 ± 0.01 Ma was obtained from the Lemitar Tuff in the Blackington Hills (Table 3; Cather et al., 2014). In the southern Joyita Hills, it corresponds to the Tuff of Allen Well of Spradlin (1976), and new dating yields an $^{40}Ar/^{39}Ar$ sanidine age of 28.22 ± 0.01 Ma (Table 3). The Lemitar Tuff may have erupted from the Hardy Ridge caldera in the Magdalena Mountains (Chapin et al., 2004a).

The **South Canyon Tuff** is a light-gray to light-purple, densely welded, crystal-poor to moderately crystal-rich rhyolitic ignimbrite erupted from the Mount Withington caldera in the San Mateo Mountains (Chapin et al., 2004a). Crystals (around 10–20% of rock volume; Spradlin, 1976) are mostly sanidine and quartz. Lithic fragments are common. It is approximately 150–375 m thick in the study area. The South Canyon Tuff yielded $^{40}Ar/^{39}Ar$ sanidine ages of 27.68 ± 0.01 Ma (lower part) and 27.67 ± 0.02 Ma (upper part) in the Blackington Hills (Table 3). The unit was mapped as Potato Canyon Formation (units Tpc1 and Tpc2) by Spradlin (1976) in the southern Joyita Hills, where it yielded an $^{40}Ar/^{39}Ar$ sanidine age of 27.65 ± 0.01 Ma (Table 3).

Fanning dips in the stratigraphic interval from the Luis Lopez Formation to the South Canyon Tuff in the Blackington Hills suggest an approximately 29.0–27.7 Ma growth relationship in the hanging wall of the Bustos fault (an upper-plate splay of the Quebradas detachment fault; see Chapter 5).

Intrusive Rocks

Basaltic andesite and andesite dikes and sills crop out in sparse, scattered exposures in many parts of the study area but have not been characterized petrographically or geochemically. These rocks are commonly altered to greenish hues (Fig. 65). Most intrusive rocks are undated, but most are likely equivalents of the La Jara Peak Basaltic Andesite, which ranges in age from approximately 35 to 24 Ma regionally. Most dikes trend east or northeast. In the Sierra de la Cruz quadrangle near 342500E, 3785000N (zone 13, NAD 27; Plate 1), a northeast-trending dike intruded the upper Yeso Group and formed an anticline in the overlying beds, similar to the dike-anticline relationship described by Cather (2009b) in areas to the east. A dike in NW1/4 sec. 8, T. 2 S., R. 3 E., Sierra de la Cruz quadrangle

Figure 65. Dike, ~2 m wide, intruded into red beds of the Abo Formation in north-central Sierra de la Cruz quadrangle. Hat for scale. View is to the southwest from 343802E, 3786788N (zone 13, NAD 27).

(Plate 1) yielded an $^{40}Ar/^{39}Ar$ biotite integrated age of 34.68 ± 0.11 Ma (Table 3; Green et al., 2013), which has important implications for the timing of slip on the Quebradas detachment (see Chapter 5).

Basalt of Black Mesa

Two superposed lava flows of dark-gray, locally vesicular basalt crop out in the northeast corner of the Sierra de la Cruz quadrangle at Black Mesa (Plate 1). Together these lavas are approximately 20–30 m thick and erupted from vents along the Montosa fault, just east of the quadrangle (Lucas et al., 2009c, stop 3). An imprecise $^{40}Ar/^{39}Ar$ isochron age of 3.68 ± 0.34 Ma was obtained from the upper flow (Table 3). The younger flow is an olivine-bearing alkalic basalt (50.8 wt.% SiO_2, 6.26% total alkalies, 6.0% MgO; R.M. Chamberlin, personal communication, 2018). The older flow has not been dated or chemically characterized.

UPPER OLIGOCENE–MIDDLE PLEISTOCENE SANTA FE GROUP OF THE QUEBRADAS REGION

Steven M. Cather

Introduction

The Santa Fe Group consists of sedimentary and minor volcanic rocks that fill the basins of the Rio Grande rift, but it does not include younger, inset terrace deposits and alluvium (Spiegel and Baldwin, 1963). In central New Mexico near Socorro, two formations compose the Santa Fe Group. These are the upper Oligocene–upper Miocene Popotosa Formation (lower Santa Fe Group) and the upper Miocene–lower Pleistocene Sierra Ladrones Formation (upper Santa Fe Group). In most areas

of central New Mexico, the Popotosa Formation accumulated as piedmont and ephemeral lake deposits within closed, early rift basins (Denny, 1940; Bruning, 1973; Lozinsky and Tedford, 1991). In the southern Joyita Hills, however, the Popotosa Formation may not be related to rifting but instead may have been deposited within a local half graben related to the final episode of top-east slip on the Quebradas detachment fault (see Chapter 5).

The Popotosa and Sierra Ladrones formations are locally divided by an angular unconformity (Denny, 1940) related to an episode of rapid half-graben tilting and subsidence that culminated around 10–5 Ma (Cather et al., 1994b; Chapin and Cather, 1994). Rapid subsidence-induced tilting, offlap, and erosion of the hanging-wall dip slope and subsequent onlap of the Sierra Ladrones Formation produced the angular unconformity. In at least some basins, this unconformity gives way to conformity in the area of maximum subsidence of the half graben (Cather et al., 1994b).

The Sierra Ladrones Formation mostly consists of interfingering piedmont and axial-river deposits. Deposition of the Sierra Ladrones Formation commenced after unconformity development. The Rio Grande spilled southward into the Socorro Basin at 7.4–7.0 Ma (Koning et al., 2024). Incision in most rift basins began around 800 ka (Connell et al., 2013), marking the end of deposition of the Sierra Ladrones Formation.

Popotosa Formation

The Popotosa Formation in the study area is conglomeratic and contains mostly volcanic pebbles and cobbles. Paleoflow was generally westward (Plate 1). It crops out only in the Mesa del Yeso quadrangle, where it locally underlies the Sierra Ladrones Formation and overlies Oligocene volcanic rocks with angular unconformity. The underlying volcanic rocks range from the La Jencia Tuff to the South Canyon Tuff. The Popotosa Formation on the Mesa del Yeso quadrangle is several tens of meters thick and interpreted to represent proximal piedmont deposits. Although undated in the study area, regionally the Popotosa Formation ranges from late Oligocene to late Miocene in age (Chapin and Cather, 1994).

Sierra Ladrones Formation

The Sierra Ladrones Formation (upper Santa Fe Group) in the study area consists of two broad lithofacies associations: piedmont deposits and axial-fluvial deposits associated with the ancestral Rio Grande. **Piedmont deposits** were divided into three map units based on textural lithofacies, following Cather (1997): QTspc—conglomerate:sandstone ratio greater than 2:1, QTspcs—conglomerate:sandstone ratio between 2:1 and 1:2, and QTsps—conglomerate:sandstone ratio of less than 1:2 (Plate 1). Piedmont deposits crop out in three areas as (1) an extensive, west-facing depositional system exposed in the eastern Socorro Basin; (2) an incompletely exposed piedmont system that drained southeastward toward the Jornada del Muerto; and (3) high-elevation gravels that represent the fill of topographically inverted, west-draining paleovalleys in the northeastern part of the study area. Only the upper part of the formation is exposed in the study area.

In the eastern Socorro Basin, piedmont deposits consist of buff to reddish-brown alluvial conglomerate, sandstone, and mudstone that generally become finer grained to the west, away from the source region (see paleocurrent arrows on Plate 1). These deposits are poor aquifers compared with the axial-fluvial lithofacies (e.g., Hawley and Kernodle, 2000). Conglomerate is poorly sorted and forms tabular and lenticular beds (Fig. 66). Most conglomerate is clast-supported and was deposited by stream-flow processes, but matrix-supported debris-flow deposits are common in proximal deposits. Sandstone is typically tabular bedded, medium to very coarse grained, commonly pebbly, and exhibits trough cross-bedding or horizontal stratification. Volcanic rocks were the dominant source for piedmont deposits of the Sierra Ladrones Formation in the west-central and northwestern parts of the Mesa del Yeso quadrangle; elsewhere in the study area, recycled sedimentary detritus predominates. Mudstone is mostly sandy, reddish-brown in color, and occurs in tabular beds. Mudstone is common only in distal piedmont deposits of the Socorro Basin.

Plate 1 shows that piedmont deposits extend farther basinward near Arroyo de Alamillo, Arroyo de la Parida, and Arroyo de las Cañas than elsewhere in the eastern Socorro Basin. This suggests that precursors to these arroyos were important detrital

Figure 66. Piedmont lithofacies of the Sierra Ladrones Formation consisting of subequal parts of conglomerate and sandstone (Plate 1, map unit QTspcs) exposed in the lower reaches of Arroyo de las Cañas. View is to the south from 333247E, 3765579N (zone 13, NAD 27), southern Loma de las Cañas quadrangle.

sources for the piedmont system during late Sierra Ladrones time. High-elevation gravels in the northern Sierra de la Cruz quadrangle appear to have filled ancestral drainages of Arroyo de Alamillo, Cibola Canyon, and Palo Duro Canyon. These gravels are tentatively correlated with the Sierra Ladrones Formation because their elevation trends can be projected westward to near the top of the Santa Fe Group in the eastern Socorro Basin. They are inset against and younger than the 3.7 Ma basalt at Black Mesa.

The **axial-river lithofacies** (Plate 1, map unit QTsa) mostly consists of sandstone, mudstone, and conglomerate deposited in channels of the ancestral Rio Grande (Fig. 67) or on its floodplain. Axial-river sandstone forms important aquifers in many basins of the Rio Grande rift (Hawley and Kernodle, 2000). Sandstone is light gray, cross-bedded, and poorly indurated. Pebbles are well rounded to subrounded quartzite, granite, gneiss, sandstone, chert, volcanic lithics, siltstone, schist, phyllite, limestone, obsidian, and pumice. Pebble imbrication and cross-bedding indicate paleoflow was generally toward the south (Plate 1). Mudstone ranges in color from reddish brown to greenish gray.

Half-meter-scale, flat-lying, laterally extensive zones of carbonate cementation are present in the axial-river lithofacies near San Pedro Arroyo in the San Antonio quadrangle. These zones of cementation appear to represent fossil water tables (e.g., Mack et al., 2000).

A local **mud-rich lacustrine lithofacies** (Plate 1, map unit QTsm) was mapped near 328000E, 3785800N (zone 13, NAD 27) in the Mesa del Yeso quadrangle. It probably represents a local sag-pond deposit in the hanging wall of the Alamillo fault.

In the central part of the San Antonio quadrangle, a remarkable **pumice and ash deposit** (Plate 1, map unit QTsap) is associated with axial-river deposits of

the Sierra Ladrones Formation. Informally termed the Bosquecito pumice, it consists of pumice- and ash-rich flood and debris-flow deposits as much as 5 m thick (Fig. 68) derived from the 1.6 Ma Otowi Member of the Bandelier Tuff (see detailed description and interpretation in Cather and McIntosh [2009]). It is bounded on the east by a poorly exposed paleoscarp related to a west-down normal fault. The Otowi Member erupted from the Toledo caldera and dammed the ancestral Rio Grande at White Rock Canyon (Reneau and Dethier, 1996). Subsequent breaching of this dam generated a large flood that is recorded by the Bosquecito pumice and by pumiceous deposits elsewhere in New Mexico (Dunbar et al., 1996; Mack et al., 1996).

The **transitional axial–piedmont lithofacies** (Plate 1, map unit QTst) records a zone of interfingering of piedmont and axial-river deposits. Transitional deposits (sensu Cather, 1997) were mapped in the area of overlap between the basinward extent of piedmont exposures and the eastern limit of axial-river deposits. Lithologic characteristics are similar to the piedmont lithofacies and axial-fluvial lithofacies.

The basal contact of the Sierra Ladrones Formation in the Socorro Basin is exposed where the upper part of the unit laps eastward beyond the rift-bounding normal faults. In such exposures, the Sierra Ladrones is thin and unconformably overlies rocks ranging from Proterozoic basement to the Popotosa Formation. A small outcrop of the La Jara Peak Basaltic Andesite exposed beneath the Sierra Ladrones Formation near 331500E, 3773000N (zone 13, NAD 27; Plate 1) indicates the fill of the

Figure 67. Ancestral Rio Grande fluvial deposits of the Sierra Ladrones Formation exposed along the south side of Arroyo de la Parida near 328280E, 3777580N (zone 13, NAD 27), Mesa del Yeso quadrangle. Note large-scale cross-beds and red and greenish-gray mud balls. Red beds of Quaternary terrace alluvium disconformably overlie these fluvial deposits.

Figure 68. Image of the southwestern part of the Bosquecito pumice beds (Sierra Ladrones Formation) exposed in the northeastern corner of sec. 34, T. 4 S., R. 1 E., San Antonio quadrangle. Buff-colored fine sediments at the base of the image are nonpumiceous floodplain deposits of the ancestral Rio Grande. These are overlain by gray, water-laid ash, which is in turn overlain by a pumiceous debris-flow deposit with a reverse-graded base (above the hammer).

Socorro Basin east of the Coyote fault is also thin. Similarly, a "basalt" (probably La Jara Peak Basaltic Andesite; R.M. Chamberlin, personal communication, 2017) encountered in a water well at 212 ft (64.6 m) depth in west-central sec. 17, T. 2 S., R. 1 E. indicates the Sierra Ladrones Formation is thin in that part of the eastern Socorro Basin (see Office of the State Engineer file number RG 91116). Elsewhere, the lower contact was down-faulted into the subsurface of the Socorro Basin by a series of generally north- to northwest-striking, left-stepping, west-down normal faults. The thickness of the Sierra Ladrones Formation in the study area west of these faults is unknown. In the western Socorro Basin near Socorro, it is 345 m thick in the Evergreen test well (Machette and Chamberlin, 2015).

The approximate depositional top of the Sierra Ladrones Formation is exposed in the southwestern part of the study area, where it is capped by the Las Cañas geomorphic surface (Plate 1). This surface is underlain by a pedogenic calcrete characterized by stage IV–V morphology (Fig. 69; McGrath and Hawley, 1987). It is locally offset by the Coyote fault. Except where the Las Cañas geomorphic surface is preserved, the top of the Sierra Ladrones Formation has been eroded and is in places overlain by post-Santa Fe Group deposits.

Regionally, the age of the Sierra Ladrones Formation is approximately 5–0.8 Ma (Chapin and Cather, 1994; Connell et al., 2013). Vertebrate fossils recovered from axial-river deposits near Arroyo de la Parida indicate a middle Blancan age (approximately 3.2–2.2 Ma; Morgan et al., 2009). The Bosquecito pumice beds of the Sierra Ladrones Formation were deposited soon after the 1.6 Ma eruption of the lower Bandelier Tuff (Cather and McIntosh, 2009). Clasts of 1.43 Ma Rabbit Mountain obsidian are present in the top of the axial-fluvial lithofacies north of Arroyo de la Parida, and clasts of 1.25 Ma upper Bandelier Tuff are present in the Sierra Ladrones Formation to the north of the study area in the Becker SW quadrangle (D.W. Love, personal communication, 2018).

Figure 69. Las Cañas geomorphic surface with prominent light-gray pedogenic calcrete. Surface caps faulted and tilted beds of the Torres Member of the Los Vallos Formation and thin conglomeratic piedmont deposits of the Sierra Ladrones Formation. Note dereddening (yellow beds) beneath limestones of the Torres Member, caused by downward leaching of organic-rich fluids from the limestones. Light-gray terraces capping small mesas above the arroyo at the center of the image are Quaternary gypsiferous deposits related to downvalley paleoflow from nearby Ojo de las Cañas, which is out of view upstream to the left. View is to the south-southeast across Arroyo de las Cañas from 334743E, 3766460N (zone 13, NAD 27), southeastern Loma de las Cañas quadrangle).

POST-SANTA FE GROUP QUATERNARY DEPOSITS OF THE QUEBRADAS REGION

Steven M. Cather

Following the end of Santa Fe Group deposition at around 800 ka (Connell et al., 2013), accumulation of sediments continued episodically during an overall degradational regime. These deposits range in age from middle Pleistocene to Holocene but were not studied in detail. Map units were delineated on the basis of depositional environment (sand and gravel within and adjacent to active arroyo channels and the Rio Grande, axial-fluvial floodplain deposits, piedmont alluvium, colluvium, landslide deposits, and eolian deposits) and landscape position (piedmont deposits in higher landscape positions are assumed to be older). Old, intermediate, and young terraces of piedmont valley-fill (Qvo, Qvi, and Qvy, respectively) were mapped east of the Rio Grande based on relative elevations above modern stream grade (note that Qvi was mapped only on the Bustos Well quadrangle). Units of piedmont valley-fill may not be time-correlative between drainages.

In the San Antonio quadrangle west of the Rio Grande, four terrace levels of piedmont alluvium were recognized (from oldest to youngest, Qv2, Qv3, Qv4, and Qv5). A similar stratigraphy was recognized by Chamberlin et al. (2002) in the adjoining Luis Lopez quadrangle. Since the completion of mapping for this study in 2014, Sion et al. (2020) and Phillips and Sion (2022) have named, correlated, and dated many terrace deposits within the study area.

Ranch house ruins at Tomas Baca Well. The sandstone blocks are from the Permian Meseta Blanca Formation. *Photo by Steve Cather*

CHAPTER 5: STRUCTURAL GEOLOGY OF THE QUEBRADAS REGION

Steven M. Cather and Gary J. Axen

INTRODUCTION

Geologic structures in the Quebradas region are complex and of diverse origin. They include (1) Laramide west-up reverse faults and associated fault-propagation folds; (2) northeast-striking zones of Laramide dextral strike-slip faults with linking contractile and extensional step-overs; (3) a regional Paleogene–early Neogene, top-east decollement within the upper Yeso Group, termed the Quebradas detachment fault, and associated normal-sense, hanging-wall splay faults and rollover anticlines; and (4) Neogene and Quaternary normal faults related to rifting.

Laramide faults were commonly reactivated during Rio Grande rifting, obscuring the history of many faults. Reactivation may also explain the rarity of verifiable late Paleozoic structures in the study area. Except for a Late Pennsylvanian fault described by Nelson et al. (2017), no examples of Ancestral Rocky Mountains faults have been documented in the study area. More such faults surely must exist given the proximity of Ancestral Rocky Mountain uplifts (see Chapter 2 discussion of the Bursum Formation).

Note that not all strike-and-dip data are presented on Plate 1. Refer to the individual geologic quadrangles for the complete dataset and for a better depiction of small exposures (Cather, 2002; Cather et al., 2004, 2007, 2012, 2014; Cather and Colpitts, 2005). The following discussion is drawn in part from those maps.

LARAMIDE REVERSE FAULTS AND FOLDS

Reverse faults and folds of Laramide age are largely restricted to the Tajo and Gallina structural zones (Fig. 70). Reverse faults in these zones (most of which are smaller than can be depicted at the present scale of mapping) dip moderately west and are associated with asymmetric and overturned folds. These contractile zones appear to be associated with the tips of underlying, eastward-thrusted basement wedges. Such basement wedges are responsible for much of the structural elevation along the east flank of the Socorro Basin.

Most other folds in the study area are not demonstrably contractile. Asymmetric rollover anticlines associated with listric normal-fault splays occur within the hanging wall of the Quebradas detachment; these extensional folds are discussed below. Remaining folds in the study area are widely scattered, gentle warpings with fold axes that trend mostly north but range from northwest to northeast. They typically are broad, upright, and open and plunge gently. Limb dips are around 20° or less. Developed largely in Paleozoic and Mesozoic strata, these folds are mostly of indeterminate origin. Some may be contractile, but others are likely gentle warps caused by rift- or detachment-related deformation.

Tajo Structural Zone

An arcuate array of reverse faults and associated folds, herein termed the Tajo structural zone (formerly the Amado–Cañas structural zone of Cather [2009a]), occupies the central part of the Loma de las Cañas quadrangle (Fig. 70, Plate 1). The structural zone is about 11 km in north–south extent and about 4 km at its widest point. Reverse faults within the Tajo structural zone dip moderately west (although only one major reverse fault is depicted on Plate 1, there are numerous small reverse faults in the Tajo structural zone; see, for example, Smith et al. [1983], fig. 1-48.2a). Folds range from open to tight and are in places overturned toward the east or northeast (Fig. 71).

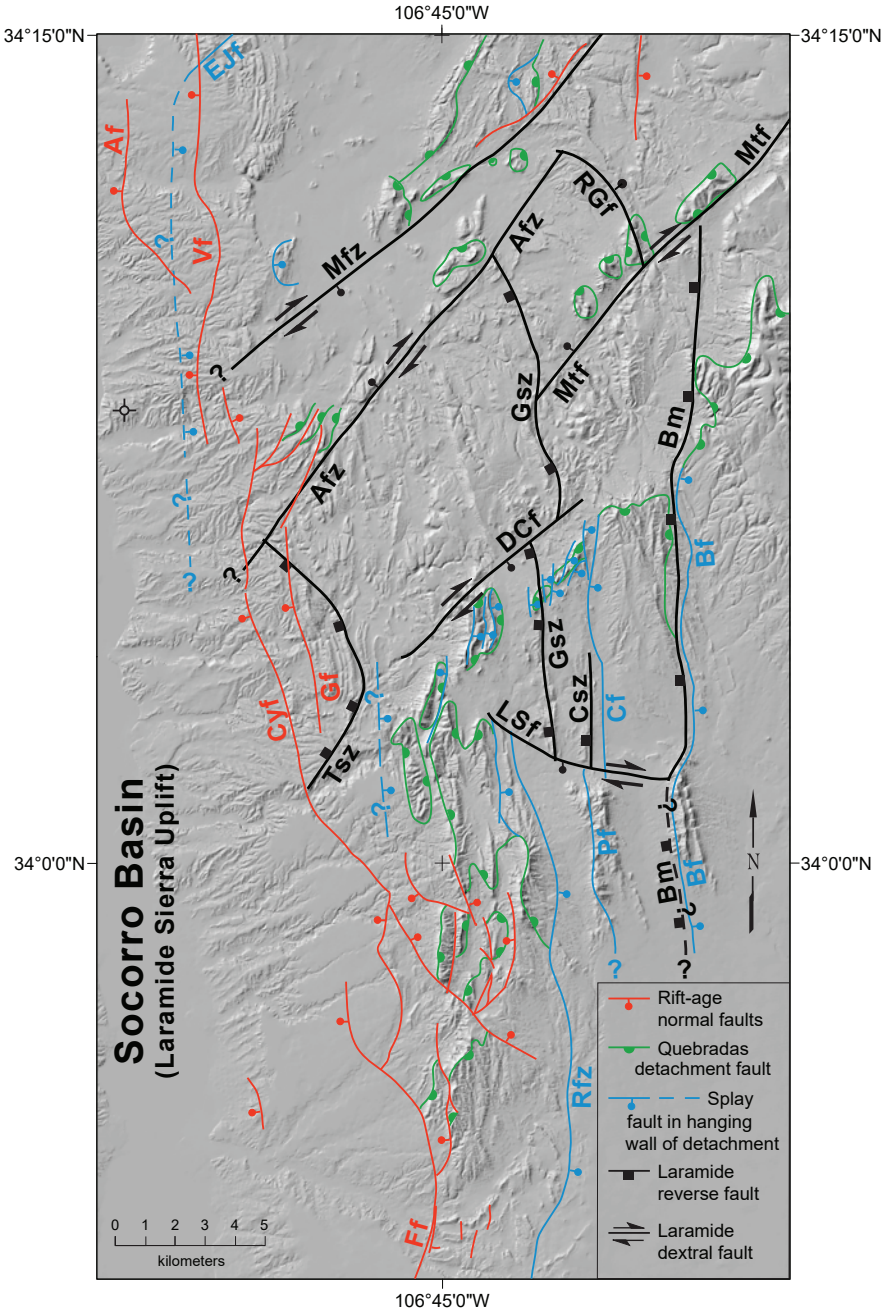

Figure 70. Index map of selected structures of known origin in the study area showing simplified configurations for Laramide basement structures (black lines), middle Eocene–middle Miocene Quebradas detachment fault (green), splay faults in the hanging wall of the detachment (blue), and rift-age normal faults (red). Laramide reverse faults (square teeth on upper plate) mark the inferred eastern edges of basement wedges associated with the transpressional Sierra Uplift to the west. Most of these basement faults are blind beneath folds and faults developed in Phanerozoic strata. Tips of these wedges are interpreted to underlie the Tajo structural zone (**Tsz**), the Gallina structural zone (**Gsz**), the Cañas structural zone (**Csz**), and the Bustos monocline (**Bm**). The south-down Landing Strip fault zone (**LSf**; bar and ball on downthrown side) is a dextral-oblique zone that marks the southern edge of basement wedges to the north. The northeast-striking Milagro (**Mfz**), Amado (**Afz**), Montosa (**Mtf**), and Del Curto (**DCf**) fault zones are probable Laramide dextral structures. The northern part of the Gallina structural zone acted as a contractional step-over between the Del Curto fault zone and the Montosa fault zone and, to a lesser extent, the Amado fault zone to the north. The northern part of the Bustos monocline may have acted as a contractile step-over between the Landing Strip fault zone and the Montosa fault zone. The Rancho Grande fault zone (**RGf**) may have served as an extensional step-over between the Montosa and Amado fault zones. Listric splay faults (bar and ball on downthrown block; dashed and queried where speculative) are associated with rollover anticlines (not shown) and merge downward with the top-east Quebradas detachment fault (rounded teeth on upper plate). Named splay faults are the East Joyita fault (**EJf**), Cañas fault (**Cf**), Ranchito fault zone (**Rfz**), Pinos fault (**Pf**), and Bustos fault (**Bf**). Neogene normal faults (bar and ball on downthrown block) are related to the Rio Grande rift and include the Alamillo fault (**Af**), Veranito fault (**Vf**), Coyote fault (**Cyf**), Gonzales fault (**Gf**), and Fite fault (**Ff**). The well symbol in the eastern Socorro Basin depicts a water well (Office of the State Engineer file number RG 91116) where volcanic strata were encountered at a depth of 212 ft (64.6 m) and may mark the footwall of a detachment-related splay fault (dashed and queried blue line to the east; see text).

East-vergent, asymmetric to overturned folds associated with the Tajo structural zone range in trend from north-northeast to northwest. They are locally Z-shaped (Rejas, 1965) and exhibit axial planes that dip approximately 30°–70° to the west. Because folds within the Tajo structural zone are associated with Laramide reverse faulting, we interpret them as fault-propagation and fault-bend folds (e.g., Hook and Brennan, 2022). This is particularly evident for an overturned syncline-anticline pair separated by a reverse fault, all of which cross Arroyo del Tajo west of the Quebradas road. These folds continue north and die out past the mapped fault tip. Smaller-scale and somewhat chaotic folds formed in the core of the larger fault-propagation syncline immediately to the east.

The Tajo structural zone deformed strata as young as the Leonardian Yeso Group. These strata postdate the Ancestral Rocky Mountains orogeny (e.g., Kues and Giles, 2004), so the Tajo structural zone is Laramide in age. The Tajo structural zone is a remnant salient on the eastern front of the transpressional Laramide Sierra Uplift, which was structurally inverted to form the Socorro Basin of the Rio Grande rift (Cather, 1983, 2009a). Although the Eocene Baca Formation primarily records its development, the Sierra Uplift began to be unroofed during the Late Cretaceous, as shown by exposures 2.5 km northeast of Puertecito of Bowling Green, where the uppermost part of the Coniacian–Santonian(?) Crevasse Canyon Formation contains rounded siliceous pebbles and sparse Paleozoic limestone pebbles that were derived from the southwest. The siliceous pebbles were probably recycled from the Shinarump Member of the Triassic Chinle Formation. The Sierra Uplift persisted as a positive area during deposition of lower Spears Group and then began to be structurally inverted around 36 Ma (Cather, 1990).

The hanging wall of the Tajo structural zone encompasses most of the Proterozoic exposures in the study area—a testament to its Laramide structural relief, although most of these exposures also lie in the footwall of west-dipping, rift-age normal faults (Plate 1). South of Arroyo del Tajo, Paleozoic rocks of the Tajo structural zone are overlain by down-faulted

Figure 71. East-vergent, overturned syncline developed within Abo (red beds at far left) and variegated Yeso strata of the Tajo structural zone. View is to the northeast across Arroyo de las Cañas from 334265E, 3765709N (zone 13, NAD 27), central Loma de las Cañas quadrangle.

exposures of the Eocene Baca Formation and Paleogene volcanic rocks, but no Mesozoic strata crop out. The limited strike-extent of these faults suggests they are not major structures. These relations suggest the Tajo structural zone was erosionally stripped of Mesozoic rocks prior to onlap of the Baca Formation. The Baca Formation there contains much Proterozoic detritus, indicating Precambrian exposures were widespread on the Sierra Uplift during the middle Eocene. The only other Proterozoic rocks exposed in the study area are in the Joyita Hills, and these owe their structural relief to a combination of Ancestral Rocky Mountain, Laramide, and rift-age uplift (Beck and Chapin, 1994).

Gallina Structural Zone

A faulted, north-trending, complex anticlinorium, herein termed the Gallina structural zone, is present in the central and northern part of the Bustos Well quadrangle and continues northward into the southwestern part of the Sierra de la Cruz quadrangle (Fig. 70, Plate 1). The Gallina structural zone is Laramide in age because beds as young as the Leonardian Yeso Group that postdate the Ancestral Rocky Mountain orogeny are locally overturned and cut by reverse faults. Near cross section C–C′ (Plate 2), the structural zone appears to be truncated by, but does not fold, the overlying Quebradas detachment fault and thus is probably older. The Quebradas detachment began to form during deposition of the Baca Formation (middle Eocene; see below), so the Gallina structural zone is probably early Eocene or older. Numerous faults within the structural zone, however, were reactivated during Neogene extension.

The Gallina structural zone is 17 km long and 0.5–1 km wide, and consists of two en-echelon segments offset by the Del Curto fault west of La Montanera (Fig. 1). There, the Gallina structural zone steps around 1.5 km to the right across the northeast-striking Del Curto fault (see below). The Gallina structural zone extends from the Landing Strip fault zone on the south to the Amado fault zone on the north (Fig. 70, Plate 1). Four kilometers south of the Amado fault zone, the northeast-striking, dextral Montosa fault zone terminates to the southwest against the Gallina structural zone (Brown, 1987). North of this intersection, the Gallina structural zone consists of steep faults bounding gently tilted blocks and paralleled by open folds typically with gentle limb dips.

South of the Montosa fault, bedding attitudes within the Gallina structural zone are notably steeper and in places are overturned and cut by minor reverse faults. Folds are mostly east-vergent and are locally overturned (Brown, 1987). They mostly trend north (Behr, 1999) but are difficult to depict at the present map scale (see Brown [1987] for a more detailed map). The axial plane of this part of the anticlinorium dips west (Brown, 1987).

The Gallina structural zone appears to mark the eastern edge of a buried Laramide basement wedge, but it also served as a local step-over between northeast-striking dextral faults. We interpret the Gallina structural zone as a complexly broken fault-propagation fold that formed above a blind, west-dipping Laramide reverse fault, analogous to some folds in the Tajo structural zone. The strongest evidence is that deeper stratigraphic levels are exposed west of the Gallina structural zone than immediately to the east (Plate 2, cross section C–C′). Preservation of Mesozoic strata south of the Landing Strip fault zone suggests that it served as the southern bounding structure to this inferred Laramide basement uplift.

Relationships between the Gallina structural zone and dextral fault zones suggest that the inferred basement uplift itself was locally broken by strike-slip faults. We interpret the part of the Gallina structural zone between the dextral Del Curto fault and the Montosa fault zone as a restraining step-over, as did Brown (1987). Contraction across the Gallina structural zone between the Del Curto fault and the Montosa fault zone suggests significant dextral slip transfer. In contrast, the Gallina structural zone between the Montosa and Amado fault zones was less contractile, as shown by the gentle dips of fold limbs in the Gallina structural zone there.

Bustos Monocline

Another west-up, early Laramide structure, along which the Bustos splay fault later developed, is inferred due to a projected 100–150 m discrepancy in the elevation of the Quebradas detachment between La Montanera on the west and La Cebolla on the east. Outcrop evidence for such a structure is scant due to obscuring effects along the younger, detachment-related Bustos fault. The pre-detachment structure, herein termed the Bustos monocline, may

have developed over the eastern edge of a basement wedge, similar to the Gallina and Tajo structural zones to the west. Alternatively, the elevation discrepancy could be explained by an east-facing footwall ramp of the Quebradas detachment itself, if the detachment stepped downsection within the Los Vallos Formation toward the east. Such an interpretation, however, would require a thin Los Vallos section in the La Cebolla area, which is not observed.

Evidence for an east-facing monocline exists only in the area north of the Landing Strip fault zone (Fig. 70). South of there, the existence of a monoclinal precursor to the Bustos fault is speculative due to Cenozoic cover. The northern part of the Bustos monocline may have acted as a contractile step-over between the Landing Strip and Montosa fault zones.

Cañas Structural Zone

The Cañas structural zone is a north-trending zone of faults and folds that lies 1.5 km east of the southern part of the Gallina structural zone. In the south-central part of the Bustos Well quadrangle, it has a north–south extent of at least 6 km (Fig. 70, Plate 1). Unlike the Gallina structural zone, the anticline in the southern part of the Cañas structural zone is only weakly asymmetric. The anticline is truncated on the north by an arcuate, west-up, probably west-dipping (based on its trace) fault that also cuts the east limb of the fold. This probable reverse fault suggests the anticline may have formed as a Laramide fault-propagation fold, but this is speculative. The Cañas structural zone terminates southward at the Landing Strip fault zone.

LARAMIDE NORTHEAST- AND EAST-STRIKING FAULT ZONES AND RELATED STRUCTURES

Montosa Fault Zone

The Montosa is a well-known fault zone that strikes northeast through the central and northeastern part of the Sierra de la Cruz quadrangle (Fig. 70). To the north of the quadrangle, the Montosa bends to a north-northeasterly strike in the vicinity of U.S. Route 60 (Scott et al., 2005). There, it is a markedly contractile, west-up, dextral-reverse fault with evidence of late Cenozoic normal reactivation (see Cather [2009c] for a history of thought on this fault). Its Laramide age is indicated by Eocene apatite fission-track cooling ages from its hanging wall (Kelley et al., 1992). In the Sierra de la Cruz quadrangle, however, the Montosa is a poorly exposed, anastamosing system of steep faults with mostly normal separation (Colpitts, 1986). It shows little evidence of Laramide shortening; only a few, mostly open folds are associated with the fault zone. The axes of the folds are subhorizontal and trend subparallel to the Montosa fault zone (Behr, 1999).

Although no fault kinematic data were collected during the present study, previous workers interpreted dextral components of Laramide slip on the Montosa fault zone (Cabezas, 1991; Hayden, 1991; Behr, 1999). The anastamosing pattern of the Montosa fault zone in the study area and its increasingly contractile behavior as it bends left in areas to the north support such interpretation. The lack of significant offset of aeromagnetic patterns across the fault suggests the magnitude of dextral slip was small, probably no more than a few kilometers (Cather et al., 2006). The Montosa fault zone terminates southwestward against the Gallina structural zone, which served as a restraining step-over across which dextral slip was transferred to the Del Curto fault to the south (Brown, 1987).

Evidence for Neogene extensional reactivation of the Montosa fault zone has been noted previously by Behr (1999), based in part on the kinematics of minor faults within the Montosa zone near Gallina Well. She noted early populations of mostly north-northeast-striking reverse faults and northeast-striking, subvertical dextral faults. Most normal faults strike north-northeast. Slickenlines on some of the normal faults cross-cut earlier dextral striae (Behr, 1999).

In the study area, the Montosa fault zone is an array of mostly northwest-down, normal-separation faults that offset the Quebradas detachment fault by about 0.5 km, based on projection of the detachment from the La Cebolla area (see cross section B–B′, Plate 2). Extensional reactivation probably occurred during the middle to late Miocene, when rifting was most active in the Socorro region (Cather et al., 1994b). Extension partly postdated exhumation and cooling along the fault, as recorded by apatite fission-track data that show the southern part of the Montosa fault zone cooled through the approximately 120°C isotherm around 24–14 Ma (Behr, 1999). The Montosa fault zone does not cut the 3.7 Ma basalt

at Black Mesa in the northeastern part of the study area (Lucas et al., 2009c, stop 3), indicating extension ended by the middle Pliocene.

Amado, Rancho Grande, and Milagro Fault Zones

Two systems of steep, northeast-striking faults are present in the northern part of the study area: the Amado and Milagro fault zones (Fig. 70). These fault zones are similar in orientation to, but locally more complex than, the Montosa fault system. The Amado and Milagro fault zones cut rocks as young as Upper Cretaceous but, locally in the southern Valle del Ojo de la Parida, do not cut the overlying Paleogene section. They were thus initially Laramide structures. They may share with the Montosa fault zone a history of Laramide dextral slip followed by local extensional reactivation during the Neogene.

The **Amado fault zone** (Rejas, 1965) is at least 17 km long and 1–2 km wide (Fig. 70, Plate 1). Parts of this fault zone were termed the Cañoncito de la Uva fault zone and Stapleton-Alamillo fault zone by Colpitts (1986) and the Parida structural zone by Cather (2009a), but subsequent mapping shows they are continuous with the Amado fault zone first defined by Rejas in 1965. A northeast-striking fault within the Amado zone is truncated by the Quebradas detachment fault 2.5 km southeast of Mesa del Yeso. Elsewhere, however, such as in the Cerrillos del Coyote in NE1/4 sec. 23 and NW1/4 sec. 24, T. 2 S., R. 1 E., the Amado fault zone cuts the detachment fault, possibly resulting from Neogene extensional reactivation within the zone (Fig. 72).

In the Loma de las Cañas quadrangle, the Amado fault zone juxtaposes differing lithofacies and thicknesses of members of the Pennsylvanian Atrasado Formation (Rejas, 1965; see Chapter 2). Most notably, exposures of the Tinajas Member with markedly differing carbonate content are closely juxtaposed across a strand of the Amado fault zone

Figure 72. Faulted and variably tilted Yeso Group beds within the Amado fault zone exposed in the Cerrillos del Coyote. Unseen strands of the Amado fault zone divide several tilted blocks in this image (see Plate 1). Variegated beds in the foreground are the Meseta Blanca Formation. Limestone capping cuestas on the skyline is the Torres Member of the Los Vallos Formation. View is to the northeast from 333147E, 3776601N (zone 13, NAD 27), northern Loma de las Cañas quadrangle.

in S1/2 sec. 26 and N1/2 sec. 35, T. 2 S., R. 1 E. We interpret these juxtapositions as largely the result of Laramide dextral slip on faults of the Amado zone, an interpretation similar to that of Rejas (1965). It is possible, however, that syndepositional growth faulting during the Pennsylvanian contributed to the observed stratigraphic discrepancies, although no evidence for soft-sediment deformation was noted.

Throughout much of its length, the Amado fault zone is down to the northwest. Because of this, outcrops provide differing perspectives of the Quebradas detachment fault across the Amado zone (see below). To the northwest lie exposures of mostly upper-plate rocks, whereas primarily footwall strata crop out to the southeast. Within the Amado fault zone itself, the Quebradas detachment fault is commonly exposed.

The Amado fault zone can be traced to the southwest where it is truncated by the Neogene Coyote normal fault along the eastern margin of the Socorro Basin. In the Sierra de la Cruz quadrangle, the fault zone terminates to the northeast against the **Rancho Grande fault zone** (Fig. 70, Plate 1). The Rancho Grande fault zone, named for a nearby well, consists of several north-northwest-striking normal faults. These faults are mostly northeast-down and exhibit only moderate separation (typically a few tens of meters). The Rancho Grande fault zone in turn probably terminates southward against the Montosa fault (Fig. 70), but the fault intersection is obscured by the upper plate of the Quebradas detachment fault (Plate 1). It is possible the Rancho Grande fault zone served as a releasing bend that transferred dextral slip between the Amado and Montosa fault zones. If so, the normal faults within the Rancho Grande fault zone are likely Laramide. Transfer of dextral slip between the Amado and Montosa fault zones was not large, as shown by only modest extension across the Rancho Grande fault zone.

The **Milagro fault zone** in the study area is about 15 km in length and as much as 1 km wide (Fig. 70, Plate 1). In contrast to the Amado fault zone, it is mostly down to the southeast. Much of the Milagro fault zone is covered by Quaternary deposits in the Valle del Ojo de la Parida. Scattered outcrops of Upper Cretaceous strata there, however, require intervening, buried faults to explain their anomalous juxtaposition. The Milagro fault zone can be traced at least 4 km northeastward beyond the study area to where it disappears beneath Quaternary deposits in the southern part of the Becker SW quadrangle (Allen et al., 2013b). Farther north, the frontal fault of Los Pinos Mountains is approximately on trend with the Milagro fault zone. The fault zone extends southwestward to the southern Joyita Hills where it is buried by Paleogene strata, indicating a Laramide history. Local Neogene reactivation is suggested, however, where a strand of Milagro fault zone cuts the Quebradas detachment in the northwestern part of the Sierra de la Cruz quadrangle near 341900E, 3788400N (zone 13, NAD 27).

Del Curto Fault

The Del Curto fault is a steep, northeast-striking fault about 5 km in length in the northwestern part of the Bustos Well quadrangle (Fig. 70, Plate 1). Brown (1987) interpreted it as a dextral strike-slip fault based on the presence of local horizontal slickenlines and adjacent small folds that plunge 15°–80° to the southwest. The Del Curto fault may have transferred a modest amount of dextral slip northward to the Montosa and Amado fault zones via a contractile step-over (the Gallina structural zone; see above).

Landing Strip Fault Zone

The Landing Strip fault zone developed along an east-trending, south-facing monocline in the southern part of the Bustos Well quadrangle. The Gallinas and Cañas structural zones terminate southward against the Landing Strip fault zone. These structural zones probably represent deformation above blind reverse faults that mark the edges of east-directed Laramide basement wedges. The Bustos monocline and its associated wedge-edge may end against it as well (the continuation of the Bustos monocline southward from its intersection with the Landing Strip fault zone is speculative). Greater contraction on the north side of the Landing Strip fault zone (Fig. 70) indicates a component of dextral slip. The Landing Strip fault zone thus may have originated by monoclinal draping of strata over the southern margins of these obliquely rising Laramide wedge blocks, followed by faulting as Laramide deformation continued.

The younger, detachment-related Ranchitos fault system and Pinos fault do not project north of the Landing Strip fault zone because the Quebradas detachment, which typically follows gypsum beds in the upper part of the Los Vallos Formation, was upturned and eroded there (see below). In this

sense, the south-facing monocline of the Landing Strip fault zone probably formed a template for a younger, south-facing lateral ramp within the top-east Quebradas detachment.

PALEOGENE–EARLY NEOGENE DETACHMENT FAULTS AND ASSOCIATED STRUCTURES

Quebradas Detachment Fault

Low-angle normal faults form a widespread detachment system in the upper gypsiferous part of the Los Vallos Formation (upper Yeso Group) of the Quebradas region (Fig. 70, Plate 1). The study area affords views of various depths of exposure of the detachment system. A broad, trapezoid-shaped, uplifted block between the Tajo structural zone and the northern part of the Gallina structural zone provides a view of the lower plate of the detachment fault. Numerous mesas near the northern, southern, and eastern edges of the block expose the detachment system and associated structures in three dimensions. The northwestern and, in particular, east-central parts of the study area provide informative perspectives of the upper plate of the detachment system.

To describe the detachment faults, we use terminology originally developed for thrust systems. Fensters are erosional windows through the upper plate; klippen are isolated erosional remnants of the upper plate. Parts of the fault subparallel to bedding in the hanging wall or footwall are called hanging-wall or footwall flats, respectively. Detachment faults that cut across strata of the hanging wall or footwall are called hanging-wall or footwall ramps, respectively. Duplexes are tabular to lenticular bodies of rock enclosed by subparallel faults where the detachment bifurcates.

Detachment faults are most easily recognized where they form hanging-wall or footwall ramps. Normal displacement of strata within a hanging-wall ramp down onto a footwall flat creates a rollover anticline (sometimes called a reverse-drag fold), and such structures are common in the study area (Figs. 73A–D). Due to erosion, however, it is not generally known if a specific rollover anticline formed above a ramp that connected detachment flats stepping between differing stratigraphic horizons or if the rollover anticline instead formed above a listric splay fault in the upper plate of the detachment. The disproportionately large number of preserved hanging-wall ramps and rollover anticlines in the Quebradas region suggests that most mapped rollover anticlines formed above listric upper-plate splay faults and that many footwall ramps have been removed by erosion. In most cases, hanging-wall anticlines involve tilted beds of resistant Glorieta Sandstone and San Andres Formation, whereas footwall ramps commonly contain weak Yeso strata. Figure 73E shows an unusual example of a preserved footwall ramp associated with a listric splay in the hanging wall of the Quebradas detachment.

Detachment faults in the upper Yeso Group have been recognized since the 1980s in the region east of Socorro (see summaries of previous work in Smith [1983] and Cather [2009a, 2009b]). Prior to the mapping of the Bustos Well quadrangle (Cather et al., 2014), it was uncertain whether these faults represented a series of isolated detachments or were part of a regionally interconnected system. The source of this uncertainty is that detachment faults are obvious features only where fault ramps or splay faults have caused omission or angular truncation of strata or in rare locations where the fault plane itself is exposed (Fig. 73F). Recognizing detachment faults where a hanging-wall flat overlies a footwall flat is difficult, particularly where the gypsiferous host strata are poorly exposed. The closely spaced exposures of hanging-wall ramps in the northern Bustos Well quadrangle (see cross section C–C′, Plate 2), however, show that a throughgoing detachment fault, herein termed the Quebradas detachment fault, must be present. From this relationship, we infer that the Quebradas detachment must connect the other, more widely spaced ramps exposed elsewhere in the study area.

Throughout the study area, the principal slip surface of the Quebradas detachment is one or more faults within the upper Los Vallos Formation. In areas of limited exposure, the detachment fault is depicted as forming the contact between the Los Vallos Formation and the Glorieta Sandstone. Bedding-parallel faults are also present locally in the lower San Andres Formation (e.g., Fig. 73B). For scale considerations, these are commonly depicted at the Glorieta/San Andres contact.

In many places in the study area, detachment faults have excised parts of the upper Torres, Cañas, and/or Joyita Members of the Los Vallos Formation.

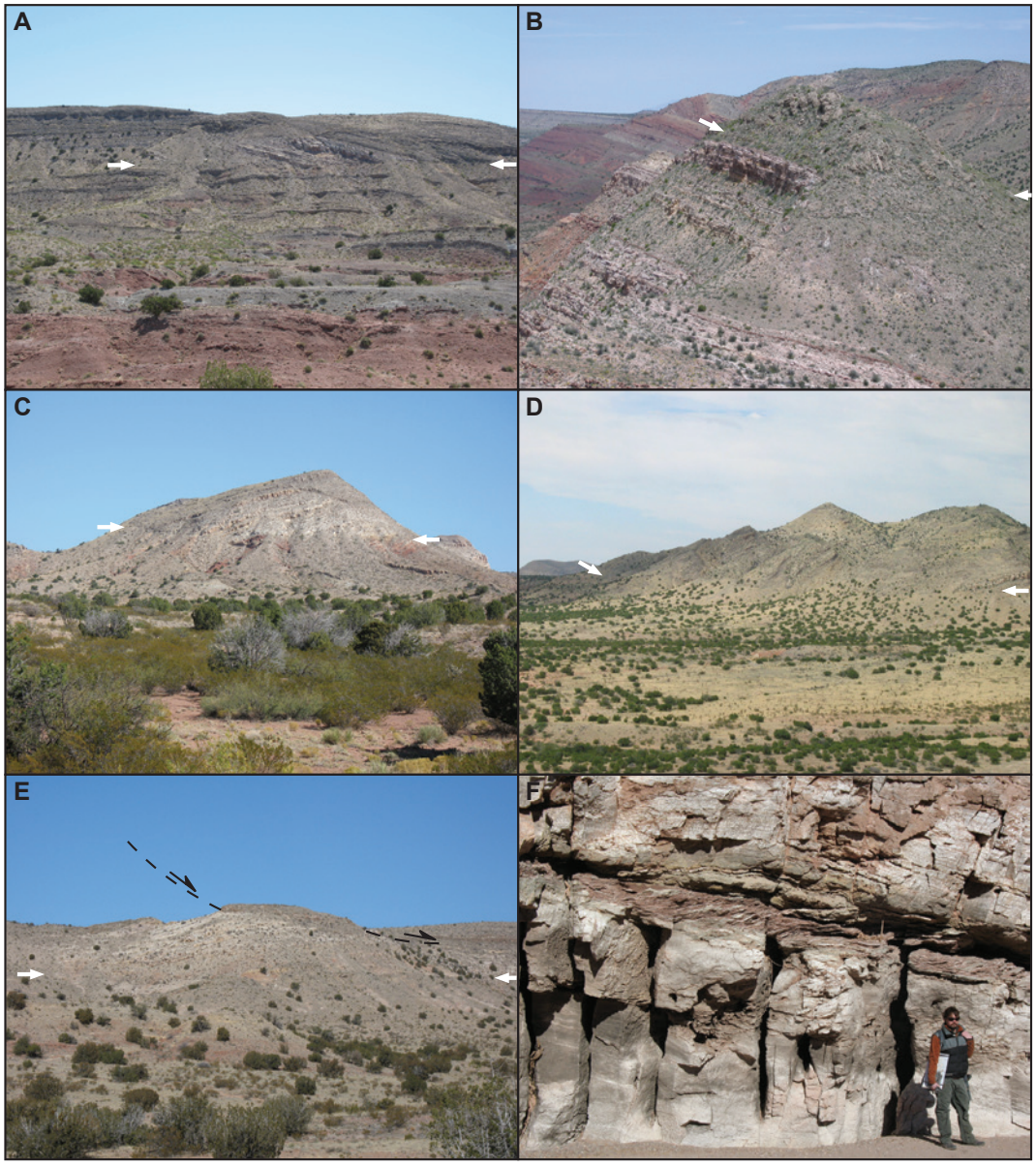

Figure 73. Images of the Quebradas detachment fault and related structures. **(A)** Detachment fault exposed in the southwestern corner of the Bustos Well quadrangle showing southwest-dipping beds of Glorieta Sandstone and the San Andres Formation in a hanging-wall ramp above the detachment fault (trace is marked by arrows). Subhorizontal beds of the upper Yeso Group (Los Vallos Formation) form a footwall flat. View is to the southeast from 338081E, 3763713N (all UTM locations are zone 13, NAD 27). **(B)** Splay fault (trace is marked by arrows) separates a hanging-wall ramp with steep (~70°) east-dipping limestone beds of gray San Andres Formation (at the top of the hill in the foreground) from a footwall containing gently dipping, light-gray beds of the Glorieta Sandstone and the basal limestone of the San Andres Formation. East-dipping hanging-wall ramps such as this are uncommon. This example formed above an antithetic (west-dipping) hanging-wall splay fault that flattened downsection into the lower San Andres Formation. The upper, steep part of the splay is now eroded in the area east of this outcrop. View is to the north-northeast from near 337800E, 3768050N. **(C)** West-dipping Glorieta and San Andres strata form a hanging-wall ramp above the Quebradas detachment fault (trace marked by arrows). Footwall rocks (red) are the Los Vallos Formation. View is to the north-northeast from 342787E, 3780177N. Sierra de la Cruz is visible in the distance on the right. **(D)** West limb of a rollover anticline related to the Bustos fault with west-dipping Glorieta and San Andres strata in the hanging wall of the Quebradas detachment (trace is marked by arrows) near La Cebolla. The footwall of the detachment fault consists of the Los Vallos Formation, which holds up the smooth slope beneath the lower one-third of the escarpment. View is to the north from 346758E, 3777402N, east-central Sierra de la Cruz quadrangle. **(E)** Example of a footwall ramp where a listric hanging-wall splay fault truncates beds of west-dipping Glorieta Sandstone in its footwall (eroded part of fault shown by dashed line). Dark-gray beds of San Andres limestone form the hanging wall. The Glorieta exposures here lie within the hanging wall of another listric splay nearby to the west (unseen to the left in this view) that caused the westward tilt of the Glorieta beds. Both listric splays sole downward into the Quebradas detachment (trace marked by arrows), which lies poorly exposed near the top of the smooth Yeso slope. View is to the north-northwest from 340954E, 3769885N, west-central Bustos Well quadrangle. **(F)** Rare exposure of Quebradas detachment fault, here cutting gypsum beds of the Cañas Member of the Los Vallos Formation. View is to the north in Arroyo de las Cañas from 338080E, 3766206N, southeastern Loma de las Cañas quadrangle. Note top-east, asymmetrical shear fabric.

We have seen no examples of contractile stratal repetition by a detachment fault. The detachment fault occurs at various stratigraphic levels within the approximately 200-m-thick Los Vallos Formation, and eastward it tends to descend stratigraphically in an irregular fashion (i.e., stratal excision of the upper part of the Los Vallos Formation is more common in the eastern part of the study area).

The Quebradas detachment fault can be regarded as a normal fault in the sense that, prior to Neogene rifting, the enclosing Permian strata dipped regionally eastward due to the structural elevation by basement fault blocks within and east of the Laramide Sierra Uplift, and slip was top-east (see below). In many areas, these strata may host two or more subparallel detachment faults, but they are commonly difficult to recognize because of inadequate exposure. Duplexes within the detachment system have been mapped only in the region between Cerro del Viboro and Loma de las Cañas, in the area west of La Montanera, near La Cebolla, and at the Yeso Group type section 3 km southeast of Mesa del Yeso (Plate 1, Fig. 1).

An area of unusually complex structure is present in the west-central part of sec. 32, T. 2 S., R. 3 E., in the northeastern part of the Bustos Well quadrangle, where Triassic and Upper Cretaceous strata and the San Andres Formation lie in fault contact above subhorizontal detachment faults on footwall strata of the Los Vallos Formation. This area needs to be remapped at a larger scale. The geology depicted there on Plate 1 is generalized.

Footwall Folds and Faults

Gypsiferous strata in the Torres and Cañas Members of the Los Vallos Formation commonly host numerous small faults and complex folds (Figs. 74 and 75). These structures probably were caused by shear related to slip on the Quebradas detachment fault.

Folds range from open to tight to isoclinal, typically plunge gently or moderately, and exhibit wavelengths of several meters to many tens of meters. Fold axes range in trend from north-northwest to northeast and average approximately 035° in the northern part of the study area (Linden, 1990). Overturned folds are common in gypsiferous parts of the upper Yeso Group (type 1 folds of Colpitts [1986]) and mostly trend north to northeast. They show variable vergence; both east- and west-dipping axial planes in subequal proportions were observed by Colpitts (1986) and during mapping for this study. Linden (1990), however, noted that west-vergent folds are more common. Only relatively large intrastratal folds within the Yeso Group are depicted on Plate 1.

Los Vallos Formation beds beneath the Quebradas detachment are locally cut by numerous small faults that exhibit either thrust or normal separation. No kinematic data were collected for these. Most faults are too small to be mapped at the scale of this study (note, however, an intra-Yeso thrust fault was mapped in sec. 6 and 7, T. 2 S., R. 3 E.).

Hanging-Wall Splay Faults

The Quebradas detachment fault displays numerous listric normal faults in its hanging wall (Fig. 70, Plate 1). Asymmetric rollover anticlines and hanging-wall ramps are associated with these splays (Figs. 73A–D). These extension-related folds generally trend north or north-northeast; rare examples trend northeast or northwest. The steep limbs of most rollover anticlines face west, opposite the dip direction of their associated splay fault.

Where best exposed in a series of klippen between the southeastern Loma de las Cañas quadrangle and southeastern Sierra de la Cruz quadrangle, the upper plate of the detachment contains at least 13 rollover anticlines and associated hanging-wall ramps. The Quebradas detachment fault does not appear to step up- or downsection in its footwall in a systematic fashion within these klippen. Most of these anticlines are thus likely related to now-eroded listric normal fault splays that soled into footwall flats of the detachment rather than to ramps within the detachment itself. The rollover geometry indicates most of these listric faults are synthetic to slip on the detachment (i.e., the faults dip east, in the direction of upper-plate slip on the detachment; see below), except for one that is antithetic and one that is oblique.

A major, geometrically well-constrained hanging-wall splay is the **Bustos fault** (Fig. 70, Plate 1). This north-striking, east-down normal fault extends approximately 18 km from the Cañon Agua Buena quadrangle northward into the La Cebolla region (Fig. 1), where it forms a prominent rollover anticline (Fig. 73D; note that the curved, onion-like strata exposed in this anticline are likely the source of the term La Cebolla). Because the modern erosion surface is beveled to deeper structural and stratigraphic

Figure 74. Intraformational faulting and folding in the Torres Member of the Los Vallos Formation beneath the Quebradas detachment. View is to the northwest from 346226E, 3776945N (zone 13, NAD 27), east-central Sierra de la Cruz quadrangle.

Figure 75. Folded beds of red mudstone and white gypsum in the Torres Member of the Los Vallos Formation. Hat for scale. View is to the southwest from 343033E, 3769428N (zone 13, NAD 27), Bustos Well quadrangle.

levels northward along its trace, the Bustos fault can be shown to sole downsection into the Quebradas detachment fault north of Cuesta de la McBride (e.g., Axen et al., 2012). There, the detachment consists of one or two fault strands within the Los Vallos Formation.

In the Blackington Hills area, the 35.4 Ma Datil Well Tuff in the hanging wall of the Bustos fault was tilted approximately 30° relative to footwall strata, with only about 1 km of stratigraphic separation on the fault, implying a strongly listric fault geometry (Cather et al., 2007). An unidentified ignimbrite and the Luis Lopez Formation are more deeply inset within paleovalleys (about 30–60 m deep) in the footwall of the Bustos fault than to the east in the hanging-wall block. These relations suggest the footwall of the Bustos fault was more deeply eroded than the hanging wall, probably because of east-down slip during volcanism. Fanning dips in the upper part of the ignimbrite succession in the hanging wall also suggest slip was occurring on the Bustos fault from about 29.0 Ma to 27.7 Ma. The fault cuts rocks as young as the 27.7 Ma South Canyon Tuff.

At the north end of the Blackington Hills, the Bustos fault bends to the east at its intersection with the Landing Strip fault zone, probably a deflection around the corner of an older, fault-bounded Laramide basement wedge (Fig. 70). North of this intersection, the Bustos fault was likely superimposed on the east-facing limb of the Laramide Bustos monocline (see above). East of La Montanera, a complex, subhorizontal part of the detachment lies in the footwall of the Bustos fault, placing duplexes of San Andres Formation and Mesozoic strata in the upper plate on folded Los Vallos Formation in the lower plate. North of La Montanera, the Bustos splay fault dips 40° east and places Eocene Baca Formation and Cretaceous strata in a hanging-wall ramp over complexly folded and faulted Los Vallos Formation of the detachment footwall. The Los Vallos Formation does not appear to thin eastward appreciably across the Bustos fault, suggesting that the detachment paralleled east-dipping Los Vallos strata within the older Bustos monocline. Where the Bustos fault soles into the Quebradas detachment near La Cebolla, Los Vallos beds constitute the footwall and a rollover anticline in the Glorieta and San Andres strata occupies the hanging wall. North and east of La Cebolla, the detachment fault again follows an upper-plate flat beneath the Glorieta Sandstone.

The **Ranchito fault zone** is as much as 1 km wide and consists of several east-down, north-striking normal faults that dip approximately 25°–35° to the east at its north end, juxtaposing the Permian San Andres Formation with Mesozoic and Paleogene strata in the southern Bustos Well quadrangle and the northern Cañon Agua Buena quadrangle (Fig. 70, Plate 1). The hanging wall of the fault features a faulted, poorly developed rollover anticline involving strata as young as Oligocene. The fault is locally buried by the Sierra Ladrones Formation. The Ranchito fault zone formed a half graben within the southern Carthage–La Joya Basin during deposition of the middle Eocene Baca Formation (see below).

The Ranchito fault zone does not extend north of the Landing Strip fault zone and was probably eroded from the upthrown block north of the Landing Strip fault zone. Because the Ranchito fault does not cut the pre-Yeso beds exposed north of the Landing Strip fault zone, we infer that it soled downward into the Quebradas detachment fault, similar to the Bustos fault to the east. The Landing Strip fault zone probably is older (early Laramide) than the Quebradas detachment because the Landing Strip fault zone bounds the southern edge of the basement wedge underlying the Gallina structural zone, which appears to be older than the Quebradas detachment (see above). The Quebradas detachment thus likely developed as a south-facing lateral ramp within the preexisting, south-facing faulted monocline of the Landing Strip fault zone.

The west-northwest-trending gravity profile C–C′ of Sanford (1968) crosses the Ranchito fault zone near U.S. Route 380. There, an approximately 15 mGal gravity gradient roughly corresponds with the Ranchito fault zone. In a simplistic model assuming no stratal tilting, Sanford (1968) interpreted an east-down fault there that offsets Proterozoic basement by about 2 km—an interpretation seemingly incompatible with a shallow, detachment-related origin of the Ranchito fault zone. Moreover, the Ranchito fault zone near U.S. Route 380 juxtaposes the Crevasse Canyon and Baca Formations against the Tres Hermanos Formation, a stratigraphic separation of only 500–600 m. Therefore, the Ranchito fault zone cannot explain the entire gravity gradient. The gravity gradient may be related to (1) an older, buried fault of Ancestral Rocky Mountains age; (2) density contrast within Proterozoic basement

rocks; or (3) an unmapped fault beneath the alluvium nearby to the east.

Similar to the Ranchito fault zone nearby to the west, the north-striking, east-down **Pinos fault** cannot be traced into pre-Yeso strata north of the Landing Strip fault zone, and thus is likely also a hanging-wall splay of the Quebradas detachment fault (Fig. 70, Plate 1). A dacite lava flow (Plate 1, map unit Tdl) is largely confined to the area of maximum hanging-wall subsidence near the Pinos normal fault, where it overlies the upper Spears Group, Datil Well Tuff, and Rock House Canyon Tuff. In three places in sec. 26, T. 3 S., R. 2 E., however, the dacite lapped westward across the Pinos fault and unconformably overlies Upper Cretaceous strata and the Baca Formation on the footwall. Little or no separation of the dacite by the fault has occurred. The Pinos fault thus records about 1.3 km of east-down, normal stratigraphic separation prior to eruption of the 34.0 Ma dacitic flow (Plate 1; see also cross section D–D´, Plate 2).

The Ranchito fault zone, Pinos fault, and Bustos fault may have developed and/or were abandoned sequentially from west to east. The Ranchito fault zone was active during the middle Eocene (i.e., during deposition of the Baca Formation, see above). This is the oldest evidence for slip on any upper-plate splay fault in the study area. Its younger history is unknown other than it cuts rocks as young as the 34.8 Ma Rock House Canyon Tuff. The Pinos fault also cuts rocks as young as the Rock House Canyon Tuff but does not appreciably offset the 34.0 Ma dacite lava where it laps westward across the fault. Slip on the Bustos fault, at least in part, postdates that on the Pinos fault. Fanning of dips in volcanic strata in the hanging wall of the Bustos fault suggests slip occurred approximately 29.0–27.7 Ma, and offset of the South Canyon Tuff by the Bustos fault indicates considerable slip also occurred after 27.7 Ma.

The Ranchito fault zone and Pinos fault clearly do not cut the Landing Strip fault zone; therefore, the combined horizontal separation (heave) of the Ranchito fault zone and the Pinos fault was transferred eastward along the Landing Strip fault zone, causing sinistral slip relative to the lower plate exposed to the north. If the Ranchito fault zone and Pinos fault are younger than (or contemporaneous with) the Bustos fault, sinistral slip on the Landing strip fault zone should have bent or cut the Bustos fault and its hanging wall in a sinistral sense. Neither effect is observed. In fact, the Bustos fault and its hanging wall are warped in the opposite sense, probably because they were bent around the wedge-block corner at the intersection between the Landing Strip fault zone and the Bustos fault as deformation proceeded. This provides a geometric argument that the Bustos fault is younger than the Ranchito fault zone and the Pinos fault. Based on the age relations stated above, slip on the Bustos fault probably began around 34–28 Ma.

The **Cañas fault** juxtaposes Mesozoic and Paleogene strata against Permian beds and terminates southward against the Landing Strip fault zone in SE1/4 sec. 23, T. 3 S., R. 2 E. of the Bustos Well quadrangle (Fig. 70, Plate 1). This normal fault probably is a hanging-wall splay of the Quebradas detachment because most of its slip may have been transferred to the detachment 8 km to the north. Critical fault relations in this area, however, are obscured by Quaternary alluvium. The Cañas fault developed along the earlier Cañas structural zone, perhaps in a manner similar to that of the Bustos fault and its antecedent Bustos monocline.

The structural context of the **East Joyita fault** is unclear. In the Joyita Hills, in the northern part of the study area, it juxtaposes Proterozoic biotite gneiss against a drag(?) syncline developed in the Popotosa Formation and Oligocene volcanic rocks in its hanging wall (Fig. 70, Plate 1). Farther north where it is better exposed, the East Joyita fault has been variously interpreted as an eastward-flattening detachment (Beck, 1993) or as a rotated planar normal fault related to rifting (de Moor et al., 2005). We think it is possible the East Joyita fault is a listric splay of the Quebradas detachment. The southward continuation of the East Joyita fault may have caused the westward tilting of volcanic units in the southern Joyita Hills (see the following discussion of the Socorro accommodation zone).

An unnamed listric, shovel-shaped normal fault that cuts volcanic rocks along the southwestern side of the Valle del Ojo de la Parida in the central part of the Mesa del Yeso quadrangle (sec. 35, T. 1 S., R. 1 E.) also may link to the regional Quebradas detachment fault (Fig. 70, Plate 1). Alternatively, the shovel-shaped fault may be related to local slumping, as was interpreted by Smith et al. (1983, stop 2). This latter interpretation is depicted in cross section A–A´ (Plate 2).

In the northwestern part of the Sierra de la Cruz quadrangle, three small exposures of Mesozoic strata lie topographically below surrounding Permian beds (Fig. 70, Plate 1). These exposures were interpreted by Smith et al. (1983, stop 1) and Linden (1990) to lie within fensters in an allochthon of Permian strata that had been thrust over Mesozoic rocks (type B allochthon of Linden [1990]). Mapping by one of us (SMC), however, shows the Mesozoic beds are not in thrust contact with Permian strata but rather are down-dropped inliers within small half grabens bounded by normal faults. Indeed, there is no evidence for older-over-younger faulting anywhere in the study area, except in the Tajo and Gallina structural zones. The northernmost half graben is bounded on the west by an arcuate, east-down normal fault that likely soles into the Quebradas detachment. Relations between the remaining half grabens and the Quebradas detachment are unclear due to poor exposure.

Quebradas Detachment Kinematics and Age

Prior to this study, Linden (1990) provided the only kinematic data for the detachment. During his dissertation research, he evaluated several types of kinematic indicators in the northern part of the study area, including (1) fold-axis trends and fold asymmetry in the footwall of the detachment, (2) calcite c-axes within extensional fractures in the hanging wall, (3) slickenline orientations on associated low-angle faults, (4) extensional fractures in the hanging wall, and (5) gypsum fibers in footwall veins (Table 4). He noted that bidirectional indicators are of variable azimuth but suggested that upper-plate slip was generally toward the east or west. Unidirectional shear indicators collected by Linden (1990) are contradictory; the dominant asymmetry of footwall folds indicates top-northwest detachment slip, whereas Riedel shears on low-angle faults indicate top-east slip.

Linden (1990) thought detachment faulting may have been diachronous and/or involved more than one detachment system that slipped in different directions. He envisioned a major allochthon that slid gravitationally to the west-northwest off the uplifted, southeastern side of the Montosa fault. Linden (1990) proposed 4–6 km of upper-plate transport to account for the purported Permian-over-Mesozoic faulting in the northwestern part of the Sierra de la Cruz quadrangle, which he interpreted as thrusting at the toe of the allochthon (see above for a contrasting interpretation). Linden (1990) interpreted detachment faulting to have occurred in the Paleocene because he saw no evidence for involvement of the Eocene Baca Formation.

Mapping during the present study sheds new light on the age and kinematics of the Quebradas detachment. A rare exposure of asymmetric shear fabrics within the fault at Arroyo de las Cañas shows the fault is top-east (Fig. 73F). Because most upper-plate normal faults in extensional parts of landslides dip in the direction of upper-plate slip (Varnes, 1978), the geometry of rollover anticlines can be used to approximate the dip direction of eroded, upper-plate normal faults (i.e., the dip direction of a splay fault is opposite to that of the steep limb of its associated rollover anticline; see green arrows on Plate 1) and therefore the slip direction of the detachment. Based on the geometry of 30 rollover anticlines scattered widely throughout the bedrock portions of the study area, the slip direction of the detachment was top-east (mean 096°; Fig. 76). Consideration of all available data (Table 4) suggests the most likely slip direction for the upper plate of the Quebradas detachment was toward the east or east-southeast.

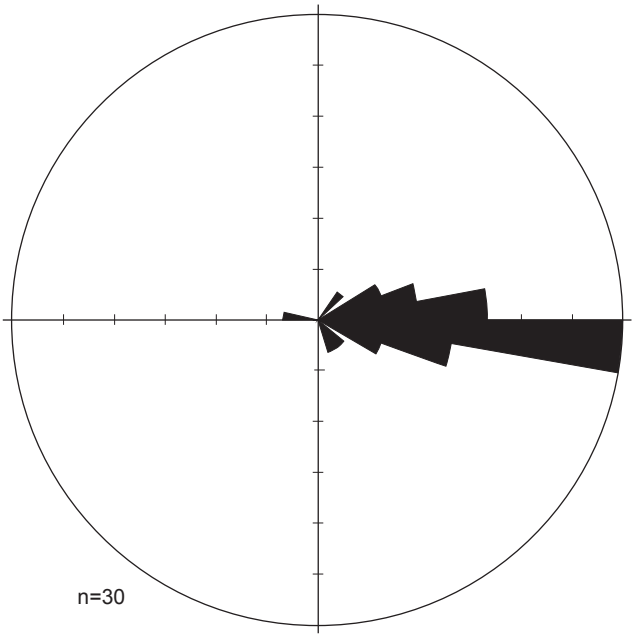

Figure 76. Rose diagram (north at top) showing inferred easterly slip direction of upper-plate splay faults, based on the geometry of associated rollover anticlines. The dip direction of the steep limb of a rollover anticline is opposite that of its associated splay fault. These splay faults in turn are assumed to be synthetic to the slip direction of the underlying Quebradas detachment (see text).

Table 4. Slip direction indicators for relative motion of the upper plate of Quebradas detachment fault.

Shear indicators	Upper plate movement direction	References
Unidirectional shear indicators		
Rollover anticline asymmetry[1]	E	This study (Fig. 76)
Fault-plane shear fabric	E	This study (Fig. 73F)
Riedel shears on low-angle faults	E	Linden, 1990
Preferred sense of fold asymmetry in FW	None	Colpitts, 1986; this study
Preferred sense of fold asymmetry in FW	NW	Linden, 1990
Bidirectional shear indicators		
Fold axes within FW[2]	Mostly ENE or WSW	Colpitts, 1986; Linden; 1990; this study
Calcite c-axes within HW veins	E or W	Linden, 1990
Slickenlines on low-angle faults within HW	Mostly WNW or ESE	Linden, 1990
Gypsum fibers within veins in FW (Torres Mbr)	E or W	Linden, 1990
Gypsum fibers within veins in FW (Joyita Mbr)	NW or SE	Linden, 1990

HW = hanging wall, FW = footwall, Mbr = Member (of Los Vallos Formation).
[1] Assumes the steep limb of the rollover anticline dips in the opposite direction from its associated hanging-wall listric splay fault, and that most splays are synthetic to the upper plate slip direction of the Quebradas detachment (see text).
[2] Assumes axes of footwall folds in the Los Vallos Formation are perpendicular to the slip direction of the upper plate of the detachment.

The Quebradas detachment fault appears to have been episodically active during the approximately 25-Myr interval between the middle Eocene and middle Miocene. New age constraints for the Quebradas detachment and its related splay faults are described in other parts of this report and are summarized here:

1. The detachment fault is younger than (i.e., not deformed by) early(?) Laramide contractile deformation in the Gallina structural zone.
2. A coarse fan deposit in the Baca Formation was localized by a paleovalley in the footwall of the Ranchito fault zone, a splay of the Quebradas detachment. This indicates slip during the middle Eocene.
3. Slip occurred on the Quebradas detachment fault before and after intrusion of a late Eocene dike near La Cebolla at 34.7 Ma (Green et al., 2013).
4. Rocks as young as the 34.8 Ma Rock House Canyon Tuff are cut by the Pinos splay fault, but a 34.0 Ma dacitic lava flow is not appreciably offset by it.
5. Slip occurred on the Bustos splay fault during late Oligocene volcanism, as shown by fanning dips in 29.0–27.7 Ma volcanic strata of the hanging wall of the fault and deeper incision of approximately 34–29 Ma paleovalleys on the footwall.
6. Slip on the Bustos fault continued after the end of volcanism because it cuts the 27.7 Ma South Canyon Tuff.
7. If westward stratal dips in the southern Joyita Hills are related to rollover folding (as we contend below), then the Popotosa Formation likely constituted the youngest strata involved in detachment faulting.
8. Normal faults within the Montosa fault zone offset the Quebradas detachment. These and other rift-related normal faults are probably middle to late Miocene in age (Cather et al., 1994b). Deep-seated rift faulting dismembered the Quebradas detachment system and likely marked its demise as a regional slip surface.

Lack of clear offset markers in the upper and lower plates makes it difficult to estimate the amount of top-east slip on the Quebradas detachment. Minimum slip can be estimated by summation of slip on upper-plate splay faults that sole into the detachment. The numerous hanging-wall splays in cross section C–C′ (Plate 2) suggest the cumulative slip there was at least 1–2 km (most are east-down, and each exhibits 100 m or more of normal separation). This estimate is conservative because the geometries of splay faults are poorly constrained due to deep erosion of the upper plate of the detachment.

The amount of top-east slip on the upper plate of the Quebradas detachment fault is better

constrained in the Bustos Well quadrangle, where more complete preservation of the upper plate allows for more accurate slip estimates for hanging-wall splays. If cross section D–D´ (Plate 2) is a reasonable depiction of the subsurface fault geometry, the slip on hanging-wall splays implies approximately 5.3 km of cumulative top-east slip on the detachment fault within the quadrangle. This estimate corresponds to upper-plate extension of about 30% but does not include probable slip contributions from now-eroded splays farther to the west.

The S-C fault fabric of the Quebradas detachment exposed in gypsiferous rocks in Arroyo de las Cañas (Fig. 73F) indicates that creep, assisted by pressure-solution, accommodated slip there. The detachment system largely resides within the evaporite-rich upper Yeso Group, so it seems likely that most slip was by creep. If 6 km of top-east slip on the detachment occurred over an approximately 30-Myr interval during the middle Eocene to middle Miocene, then the average slip rate was about 0.2 mm/yr, but it is likely that slip rate varied both spatially and temporally.

Regional Context

The Quebradas detachment system is clearly present throughout most or all of the study area, but its lateral boundaries in adjacent regions are not well defined. North of the study area, a post-Oligocene detachment fault is present in the northern Joyita Hills (Beck, 1993), and low-angle normal faults are present within Permian strata in the southern Becker SW quadrangle (Allen et al., 2013b), but no detachment faulting is evident farther north in the Abo Pass area. The Quebradas detachment crops out in the southern part of the study area at Cerro del Viboro but is not known to be present in the next Permian exposures 30 km to the south, near Little San Pascual Mountain (Geddes, 1963). The western limit of the Quebradas detachment fault presumably was on the eastern flank of the Laramide Sierra Uplift, now subsided within the Socorro Basin. The only known detachment fault west of the Rio Grande rift is near Yellow Mountain, 35 km northwest of the study area (Fig. 77). The detachment there needs further study. It lies within the upper Yeso Group, but slip

Figure 77. Detachment fault dividing east-dipping strata of Glorieta Sandstone(?) and San Andres Formation in hanging-wall ramp from orange beds of upper Yeso Group in the footwall, ~35 km northwest of the study area. This geometry suggests top-west slip on the fault. View is to the north-northwest from 296099E, 3810686N (zone 13, NAD 27), near Yellow Mountain, north of Riley, New Mexico.

was probably top-west—opposite the slip sense of the Quebradas detachment. Cather (2009b) speculated that the eastern margin of the detachment system may lie as far east as the Carrizozo area, 75 km east of the study area (Fig. 78). If it does indeed extend that far to the east, then the area of the detachment is approximately 3,600 km^2, similar to that of the Heart Mountain detachment of Wyoming (Hauge, 1993).

It is possible that the Prairie Spring, Chupadera, and Carrizozo anticlines represent the contractile toes of a mega-landslide (i.e., the upper plate of the Quebradas detachment) and the hanging-wall splays exposed in the study area formed in the extensional rear of the slide sheet (Fig. 78; Cather, 2009b). Based on unpublished geologic mapping of the northern Sierra Larga by M.W. Green, it is clear that the

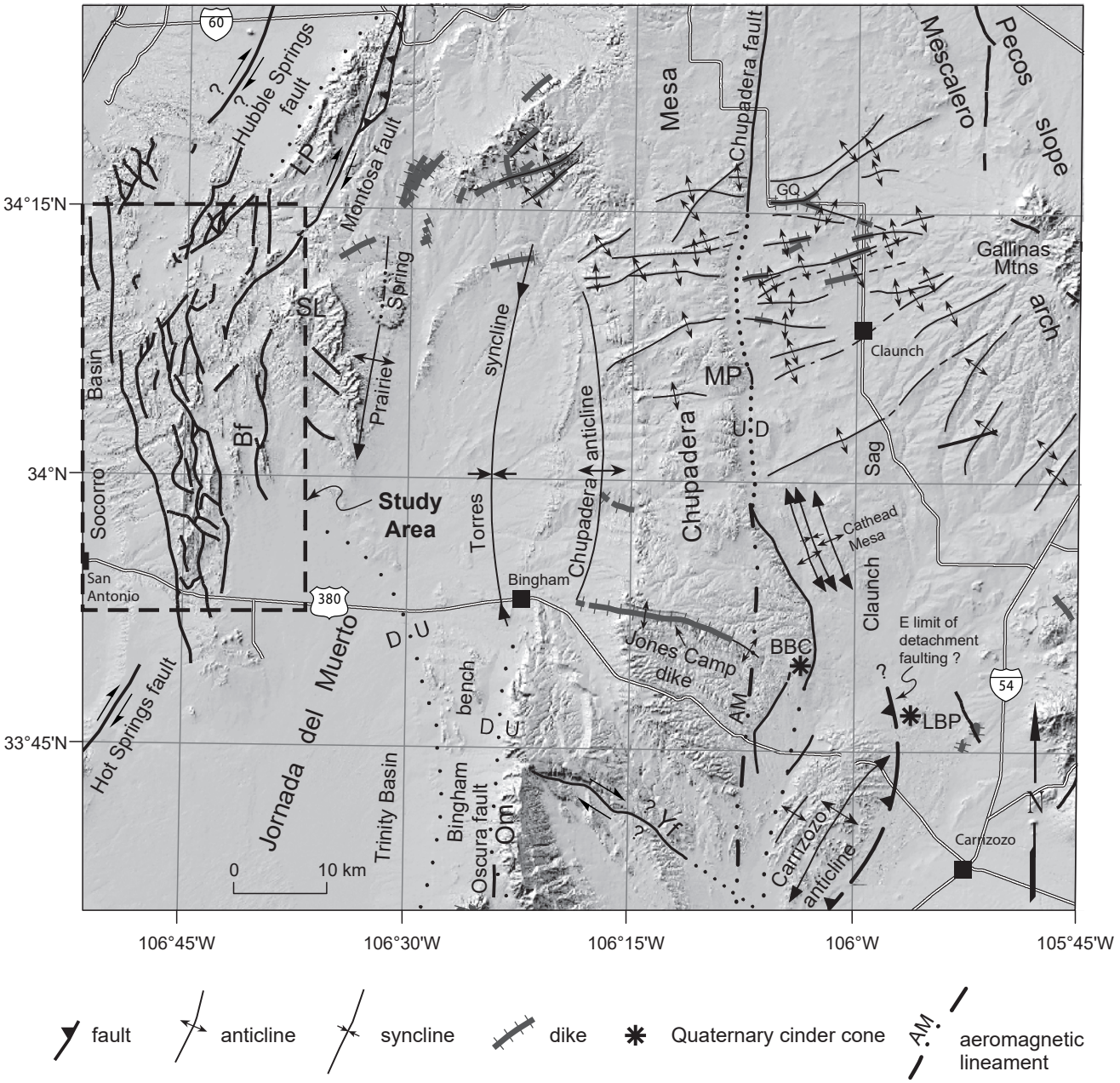

Figure 78. Digital elevation model for central New Mexico showing selected high-angle faults, folds, and igneous features in the study area (from NMBGMR [2003]) and in regions to the north, east, and south. Thickened Yeso Group in the cores of the Prairie Spring, Chupadera, and Carrizozo anticlines may represent the contractile toes of the Quebradas detachment. The Laramide Sierra Uplift encompassed what is now the Socorro Basin. Abbreviations are **Bf**—Bustos fault, **SL**—Sierra Larga, **LP**—Los Pinos Mountains, **MP**—Monte Prieto, **GQ**—Gran Quivira, **BBC**—Broken Back Crater, **LBP**—Little Black Peak, **OM**—Oscura Mountains, and **Yf**—Yates fault. Modified from Cather (2009b).

Quebradas detachment is exposed within the western limb of the Prairie Spring anticline. The easternmost upper-plate rollovers are in the northwestern part of Sierra Larga near La Cebolla. East of there, across the width of the Sierra Larga, the upper plate is essentially unfaulted, so it moved eastward as an intact allochthon that included the Prairie Spring anticline (Fig. 78). Potential continuity of the detachment with anticlines farther east, however, is uncertain because the intervening Torres syncline has not been penetrated by drilling. The thickness of the Yeso Group in the Torres syncline is unknown.

The Prairie Spring, Chupadera, and Carrizozo anticlines are largely "rootless" folds that owe much of their structural relief to contractile thickening of the upper Yeso Group in their cores. The upper Yeso Group in these anticlines is significantly thicker than in adjacent, undeformed areas (Cather, 2009b). Wells that penetrate deeper stratigraphic levels suggest that pre-Yeso strata do not conform to these folds. Thus, the eastern limit of the Quebradas detachment fault may be a blind-thrust triangle zone below one or more of these anticlines, allowing more shortening within the upper Yeso Group than is evident in the overlying San Andres and Glorieta Formations. Mechanisms for thickening of the Yeso in these anticlines have not been adequately studied but appear to be mostly the result of folding (Fig. 79) and thrust faulting (Cather, 2009b). We are not aware of any exposed thrusts that daylighted at the eastern edge of the proposed regional detachment.

Figure 79. Folds within the Los Vallos Formation (upper Yeso Group) exposed in the north-central part of the Prairie Spring anticline. Exposure is capped by Pliocene basalt of Mesa Redonda, ~8 km east of the Sierra de la Cruz quadrangle. Folds such as these contribute to the contractile thickening of the Yeso Group within the Prairie Spring, Chupadera, and Carrizozo anticlines (see Cather [2009b]). View is to the north-northeast from 3571150E, 3779237N (zone 13, NAD 27).

The north–south extents of the Prairie Spring anticline, Torres syncline, Chupadera anticline, and Carrizozo anticline are similar to that of known exposures of the Quebradas detachment fault to the west, suggesting a common origin. All lie east of a restraining bend in the Laramide Hot Springs–Montosa–Hubble Springs fault system that gave rise to the Sierra Uplift (Fig. 78), which in turn probably provided the slope on which top-east slip on the detachment initiated.

Model for Development of the Quebradas Detachment

What follows is our favored model for detachment faulting in the Quebradas region east of Socorro, in which the detached upper plate initially slid eastward off the eastern flank of the Laramide Sierra Uplift. This model incorporates the following observations:

1. Initial rise of the Sierra Uplift probably began in the Late Cretaceous, within what is now the Socorro Basin of the Rio Grande rift, as shown by the presence of pebbles recycled from Triassic strata in the upper part of the Crevasse Canyon Formation.
2. The northern part of the Sierra Uplift cooled through the approximately 110°C isotherm (about 3–5 km paleodepth) around 57–45 Ma, as shown by apatite fission-track ages of from clasts in the Baca Formation (Kelley et al., 2009). This suggests uplift continued until the middle Eocene.
3. Uplift related to east-directed Laramide reverse faulting along the flank of the Sierra Uplift extended at least as far east as the Bustos monocline and the Gallina structural zone.
4. Reverse faulting occurred prior to initiation of detachment faulting, as shown by field relations between the Gallina structural zone and the Quebradas detachment fault.
5. The Baca Formation of the southern Carthage–La Joya Basin locally exhibits an anomalous, inverted unroofing succession in which Proterozoic clasts dominate the base of the Baca Formation and give way upsection to mostly sedimentary detritus.
6. Stratigraphic relations indicate splay faults in the upper plate of the Quebradas detachment were active between the middle Eocene and late Oligocene, and perhaps until the middle Miocene.
7. The Quebradas detachment was disrupted by rift-related normal faults that were likely initiated during the middle to late Miocene.

During the Laramide orogeny, west-up basement faulting along the eastern flank of the Sierra Uplift extended as far east as the central part of the Bustos Well and Sierra de la Cruz quadrangles (Figs. 70 and 80). Reverse faults (mostly blind) produced the Tajo and Gallina structural zones and the Bustos monocline. We suggest these structures mark the eastern edges of subsurface basement wedges. Laramide basement wedges are responsible for much of the structural elevation along the eastern flank of the Socorro Basin and probably began to rise during the Late Cretaceous. (Note that Pollock et al. [2004] proposed a similar blind basement wedge along the western margin of the Laramide Nacimiento Uplift in northern New Mexico.)

By early Eocene time, widespread Proterozoic exposures probably existed on the Sierra Uplift to the west, but subsidence and sedimentation had not yet begun in the late Laramide Carthage–La Joya Basin. Instead, fluvial systems transported detritus to the east beyond the study area. During middle Eocene time, an easterly topographic slope caused by uplift of underlying basement wedges became sufficient to initiate top-east gravity sliding on slip planes within weak gypsiferous beds of the upper Yeso Group. Detachment slip may have been aided by the dehydration of gypsum to anhydrite (Linden, 1990; Cather, 2009b) and by the possible former presence of halite in the upper Yeso (Green et al., 2013). Development of mostly east-down normal-fault splays in the hanging wall of the detachment caused at least one half graben to develop (along the Ranchito fault zone) in which the Baca Formation was deposited (Fig. 80). Clasts in the Baca were initially dominated by Proterozoic lithotypes derived from the Sierra Uplift. Proterozoic clasts were increasingly supplanted by Mesozoic and Paleozoic sedimentary lithotypes as the footwall of the Ranchito fault became incised by streams.

Slip on the Quebradas detachment may have been episodic. It is unclear if detachment slip continued during deposition of the lower Spears Group in the middle and late Eocene. Fanning dips, onlap

of a dacitic lava across the footwall of the Pinos fault, and increased erosion depth on the footwall of the Bustos fault, however, suggest deformation occurred during the subsequent Oligocene ignimbrite flare-up. Synvolcanic detachment faulting may have been enhanced by gravity-driven spreading of the volcanic field (e.g., Borgia et al., 2000; Le Corvec and Walter, 2009). A locus of Spears-age volcanism was centered on the Sierra Uplift (Cather, 1990), which subsequently became structurally inverted to form the Socorro Basin. If gravitational loading by volcanic accumulation caused lateral spreading and renewed top-east detachment faulting in the Quebradas region, it might be expected that top-west faulting would have occurred in the region west of the rift. The previously described detachment fault near Yellow Mountain may be an example of this.

Detachment faulting in the east-central part of the study area may have been accompanied by sequential west-to-east development of hanging-wall splays (the Ranchito, Pinos, and Bustos faults). These splay faults appear to merge downward with the Quebradas detachment. Upper-plate extension in the study area may have been compensated by contractile folding and faulting in the Prairie Spring, Chupadera, and Carrizozo anticlines to the east (Fig. 78; Cather, 2009b). Kinematic links to folds east of the Prairie Spring anticline, however, have yet to be demonstrated.

The end of detachment faulting postdates the youngest volcanic unit in the study area—the 27.7 Ma South Canyon Tuff. This tuff is cut by the Bustos fault, an upper plate splay of the Quebradas detachment. The same tuff also is down-faulted against Proterozoic basement by the East Joyita fault at the north end of a west-tilted volcanic section capped by Popotosa Formation in the southern Joyita Hills. We suggest westward tilting of volcanic strata in the southern Joyita Hills occurred during detachment faulting (see below). If so, the end of detachment faulting postdates deposition of the Popotosa Formation (lower Miocene?), which is also west-tilted. During the middle to late Miocene culmination of rifting (Chapin and Cather, 1994), rift-related normal faults disrupted the detachment and probably prevented further regional slip on the fault.

Evaporite-hosted detachment faulting in the study area is a well-exposed, incipient example of what is termed "raft tectonics" (*tectonique en radeaux*) in petroleum geology literature. Raft tectonics has been described in many places, including offshore Angola, Tunisia, northwestern Europe, the Gulf of Guinea, and the Gulf of Mexico (Burollet, 1975; Duval et al., 1992; Lundin, 1992; Guglielmo et al., 1997; Mauduit et al., 1997; Vila et al., 1998; Penge et al., 1999; Pilcher et al., 2014). The study area differs from these examples in that it does not host extreme upper-plate extension or evaporite diapirism.

Variations on the model for formation of the Quebradas detachment fault are possible and compatible with the model proposed above. These may help explain minor problems with the model, such as how the Quebradas detachment may have remained active until middle Miocene time, well after the end of the Laramide orogenesis in this part of New Mexico (the first two variants assume post-Laramide, volcanism-induced lateral spreading was not important).

In the first variant of the model, the detachment was initiated as a rootless, east-directed, late Laramide landslide as proposed above, and it ended eastward in the Prairie Spring anticline and possibly the Torres syncline, Chupadera anticline, and Carrizozo anticline (Fig. 78). In this variant, the eastern limb of the Torres syncline formed as a fault-propagation drape fold (or forced fold) above a subsurface, northward continuation of the west-down Oscura normal fault. This would have allowed some of the late slip on the eastern part of the detachment to be accommodated by heave on the blind northern extension of the west-dipping Oscura fault. A second but less likely early rift-age variant allows the detachment to be rooted eastward into the basement, so that slip on it accommodated late detachment-related upper crustal extension to the west. In this variant, the root zone probably lies under the Torres syncline.

A third variation is that the detachment initially developed as an east-directed, stratigraphically controlled thrust related to development of the Laramide Sierra Uplift. It could have initiated as an eastward splay from a reverse fault that raised the uplift, or it may have initiated as an out-of-syncline thrust before the associated reverse fault propagated to the surface. In this model, subsequent east-directed gravity sliding off the uplift would have then reutilized the detachment.

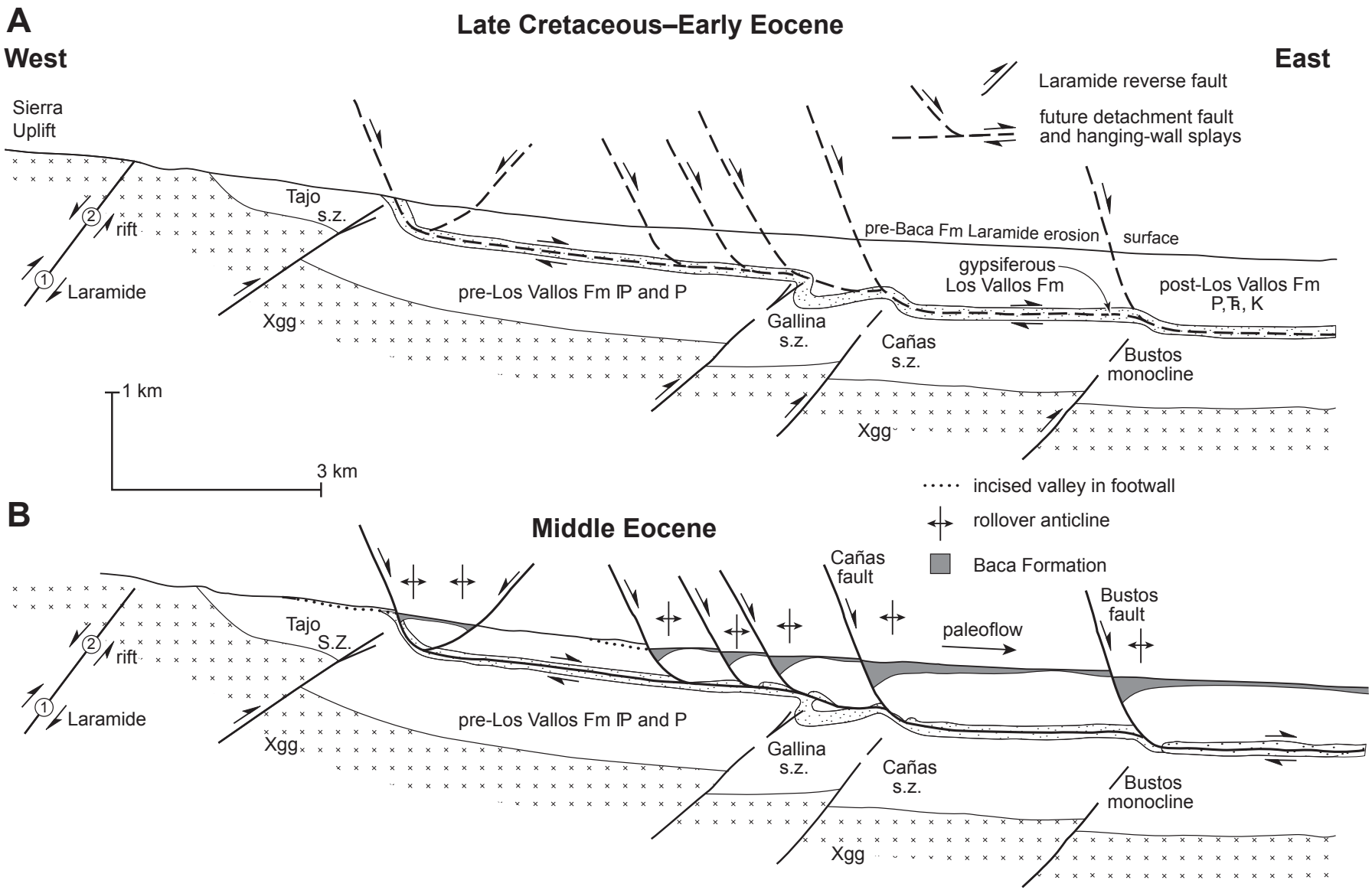

Figure 80. Schematic cross-sectional model for development of (A) Laramide basement wedges and (B) subsequent late Laramide (middle Eocene) initiation of top-east slip on the Quebradas detachment and associated hanging-wall splay faults and rollover anticlines. Line of section is approximately along 34°03′ in the Loma de las Cañas and Bustos Well quadrangles (~3 km north of the Landing Strip fault zone). Note that depositional control of the Baca Formation by splay faults has only been demonstrated for the Ranchito fault zone, south of the Landing Strip fault zone. The Quebradas detachment continued to slip until the middle Miocene. **s.z.**—structural zone. Scale is approximate.

NEOGENE RIFT-RELATED NORMAL FAULTS

Most rift-related normal faults in the study area dip moderately to steeply (50°–75°). They generally strike northwest or north, but several faults within the northeast-striking Milagro, Amado, and Montosa fault zones experienced normal reactivation during the late Cenozoic. Rift-age normal faults are most commonly found along the eastern margin of the Socorro Basin, but examples are scattered throughout many parts of the study area (Fig. 70, Plate 1). Unlike the older splay faults in the upper plate of the Quebradas detachment, rift-related normal faults are mostly west-down, not strongly listric, and not associated with rollover anticlines.

A series of north-striking normal faults, locally linked by left-stepping, northwest-striking normal faults, defines the eastern margin of the Socorro Basin in the study area. These faults include, from north to south, the **Alamillo**, **Veranito**, **Coyote**, **Gonzales**, and **Fite faults** (Fig. 70, Plate 1). Several of these faults offset and control the thickness of the Sierra Ladrones Formation. They are thus clearly related to late rift extension, although the timing of their origin remains uncertain. The Coyote fault defines the western edge of a structural bench in the eastern Socorro Basin on which thin piedmont deposits of the Sierra Ladrones Formation overlie Paleogene volcanic rocks.

Only three faults in the study area have demonstrable Quaternary normal separation, although it is difficult to evaluate the possibility of Quaternary slip on many other faults in bedrock areas because of insufficient age control. A poorly exposed fault that bounds the eastern margin of the Bosquecito pumice deposit near 332000E, 3755300N (zone 13, NAD 27) exhibits about 5–10 m of west-down separation that has occurred since 1.6 Ma. About 10 m of west-down separation of the Las Cañas geomorphic surface has occurred on the Coyote fault since about 0.8 Ma and represents the youngest verifiable episode of normal faulting in the Quebradas region. Possible sag-pond deposits in the upper Sierra Ladrones Formation (map unit QTsm) near 328000E, 3785800N (zone 13, NAD 27) suggest slip may have occurred on the Alamillo fault during the Quaternary.

Balch (1997) studied three swarms of seismicity that occurred in 1985–1986 at 5.0–8.5 km depth in the Mesa del Yeso and Loma de las Cañas quadrangles. The southern two swarms are closely associated with the Coyote fault. Nearly all focal mechanisms calculated for the three swarms were strike-slip, with T-axes in the southwestern quadrant. These results are suggestive of sinistral slip when resolved on north-striking faults.

Relatively few faults in the Sierra de la Cruz quadrangle can be shown to be Neogene. These include steep, north-striking normal faults in the north-central part of the quadrangle near Cibola Spring, part of the Milagro fault zone where it cuts the Quebradas detachment fault, and the above-described extensional reactivation of parts of the Montosa fault zone (Fig. 70, Plate 1).

The footwall of the Quebradas detachment fault, well exposed between the Laramide Tajo and Gallina structural zones, is broken by numerous, mostly north-striking, high-angle faults (Plate 1). Several have west-down separation, but the fault dip direction is indeterminate for most. Given their position between two major Laramide contractile structures, it is possible these faults originated as steep reverse faults and were subsequently reactivated as normal faults. More work is needed in this area.

In the region around and north of Cerro del Viboro, the Quebradas detachment is cut by several steep faults with normal separation (Fig. 70, Plate 1; Fagrelius, 1982; Craig, 1992). These faults strike north to west-northwest and are presumably rift related. Along U.S. Route 380 in the Cañon Agua Buena quadrangle, numerous north-striking normal faults offset the Upper Cretaceous Dakota Sandstone. Some of these faults did not propagate through the underlying Triassic Chinle Formation or the overlying Upper Cretaceous Mancos Shale, which were instead deformed by distributed minor faults and folds.

SOCORRO ACCOMMODATION ZONE AND DIP DOMAINS

The Socorro accommodation zone (SAZ; originally termed the Socorro transverse shear zone by Chapin et al. [1978]) is an east-northeast-trending structural zone within the Rio Grande rift of central New Mexico (Chapin, 1989). Where best expressed west of the Socorro rift basin, it is an approximately 60-km-long, 2-km-wide zone that divides mostly west-tilted Neogene fault blocks on the north from

east-tilted ones to the south. The SAZ follows part of an inferred basement flaw of Precambrian(?) age—the Morenci lineament (Chapin et al., 1978). The lineament also served as a Cenozoic magmatic locus. Most workers (e.g., Chapin et al., 1978; Chapin, 1989; Chamberlin et al., 2004) extend the SAZ across the Socorro Basin to the Quebradas region, where it corresponds to the northeast-striking Amado fault zone, which locally divides mostly west-tilted strata to the north from variably tilted rocks to the south.

Mapping for this study indicates that, unlike most areas west of the Socorro Basin, the geographic distribution of dip domains in the Quebradas region is quite complex and cannot be solely attributed to rifting (Fig. 81). Most areas of significant stratal tilting in the Quebradas region are within Laramide structural zones or detachment-related rollover anticlines. Tilted strata that can be confidently attributed to rifting are limited to the Sierra Ladrones Formation of the eastern Socorro Basin. These beds typically exhibit very gentle dips (0°–7°) and locally varying dip direction (Fig. 81, Plate 1).

A region of westward stratal tilts occurs in the La Cebolla–Blackington Hills–Cañon Agua Buena area (Fig. 81). Dips within this domain are typically 15°–50° west. These dips are clearly related to rollover anticlines associated with the Ranchito, Pinos, and Bustos splay faults in the upper plate of the Quebradas detachment and thus predate rifting.

The only other large area of westward stratal dips lies north of the Amado fault zone in the southern Joyita Hills. Because these exposures are in the upper plate of the Quebradas detachment (as shown by westward projection of detachment faults exposed along the eastern side of Valle del Ojo de la Parida), we suspect stratal tilting there is also the result of detachment faulting, not rifting. We note that footwall unloading along the west-down Alamillo and Veranito rift faults in the Socorro Basin should produce eastward tilting of the southern Joyita Hills, not westward as observed.

We suggest westward tilting of volcanic units and Popotosa Formation in the southern Joyita Hills occurred within a broad rollover anticline, analogous to west-dipping volcanic strata elsewhere in the study area. If so, an associated east-down splay fault must be present nearby to the west, beneath fill of the Socorro Basin (see Fig. 70). A gravity survey (Sanford, 1968) indicates a modest gravity high in the Socorro Basin near the western edge of the study area, north of 34°06′. The gravity high may represent the footwall of an east-dipping splay fault or perhaps the headwall scarp of the Quebradas detachment itself. This interpretation is supported by a driller's log for a water well (Office of the State Engineer file number RG 91116) on the gravity high in W1/2 sec. 17, T. 2 S., R. 1 E., Mesa del Yeso quadrangle (see well location in Fig. 70). The log indicates "basalt" overlying "granite" (probably La Jara Peak Basaltic Andesite overlying Lemitar Tuff; R.M. Chamberlin, personal communication, 2018), beneath 64.6 m of Sierra Ladrones Formation.

If this interpretation is correct, a significant east-down fault offsets the Oligocene volcanic section and Popotosa Formation (but not the Sierra Ladrones Formation) between the well and the southern Joyita Hills. East-down separation on this buried fault is at least 1.5 km, based on projection of west-tilted volcanic strata exposed in the southern Joyita Hills toward the well described above. Throw on the younger, west-down Veranito fault (Fig. 70) is poorly constrained but would add to the 1.5 km value. The east-down fault may join northward with the East Joyita fault (Fig. 70; fault is not shown on Plate 1), which exhibits at least 3.7 km of east-down stratigraphic separation. The East Joyita fault was interpreted by Beck (1993) as a detachment structure (cf. de Moor et al. [2005], who instead interpreted it as a low-angle, basement-rooted rift fault).

We conclude that evidence for extrapolation of the SAZ east of the Socorro Basin is not compelling. If the SAZ were indeed developed along an ancient, regional basement flaw (i.e., the Morenci lineament of Chapin et al. [1978]), it is likely this feature would have been offset dextrally during the Laramide orogeny. The best estimate for Ancestral Rocky Mountain and Laramide dextral slip in what is now the Socorro Basin is approximately 26 km (Cather and Harrison, 2002; Cather, 2009b). Offset of the projected trend of the Morenci lineament by this amount would place it at the southern edge of the study area, near Carthage. Stratal draping over faults developed along the lineament may explain the anomalous southerly and southeasterly stratal dips in this area (Fig. 81, Plate 1). In addition, several aeromagnetic features near Carthage correspond to the 065° trend of the Morenci lineament (Kucks et al., 2001; see also plate 4 in Lueth et al. [2009]). Alternatively, the Morenci lineament may simply end at Socorro, as does the SAZ.

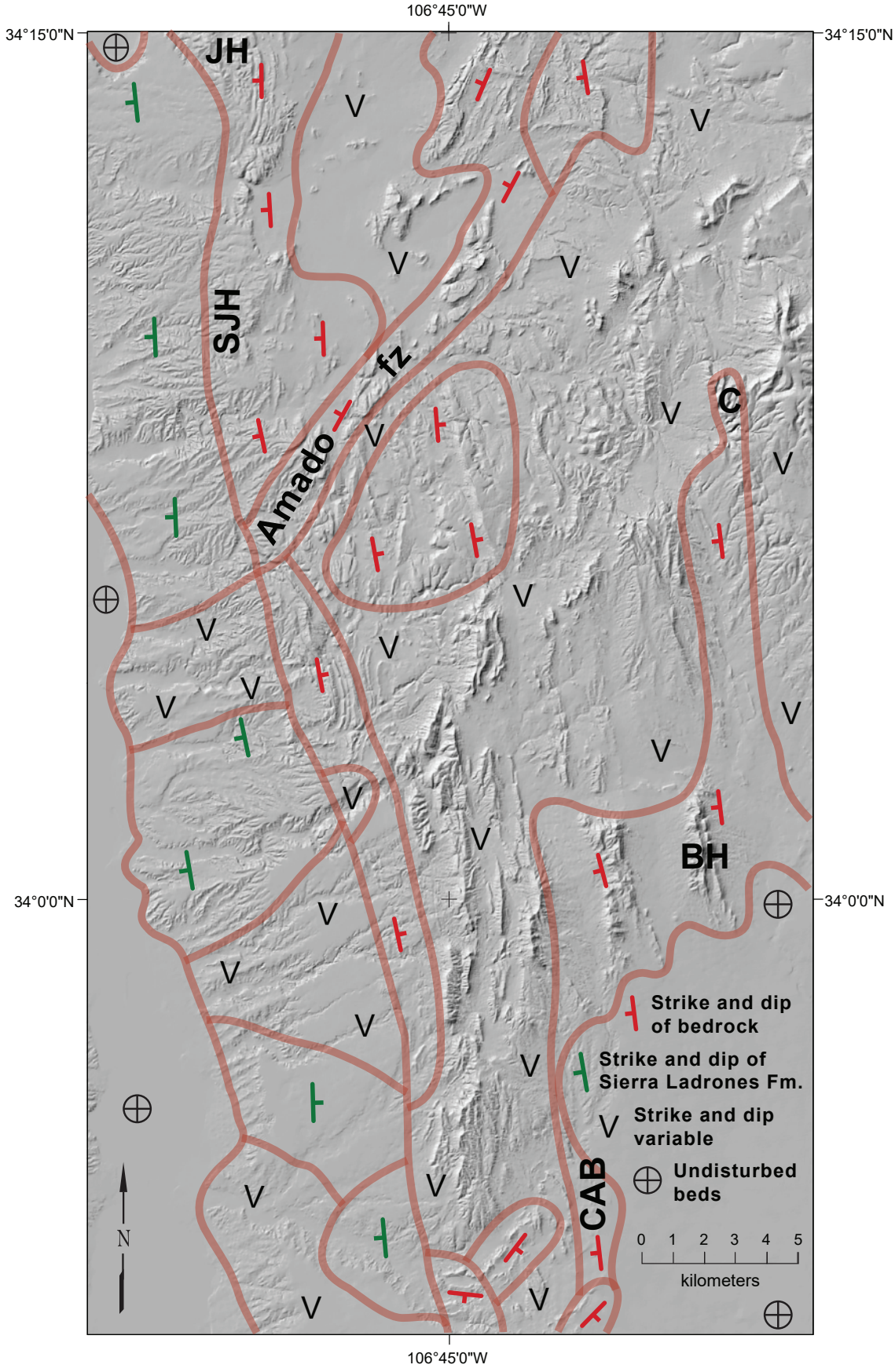

Figure 81. Digital elevation model for the study area showing generalized dip domains. Abbreviations are **Amado fz**—Amado fault zone, **BH**—Blackington Hills, **C**—La Cebolla, **CAB**—Cañon Agua Buena, **JH**—Joyita Hills, and **SJH**—southern Joyita Hills.

CHAPTER 6: MINERAL RESOURCES OF THE QUEBRADAS REGION

Virginia T. McLemore

INTRODUCTION

Mining history in the Quebradas area is not as well known as that in other parts of New Mexico. Two mining districts (Socorro and Chupadero) and two coal fields (Carthage and Jornada del Muerto) are present in the Quebradas area (Fig. 82). Uranium was mined from the Socorro district. Copper, silver, clay, and fluorite were mined from the Chupadero district, whereas limestone and clay were mined from the Carthage coal field. The Carthage coal field is described separately (Chapter 7). Flagstone was mined from several small quarries in the area, but not much is known about their history.

This work is part of ongoing studies of mineral deposits in New Mexico and includes updates and revisions of prior work by McLemore (1983a, 1983b, 2017) and North and McLemore (1986, 1988). Chemical analyses of selected mineralized samples are in Appendix 2. Published and unpublished data on mines and mills within the Quebradas area were inventoried and compiled in the New Mexico Mines Database (McLemore et al., 2005a, 2005b), and a summary is in Appendix 3.

SOCORRO MINING DISTRICT

The Socorro mining district (Fig. 83), as defined by Jones (1915) and McLemore and Chenoweth (1989), was first prospected during the late 1950s and has been known by several names, including Encarnacion, Agua Torres, Carthage, Little Davie, Lucky Don, and Marie districts. It is estimated that approximately $70,000 worth of uranium (U) and vanadium (V) was produced from Rio Grande rift (RGR) copper-silver (± uranium) vein deposits (McLemore, 2017). Additional mineral deposits in the Socorro district include sandstone uranium, volcanogenic uranium, RGR barite-fluorite-galena (± silver, copper), sedimentary copper (Cu), and gypsum.

Mining History and Production

The Lucky Don and Little Davie mines were discovered in the early 1950s by E.R. Caprio. In July 1955, Holly Uranium Corporation filed an application for certification of the Lucky Don Group with the U.S. Atomic Energy Commission. Certification from the U.S. Atomic Energy Commission (AEC) was required to obtain federal grants for development of the mines. A second application from the company was filed in November 1955, covering the Little Davie mine. Also known as the Bonanza mine, the Lucky Don mine was active during 1955–1956, 1960, and 1962–1963 (Hilpert, 1969; Anderson, 1981).

Uranium in the Lucky Don and Little Davie mines is hosted by limestone of the Permian San Andres Formation. At Lucky Don, an adit was originally driven into the San Andres Formation for about 30–40 ft; the mine was later blasted after the ore ran out. Today, the mine consists of a cut face approximately 170 ft long, four short adits cut in the quarry face, a wooden loading bin, and three waste-rock piles with a volume of approximately 32,000 ft^3. Blasted ore was sorted by hand and trammed to a 15- to 20-short-ton ore chute on the side of the hill (Fig. 84). Total production from the Lucky Don mine by the McKedy Mines and Exploration Company amounted to 847 short tons of ore yielding 4,035 lbs U_3O_8 and 3,309 lbs V_2O_5 (Table 5).

The Little Davie mine includes a 6-ft-deep pit, a face cut (Fig. 85), and a waste-rock pile. Ore from Little Davie was loaded into a pickup and hauled to the ore chute at Lucky Don. Equipment used in mining included a compressor (125 ft^3/min),

jackhammer, wheelbarrows, and picks and shovels. Total production from the Little Davie mine amounted to 17 short tons yielding 60 lbs U_3O_8 and 71 lbs V_2O_5 (Table 6).

The Agua Torres (Fig. 86) and Marie (Fig. 87) mines are north of the Lucky Don–Little Davies mines within the Sevilleta National Wildlife Refuge, along a north-trending, rift-related normal fault juxtaposing Permian Abo Formation against Pennsylvanian Atrasado Formation (Fig. 83). Production from the Agua Torres mine amounted to 149 short tons of ore yielding 325 lbs U_3O_8 and 315 lbs V_2O_5 (Table 7). Production from the Marie mine amounted to 43 short tons of ore yielding 129 lbs U_3O_8 and 88 lbs V_2O_5 (Table 8). Both mines consist of several pits and open cuts. Other smaller prospects are found along the fault between the Agua Torres and Marie mines (Fig. 83, Appendix 3).

Table 5. Production from the Lucky Don mine (from U.S. Department of Energy files).

Year	Shipper	Short tons	U_3O_8 (%)	V_2O_5 (%)
1955	McKedy Mining and Exploration Co.	48.39	0.34	0.32
1956	Holly Uranium Corp.			
1956	Umino Co.	46		
1956	Three Bear Mining			
1960	McKedy Mining and Exploration Co.	27	0.16	
1962	R.H. Lummus	50	0.50(?)	
1963	R.H. Lummus	20		
Total		**964.94**	**0.23**	**0.43**

Table 6. Production from the Little Davie mine (from U.S. Department of Energy files).

Year	Shipper	Short tons	U_3O_8 (%)	V_2O_5 (%)
1955	McKedy Mining and Exploration Co.	17	0.18	0.21
Total		**17**	**0.18**	**0.21**

Table 7. Production from the Agua Torres mine (from U.S. Department of Energy files).

Year	Shipper	Short tons	U_3O_8 (%)	V_2O_5 (%)
1955	Campbell Farming Corp.	118	0.11	0.10
1956	Campbell Farming Corp.	31	0.10	0.14
Total		**149**	**0.11**	**0.11**

Table 8. Production from the Marie mine (from U.S. Department of Energy files).

Year	Shipper	Short tons	U_3O_8 (%)	V_2O_5 (%)
1956	Campbell Farming Corp.	46	0.14	0.10
Total		**46**	**0.14**	**0.10**

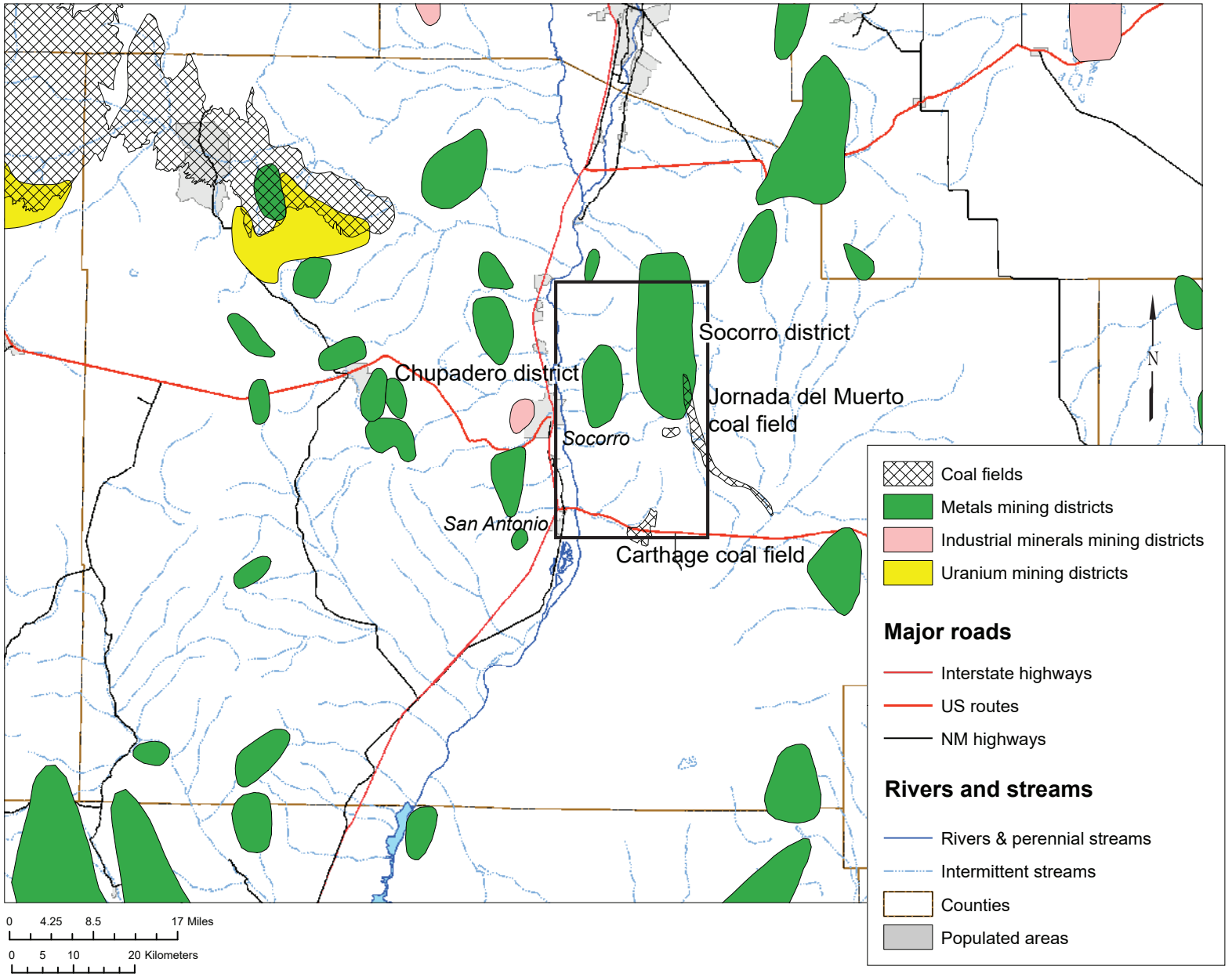

Figure 82. Mining districts of central New Mexico with locations of Socorro and Chupadero mining districts and Carthage and Jornada del Muerto coal fields. The black box is the location of the Quebradas region (Plate 1).

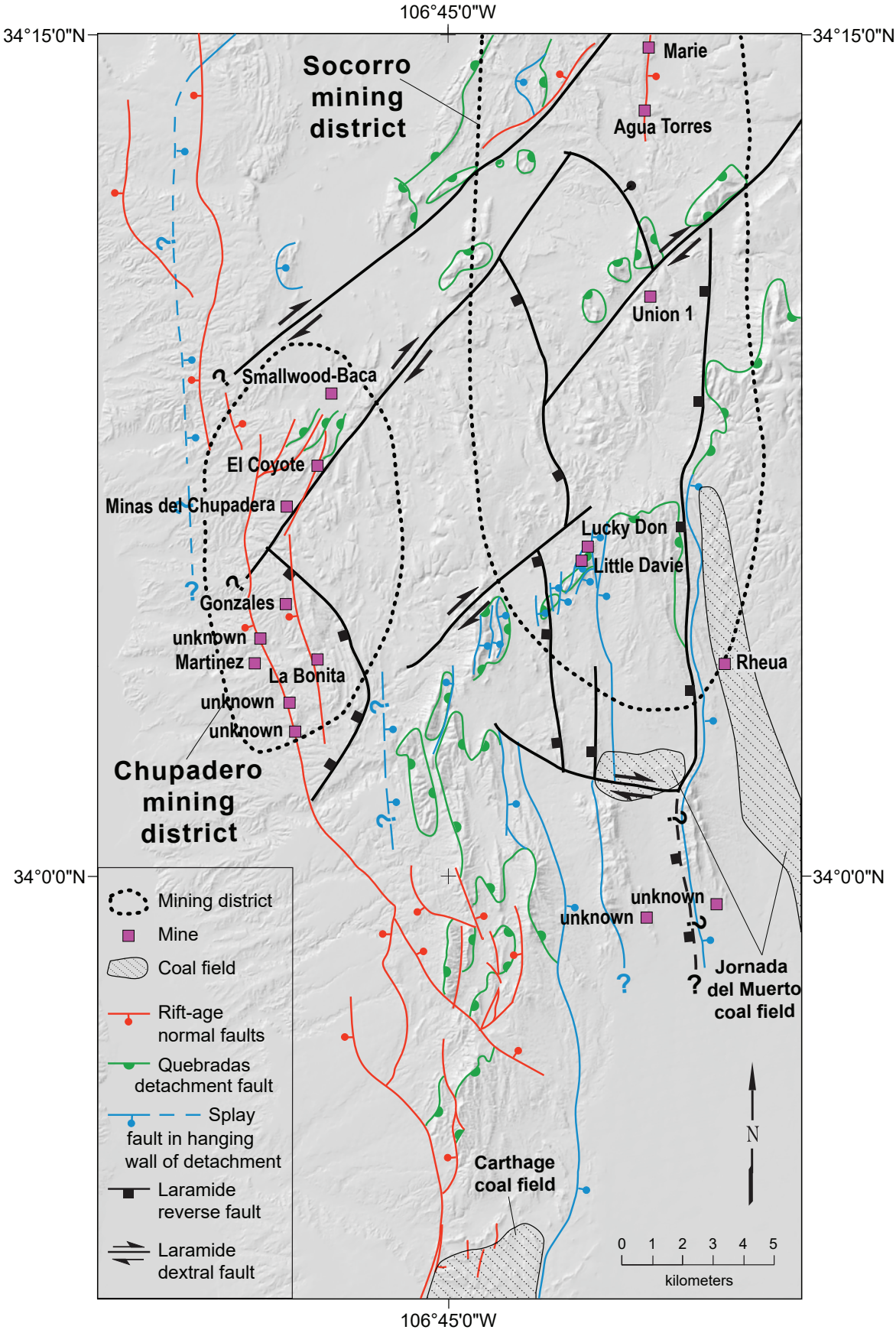

Figure 83. Digital elevation map of the Quebradas region showing mining districts, coal fields, mines, and simplified structures from Figure 70. Information on individual mines is provided in Appendix 2.

Figure 84. Ore bin at the Lucky Don mine. *Photo by V.T. McLemore, 3/26/2016*

Figure 85. Short adit at the Little Davie mine. *Photo by John Asafo-Akowuah, 8/9/2016*

Figure 86. Agua Torres pit, looking south. *Photo by V.T. McLemore, 6/15/2017*

Figure 87. Marie mine, looking west. *Photo by V.T. McLemore, 6/15/2017*

Rio Grande Rift Copper-Silver (± Uranium) Vein Deposits

Rio Grande rift (RGR) copper-silver (± uranium) vein deposits (McLemore, 1999; McLemore and Chenoweth, 2017; McLemore and Lueth, 2017) are found in the Socorro district. These formed near the surface along late Paleogene to Neogene faults in basins of the Rio Grande rift. Uranium and vanadium, with trace amounts of copper, are found along the footwalls of the north- or northeast-trending faults in two major areas in the Socorro district: the Lucky Don–Little Davie and Agua Torres–Marie areas. These deposits are similar to the Jeter mine in the Ladron Mountains, where 58,562 lbs of U_3O_8 and 3,202 lbs of V_2O_5, worth approximately $500,000, were produced (McLemore, 1983a, 1983b). These deposits also are similar to the La Bajada mine near Santa Fe, where 27,111 lbs of U_3O_8, 5,345 lbs of copper, and some silver and vanadium, worth approximately $310,000, were produced (McLemore, 1999, 2017).

Secondary uranium and copper minerals (tyuyamunite, carnotite, uraninite, malachite, azurite, and uranophane) are found in small tabular deposits along a northeast-trending, brecciated fault zone in silicified and recrystallized limestones of the Los Vallos Formation of the Permian Yeso Group and the San Andres Formation at the Lucky Don and Little Davie mines. The Lucky Don deposit was approximately 50 ft wide, 35 ft long, and 300–400 ft thick; the Little Davie deposit was smaller. Production grades (i.e., concentration of valuable commodity) amounted from 0.16% to 0.3% U_3O_8 (Tables 5 and 6). Selected samples were assayed at 0.38% and 1.4% U_3O_8 (McLemore, 1983a). Composite dump samples contained 126.5 ppm U and 160.5 ppm U at Lucky Don and Little Davie, respectively (Appendix 2). The Lucky Don sample also was high (241 ppm) in arsenic (As; Appendix 2).

Similar small deposits are found at the Agua Torres and Marie mines in Pennsylvanian limestone along another north-trending fault separating the Atrasado Formation from the Abo Formation. Carnotite and tyuyamunite form thin fracture coatings and disseminations within limestone (Fig. 88). Ore shipments as high as 0.23% U_3O_8 were reported from these mines (New Mexico Bureau of Geology and Mineral Resources [NMBGMR] files). Pierson et al. (1982) reported 125–148 ppm U from these two deposits. Composite dump and select samples from the two mines ranged from 240 to >1,000 ppm U, 122 to 1,280 ppm V, and 14.3 to >250 ppm As (Appendix 2). The adjacent Abo sandstone does not contain uranium mineralization. A National Uranium Resource Evaluation (NURE) water sample from a well near Agua Torres contained 42.37 ppb U (Planner et al., 1981), indicating anomalously high uranium is present in waters along the Bustos fault, perhaps further indicating additional uranium deposits in the subsurface.

Several other small prospects were developed looking for additional deposits (Fig. 83, Appendix 3), but only small amounts of uranium minerals were found. A NURE water sample from a well south of the Rheua prospect contained 118.99 ppb U (Planner et al., 1981), indicating anomalously high uranium present in waters along this fault and perhaps indicating additional uranium deposits in the subsurface.

Rio Grande rift copper-silver (± uranium) vein deposits were probably formed by low-temperature mineralizing waters, possibly a result of dewatering of rift basins. If this origin is correct, these deposits may be similar in origin to the RGR barite-fluorite-galena deposits (McLemore et al., 1998; Partey et al., 2009; McLemore and Lueth, 2017). Deposition occurred in open-space fillings in favorably reducing environments along the fault in the presence of organic material, similar to the formation of sandstone-uranium and sedimentary-copper deposits.

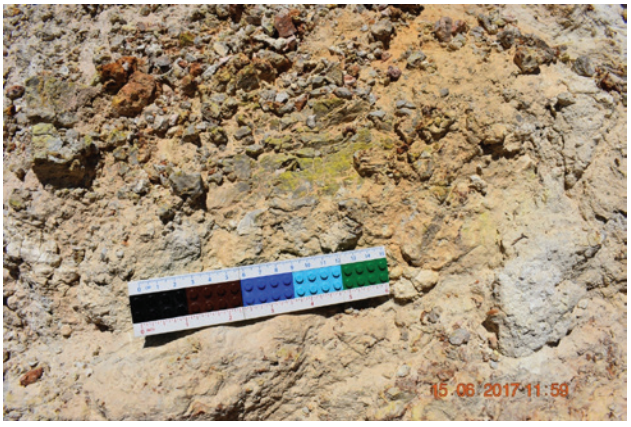

Figure 88. Mineralized (carnotite, tyuyamunite) and altered limestone at the Marie mine. *Photo by V.T. McLemore, 6/15/2017*

Sandstone-Uranium and Volcanogenic-Uranium Deposits

Small, uneconomic sandstone-uranium deposits are found in sandstone and shale of the Triassic Chinle Formation in the northern Socorro district (e.g., T.D. Campbell mine; Fig. 83). Small, uneconomic volcanogenic uranium deposits in rocks of the Oligocene Mogollon Group are found south of the Socorro district and east of the Jornada del Muerto coal field in the Blackington Hills (Fig. 83, Appendix 3). None of the deposits have economic potential.

Rio Grande Rift Barite-Fluorite-Galena (± Silver, Copper) Deposits

Rio Grande rift barite-fluorite-galena (± silver, copper) deposits are located in the eastern Socorro district (McLemore, 2017; McLemore and Lueth, 2017). These deposits are found within or near the Rio Grande rift in central New Mexico and are low-temperature, open-space fillings with little or no replacement; they are not associated with any magmatic activity and are similar to Mississippi Valley-type (MVT) deposits (McLemore et al., 1998; Partey et al., 2009; McLemore and Lueth, 2017). Rio Grande rift deposits are widespread in New Mexico and predominantly comprise barite, fluorite, and galena, although they can locally contain significant amounts of silver, copper, and zinc. Rio Grande rift deposits were formed by low-temperature basin brines migrating along fractures, faults, and unconformities during diagenesis or later compaction of sedimentary basins (Partey et al., 2009; McLemore and Lueth, 2017). In contrast to MVT deposits (Partey et al., 2009; Leach et al., 2010), however, RGR deposits in New Mexico formed along continental basins along the Rio Grande rift (Partey et al., 2009). Deposits in the Socorro district are small, with no future economic potential.

Stratabound Sedimentary-Copper Deposits

Stratabound (i.e., sedimentary-rock-hosted) sedimentary-copper deposits containing copper and silver (and locally lead, zinc, uranium, vanadium, and molybdenum) are found throughout New Mexico and are in Permian sandstone and shale in the Socorro district (Appendix 3; Lasky, 1932; McLemore and Lueth, 2017). These deposits were also called red-bed or sandstone-copper deposits by previous workers (Soulé, 1956; Phillips, 1960; Cox and Singer, 1986). The mineralized bodies typically are preserved as lenses or blankets of disseminated and/or fracture coatings of copper minerals, predominantly chalcopyrite, chalcocite, digenite, malachite, and azurite, with local uranium minerals, galena, sphalerite, and barite. Only small deposits are found in the Socorro district, however, and there is no future economic potential.

Gypsum Deposits

Gypsum is found throughout the Quebradas area in the Cañas Member of the Los Vallos Formation of the Yeso Group, and many prospect pits were dug on unpatented mining claims in the Socorro district (Appendix 3). Gypsum beds are generally thin (<10 ft thick), typically lens shaped, and discontinuous because of faulting. Gypsum is currently mined in the White Mesa district, Sandoval County, from the Jurassic Todilto Formation and used for cement, agriculture, plasters, and wallboard (McLemore and Austin, 2017). It is unlikely that gypsum in the Quebradas area will be mined in the near future because of small tonnage and the distance to wallboard factories in Albuquerque, New Mexico, and Juárez, Mexico.

Mineral Resource Potential of the Socorro District

Uranium-mineralized areas are sporadic and discontinuous along north- or northeast-trending faults. The uranium mines appear to be mined out. Some drilling occurred east and south of the Lucky Don mine without success (NMBGMR files). The presence of anomalously high uranium in two samples from water wells indicates uranium is present along some of these faults and the potential for additional similar, small uranium deposits is high. The potential for current economic development of any of these deposits is low, however, because of low tonnage and long distance to the only uranium mill operating in the United States at Blanding, Utah.

CHUPADERO MINING DISTRICT

The Chupadero mining district, as defined by File and Northrop (1966) and Mardirosian (1971), was first prospected during the late 1800s and has been known by several names, including Minas del Chupadero, Chupadera, De La Parida, Del La Parida, La Parida, Escondida, and Presilla mines. It is estimated that less

than $1,000 worth of copper and silver was produced from the district (McLemore, 2017), although additional fluorite, barite, and clay were mined, for a total estimated production from the district of about $2,000. Mineral deposits include sedimentary copper, RGR barite-fluorite-galena, and sedimentary clay (Fig. 83). Limestone and gypsum are abundant in the district but are uneconomic because of impurities, insufficient thickness, and faulting that offsets or otherwise disrupts the continuity of the deposit.

Mining History and Production

From 1959 to 1960, 2,000 short tons of copper and an unknown amount of silver were produced from Minas del Chupadera (McLemore, 2017). Gonzales P. Innebicher owned the property in 1942. Humphreys Gold Corporation of Denver, Colorado, acquired the property in 1943, and J.J. McPhaul of Magdalena, New Mexico, acquired the property in 1949 (Clippinger, 1946). Approximately 50 short tons of fluorite and some barite were produced from the Gonzales mine (Williams, 1966; McAnulty, 1978; McLemore et al., 1998). Barite was produced from several pits in the northeastern part of the district by Ranger Industries in the 1970s and early 1980s, but the total amount is unknown.

Clay (mostly kaolinite) was produced from the Buster and Houlette mines, south and west of the Gonzales fluorite mine (Lasky and Wootton, 1933; Talmage and Wootton, 1937), and the clay was used as flux in the Billings (Rio Grande Smelting Works, 1883–1894) and Graphic (1885–1888) smelters in Socorro. Probably fewer than 1,000 short tons were produced, estimated from the size of the pit. Fire bricks also were made from the Buster clay (Talmage and Wootton, 1937). The clay was hauled by wagons across the Rio Grande to Socorro.

Stratabound Sedimentary-Copper Deposits

Stratabound sedimentary-copper deposits containing copper and silver (and local lead, zinc, uranium, vanadium, and molybdenum) are present throughout New Mexico and are found in Permian and Pennsylvanian sandstone and shale in the Chupadero district (Lasky, 1932; McLemore and Lueth, 2017). The largest deposits in the Socorro area are at the Minas del Chupadera mine (Fig. 89), where approximately 2,000 short tons of ore (grading 2% Cu) were mined during 1958–1960 from the North and South pits (Jaworski, 1973). The sedimentary-copper deposits are in sandstone and siltstone of the upper Moya Member of the Atrasado Formation. Malachite and azurite are predominant copper minerals, with minor amounts of tenorite, cuprite, delafossite, and chrysocolla (Figs. 90 and 91). Copper minerals are found as interstitial cement, fracture fillings, and coatings, concretions, and replacements of organic plant material. Calcite and iron oxides are common. A leaching operation was attempted during the 1960s but was unsuccessful (Fig. 92; Jaworski, 1973).

Small occurrences of copper oxides and chalcocite are found in small, scattered stratabound sedimentary-copper deposits in the Permian Abo and Bursum Formations in the northern area of the Chupadero district. The copper-rich zones rarely exceed 1–2 ft in thickness and typically are less than 50 ft long. These deposits are small and have no future economic potential.

Igneous and Metamorphic Rocks with Disseminated Uranium Deposits

The Rocky Mountain Energy Company found uranium and rare earth elements (REE) along fractures and joints in weathered and altered Tajo granite of Proterozoic age, which they called the Arroyo project (Appendices 2 and 3; McLemore, 1983a, 1983b). Six outliers of medium- to coarse-grained granite (formerly termed quartz monzonite) are exposed along north-trending faults in the Quebradas area, and most contain radioactive zones (McLemore, 1983b). The Tajo granite contains metamorphic xenoliths in exposures in sec. 11 and 12, T. 3 S., R. 1 E. (Fig. 93). Pegmatite and aplite dikes are rare. Purple fluorite, hematitization, and silicification are associated with northwest- to northeast-trending, uranium-rich, radioactive fracture zones in the granite (McLemore, 1983b). One sample reportedly contained 4,350 ppm U (Krason et al., 1982). Samples collected for this project contained as much as 262 ppm U and 282 total REE (Appendix 2). Rio Grande rift barite-fluorite-galena veins are found along fault contacts of the exposures (see below).

The chemical composition of the mineralized Tajo granite is unusual for Precambrian granites in New Mexico (McLemore, 1983b). The Tajo granite is grossly similar in major-element chemistry to high-silica (Si) and high-potassium (K) granites in the state (Condie and Budding, 1979).

Figure 89. Adit at Minas del Chupadera, with ore stockpiles in the foreground, looking northeast.
Photo by V.T. McLemore, 1/24/2016

Figure 90. Malachite and delafossite within sandstones at the adit of Minas del Chupadera.
Photo by V.T. McLemore, 1/24/2016

Figure 91. Chryscolla along bedding planes and disseminated within sandstone at the North Pit, Minas del Chupadera. *Photo by V.T. McLemore, 1/24/2016*

Figure 92. Leach tanks at Minas del Chupadera, looking east. *Photo by V.T. McLemore, 1/24/2016*

Figure 93. Fractured and altered Tajo granite.
Photo by V.T. McLemore, 12/26/2016

Tajo granite is enriched in rubidium (Rb), U, and thorium (Th) and depleted in CaO, Na_2O, Al_2O_3, and strontium (Sr) relative to most Precambrian granites (Condie and Budding, 1979; McLemore, 1983b). This is due in part to silicification and hematitization related to the uranium mineralization. The chemical trends in the Tajo granite, however, differ from chemical trends observed in other altered Precambrian granites in New Mexico. Most Precambrian granites in New Mexico that are altered by albitization and epidotization are enriched in Na_2O, CaO, and Fe_2O_3 and depleted in K_2O, Rb, Sr, TiO_2, and Al_2O_3 relative to unaltered granites (Condie and Budding, 1979).

The uranium and REE potential of the Tajo granite is uncertain. The subsurface extent of the Tajo granite within the highly faulted Rio Grande graben is unknown. The Tajo granite exhibits the mineralogy and chemistry typical of uraniferous granites that also contain high REE compared to most granites (Mathews, 1978). Thus, the Tajo granite could provide a local source for uranium and could host a significant U-Th-REE deposit at depth. The U-Th-REE deposits in Tajo granite may be similar to the Bokan Mountain U-Th-REE deposits of Alaska that contain significant structurally controlled U, Th, and REE (MacKevett, 1963; Thompson, 1988; Long et al., 2010). The Ross Adams mine produced approximately 100,000 short tons of approximately 1% U_3O_8 from uranium deposits in the Bokan Mountain granite between 1957 and 1971. The Bokan Mountain deposit is classified as an intrusive uranium deposit (International Atomic Energy Agency, 2009).

More than 200 uranium occurrences are found in igneous and metamorphic rocks (pegmatites, alkaline rocks, granitic rocks, carbonatites, and caldera-related volcanogenic deposits) in New Mexico, including the Tajo granite, but most in New Mexico are probably uneconomic (McLemore, 1983a; McLemore and Chenoweth, 2017). Additional study, and ultimately drilling, are needed to determine the economic potential of the U-Th-REE deposits in the Tajo granite.

Rio Grande Rift Barite-Fluorite-Galena (± Silver, Copper) Deposits

Rio Grande rift barite-fluorite-galena (± silver, copper) deposits also are present in the Chupadero district (McLemore and Lueth, 2017). Fluorite and barite are found along a brecciated fault zone between Proterozoic Tajo granite and sandstone and siltstone of the Sandia Formation at the Gonzales and La Bonita mines (Lasky, 1932; Rothrock et al., 1946; Williams, 1966; McLemore et al., 1998; Partey et al., 2009). The mineralized zone, consisting of two veins, is approximately 500 ft long, 1–5 ft wide, and trends 335°–345°, dipping 74°–90°W along the Tajo structural zone. Quartz and trace pyrite and galena are also found. Two adits and several prospect pits and shallow shafts developed the mineralized zone (Gonzales and La Bonita mines). The Martinez mine southwest of the Gonzales mine is along another fault between the Proterozoic granite and Sandia Formation sandstone and siltstone (Fig. 83).

Rio Grande rift deposits mostly containing barite, with little fluorite and galena, are found in the northeastern part of the Chupadero district and were mined by Ranger Industries in the 1970s and early 1980s. Ore was processed at the Ranger Industries mill in Escondida, New Mexico. Barite formed as lenses and veins along faults in San Andres limestone, and the mineralized zone is as much as 9 ft thick.

Fluorite at the Gonzales mine ranged in temperature of homogenization from 143° to 189°C, and the fluids contained 1.1–8.1 eq.wt.% NaCl (Hill, 1994). The deposit may be as young as 8 Ma according to apatite fission-track cooling dates of the granitic host rock (Kelley et al., 1992).

Using chlorine isotopes as a proxy for fluorine, Partey et al. (2009) indicated a potential magmatic source for some of the fluorine at the Hansonburg district. Stable isotope analysis of waters involved in mineralization (i.e., both fluid inclusion and waters calculated to be in equilibrium with various minerals) indicated they are predominantly of meteoric origin, having accumulated in local sedimentary basins, possibly of varying age, and having subsequently been heated by high heat flow, magmatic activity, basinal-sediment compaction, or radiogenetic heat from Precambrian plutons (McLemore et al., 1998; Partey et al., 2009; McLemore and Lueth, 2017). Warm, convecting waters leached barium, sulfate, silver, and other ions from source rocks such as arkosic sediment, evaporite, Precambrian rock, and mineral deposits. In central New Mexico, these basins were continental instead of marine, as in the classic Mississippi Valley area; thus, faults and continental brines were important in forming RGR deposits. Precipitation occurred as fluids cooled, pressure decreased, and/or the mineralized hydrothermal fluids mixed with subsurface brines or meteoric water.

Gypsum

Gypsum is found throughout the Quebradas area in the Cañas Member of the Los Vallos Formation of the Yeso Group, and many prospect pits were dug on unpatented mining claims, including the Chupadero district (Appendix 3). Gypsum beds are generally thin (<10 ft thick) and typically lens shaped but discontinuous because of faulting. Samples collected in the Sierra de las Cañas Wilderness Study Area contained 97–99% $CaSO_4 \cdot H_2O$ (Moore et al., 1988), where an estimated 50,000 short tons of gypsum suitable for cement, agriculture, plaster, and manufacture of wallboard were estimated to occur (Korzeb, 1986). Gypsum currently is mined in the White Mesa district, Sandoval County, from the Todilto Formation (McLemore and Austin, 2017). It is unlikely that gypsum in the Quebradas area will be mined in the near future because of small tonnage and long distances to wallboard factories in Albuquerque and Juárez.

Limestone

Limestone is abundant in the Quebradas area in the Permian Madera Group, Yeso Group, and San Andres Formation. Limestone is used in cement, as an aggregate in concrete and asphalt, in crushed stone, and in many other products (McLemore and Austin, 2017). Limestone was quarried at Fraley, near Carthage (see below). Economic potential for limestone in the Quebradas area is low, however, because of long distances to potential markets and the abundance of other limestone throughout New Mexico (McLemore and Austin, 2017).

Fire Clay

Clay from the Buster and Houlette mines was mined from a 1- to 2-ft-thick, faulted shale within the Madera Group. Shale consists of kaolinite, minor illite, quartz, and minor gypsum and iron oxides. Locally, the clay is classified as a fire clay and is suitable for manufacturing bricks. The economic potential is low, however, because there is no clay industry in the Socorro area.

Mineral Resource Potential of the Chupadero District

Although several commodities were produced from the Chupadero district in the past, none except perhaps the Arroyo prospect in the Tajo granite have any future economic potential because of small tonnage, low grade, and distance to existing markets. Additional study and drilling are needed to determine the economic potential of the U-Th-REE deposits in the Arroyo prospect in the Tajo granite.

JORNADA DEL MUERTO COAL FIELD

The western area of the small Jornada del Muerto coal field extends into the Quebradas area (Figs. 82 and 83), where coal beds as much as 4 ft thick are found in the Dilco Member of the Cretaceous Crevasse Canyon Formation (Tabet, 1979). The coal is a high-volatile C-bituminous coal with as much as 1.3–1.4% sulfur (S). Coal was produced from the Law mine prior to 1927, but production figures are unknown (Tabet, 1979). Most coal elsewhere in the district is uneconomic because it is too thin, faulted, steeply dipping (24°–45°), and overlain by thick overburden. Furthermore, mineral ownership of the area is mixed federal and private, and leasing of remaining coal would be difficult.

CARTHAGE AND SAN ANTONIO AREAS

Fraley Limestone Quarry

In the 1860s, Estanislao Montoya acquired the mineral ownership of limestone in the Carthage coal field when he acquired ownership of the coal. The limestone belongs to the Permian San Andres Formation. At that time, the area was part of the Old Socorro Land Grant (Eveleth and Harden, 2011). In 1882, James Fraley obtained ownership of the limestone quarry and planned for a large operation (Fig. 94). In 1883, Atchison, Topeka and Santa Fe (AT&SF) Railroad constructed a spur into Carthage, New Mexico, including a switch about 3 mi west of Carthage to access the limestone quarry and the town of Fraleyville or Fraley that grew around the quarry (Eveleth et al., 2009; Eveleth and Harden, 2011). The first kiln was in operation by March 1884. Fraley supplied lime to the Billings (1883–1894) and Graphic (1885–1888) smelters in Socorro, as well as to smelters throughout central and southwestern New Mexico. In 1897, limestone was quarried from the mine to supply rip-rap and ballast for the AT&SF Railroad west of Albuquerque. The railroad to Carthage was abandoned in 1897. In 1899, the validity of the Old Socorro Land Grant, under which Montoya obtained mineral ownership, was limited to lands settled and cultivated by February 2, 1848, which resulted in the return of Carthage and Fraley to federal government ownership.

Total production is unknown, but Fraley shipped 13,497 short tons of limestone in 1887 and 13,000 short tons in 1888. In addition, a large amount of lime was shipped to Socorro and elsewhere in central and southern New Mexico for use in construction and as a flux in the smelters.

Figure 94. Fraley limestone quarry, looking north. *Photo by V.T. McLemore, 4/8/2017*

Miscellaneous Mills and Deposits

A small roofing tile plant operated in San Antonio, New Mexico, prior to 1937 (Lasky and Wootton, 1933; Talmage and Wootton, 1937). Local Quaternary adobe clay was used in a single kiln operated by two to three men to make adobe. The tiles were shaped using a wooden mold. Although clay shipped from Carthage was sporadically used to make bricks and tiles at the plant, there are no production records. Tile manufactured at this plant was used on the Socorro City Hall in 1933 (Lasky and Wootton, 1933).

Two separate barite mills operated in San Antonio, mostly processing ore from the Hansonburg district (Fig. 95). Production records are not available.

A small deposit of water-laid pumice near Bosquecito, New Mexico, was mined and sold for use as scouring powder or sawed blocks for polishing (see Quaternary section of Chapter 4; Ellis, 1929; Talmage and Wootton, 1937). Settlers collected pumice for use in coking ovens in San Antonio before 1915. The pumice also was used to manufacture cinder blocks (Clippinger, 1946). The deposit was originally thought to be tripoli or diatomite (Herrick, 1896), which are also used as abrasives, but subsequent studies correctly identified it as pumice (Talmage and Wootton, 1937). A mining permit was issued to a company in 2006, but no production occurred.

SUMMARY

Although coal, uranium, vanadium, clay, fluorite, barite, copper, silver, pumice, and limestone have been produced in the Quebradas area, it is unlikely that any mineral production will occur in the near future because of small tonnage, low grades, and long distances to existing mills and processing plants. Additional studies and ultimately drilling are needed to determine the economic potential of the U-Th-REE deposits in the Tajo granite.

Figure 95. San Antonio barite mill, circa 1960. *NMBGMR Photo and Document Archive, Resource ID 1430*

Ruins of the superintendent's house at the abandoned coal mining town at Carthage. *Photo by Martha Cather*

CHAPTER 7: THE CARTHAGE COAL FIELD

Gretchen K. Hoffman

INTRODUCTION

The Carthage coal field is located about 15 mi southeast of Socorro and about 10 mi east of San Antonio, just south of U.S. Route 380. The Carthage field encompasses about 10 mi^2 on the eastern flank of the Rio Grande rift and comprises a series of small fault blocks. The area contains two Upper Cretaceous coal-bearing units. The Carthage Member of the Tres Hermanos Formation has multiple coal seams that rarely exceed 2 ft in thickness (Osburn, 1983), and the Crevasse Canyon Formation has two coal seams ranging in thickness from 4 to 7 ft (Figs. 34A and 34B). Most coal production was from coal seams in the latter. The lower coal bed of the Crevasse Canyon, the Carthage seam, was the main source of coal extracted in the Carthage field beginning in the 1860s (Fig. 46). This is excellent coking coal and relatively high in Btu value (12,531 Btu/lb; Hoffman, 1996). The quality of the coal and proximity of the Carthage field to smelters in the southwestern United States created the first surge of coal mining activity in the 1880s. Carthage experienced multiple pulses of coal development until 1963. Over 2 million short tons of coal were produced from the Carthage area mines from 1882 to 1963 (Mine Inspector for the Territory of New Mexico, 1894–1911; State Inspector of Mines, 1912–1968). Most of the easily accessible coal has been removed from the field, and the faulted and tilted structure of the area does not lend itself to large-scale mining practices.

FIRST SUSTAINED COAL MINING OPERATION IN NEW MEXICO

After New Mexico became a territory, the United States government built several forts along the Rio Grande valley to protect new settlements. Fort Craig was established in 1854 and Fort Selden in 1865. Blacksmiths at the forts needed coal, and Estanislao Montoya, a brigadier general with the New Mexico militia, met this need from a coal source on family land east of San Antonio, New Mexico. The coal mine opened in 1862 near the Government mine (Fig. 96) and was the first to operate on a sustained basis in the New Mexico Territory (Hereford, 2003). In 1872, Montoya became a sutler—a civilian who supplied provisions to soldiers—and he continued to supply coal to several forts, including Craig, Bayard, Stanton, and Selden, until 1877 (Haines, 1891).

RAILROAD EXPANSION— SAN PEDRO COAL AND COKE

Following the Civil War, the western United States saw significant expansion that included development of railroads, settlements, and industry. In 1877, the Santa Fe Railroad sent surveyors into the western territories looking for rail routes with nearby water and coal resources. As a result of these surveys, the Carthage coal area was one of the first developed by the Santa Fe Railroad. The proximity of the field to the main rail line running along the Rio Grande and the coking quality of the coal made Carthage coal marketable to smelters in New Mexico, Arizona, and old Mexico (Hereford, 2003).

Thomas Peter, a former director of the Santa Fe Railroad, and Estanislao Montoya formed a partnership with the Santa Fe Railroad and established the subsidiary San Pedro Coal and Coke in July 1881 (Hereford, 2003). Montoya and Peter received 45% of San Pedro Coal and Coke stock for the 6 mi^2 of land encompassing the Carthage coal area. Mining at the San Pedro mine (Carthage No. 1; Fig. 96) began in 1882 in a 4- to 4.5-ft-thick coal seam near the base of the Crevasse Canyon Formation, called the Carthage coal seam in literature (Gardner, 1910).

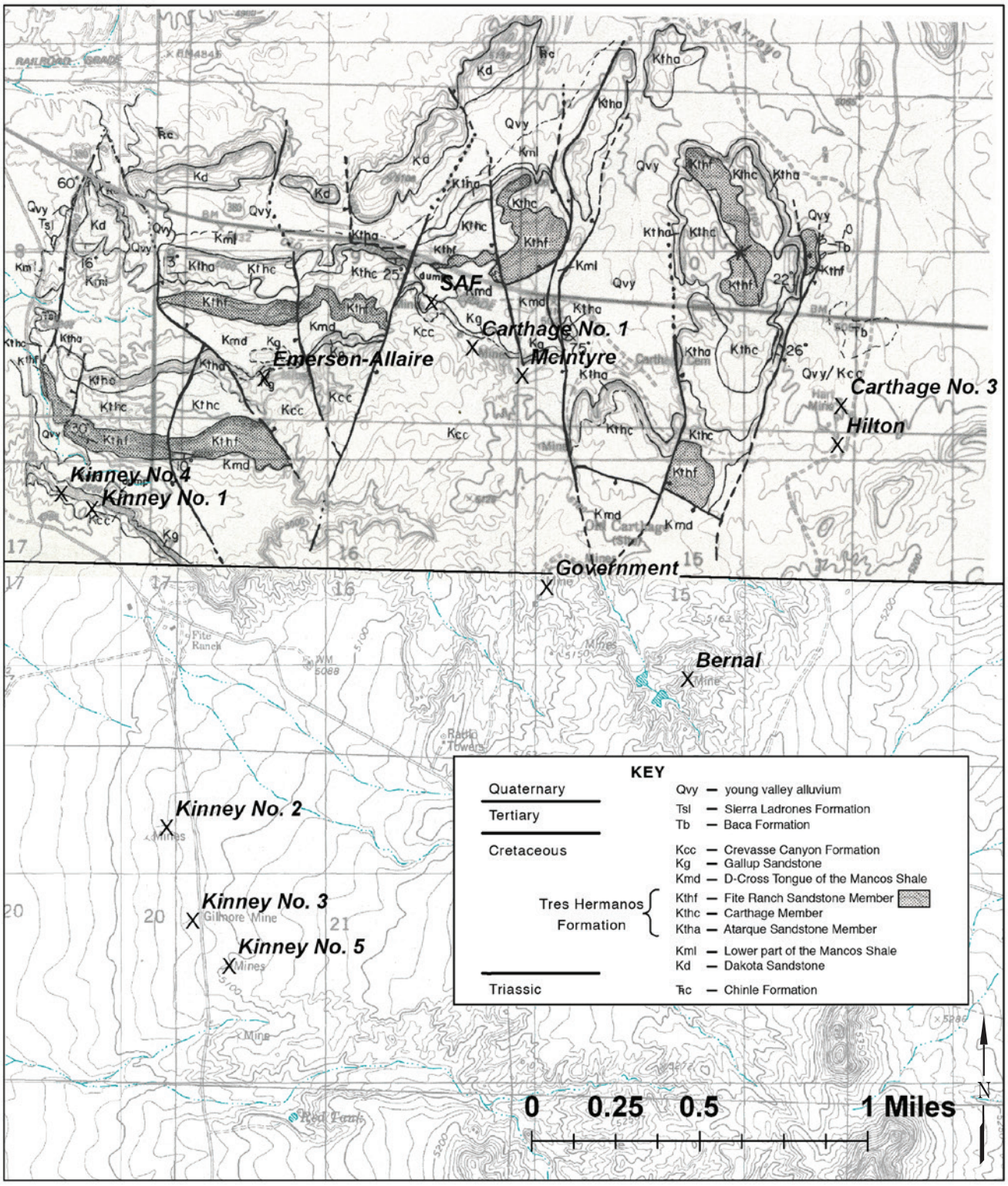

Figure 96. Geologic map and location of mines (shown by Xs) in the Carthage coal field. The north half of the figure (above line) is from Smith et al. (1983, fig. 1-60.55; geologic mapping by O.J. Anderson and J.C. Osburn). Note that this map differs in several details from Plate 1. Mine locations are from the 1904 map of the Carthage field, by Southern Fuel Co. in the New Mexico Bureau of Geology mine map archives (1550) and from locations in Nickelson (1979). Note Carthage No. 3 on the map has aliases: the Hart, Soto, or Baca mine.

The Santa Fe Railroad created another subsidiary in 1882, the New Mexican Railroad, and built a rail spur from the San Pedro Coal and Coke mines to the main rail line that was completed in May 1883 (Meade, 2001). With the rail spur in place, the San Pedro mines could economically transport coal to the main rail line at San Antonio.

San Pedro Coal and Coke built 12 coke ovens in San Antonio in 1882 to supply coke for smelting ores. Coke is a carbon byproduct produced by burning coal in an oxygen-deficient atmosphere. Carbon from coke is a reducing agent in the smelting process used to drive off impurities from the ore, leaving the pure metal behind. By 1884, there were 70 coke ovens in San Antonio supplying coke to smelters near Socorro and those in Arizona (Fig. 97). Coke from these mines also supplied the lime kilns at Fraley, New Mexico, just north of U.S. Route 380. Coke production only lasted for 9 years, from 1883 to 1891. Peak production in 1887 was more than 13,000 tons (Mineral Resources of the U.S., 1883, 1884, 1887). By 1893, 11 years after its first production, the San Pedro No. 1 mine closed (Mine Inspector for the Territory of New Mexico, 1894–1911), and the coke ovens were demolished. By August 1893, mine machinery and houses at Carthage were relocated to Cerrillos, a coal area south of Santa Fe, New Mexico, where the Santa Fe Railroad owned property. From 1885 through 1892, San Pedro Coal and Coke had yearly production rates of more than 50,000 short tons (Fig. 98; Mine Inspector for the Territory of New Mexico, 1894–1911). Closure of the San Pedro mines was partly due to the geologic conditions. Coal seams commonly pinch out due to the fluvial paleoenvironment. Fault offsets of seams complicated mining and led to reports that easily minable coal was depleted in the Carthage area. The mine inspector reported the mining of pillars in San Pedro mines (Mine Inspector for the Territory of New Mexico, 1894–1911), indicating that the operations were preparing for closure. It was assumed no more economic coal existed in the Carthage area (Gardner, 1910).

Figure 97. Coke ovens at San Antonio, New Mexico. Inscription on back of photo: "Mother's Day, Sunday, May 6th, 1888, was a rare down day for the San Pedro Coal & Coke Co ovens at San Antonio, New Mexico. Company officials, including superintendent Sullivan (center) and Walter Faddis (left), take advantage of the situation to show the ovens to their wives and Mrs. Smith (right). Faddis' two sons and the family dog were also along for the occasion." *NMBGMR Photo and Document Archive, Resource ID 1318, photo by Joseph E. Smith, courtesy of Avery Smith*

Economic conditions also played a role in closing the San Pedro mines. Major expansion occurred in the 1880s (Hereford, 2003), and companies became overextended, particularly the railroads. The Santa Fe Railroad went into receivership in December 1893. By December 1895, the railroad had reorganized as AT&SF Railroad. This new company acquired San Pedro Coal and Coke stock and dissolved the previous company in 1897 (Hereford, 2003). The rail spur from the main line to the mines was abandoned in February 1896, but trains continued to operate on the spur until March of 1897. As part of the abandonment agreement, tracks were removed, but the bridge over the Rio Grande was deeded to Socorro County (Socorro County Records, Quitclaim deed, v. 42, folio 377; Hereford, 2003). San Pedro Coal and Coke produced over 563,000 tons of coal during their 11 years of operation.

CARTHAGE COAL COMPANY

The next chapter of coal development in the Carthage field was begun in 1894 by the Carthage Coal Company, owned by Austin Goodall and Felipe Portigliatti. Their mine, originally called the Carthage mine, was 12 mi east of San Antonio and east of the San Pedro mines (Fig. 96). By 1903, the mine was known as the Hilton mine (Mine Inspector for the Territory of New Mexico, 1894–1911). Coal at the Hilton mine was 4.5 ft thick and probably in the Carthage seam of the Crevasse Canyon Formation.

Because land issues caused delays in validating the claim, the original owners sold the company in 1895–1896 to Giacoma Lovera and Mary Hilton, wife of local merchant August Hilton and mother of Conrad Hilton. Coal from the Hilton mine was transported by wagon 12 mi to San Antonio for shipment to Silver City, Socorro, and Belen, New Mexico, and El Paso, Texas. The primary market for this coal was as heating fuel for homes, with lesser amounts going to nearby smelters. The Carthage Coal Company operated two other mines, the Government and Bernal mines (Fig. 96). The Government mine slope (inclined opening on the coal seam) was opened on a 5.75-ft seam, near the old U.S. Army mine (Hereford, 2003).

In 1904, August Hilton, now a partner in the Carthage Coal Company, considered rebuilding the rail spur. Hilton could not fund the expansion, so he approached investors. Hilton's business transactions, as well as deals by other investors wanting to secure the rights to the rail line, resulted in 2 years of litigation that idled the mines before a settlement was reached on the rights to build the rail spur and operate the coal mines (Hereford, 2003). In an effort to develop a competing coal source and receive rights to build the railroad, the Southern Fuel Company, owned by investors in Colorado, opened the McIntyre mine near the original Carthage coal mine. The McIntyre or Manilla mine, leased to John McIntyre for operation (Gardner, 1910), never reported any production, possibly because the steep dip (25°) of the seam hindered mining (Mine Inspector for the Territory of New Mexico, 1894–1911 [1906]; Hereford, 2003).

Eventually, the lawsuits were settled in early 1906, and Powell Stackhouse and Charles Eddy emerged from the negotiations as owners of the renamed Carthage Fuel Company and the New Mexico Midland Railroad. The mines resumed production in 1906. The New Mexico Midland branch was completed the same year, with new tipples built at the mines for loading the rail cars. Yearly production in 1906 was 11,067 tons and increased to 50,322 tons by 1907 (Fig. 98; Mine Inspector for the Territory of New Mexico, 1894–1911).

On December 31, 1907, an explosion in the Bernal mine killed 11 miners. Mines in the Carthage field were not gaseous, but the coal dust was highly flammable (Mine Inspector for the Territory of New Mexico, 1894–1911 [1907]). Blasting powder was used in the mines until this time to break coal. After 1909, however, the mine inspector reported that explosives were seldom used in the Carthage-area mines and most coal was removed by pick and shovel (Mine Inspector for the Territory of New Mexico, 1894–1911). Faulting in the Carthage field and well-developed cleats, from a naturally occurring fracture system formed during the processes that turn peat into coal, made the coal relatively easy to break and remove without blasting (Gardner, 1910).

In 1911, the Mexican Revolution curtailed the market for Carthage coal to Mexico, but coal continued to be shipped to the Santa Rita copper mines in southern New Mexico and to other towns in the southwestern United States. Three years later, Carthage Fuel supplied coal to a central power plant

that provided electricity to all their coal mines (State Inspector of Mines, 1912–1968 [1914]).

A fire began in the Government mine on February 22, 1918. The mine was sealed to contain and extinguish the fire. A safety team from the U.S. Bureau of Mines and the Dawson mine manager from near Raton, New Mexico, came to Carthage and determined the level of carbon monoxide in the mine was unsafe. The air was unsafe for mine entry until March, and the area where the fire occurred remained sealed until May 5, 1918 (State Inspector of Mines, 1912–1968 [1918]).

Coal seams in the Hilton and Bernal mines were mined out and closed by 1918. Finlay (1922) estimated 40 acres of coal had been extracted at each of the mines. The Government mine continued to operate until 1926, when all pillars were removed for the remaining easily accessible coal (State Inspector of Mines, 1912–1968 [1923, 1926]). From 1922 to 1924, the Carthage Fuel Company operated the Carthage No. 3 mine, north of the Hilton mine. All Carthage Fuel mines ceased operations after 1925. Total production from these mines for 31 years was more than 894,000 tons (Fig. 98).

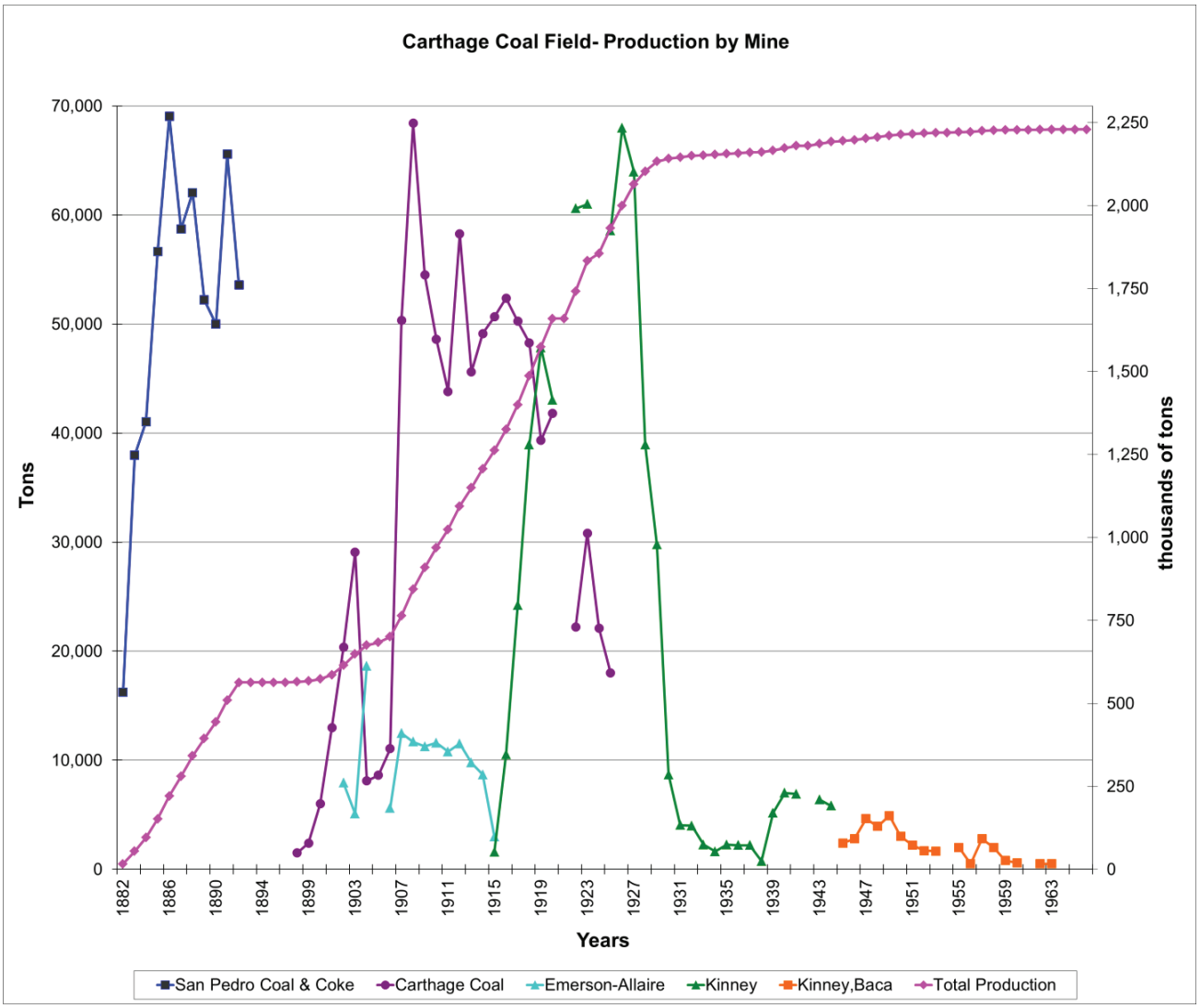

Figure 98. Carthage coal field production for individual mines (left scale) and total cumulative production (right scale). Data from Mine Inspector for the Territory of New Mexico (1894–1911) and State Inspector of Mines (1912–1968).

OTHER NOTABLE OPERATIONS

A few mines owned by other individuals and companies operated in the Carthage area and later southwest of Carthage at Tokay, New Mexico. The SAF mine, located northwest of the Carthage No. 1 mine, was started by the AT&SF Railroad in the 1890s (Fig. 96). Records from 1901–1902 show it was operated by the San Antonio Fuel Company with Robert Law as superintendent (Mine Inspector for the Territory of New Mexico, 1894–1911). The mine closed in 1907. The Emerson-Allaire mine began operating in 1902 (Fig. 96); the coal seam mined at this location was 6 ft thick with a 20° dip. In 1904, the main slope was closed because of what the mine inspector called a squeeze. This phenomenon indicates floor or roof problems resulting from expansion of the floor rock, most likely consisting of shale, or settling of the roof. Supporting pillars may have been inadequate to support the roof, causing unsafe mining conditions. Two other slopes were opened at the Emerson-Allaire mine, one above the sandstone overlying the original slope. By 1908, a tram connected the Emerson-Allaire mine to the New Mexico Midland railroad. Operations closed in 1916, with total production from this mine of 128,036 tons (Fig. 98; Mine Inspector for the Territory of New Mexico, 1894–1911; State Inspector of Mines, 1912–1968).

The Kinney mine, operated by B.H. Kinney, opened in 1914 southwest of the Carthage Fuel Company mines (Fig. 96). The dip of the coal in this area was less than at the Carthage mines, only 6°—more favorable for mining coal. Production began in 1915, and by 1917 construction of a rail spur connected the Kinney mines to the New Mexico Midland Railroad. A water system was installed and tipple and chutes were constructed in 1917. By 1918, there were several dwellings for miners on the mesa above the Kinney mine, and a U.S. Postal Office was built, establishing the settlement of Tokay. Resistant beds in the Upper Cretaceous Gallup Sandstone hold up the mesa where Tokay is located. In 1925, the No. 2 mine slope opened on a 4- to 4.5-ft-thick coal seam. Production began in 1926, and by 1927, all production for the Kinney operations was from the No. 2 mine. Coal from this mine was shipped to El Paso for use as home heating fuel (State Inspector of Mines, 1912–1968).

Kinney opened three other mines, numbered Kinney 3–5. By the late 1920s, fuel oil and natural gas were replacing coal for home heating, particularly in El Paso, which had pipelines bringing oil and gas from other parts of Texas. These factors, along with the Great Depression, cut production at Kinney mines by over 50% from 1927 to 1929. In late 1930, J.E. Gilmore acquired the Kinney mine and sold coal in Albuquerque and Socorro. By August 1931, the New Mexico Midland Railroad ceased operating after monetary losses for several years. All coal from Carthage was transported by truck. The Gilmore mine ceased operations in 1937. Kinney repossessed the mine in 1939 and continued to operate the mine for another 10 years (State Inspector of Mines, 1912–1968 [1949]; Hereford, 2003).

In 1935, Jack Hart started the Hart mine, opening a new slope on the old Hilton mine property, and he continued mining until 1939. Ralph Soto obtained the mine in 1947 and operated it for 1 year as the Soto mine. The property was sold to A.B. Baca in 1948, who operated the mine as the Carthage or Carthage No. 3 mine until 1968 (Fig. 96; State Inspector of Mines, 1912–1968 [1968]). The Carthage and Carthage No. 3 mine names cause confusion because both were associated with the Hilton mine location when the Carthage Coal Company first opened the mine. The Soto, Hart, and Carthage No. 3 operations mined the coal within the fault blocks north of the original Hilton mine (Nickelson, 1979, p. 64). They supplied coal locally, including to public schools in Socorro (F.E. Kottlowski, personal communication, 1993). From 1945 to 1963, total production from the Carthage mines was only 37,000 tons (State Inspector of Mines, 1912–1968).

There was some interest in the Carthage coal field in 1980 when Cactus Industries opened the Tres Hermanos mine. By 1981, however, development ceased at the property when the company realized the coal reserves were insufficient to supply the proposed market (Martinez, 1981). No production was reported for this mine.

From 1882 to 1963, 2.23 million short tons of coal were produced from the Carthage field (Fig. 98). The highest years of production for the Carthage field were 1886 (69,000 tons) at the San Pedro Coal mines, 1908 (>68,000 tons) by Carthage Coal, and 1926 (approximately 68,000 tons) at the Kinney mines. Almost all coal mined in the Carthage field was from the Crevasse Canyon Formation coal seams.

REFERENCES CITED

Allen, J.R.L., 1970, A quantitative model of grain size and sedimentary structures in lateral deposits: Geological Journal, v. 7, no. 1, p. 129–146. https://doi.org/10.1002/gj.3350070108

Allen, B.D., Love, D.W., and McCraw, D.J., 2013a, Uppermost Pennsylvanian Bursum Formation near Cibola Spring, Sevilleta National Wildlife Refuge, Socorro County, New Mexico, *in* Lucas, S.G., Nelson, J.W., DiMichele, W.A., Spielmann, J.A., Krainer, K., Barrick, J.E., Elrick, S., and Voigt, S., eds., The Carboniferous-Permian transition in central New Mexico: New Mexico Museum of Natural History and Science Bulletin 59, p. 233–238.

Allen, B.D., Love, D.W., McCraw, D.J., and Rinehart, A.J., 2013b, Geologic map of the Becker SW quadrangle, Socorro County, New Mexico: New Mexico Bureau of Geology and Mineral Resources Open-File Geologic Map 233, scale 1:24,000. https://doi.org/10.58799/OF-GM-233

Altares III, T., 1990, Stratigraphic description and paleoenvironments of the Bursum Formation, Socorro County, New Mexico [MS thesis]: Socorro, New Mexico Institute of Mining and Technology, 184 p.

Anderson, O.J., 1981, Abandoned or inactive uranium mines in New Mexico: New Mexico Bureau of Mines and Mineral Resources Open-File Report 148, 778 p. https://doi.org/10.58799/OFR-148

Anderson, O.J., 1987, Geology and coal resources of Atarque Lake 1:50,000 quadrangle, New Mexico: New Mexico Bureau of Mines and Mineral Resources Geologic Map 61, scale 1:50,000. https://doi.org/10.58799/GM-61

Anderson, O.J., and Osburn, J.C., 1983, Geologic map and cross section of Cretaceous rocks along and south of U.S. 380 in the vicinity of Carthage, New Mexico, *in* Chapin, C.E., and Callender, J.F., eds., Socorro Region II: New Mexico Geological Society Fall Field Conference Guidebook 34, p. 24. https://doi.org/10.56577/FFC-34

Arendt, W.W., 1971, The geology of the Joyita Hills, Socorro County, N.M. [MS thesis]: Albuquerque, University of New Mexico, 75 p.

Aubrey, W.M., 1991, Geologic framework of Cretaceous and Tertiary rocks in the Southern Ute Indian Reservation and adjacent areas in the northern San Juan Basin, southwestern Colorado, *in* Zech, R.S., ed., Geologic framework and stratigraphy of Cretaceous and Tertiary rocks of the Southern Ute Indian Reservation, southwestern Colorado: U.S. Geological Survey Professional Paper 1505-B, 24 p. https://doi.org/10.3133/pp1505BC

Aubrey, W.M., 1992, New interpretations of the stratigraphy and sedimentology of uppermost Jurassic to lowermost Upper Cretaceous strata in the San Juan Basin of northwestern New Mexico: U.S. Geological Survey Bulletin 1808-J, p. J1–J17.

Axen, G., Flores, S., Cather, S.M., and Green, M., 2012, Neogene decollment-style faulting in Permian Yeso Formation, Sierra Larga, Socorro County, New Mexico: Geological Society of America Abstracts with Programs, v. 44, p. 28.

Baars, D.L., 1962, Permian System of Colorado Plateau: American Association of Petroleum Geologists Bulletin, v. 46, no. 2, p. 149–218. https://doi.org/10.1306/BC74376F-16BE-11D7-8645000102C1865D

Bachman, G.O., 1953, Geology of a part of northwestern Mora County, New Mexico: U.S. Geological Survey Oil and Gas Investigations Map OM-137, scale 1:48,000. https://doi.org/10.3133/om137

Baker, B.W., 1981, Geology and depositional environments of Upper Cretaceous rocks, Sevilleta Grant, Socorro County, New Mexico [MS thesis]: Socorro, New Mexico Institute of Mining and Technology, 159 p.

Balch, R.S., 1997, Earthquake swarm studies in the central Rio Grande rift—Specific and general results [PhD dissertation]: Socorro, New Mexico Institute of Mining and Technology, 221 p.

Baldwin, B., and Muehlberger, W.R., 1959, Geologic studies of Union County, New Mexico: New Mexico Bureau of Mines and Mineral Resources Bulletin 63, 171 p. https://doi.org/10.58799/B-63

Barrick, J., Lucas, S.G., and Krainer, K., 2013, Conodonts of the Atrasado Formation (uppermost Middle to Upper Pennsylvanian), Cerros de Amado region, central New Mexico, USA, *in* Lucas, S.G., Nelson, J.W., DiMichele, W.A., Spielmann, J.A., Krainer, K., Barrick, J.E., Elrick, S., and Voigt, S., eds., The Carboniferous-Permian transition in central New Mexico: New Mexico Museum of Natural History and Science Bulletin 59, p. 239–252.

Bauch, J.H.A., 1982, Geology of the central area of the Loma de las Cañas quadrangle, Socorro County, New Mexico [MS thesis]: Socorro, New Mexico Institute of Mining and Technology, 116 p.

Beck, W.C., 1993, Structural evolution of the Joyita Hills, Socorro County, New Mexico [PhD dissertation]: Socorro, New Mexico Institute of Mining and Technology, 187 p.

Beck, W.C., and Chapin, C.E., 1994, Structural and tectonic evolution of the Joyita Hills, central New Mexico—Implications of basement control on Rio Grande rift, *in* Keller, G.R., and Cather, S.M., eds., Basins of the Rio Grande rift—Structure, stratigraphy, and tectonic setting: Geological Society of America Special Paper 291, p. 187–204. https://doi.org/10.1130/SPE291-p187

Behr, R.-A., 1999, Structure and thermochronologic constraints on the movement history of the Montosa fault, central New Mexico [MS thesis]: Socorro, New Mexico Institute of Mining and Technology, 129 p.

Blakey, R.C., and Gubitosa, R., 1983, Late Triassic paleogeography and depositional history of the Chinle Formation, southern Utah and northern Arizona, *in* Reynolds, M.W., and Dolly, E.D., eds., Mesozoic paleogeography of the west-central United States, Rocky Mountain Paleogeography Symposium 2, Denver, CO: Society of Economic Paleontologists and Mineralogists, Rocky Mountain Section, p. 57–76.

Borgia, A., Delaney, P.T., and Denlinger, R.P., 2000, Spreading volcanoes: Annual Review of Earth and Planetary Sciences, v. 28, p. 539–570. https://doi.org/10.1146/annurev.earth.28.1.539

Broadhead, R.F., and Jones, G., 2004, Oil, natural gas, and helium potential of the Chupadera Mesa area, Lincoln and Socorro Counties, New Mexico: New Mexico Bureau of Geology and Mineral Resources Open-File Report 478, 95 p. plus CD-ROM. https://doi.org/10.58799/OFR-478

Brose, R.J., Lucas, S.G., and Krainer, K., 2013, The Permian San Andres Formation in central and western New Mexico, *in* Lucas, S.G., Nelson, J.W., DiMichele, W.A., Spielmann, J.A., Krainer, K., Barrick, J.E., Elrick, S., and Voigt, S., eds., The Carboniferous-Permian transition in central New Mexico: New Mexico Museum of Natural History and Science Bulletin 59, p. 213–226.

Brown, K.B., 1987, Geology of the southern Cañoncita de la Uva area, Socorro County, New Mexico [MS thesis]: Socorro, New Mexico Institute of Mining and Technology, 89 p.

Bruning, J.E., 1973, Origin of the Popotsa Formation, north-central Socorro County, New Mexico [PhD dissertation]: Socorro, New Mexico Institute of Mining and Technology, 132 p.

Burollet, P.F., 1975, Tectonique en radeaux en Angola: Bulletin de la Société Géologique de France, v. S7-XVII, no. 4, p. 503–504. https://doi.org/10.2113/gssgfbull.S7-XVII.4.503

Cabezas, P., 1991, The southern Rocky Mountains in west-central New Mexico—Laramide structures and their impact on Rio Grande rift extension: New Mexico Geology, v. 13, no. 2, p. 25–37. https://doi.org/10.58799/NMG-v13n2.25

Cantrell, A.K., Suazo, T.L., Berman, D.S., Spielmann, J.A., Lucas, S.G., Henrici, A.C., and Rinehart, L.F., 2013, The Gallina Well locality, an early Permian (middle Wolfcampian) vertebrate fossil site in Socorro County, New Mexico, *in* Lucas, S.G., Nelson, J.W., DiMichele, W.A., Spielmann, J.A., Krainer, K., Barrick, J.E., Elrick, S., and Voigt, S., eds., The Carboniferous-Permian transition in central New Mexico: New Mexico Museum of Natural History and Science Bulletin 59, p. 253–264.

Cappa, J.A., 1975, The depositional environment, paleocurrents, provenance, and dispersal patterns of the Abo Formation in part of the Cerros de Amado area, Socorro County, New Mexico [MS thesis]: Socorro, New Mexico Institute of Mining and Technology, 153 p.

Cappa, J.A., and McMillan, J.R., 1983, Paleocurrent analysis of early Permian Abo Formation, Cerros de Amado area, Socorro County, New Mexico, *in* Chapin, C.E., and Callender, J.F., eds., Socorro Region II: New Mexico Geological Society Fall Field Conference Guidebook 34, p. 15–16. https://doi.org/10.56577/FFC-34

Cather, S.M., 1980, Petrology, diagenesis, and genetic stratigraphy of the Eocene Baca Formation, Alamo Navajo Reservation and vicinity, Socorro County, New Mexico [MA thesis]: Austin, University of Texas, 240 p. (also available as New Mexico Bureau of Mines and Mineral Resources Open-File Report 125, 262 p., 1 plate. https://doi.org/10.58799/OFR-125)

Cather, S.M., 1983, Laramide Sierra Uplift—Evidence for major pre-rift uplift in central and southern New Mexico, *in* Chapin, C.E., and Callender, J.F., eds., Socorro Region II: New Mexico Geological Society Fall Field Conference Guidebook 34, p. 99–101. https://doi.org/10.56577/FFC-34.99

Cather, S.M., 1986, Volcano-sedimentary evolution and tectonic implications of the Datil Group (latest Eocene–early Oligocene), west-central New Mexico [PhD dissertation]: Austin, University of Texas, 486 p.

Cather, S.M., 1990, Stress and volcanism in the northern Mogollon–Datil field, New Mexico—Effects of the post-Laramide tectonic transition: Geological Society of America Bulletin, v. 102, no. 11, p. 1447–1458. https://doi.org/10.1130/0016-7606(1990)102%3C1447:SAVITN%3E2.3.CO;2

Cather, S.M., 1992, Suggested revisions to the Tertiary tectonic history of north-central New Mexico, *in* Lucas, S.G., Kues, B.S., Williamson, T.E., and Hunt, A.P., eds., San Juan Basin IV: New Mexico Geological Society Fall Field Conference Guidebook 43, p. 109–122. https://doi.org/10.56577/FFC-43.109

Cather, S.M., 1997, Toward a hydrogeologic classification of map units in the Santa Fe Group, Rio Grande rift, New Mexico: New Mexico Geology, v. 19, no. 1, p. 15–21. https://doi.org/10.58799/NMG-v19n1.15

Cather, S.M., 1999, Implications of Jurassic, Cretaceous, and Proterozoic piercing lines for Laramide oblique-slip faulting in New Mexico and rotation of the Colorado Plateau: Geological Society of America Bulletin, v. 111, no. 6, p. 849–868. https://doi.org/10.1130/0016-7606(1999)111%3C0849:IOJCAP%3E2.3.CO;2

Cather, S.M., 2002 (revised 2016), Geologic map of the San Antonio 7.5-minute quadrangle, Socorro County, New Mexico: New Mexico Bureau of Geology and Mineral Resources Open-File Geologic Map 58, scale 1:24,000. https://doi.org/10.58799/OF-GM-58

Cather, S.M., 2003, Polyphase Laramide tectonics and sedimentation in the San Juan Basin, New Mexico, *in* Lucas, S.G., Semken, S.C., Berglof, W., and Ulmer-Scholle, D., eds., Geology of the Zuni Plateau: New Mexico Geological Society Fall Field Conference Guidebook 54, p. 119–132. https://doi.org/10.56577/FFC-54.119

Cather, S.M., 2004, The Laramide orogeny in central and northern New Mexico and southern Colorado, *in* Mack, G.H., and Giles, K.A., eds., The Geology of New Mexico—A geologic history: New Mexico Geological Society Special Publication 11, p. 203–248. https://doi.org/10.56577/SP-11

Cather, S.M., 2009a, Stratigraphy and structure of the Laramide Carthage–La Joya Basin, central New Mexico, *in* Lueth, V., Lucas, S.G., and Chamberlin, R.M., eds., Geology of the Chupadera Mesa: New Mexico Geological Society Fall Field Conference Guidebook 60, p. 227–234. https://doi.org/10.56577/FFC-60.227

Cather, S.M., 2009b, Tectonics of the Chupadera Mesa region, central New Mexico, *in* Lueth, V., Lucas, S.G., and Chamberlin, R.M., eds., Geology of the Chupadera Mesa: New Mexico Geological Society Fall Field Conference Guidebook 60, p. 127–137. https://doi.org/10.56577/FFC-60.127

Cather, S.M., 2009c, The Montosa fault, *in* Lueth, V., Lucas, S.G., and Chamberlin, R.M., eds., Geology of the Chupadera Mesa: New Mexico Geological Society Fall Field Conference Guidebook 60, p. 73–74. https://doi.org/10.56577/FFC-60

Cather, S.M., 2018, Revised basin geometry of the Bursum Formation (upper Virgilian–lower Wolfcampian), central New Mexico: New Mexico Geology, v. 40, no. 1, p. 6–16. https://doi.org/10.58799/NMG-v40n1.6

Cather, S.M., and Colpitts, Jr., R.M., 2005 (revised 2016), Geologic map of the Loma de las Cañas 7.5-minute quadrangle, Socorro County, New Mexico: New Mexico Bureau of Geology and Mineral Resources Open-File Geologic Map 110, scale 1:24,000. https://doi.org/10.58799/OF-GM-110

Cather, S.M., and Harrison, R.W., 2002, Lower Paleozoic isopach maps of southern New Mexico and their implications for Laramide and ancestral Rocky Mountain tectonism, *in* Lueth, V.W., Giles, K.A., Lucas, S.G., Kues, B.S., Myers, R., and Ulmer-Scholle, D.S., eds., Geology of White Sands: New Mexico Geological Society Fall Field Conference Guidebook 53, p. 85–101. https://doi.org/10.56577/FFC-53.85

Cather, S.M., and Johnson, B.D., 1984, Eocene tectonics and depositional setting of west-central New Mexico and eastern Arizona: New Mexico Bureau of Mines and Mineral Resources Circular 192, 33 p. https://doi.org/10.58799/C-192

Cather, S.M., and Johnson, B.D., 1986, Eocene depositional setting and tectonic framework of west-central New Mexico and eastern Arizona, *in* Peterson, J.A., ed., Paleotectonics and sedimentation in the Rocky Mountain region: American Association of Petroleum Geologists Memoir 41, p. 623–652.

Cather, S.M., and McIntosh, W.C., 2009, Flood deposits of lower Bandelier pumice and ash near Bosquecito, central New Mexico, *in* Lueth, V., Lucas, S.G., and Chamberlin, R.M., eds., Geology of the Chupadera Mesa: New Mexico Geological Society Fall Field Conference Guidebook 60, p. 44–45. https://doi.org/10.56577/FFC-60

Cather, S.M., McIntosh, W.C., and Chapin, C.E., 1987, Stratigraphy, age, and rates of deposition of the Datil Group (upper Eocene–lower Oligocene), west-central New Mexico: New Mexico Geology, v. 9, no. 3, p. 50–54. https://doi.org/10.58799/NMG-v9n3.50

Cather, S.M., Chamberlin, R.M., and Ratté, J.C., 1994a, Tertiary stratigraphy and nomenclature for western New Mexico and eastern Arizona, *in* Chamberlin, R.M., Kues, B.S., Cather, S.M., Barker, J.M., and McIntosh, W.C., eds., Mogollon Slope (west-central New Mexico and east-central Arizona): New Mexico Geological Society Fall Field Conference Guidebook 45, p. 259–266. https://doi.org/10.56577/FFC-45.259

Cather, S.M., Chamberlin, R.M., Chapin, C.E., and McIntosh, W.C., 1994b, Stratigraphic consequences of episodic extension in the Lemitar Mountains, central Rio Grande rift, *in* Keller, G.R., and Cather, S.M., eds., Basins of the Rio Grande rift—Structure, stratigraphy, and tectonic setting: Geological Society of America Special Paper 291, p. 157–170. https://doi.org/10.1130/SPE291-p157

Cather, S.M., Connell, S.D., Lucas, S.G., Picha, M.G., and Black, B.A., 2002, Geology of the Hagan 7.5-minute quadrangle, New Mexico: New Mexico Bureau of Geology and Mineral Resources Open-File Digital Geologic Map 50, scale 1:24,000. https://doi.org/10.58799/OF-GM-50

Cather, S.M., Colpitts, Jr., R.M., Hook, S.C., and Heizler, M.T., 2004 (revised 2016), Geologic map of the Mesa del Yeso 7.5-minute quadrangle, Socorro County, New Mexico: New Mexico Bureau of Geology and Mineral Resources Open-File Geologic Map 92, scale 1:24,000. https://doi.org/10.58799/OF-GM-92

Cather, S.M., Karlstrom, K.E., Timmons, J.M., and Heizler, M.T., 2006, Palinspastic reconstruction of Proterozoic basement-related aeromagnetic features in north-central New Mexico—Implications for Mesoproterozoic to Late Cenozoic tectonism: Geosphere, v. 2, p. 299–323. https://doi.org/10.1130/GES00045.1

Cather, S.M., Osburn, G.R. and Hook, S.C., 2007 (revised 2016), Geologic map of the Cañon Agua Buena 7.5-minute quadrangle, Socorro County, New Mexico: New Mexico Bureau of Geology and Mineral Resources Open-File Geologic Map 146, scale 1:24,000. https://doi.org/10.58799/OF-GM-146

Cather, S.M., Colpitts, Jr., R.M., Green, M., Axen, G.J., and Flores, S., 2012 (revised 2016), Geologic map of the Sierra de la Cruz 7.5-minute quadrangle, Socorro County, New Mexico: New Mexico Bureau of Geology and Mineral Resources Open-File Geologic Map 227, scale 1:24,000. https://doi.org/10.58799/OF-GM-227

Cather, S.M., Zeigler, K.E., Mack, G.H., and Kelley, S.A., 2013, Toward standardization of Phanerozoic stratigraphic nomenclature in New Mexico: Rocky Mountain Geology, v. 48, p. 101–124. https://doi.org/10.2113/gsrocky.48.2.101

Cather, S.M., Osburn, G.R., McIntosh, W.C., Heizler, M.T., Hook, S.C., Axen, G.J., Flores, S., and Green, M., 2014 (revised 2016), Geologic map of the Bustos Well 7.5-minute quadrangle, Socorro County, New Mexico: New Mexico Bureau of Geology and Mineral Resources Open-File Geologic Map 237, scale 1:24,000. https://doi.org/10.58799/OF-GM-237

Chamberlin, R.M., 1983, Cenozoic domino-style crustal extension in the Lemitar Mountains, New Mexico—A summary, *in* Chapin, C.E., and Callender, J.F., eds., Socorro Region II: New Mexico Geological Society Fall Field Conference Guidebook 34, p. 111–118. https://doi.org/10.56577/FFC-34.111

Chamberlin, R.M., and Harris, J.S., 1994, Upper Eocene and Oligocene volcaniclastic sedimentary stratigraphy of the Quemado–Escondido Mountain area, Catron County, New Mexico, *in* Chamberlin, R.M., Kues, B.S., Cather, S.M., Barker, J.M., and McIntosh, W.C., eds., Mogollon Slope (west-central New Mexico and east-central Arizona): New Mexico Geological Society Fall Field Conference Guidebook 45, p. 269–275. https://doi.org/10.56577/FFC-45.269

Chamberlin, R.M., Eggleston, T., and McIntosh, W.C., 2002, Geologic map of the Luis Lopez quadrangle, Socorro County, New Mexico: New Mexico Bureau of Geology and Mineral Resources Open-File Geologic Map 53, scale 1:24,000. https://doi.org/10.58799/OF-GM-53

Chamberlin, R.M., McIntosh W.C., and Eggleston T.L., 2004, $^{40}Ar/^{39}Ar$ geochronology and eruptive history of the eastern sector of the Oligocene Socorro caldera, central Rio Grande rift, New Mexico, *in* Cather, S.M., McIntosh, W.C., and Kelley, S.A., eds., Tectonics, geochronology, and volcanism in the Southern Rocky Mountains and Rio Grande rift: New Mexico Bureau of Geology and Mineral Resources Bulletin 160, p. 251–279. https://doi.org/10.58799/B-160

Chamberlin, R.M., McIntosh, W.C., Heizler, M.T., and Koning, D.J., 2022, A new constraint on the onset of Cenozoic crustal extension in the central Rio Grande rift near Socorro, New Mexico, *in* Koning, D.J., Hobbs, K.M., Phillips, F.M., Nelson, W.J., Cather, S.M., Jakle, A.C., and Van Der Werff, B., eds., Socorro Region III: New Mexico Geological Society Fall Field Conference Guidebook 72, p. 60–62. https://doi.org/10.56577/FFC-72

Chang, C., and Liu, L., 2021, Investigating the formation of the Cretaceous Western Interior Seaway using landscape evolution simulations: Geological Society of America Bulletin, v. 133, no. 1–2, p. 347–361. https://doi.org/10.1130/B35653.1

Chapin, C.E., 1989, Volcanism along the Socorro accommodation zone, Rio Grande rift, New Mexico, *in* Chapin, C.E., and Zidek, J., eds., Field excursions to volcanic terranes in the western United States, Volume 1—Southern Rocky Mountain region: New Mexico Bureau of Mines and Mineral Resources Memoir 46, p. 46–57. https://doi.org/10.58799/M-46

Chapin, C.E., and Cather, S.M., 1981, Eocene tectonics and sedimentation in the Colorado Plateau-Rocky Mountain area, *in* Dickinson, W.R., and Payne, W.D., eds., Relation of tectonics to ore deposits in the southern Cordillera: Arizona Geological Society Digest, v. 14, p. 173–198.

Chapin, C.E., and Cather, S.M., 1983, Eocene tectonics and sedimentation in the Colorado Plateau-Rocky Mountain area, *in* Lowell, J.D., ed., Rocky Mountain foreland basins and uplifts: Rocky Mountain Association of Geologists, p. 33–56.

Chapin, C.E., and Cather, S.M., 1994, Tectonic setting of the axial basins of the northern and central Rio Grande rift, *in* Keller, G.R., and Cather, S.M., eds., Basins of the Rio Grande rift—Structure, stratigraphy and tectonic setting: Geological Society of America Special Paper 291, p. 5–26. https://doi.org/10.1130/SPE291-p5

Chapin, C.E., Chamberlin, R.M., Osburn, G.R., White, D.L., and Sanford, A.R., 1978, Exploration framework of the Socorro geothermal area, New Mexico, *in* Chapin, C.E., and Elston, W.E., eds., Field guide to selected cauldrons and mining districts of the Datil-Mogollon volcanic field: New Mexico Geological Society Special Publication No. 7, p. 114–129. https://doi.org/10.56577/SP-7

Chapin, C.E., McIntosh, W.C., and Chamberlin, R.M., 2004a, The late Eocene–Oligocene peak of Cenozoic volcanism in southwestern New Mexico, *in* Mack, G.H., and Giles, K.A., eds., The Geology of New Mexico—A geologic history: New Mexico Geological Society Special Publication 11, p. 271–293. https://doi.org/10.56577/SP-11

Chapin, C.E., Wilks, M., and McIntosh, W.C., 2004b, Space-time patterns of Late Cretaceous to present magmatism in New Mexico—Comparison to Andean volcanism and potential for future volcanism, *in* Cather, S.M., McIntosh, W.C., and Kelley, S.A., eds., Tectonics, geochronology, and volcanism in the Southern Rocky Mountains and Rio Grande rift: New Mexico Bureau of Geology and Mineral Resources Bulletin 160, p. 13–40. https://doi.org/10.58799/B-160

Clippinger, D.M., 1946, Building blocks from natural lightweight materials of New Mexico: New Mexico Bureau of Mines and Mineral Resources Bulletin 24, 43 p. https://doi.org/10.58799/B-24

Cobban, W.A., 1961, The ammonite family Binneyitidae in the Western Interior of the United States: Journal of Paleontology, v. 35, no. 4, p. 737–758.

Cobban, W.A., 1977a, Characteristic marine molluscan fossils from the Dakota Sandstone and intertongued Mancos Shale, west-central New Mexico: U.S. Geological Survey Professional Paper 1009, 30 p. https://doi.org/10.3133/pp1009

Cobban, W.A., 1977b, Fossil mollusks of the Dakota Sandstone and intertongued Mancos Shale of west-central New Mexico, *in* Fassett, J.F., and James, H.L., eds., San Juan Basin III (northwestern New Mexico): New Mexico Geological Society Fall Field Conference Guidebook 28, p. 213–220. https://doi.org/10.56577/FFC-28.213

Cobban, W.A., 1986, Upper Cretaceous molluscan record from Lincoln County, New Mexico; Southwest section of AAPG transactions and guidebook of 1986 convention, Ruidoso, New Mexico: New Mexico Bureau of Mines and Mineral Resources, p. 77–89.

Cobban, W.A., 1987a, Some middle Cenomanian (Upper Cretaceous) acanthoceratid ammonites from the Western Interior of the United States: U.S. Geological Survey Professional Paper 1445, 28 p. https://doi.org/10.3133/pp1445

Cobban, W.A., 1987b, Ammonite faunas of the Sarten Sandstone (Cretaceous), Luna County, New Mexico: U.S. Geological Survey Professional Paper 1641-B, 17 p. https://doi.org/10.3133/b1641B

Cobban, W.A., 1988, The Late Cretaceous ammonite *Spathites* Kummel & Decker in New Mexico and Trans-Pecos Texas, *in* Contributions to Late Cretaceous paleontology and stratigraphy of New Mexico, Part II: New Mexico Bureau of Mines and Mineral Resources Bulletin 114, p. 4–21. https://doi.org/10.58799/B-114

Cobban, W.A., and Hook, S.C., 1979, *Collignoniceras woollgari woollgari* (Mantell) ammonite fauna from Upper Cretaceous of Western Interior, United States: New Mexico Bureau of Mines and Mineral Resources Memoir 37, 51 p. https://doi.org/10.58799/M-37

Cobban, W.A., and Hook, S.C., 1980, The Upper Cretaceous (Turonian) ammonite family Coilopoceratidae Hyatt in the Western Interior of the United States: U.S. Geological Survey Professional Paper 1192, 28 p. https://doi.org/10.3133/pp1192

Cobban, W.A., and Hook, S.C., 1984, Mid-Cretaceous molluscan biostratigraphy and paleogeography of southwestern part of Western Interior, United States: Geological Association of Canada Special Paper 27, p. 257–271.

Cobban, W.A., and Kennedy, W.J., 1989, The ammonite *Metengonoceras* Hyatt, 1903, from the Mowry Shale (Cretaceous) of Montana and Wyoming: U.S. Geological Survey Bulletin 1787-L, 30 p. https://doi.org/10.3133/b1787L

Cobban, W.A., and Scott, G.R., 1972, Stratigraphy and ammonite fauna of the Graneros Shale and Greenhorn Limestone near Pueblo, Colorado: U.S. Geological Survey Professional Paper 645, 108 p. https://doi.org/10.3133/pp645

Cobban, W.A., Hook, S.C., and Kennedy, W.J., 1989, Upper Cretaceous rocks and ammonite faunas of southwestern New Mexico: New Mexico Bureau of Mines and Mineral Resources Memoir 45, 137 p. https://doi.org/10.58799/M-45

Cobban, W.A., Walaszczyk, I., Obradovich, J.D., and McKinney, K.C., 2006, A USGS zonal table for the Upper Cretaceous middle Cenomanian-Maastrichtian of the Western Interior of the United States based on ammonites, inoceramids, and radiometric ages: U.S. Geological Survey Open-File Report 2006-1250, 46 p. https://doi.org/10.3133/ofr20061250

Cobban, W.A., Hook, S.C., and McKinney, K.C., 2008, Upper Cretaceous molluscan record along a transect from Virden, New Mexico, to Del Rio, Texas: New Mexico Geology, v. 30, no. 3, p. 75–92. https://doi.org/10.58799/NMG-v30n3.75

Colpitts, Jr., R.M., 1986, Geology of the Sierra de la Cruz area, Socorro County, New Mexico [MS thesis]: Socorro, New Mexico Institute of Mining and Technology, 166 p.

Condie, K.C., and Budding, A.J., 1979, Geology and geochemistry of Precambrian rocks, central and southern New Mexico: New Mexico Bureau of Mines and Mineral Resources Memoir 35, 58 p. https://doi.org/10.58799/M-35

Connell, S.D., Smith, G.A., Geissman, J.W., and McIntosh, W.C., 2013, Climatic controls on nonmarine depositional sequences in the Albuquerque Basin, Rio Grande rift, north-central New Mexico, *in* Hudson, M.R., and Grauch, V.J.S., eds., New perspectives on Rio Grande rift basins—From tectonics to groundwater: Geological Society of America Special Paper 494, p. 383–425. https://doi.org/10.1130/2013.2494(15)

Cox, D.P., and Singer, D.A., eds., 1986, Mineral deposit models: U.S. Geological Survey Bulletin 1693, 379 p. https://doi.org/10.3133/b1693

Craig, F.M., 1992, Geology of part of the area east and west of Quebradas road between mile markers 15 and 20, Socorro County, New Mexico [MS thesis]: Socorro, New Mexico Institute of Mining and Technology, 114 p.

Dane, C.H., Wanek, A.A., and Reeside, Jr., J.B., 1957, Reinterpretation of section of Cretaceous rocks in Alamosa Creek Valley area, Catron and Socorro Counties, New Mexico: Bulletin of the American Association of Petroleum Geologists, v. 42, p. 181–196. https://doi.org/10.1306/0BDA57C5-16BD-11D7-8645000102C1865D

Dane, C.H., Kauffman, E.G., and Cobban, W.A., 1968, Semilla Sandstone, a new member of the Mancos Shale in the southeastern part of the San Juan Basin, New Mexico: U.S. Geological Survey Bulletin 1254-F, 28 p. https://doi.org/10.3133/b1254F

Darton, N.H., 1928, "Red beds" and associated formations in New Mexico, with an outline of the geology of the state: U.S. Geological Survey Bulletin 794, 356 p. https://doi.org/10.3133/b794

Davydov, V.I., Glenister, B.F., Sinosa, C., Ritter, S.M., Chernykh, V.V., Wardlaw, B.R., and Snyder, W.S., 1998, Proposal of Aidaralash as global stratotype section and point (GSSP) for base of the Permian System: Episodes, v. 21, no. 1, p. 11–17. https://doi.org/10.18814/epiiugs/1998/v21i1/003

de Moor, M., Zinsser, A., Karlstrom, K., Chamberlin, R., Connell, S. and Read, A., 2005, Preliminary geologic map of the La Joya 7.5-minute quadrangle, Socorro County, New Mexico: New Mexico Bureau of Geology and Mineral Resources Open-File Geologic Map 102, scale 1:24,000. https://doi.org/10.58799/OF-GM-102

Denny, C.S., 1940, Tertiary geology of the San Acacia area, New Mexico: Journal of Geology, v. 48, no. 1, p. 73–106. https://www.jstor.org/stable/30056660

Dickinson, W.R., 2018, Tectonosedimentary relations of Pennsylvanian to Jurassic strata on the Colorado Plateau: Geological Society of America Special Paper 533, 184 p. https://doi.org/10.1130/2018.2533

Dickinson, W.R., and Gehrels, G.E., 2008, U-Pb ages of detrital zircons in relation to paleogeography—Triassic paleodrainage networks and sediment dispersal acrosssouthwest Laurentia: Journal of Sedimentary Research, v. 78, no. 12, p. 745–764. https://doi.org/10.2110/jsr.2008.088

Dickinson, W.R., and Gehrels, G.E., 2010, Implications of U-Pb ages of detrital zircons in Mesozoic strata of the Four Corners region for provenance relations in space and time, *in* Fassett, J.E., Zeigler, K.E., and Lueth, V., eds., Geology of the Four Corners Country: New Mexico Geological Society Fall Field Conference Guidebook 61, p. 135–146. https://doi.org/10.56577/FFC-61.135

Dickinson, W.R., Klute, M.A., Hayes, M.J., Janecke, S.U., Lundin, E.R., McKittrick, M.A., and Olivares, M.D., 1988, Paleogeographic and paleotectonic setting of Laramide sedimentary basins in the Rocky Mountain region: Geological Society of America Bulletin, v. 100, no. 7, p. 1023–1039. https://doi.org/10.1130/0016-7606(1988)100%3C1023:PAPSOL%3E2.3.CO;2

DiMichele, W.A., and Lucas, S.G., 2017, The first specimen of *Annularia spinulosa* Sternberg from the Lower Permian Abo Formation, New Mexico, and implications for rarity in the plant fossil record, *in* Lucas, S.G., DiMichele, W.A. and Krainer, K., eds., Carboniferous-Permian transition in Socorro County, New Mexico: New Mexico Museum of Natural History and Science Bulletin 77, p. 17–23.

DiMichele, W.A., Chaney, D.S., Nelson, W.J., Lucas, S.G., Looy, C.V., Quick, K., and Jun, W., 2007, A low diversity, seasonal tropical landscape dominated by conifers and peltasperms—Early Permian Abo Formation, New Mexico: Review of Palaeobotany and Palynology, v. 145, no. 3–4, p. 249-273. https://doi.org/10.1016/j.revpalbo.2006.11.003

DiMichele, W.A., Chaney, D.S., Lucas, S.G., Nelson, J.W., Elrick, S.D., Falcon-Lang, H.J., and Kerp, H., 2017, Middle to Late Pennsylvanian fossil floras from Socorro County, New Mexico, U.S.A., *in* Lucas, S.G., DiMichele, W.A. and Krainer, K., eds., Carboniferous-Permian transition in Socorro County, New Mexico: New Mexico Museum of Natural History and Science Bulletin 77, p. 25–99.

Donahue, M.S., 2016, Episodic uplift of the Rocky Mountains—Evidence from U-Pb detrital zircon geochronology and low-temperature thermochronology, with a chapter on using mobile technology for geoscience education [PhD dissertation]: Albuquerque, University of New Mexico, 201 p.

Dubiel, R.F., 1994, Triassic deposystems, paleogeography, and paleoclimate of Western Interior, *in* Caputo, M.V., Peterson, J.A., and Franczyk, K.J., eds., Mesozoic Systems of the Rocky Mountain Region, USA: Denver, Colorado, Rocky Mountain Section, Society for Sedimentary Geology (SEPM), p. 133–168.

Dunbar, N.W., McIntosh, W.C., Cather, S.M., Chamberlin, R.M., Harrison, B., and Kyle, P.R., 1996, Distal tephras from the Jemez volcanic center as time-stratigraphic markers in ancestral Rio Grande sediments from the Socorro area, *in* Goff, F., Kues, B.S., Rogers, M.A., McFadden, L.D., and Gardner, J.N., eds., Jemez Mountains Region: New Mexico Geological Society Fall Field Conference Guidebook 47, p. 69–70. https://doi.org/10.56577/FFC-47

Duval, B., Cramez, C., and Jackson, M.P.A., 1992, Raft tectonics in the Kwanza Basin, Angola: Marine and Petroleum Geology, v. 9, no. 4, p. 389–404. https://doi.org/10.1016/0264-8172(92)90050-O

Elder, W.P., 1988, Geometry of Upper Cretaceous bentonite beds—Implications about volcanic source area and paleowind patterns, western interior, United States: Geology, v. 16, no. 9, p. 835–838. https://doi.org/10.1130/0091-7613(1988)016%3C0835:GOUCBB%3E2.3.CO;2

Elder, W.P., 1989, Molluscan extinction patterns across the Cenomanian-Turonian Stage boundary in the western interior of the United States: Paleobiology, v. 15, no. 3, p. 299–320. https://doi.org/10.1017/S0094837300009465

Ellis, R.W., 1929, New Mexico mineral deposits except fuels: University of New Mexico Bulletin 167, 148 p.

Eveleth, R.W., 2015, Audley Dean Nicols' Tokay Panorama of 1927: New Mexico Geology, v. 37, no. 2, p. 52–54. https://doi.org/10.58799/NMG-v37n2.52

Eveleth, R., and Harden, P., 2011, Fraley limestone quarry and kilns, 9 p.: http://socorro-history.org/HISTORY/PH_History/201110_fraley.pdf (accessed December 2017).

Eveleth, R., Lueth, V., and Krukowski, S., 2009, Fraley limestone quarry and kilns, *in* Lueth, V., Lucas, S.G., and Chamberlin, R.M., eds., Geology of the Chupadera Mesa: New Mexico Geological Society Fall Field Conference Guidebook 60, p. 40–42. https://doi.org/10.56577/FFC-60

Fagrelius, K.H., 1982, Geology of the Cerro del Viboro area, Socorro County, New Mexico [MS thesis]: Socorro, New Mexico Institute of Mining and Technology, 135 p.

Falcon-Lang, H.J., Jud, N.A., Nelson, W.J., DiMichele, W.A., Chaney, D.S., and Lucas, S.G., 2011, Pennsylvanian coniferopsid forests in sabkha facies reveal the nature of seasonal tropical biome: Geology, v. 39, no. 4, p. 371–374. https://doi.org/10.1130/G31764.1

Feldman, H.R., Franseen, E.K., Joeckel, R.M., and Heckel, P.H., 2005, Impact of longer-term modest climate shifts on architecture of high-frequency sequences (cyclothems), Pennsylvanian of midcontinent U.S.A: Journal of Sedimentary Research, v. 75, no. 3, p. 350–368. https://doi.org/10.2110/jsr.2005.028

Ferguson, C.A., Osburn, G.R., and McIntosh, W.C., 2012, Oligocene calderas in the San Mateo Mountains, Mogollon-Datil volcanic field, New Mexico, *in* Lucas, S.G., McLemore, V.T., Lueth, V.W., Spielmann, J.A., and Krainer, K., eds., Geology of the Warm Springs Region: New Mexico Geological Society Fall Field Conference Guidebook 63, p. 74–77. https://doi.org/10.56577/FFC-63

File, L., and Northrop, S.A., 1966, County, township, and range locations of New Mexico's Mining Districts: New Mexico Bureau of Mines and Mineral Resources Circular 84, 66 p. https://doi.org/10.58799/C-84

Finlay, J.R., 1922, Report of Appraisal of Mining Properties of New Mexico, 1921–1922: Santa Fe, New Mexico State Tax Commission, 154 p.

Folk, R.L., 1974, Petrology of Sedimentary Rocks: Austin, Hemphill Publishing Co., 170 p.

Gardner, J.H., 1910, The Carthage coal field, New Mexico, *in* Campbell, M.R., ed., Contributions to economic geology 1908, Part II—Mineral fuels: U.S. Geological Survey Bulletin 381, p. 452–460. https://doi.org/10.3133/b381C

Geddes, R.W., 1963, Structural geology of Little San Pasqual Mountain and adjacent Rio Grande trough [MS thesis]: Socorro, New Mexico Institute of Mining and Technology, 64 p.

Gilbert, G.K., 1896, The underground water of the Arkansas Valley in eastern Colorado, *in* Walcott, C.D., ed., Seventeenth annual report of the United States Geological Survey to the Secretary of the Interior, 1895–1896, Part II, Economic geology and hydrography, p. 551–601. https://doi.org/10.3133/ar17_2

Green, M.W., Axen, G., and Cather, S.M., 2013, Low-angle normal faults within evaporite-rich Permian strata, Sierra Larga, NM [abstract]: New Mexico Geological Society Annual Spring Meeting, April 12, 2013, Macey Center, New Mexico Institute of Mining and Technology, Socorro, NM. https://doi.org/10.56577/SM-2013.62

Gregory, H.E., 1917, Geology of the Navajo Country—A reconnaissance of parts of Arizona, New Mexico and Utah: U.S. Geological Survey Professional Paper 93, 161 p. https://doi.org/10.3133/pp93

Guglielmo, Jr., G., Schultz-Ela, D.D., and Jackson, M.P.A., 1997, Raft tectonics in the Kwanza Basin, Angola—An animation: Austin, Texas Bureau of Geology: http://www.beg.utexas.edu/indassoc/agl/animations/AGL96-MM-003/index.html

Haines, H., 1891, History of New Mexico—From the Spanish Conquest to the present time 1530–1890: New York, New Mexico Historical Publishing Co., 591 p.

Hambleton, A.W., 1959, Interpretation of the palaoenvironment of several Missourian carbonate sections in Socorro County, New Mexico by carbonate fabrics [PhD dissertation]: Socorro, New Mexico Institute of Mining and Technology, 87 p.

Hambleton, A.W., 1962, Carbonate-rock fabrics of three Missourian stratigraphic sections in Socorro County, New Mexico: Journal of Sedimentary Petrology, v. 32, no. 3, p. 579–601. https://doi.org/10.1306/74D70D1C-2B21-11D7-8648000102C1865D

Harris, S.K., and Lucas, S.G, 2022, Vertebrate fossils in the upper Pennsylvanian (Missourian) Tinajas Member of the Atrasado Formation, Socorro County, New Mexico, *in* Koning, D.J., Hobbs, K.M., Phillips, F.M., Nelson, W.J., Cather, S.M., Jakle, A.C., and Van Der Werff, B., eds., Socorro Region III: New Mexico Geological Society Fall Field Conference Guidebook 72, p. 165–170. https://doi.org/10.56577/FFC-72.165

Hashberger, K., Leary, R., and Prush, V., 2024, Stratigraphy and provenance of the Baca Formation in the Baca and Carthage–La Joya Basins, central New Mexico [abstract]: New Mexico Geological Society Annual Spring Meeting, April 19, 2024, Macey Center, New Mexico Institute of Mining and Technology, Socorro, NM. https://doi.org/10.56577/SM-2024.2969

Hattin, D.E., 1962, Stratigraphy of the Carlile Shale (Upper Cretaceous) in Kansas: Kansas Geological Survey Bulletin 156, 166 p.

Hattin, D.E., 1975, Stratigraphy and depositional environment of Greenhorn Limestone (Upper Cretaceous) of Kansas: Kansas Geological Survey Bulletin 209, 128 p.

Hattin, D.E., 1987, Pelagic/hemipelagic rhythmites of Greenhorn Limestone (Upper Cretaceous), *in* Clemons, R.E., King, W.E., Mack, G.H., and Zidek, J., eds., Northeastern New Mexico: New Mexico Geological Society Fall Field Conference Guidebook 38, p. 237–247. https://doi.org/10.56577/FFC-38.237

Hauge, T.A., 1993, The Heart Mountain detachment, northwestern Wyoming—100 years of controversy, *in* Snoke, A.W., Steidtmann, J.R., and Roberts, S.M., eds., Geology of Wyoming: Geological Survey of Wyoming Memoir 5, v. 2, p. 530–571.

Hawley, J.W., and Kernodle, J.M., 2000, Overview of the hydrogeology and geohydrology of the northern Rio Grande basin—Colorado, New Mexico, and Texas, *in* Ortega-Klett, C.T., ed., Proceedings of the 44th Annual New Mexico Water Conference, Las Cruces, New Mexico: New Mexico Water Resources Research Institute Report 312, p. 79–102.

Hayden, S.N., 1991, Dextral oblique-slip deformation along the Montosa fault zone at Abo Pass, Valencia and Socorro Counties, New Mexico [abstract]: New Mexico Geological Society Annual Spring Meeting, April 5, 1991, Macey Center, New Mexico Institute of Mining and Technology, Socorro, NM.

Heckel, P.B., 1990, Evidence for global (glacial-eustatic) control over Upper Carboniferous (Pennsylvanian) cyclothems in midcontinent North America: The Geological Society of London Special Publication 55, p. 35–47. https://doi.org/10.1144/GSL.SP.1990.055.01.02

Heckert, A.B., and Lucas, S.G., 2002, The microfauna of the Upper Triassic Ojo Huelos Member, San Pedro Arroyo Formation, central New Mexico: New Mexico Museum of Natural History and Science Bulletin 21, p. 77–85.

Heller, P.L., and Lui, L., 2016, Dynamic topography and vertical motion of the U.S. Rocky Mountain region prior to and during the Laramide orogeny: Geological Society of America Bulletin, v. 128, p. 973–988. https://doi.org/10.1130/B31431.1

Herber, L.J., 1963a, Structural petrology and economic features of the Precambrian rocks of La Joyita Hills [MS thesis]: Socorro, New Mexico Institute of Mining and Technology, 36 p.

Herber, L.J., 1963b, Precambrian rocks of La Joyita Hills, *in* Kuellmer, F.J. ed., Socorro Region: New Mexico Geological Society Fall Field Conference Guidebook 14, p. 180–184. https://doi.org/10.56577/FFC-14.180

Hereford, J.P., 2003, Report on Carthage coal field, San Pedro Coal and Coke Co., and New Mexico Midland Railway, private report.

Herrick, C.L., 1896, The so-called Socorro tripoli: The American Geologist, v. 18, p. 135–140.

Herrick, C.L., 1900, Report of a geological reconnaissance in western Socorro and Valencia Counties, New Mexico: The American Geologist, v. 25, p. 331–346.

Herrick, C.L., 1904, A coal-measure forest near Socorro, New Mexico: Journal of Geology, v. 12, no. 3, p. 237–251. https://www.jstor.org/stable/30056704

Herrick, C.L., and Johnson, D.W., 1900, The geology of the Albuquerque sheet: Bulletin of the Scientific Laboratories of Denison University, v. 11, p. 175–239.

Hill, G.T., 1994, Geochemistry of southwestern New Mexico fluorite deposits with possible base and precious metals exploration significance [MS thesis]: Socorro, New Mexico Institute of Mining and Technology, 44 p.

Hilpert, L.S., 1969, Uranium resources of northwestern New Mexico: U.S. Geological Survey Professional Paper 603, 166 p. https://doi.org/10.3133/pp603

Hoffman, G.K., 1996, Coal resources of New Mexico: New Mexico Bureau of Mines and Mineral Resources Resource Map 20, 17 p. https://doi.org/10.58799/RM-20

Hook, S.C., 1983, Stratigraphy, paleontology, depositional framework, and nomenclature of marine Upper Cretaceous rocks, Socorro County, New Mexico, *in* Chapin, C.E., and Callender, J.F., eds., Socorro Region II: New Mexico Geological Society Fall Field Conference Guidebook 34, p. 165–172. https://doi.org/10.56577/FFC-34.165

Hook, S.C., 1984, Evolution of stratigraphic nomenclature of the Upper Cretaceous of Socorro County, New Mexico: New Mexico Geology, v. 6, no. 2, p. 28–33. https://doi.org/10.58799/NMG-v6n2.28

Hook, S.C., 2009, Bentonites and boundaries in the lower tongue of the Mancos Shale, Carthage coal field, Socorro County, New Mexico, *in* Lueth, V., Lucas, S.G., and Chamberlin, R.M., eds., Geology of the Chupadera Mesa: New Mexico Geological Society Fall Field Conference Guidebook 60, p. 23–26. https://doi.org/10.56577/FFC-60

Hook, S.C., 2010, *Flemingostrea elegans*, n. sp.—Guide fossil to marine, lower Coniacian (Upper Cretaceous) strata of central New Mexico: New Mexico Geology, v. 32, no. 2, p. 35–55. https://doi.org/10.58799/NMG-v32n2.35

Hook, S.C., 2016, Biostratigraphic importance of the small, isolated exposure of the Upper Cretaceous Dakota Sandstone at Canyon View, Palo Duro Canyon, Sevilleta National Wildlife Refuge, New Mexico, *in* Frey, B.A., Karlstrom, K.E., Lucas, S.G., Williams, S., Zeigler, K., McLemore, V., and Ulmer-Scholle, D.S., eds., Geology of the Belen Area: New Mexico Geological Society Fall Field Conference Guidebook 67, p. 31–32. https://doi.org/10.56577/FFC-67

Hook, S.C., and Brennan, P.A., 2022, Reconaissance assessments of three contractional fault-related folds along the Quebradas back country byway, Socorro County, New Mexico, *in* Koning, D.J., Hobbs, K.M., Phillips, F.M., Nelson, W.J., Cather, S.M., Jakle, A.C., and Van Der Werff, B., eds., Socorro Region III: New Mexico Geological Society Fall Field Conference Guidebook 72, p. 305–319. https://doi.org/10.56577/FFC-72.305

Hook, S.C., and Cobban, W.A., 1977, *Pycnodonte newberryi* (Stanton)—Common guide fossil in Upper Cretaceous of New Mexico: New Mexico Bureau of Mines and Mineral Resources Annual Report, July 1, 1976 to June 30, 1977, p. 48–54.

Hook, S.C., and Cobban, W.A., 1979, *Prionocyclus novimexicanus* (Marcou)—Common Upper Cretaceous guide fossil in New Mexico: New Mexico Bureau of Mines and Mineral Resources Annual Report, July 1, 1977 to June 30, 1978, p. 34–42.

Hook, S.C., and Cobban, W.A., 2007, A condensed middle Cenomanian succession in the Dakota Sandstone (Upper Cretaceous), Sevilleta National Wildlife Refuge, Socorro County, New Mexico: New Mexico Geology, v. 29, no. 3, p. 75–96. https://doi.org/10.58799/NMG-v29n3.75

Hook, S.C., and Cobban, W.A., 2010, *Flemingostrea elegans,* n. sp.—Guide fossil to marine, lower Coniacian (Upper Cretaceous) strata of central New Mexico: New Mexico Geology, v. 32, no. 2, p. 35–57. https://doi.org/10.58799/NMG-v32n2.35

Hook, S.C., and Cobban, W.A., 2011a, The Late Cretaceous oyster *Cameleolopha bellaplicata* (Shumard 1860), guide fossil to middle Turonian strata in New Mexico: New Mexico Geology, v. 33, no. 3, p. 67–89. https://doi.org/10.58799/NMG-v33n3.67

Hook, S.C., and Cobban, W.A., 2011b, Cover description: New Mexico Geology, v. 33, no. 3, p. 66, 96.

Hook, S.C., and Cobban, W.A., 2012, Evolution of the Late Cretaceous oyster genus *Cameleolopha* Vyalov 1936 in central New Mexico: New Mexico Geology, v. 34, no. 3, p. 76–95. https://doi.org/10.58799/NMG-v34n3.76

Hook, S.C., and Cobban, W.A., 2013, The Upper Cretaceous (Turonian) Juana Lopez Beds of the D-Cross Tongue of the Mancos Shale in central New Mexico and their relationship to the Juana Lopez Member of the Mancos Shale in the San Juan Basin: New Mexico Geology, v. 35, no. 3, p. 59–81. https://doi.org/10.58799/NMG-v35n3.59

Hook, S.C., and Cobban, W.A., 2015, The type section of the Upper Cretaceous Tokay Tongue of the Mancos Shale (new name), Carthage coal field, Socorro County, New Mexico: New Mexico Geology, v. 37, no. 2, p. 27–46. https://doi.org/10.58799/NMG-v37n2.27

Hook, S.C., and Cobban, W.A., 2016, The late Cenomanian oyster *Lopha staufferi* (Bergquist, 1944)—The oldest ribbed oyster in the Upper Cretaceous of the Western Interior of the United States: Acta Geologica Polonica, v. 66, no. 4, p. 609–626.

Hook, S.C., and Cobban, W.A., 2017, *Mecaster batnensis* (Coquand, 1862), a late Cenomanian echinoid from New Mexico, with a compilation of Late Cretaceous echinoid records in the Western Interior of the United States and Canada: Acta Geologica Polonica, v. 67, no. 1, p. 1–30.

Hook, S.C., Cobban, W.A., and Landis, E.R., 1980, Extension of the intertongued Dakota Sandstone–Mancos Shale into the southern Zuni Basin: New Mexico Geology, v. 2, no. 3, p. 42–44, 46. https://doi.org/10.58799/NMG-v2n3.42

Hook, S.C., Molenaar, C.M., and Cobban, W.A., 1983, Stratigraphy and revision of nomenclature of upper Cenomanian to Turonian (Upper Cretaceous) rocks of west-central New Mexico, *in* Hook, S.C., ed., Contributions to mid-Cretaceous paleontology and stratigraphy of New Mexico, Part II: New Mexico Bureau of Mines and Mineral Resources Circular 185, p. 7–28. https://doi.org/10.58799/C-185

Hook, S.C., Mack, G.H., and Cobban, W.A., 2012, Upper Cretaceous stratigraphy and biostratigraphy of south-central New Mexico, *in* Lucas, S.G., McLemore, V.T., Lueth, V.W., Spielmann, J.A., and Krainer, K., eds., Geology of the Warm Springs Region: New Mexico Geological Society Fall Field Conference Guidebook 63, p. 121–137. https://doi.org/10.56577/FFC-63.413

Huffman, Jr., A.C., 1987, Petroleum geology and hydrocarbon plays of the San Juan petroleum province: U.S. Geological Survey Open-File Report 87-450-B, 67 p. https://doi.org/10.3133/ofr87450B

Hunt, A.P., 1983, Plant fossils and lithostratigraphy of the Abo Formation (Lower Permian) in the Socorro area and plant biostratigraphy of Abo red beds in New Mexico, *in* Chapin, C.E., and Callender, J.F., eds., Socorro Region II: New Mexico Geological Society Fall Field Conference Guidebook 34, p. 157–163. https://doi.org/10.56577/FFC-34.157

Hunt, A.P., and Lucas, S.G., 1987a, Triassic stratigraphy, Carthage area, Socorro County, New Mexico, and the southeasternmost outcrops of the Moenkopi Formation [abstract]: New Mexico Geological Society Annual Spring Meeting, April 3, 1987, Macey Center, New Mexico Institute of Mining and Technology, Socorro, NM.

Hunt, A.P., and Lucas, S.G., 1987b, Southernmost outcrops of the Morrison Formation in the Carthage area, Socorro County, New Mexico: New Mexico Geology, v. 9, no. 3, p. 58–62. https://doi.org/10.58799/NMG-v9n3.58

Hunter, R.E., 1981, Stratification styles in eolian sandstones—Some Pennsylvanian to Jurassic examples from the Western Interior U.S.A, *in* Ethridge, F.G., and Flores, R.M., eds., Recent and ancient nonmarine depositional environments—Models for exploration: Society of Economic Paleontologists and Mineralogists Special Publication 31, p. 315–329.

Hyatt, A., 1903, Pseudoceratites of the Cretaceous (edited by T.W. Stanton): U.S. Geological Survey Monograph 44, 351 p. https://doi.org/10.3133/m44

International Atomic Energy Agency (IAEA), 2009, World distribution of uranium deposits with uranium deposit classification: IAEA Report IAEA-TECDOC-1629, 126 p. http://www-pub.iaea.org/MTCD/publications/PDF/TE_1629_web.pdf

Ivanov, A.O., Lucas, S.G., and Krainer, K., 2009, Pennsylvanian fishes from the Sandia Formation, Socorro County, New Mexico, *in* Lueth, V., Lucas, S.G., and Chamberlin, R.M., eds., Geology of the Chupadera Mesa: New Mexico Geological Society Fall Field Conference Guidebook 60, p. 243–248. https://doi.org/10.56577/FFC-60.243

Jaworski, M.J., 1973, Copper mineralization of the upper Moya Sandstone, Chupadero mines area, Socorro County, New Mexico [MS thesis]: Socorro, New Mexico Institute of Mining and Technology, 102 p.

Jones, F.A., 1915, The mineral resources of New Mexico: State School of Mines, Mineral Resources Study of New Mexico, 77 p.

Karlstrom, K.E., Amato, J.M., Williams, M.L., Heizler, M., Shaw, C.A., Read, A.S., and Bauer, P., 2004, Proterozoic tectonic evolution of the New Mexico region—A synthesis, *in* Mack, G.H., and Giles, K.A., eds., The Geology of New Mexico—A geologic history: New Mexico Geological Society Special Publication 11, p. 1–34. https://doi.org/10.56577/SP-11

Karlstrom, K.E., Williams, M.L., Heizler, M.T., Holland, M.E., Grambling, T.A., and Amato, J.M., 2016, U-Pb monazite and $^{40}Ar/^{39}Ar$ data supporting polyphase tectonism in the Manzano Mountains—A record of both the Mazatzal (1.66–1.60 Ga) and Picuris (1.45 Ga) orogenies, *in* Frey, B.A., Karlstrom, K.E., Lucas, S.G., Williams, S., Zeigler, K., McLemore, V., and Ulmer-Scholle, D.S., eds., Geology of the Belen Area: New Mexico Geological Society Fall Field Conference Guidebook 67, p. 177–184. https://doi.org/10.56577/FFC-67.177

Kauffman, E.G., 1965, Middle and late Turonian oysters of the *Lopha lugubris* group: Smithsonian Miscellaneous Collections, v. 148, no. 6, 92 p.

Kauffman, E.G., 1969, Cretaceous marine cycles of the Western Interior: The Mountain Geologist, v. 6, p. 227–245.

Kelley, V.C., and Wood, G.H., 1946, Geology of the Lucero Uplift, Valencia, Socorro, and Bernalillo Counties, New Mexico: U.S. Geological Survey Oil and Gas Investigations Preliminary Map 47, scale 1:63,360. https://doi.org/10.3133/om47

Kelley, S.A., Chapin, C.E., and Corrigan, J., 1992, Late Mesozoic to Cenozoic cooling histories of the flanks of the northern and central Rio Grande rift, Colorado and New Mexico: New Mexico Bureau of Mines and Mineral Resources Bulletin 145, 39 p. https://doi.org/10.58799/B-145

Kelley, S.A., Lawrence, J.R., and Osburn, G.R., 2005, Geologic map of the Youngsville 7.5-minute quadrangle, Rio Arriba County, New Mexico: New Mexico Bureau of Geology and Mineral Reources Open-File Geologic Map 106, scale 1:24,000. https://doi.org/10.58799/OF-GM-106

Kelley, S.A., Chapin, C.E., Cather, S.M., and Person, M., 2009, Thermal history of the eastern Socorro Basin, Socorro County, New Mexico, based on apatite fission-track thermochronology, *in* Lueth, V., Lucas, S.G., and Chamberlin, R.M., eds., Geology of the Chupadera Mesa: New Mexico Geological Society Fall Field Conference Guidebook 60, p. 347–358. https://doi.org/10.56577/FFC-60.347

Kennedy, W.J., Cobban, W.A., and Hook, S.C., 1988, Middle Cenomanian (Late Cretaceous) molluscan faunas from the base of the Boquillas Formation, Cerro de Muleros, Dona Anna County, New Mexico, *in* Cobban, W.A., Kennedy, W.J., and Hook, S.C., eds., Contributions to Late Cretaceous paleontology and stratigraphy of New Mexico: New Mexico Bureau of Mines and Mineral Resources Bulletin 114, p. 35–44. https://doi.org/10.58799/B-114

Kennedy, W.J., Walaszczyk, I., and Cobban, W.A., 2000, Pueblo, Colorado, USA, candidate Global Boundary Stratotype Section and Point for the base of the Turonian Stage of the Cretaceous, and for the base of the Middle Turonian Substage, with a revision of the Inoceramidae (Bivalvia): Acta Geologica Polonica, v. 50, no. 3, p. 295–334.

Kennedy, W.J., Cobban, W.A., and Landman, N.H., 2001, A revision of the Turonian members of the ammonite subfamily Collignoniceratinae from the United States Western Interior and Gulf Coast: Bulletin of the American Museum of Natural History, no. 267, 148 p. https://doi.org/10.1206/0003-0090(2001)267%3C0001:AROTTM%3E2.0.CO;2

Kennedy, W.J., Walaszczyk, I., and Cobban, W.A., 2005, The Global Boundary Stratotype Section and Point for the base of the Turonian Stage of the Cretaceous, Pueblo, Colorado, U.S.A.: Episodes, v. 28, no. 2, p. 93–104. https://doi.org/10.18814/epiiugs/2005/v28i2/003

Keyes, C.R., 1915, Foundation of exact geological correlation: Iowa Academy of Science Proceedings, v. 22, p. 249–267.

Kirk, A.R., Huffman, Jr., A.C., and Zech, R.S., 1988, Subsurface correlation of Jurassic and Cretaceous rocks having occurrences of uranium, coal, and oil—Mariano Lake-Lake Valley drilling project, northwestern New Mexico: U.S. Geological Survey Oil and Gas Investigations Chart 130. https://doi.org/10.3133/oc130

Kirkland, J.I., 1996, Paleontology of the Greenhorn cyclothem (Cretaceous: late Cenomanian to middle Turonian) at Black Mesa, northeastern Arizona: New Mexico Museum of Natural History and Science Bulletin 9, 131 p.

Koning, D.J., Heizler, M.T., and Chamberlin, R.M., 2024, Lake Socorro and the 7.4–7.0 Ma fluvial integration of the ancestral Rio Grande through the Socorro Basin, south-central New Mexico [abstract]: New Mexico Geological Society Annual Spring Meeting, April 19, 2024, Macey Center, New Mexico Institute of Mining and Technology, Socorro, NM. https://doi.org/10.56577/SM-2024.3007

Korzeb, S.L., 1986, Minerals investigations of Sierra de las Cañas wilderness study area (NM-020-038), Socorro County, New Mexico: U.S. Bureau of Mines Open-File Report MLA-51-86, 9 p.

Kottlowski, F.E., and Stewart, W.J., 1970, The Wolfcampian Joyita Uplift of central New Mexico: New Mexico Bureau of Mines and Mineral Resources Memoir 23, p. 3–31. https://doi.org/10.58799/M-23

Krainer, K., and Lucas, S.G., 2009, Cyclic sedimentation of the Upper Pennsylvanian (lower Wolfcampian) Bursum Formation, central New Mexico—Tectonics versus glacioeustasy, *in* Lueth, V., Lucas, S.G., and Chamberlin, R.M., eds., Geology of the Chupadera Mesa: New Mexico Geological Society Fall Field Conference Guidebook 60, p. 167–182. https://doi.org/10.56577/FFC-60.167

Krainer, K., and Lucas, S.G., 2013, The Pennsylvanian Sandia Formation in northern and central New Mexico, *in* Lucas, S.G., Nelson, J.W., DiMichele, W.A., Spielmann, J.A., Krainer, K., Barrick, J.E., Elrick, S., and Voigt, S., eds., The Carboniferous-Permian transition in central New Mexico: New Mexico Museum of Natural History and Science Bulletin 59, p. 77–100.

Krainer, K., and Lucas, S.G., 2015, Type section of the Permian Glorieta Sandstone, San Miguel County, New Mexico, *in* Lindline, J., Petronis, M., and Zebrowski, J., eds., Geology of the Las Vegas area: New Mexico Geological Society Fall Field Conference Guidebook 66, p. 205–210. https://doi.org/10.56577/FFC-66.205

Krainer, K., Lucas, S.G., and Vachard, D., 2009, The Upper Carboniferous Bursum Formation at Abo Pass, Socorro County, New Mexico, *in* Lueth, V., Lucas, S.G., and Chamberlin, R.M., eds., Geology of the Chupadera Mesa: New Mexico Geological Society Fall Field Conference Guidebook 60, p. 98–102. https://doi.org/10.56577/FFC-60

Krainer, K., Vachard, D., Lucas, S.G., and Ernst, A., 2017, Microfacies and sedimentary petrography of Pennsylvanian limestones and sandstones of the Cerros de Amado area, east of Socorro (New Mexico, USA), *in* Lucas, S.G., DiMichele, W.A. and Krainer, K., eds., Carboniferous-Permian transition in Socorro County, New Mexico: New Mexico Museum of Natural History and Science Bulletin 77, p. 159–197.

Krason, J., Wodzicki, A., and Cruver, S., 1982, Geology, energy, and mineral resources assessment of the Socorro area, New Mexico: U.S. Bureau of Land Management Geology, Energy, and Mineral Resources Series Report No. 1, 58 p.

Kucks, R.P., Hill, P.L., and Heywood, C.E., 2001, New Mexico aeromagnetic and gravity maps and data—A web site for distribution of data: U.S. Geological Survey Open-File Report 01-0061, version 1.0: https://pubs.usgs.gov/of/2001/ofr-01-0061/ (accessed January 2005).

Kues, B.S., 2001, The Pennsylvanian System in New Mexico—Overview with suggestions for revision of stratigraphic nomenclature: New Mexico Geology, v. 23, no. 4, p. 103–122. https://doi.org/10.58799/NMG-v23n4.103

Kues, B.S., and Giles, K.A., 2004, The late Paleozoic Ancestral Rocky Mountain system in New Mexico, *in* Mack, G.H., and Giles, K.A., eds., The Geology of New Mexico—A geologic history: New Mexico Geological Society Special Publication 11, p. 95–136. https://doi.org/10.56577/SP-11

Kues, B.S., Lucas S.G., Lerner, A.J, and Wilde, G.L., 2002, Invertebrate faunas of the lower Atrasado Formation (Pennsylvanian, Missourian), Cerros de Amado, Socorro County, New Mexico [abstract]: New Mexico Geological Society Annual Spring Meeting, April 5, 2002, Macey Center, New Mexico Institute of Mining and Technology, Socorro, NM.

Kuiper, K.F., Deino, A., Hilgen, F.J., Krijgsman, W., Renne, P.R. and Wijbrans, J.R., 2008, Synchronizing the rock clocks of Earth history: Science, v. 320, no. 5875, p. 500–504. https://doi.org/10.1126/science.1154339

Landis, E.R., Dane, C.H., and Cobban, W.A., 1973, Stratigraphic terminology of the Dakota Sandstone and Mancos Shale, west-central New Mexico: U.S. Geological Survey Bulletin 1372-J, 44 p. https://doi.org/10.3133/b1372J

Lasky, S.G., 1932, The ore deposits of Socorro County, New Mexico: New Mexico Bureau of Mines and Mineral Resources Bulletin 8, 139 p. https://doi.org/10.58799/B-8

Lasky, S.G., and Wootton, T.P., 1933, The metal resources of New Mexico and their economic features: New Mexico Bureau of Mines and Mineral Resources Bulletin 7, 178 p. https://doi.org/10.58799/B-7

Lawton, T.F., 1994, Tectonic setting of Mesozoic sedimentary basins, *in* Caputo, M.V., Peterson, J.A., and Franczyk, K.J., eds., Mesozoic systems of the Rocky Mountain Region, USA: Denver, Colorado, Rocky Mountain Section, Society for Sedimentary Geology (SEPM), p. 1–25.

Le Corvec, N., and Walter, T.R., 2009, Volcano spreading and fault interaction influenced by rift zone intrusions—Insights from analogue experiments analyzed with digital image correlation technique: Journal of Volcanology and Geothermal Research, v. 183, no. 3–4, p. 170–182. https://doi.org/10.1016/j.jvolgeores.2009.02.006

Le Maitre, R.W., et al., 1989, A classification of igneous rocks and glossary of terms, *in* Le Maitre, R.W., ed., Recommendations of the International Union of Geological Sciences Subcommission on the systematics of igneous rocks: Oxford, United Kingdom, Blackwell Scientific Publications, 35 p.

Leach, D.L., Taylor, R.D., Fey, D.L., Diehl, S.F., and Saltus, R.W., 2010, A deposit model for Mississippi Valley-type lead-zinc ores, chapter A of mineral deposit models for resource assessment: U.S. Geological Survey Scientific Investigations Report 2010–5070–A, 52 p.

Leary, R.J., Umhoefer, P., Smith, M.E., and Riggs, N., 2017, A three-sided orogen—A new tectonic model for Ancestral Rocky Mountain uplift and basin development: Geology, v. 45, no. 8, p. 735–738. https://doi.org/10.1130/G39041.1

Lee, W.T., 1916, Relation of the Cretaceous formations to the Rocky Mountains in Colorado and New Mexico: U.S. Geological Survey Professional Paper 95-C, p. 27–58. https://doi.org/10.3133/pp95C

Lee, W.T., and Girty, G.H., 1909, The Manzano group of the Rio Grande valley, New Mexico: U.S. Geologic Survey Bulletin 389, 141 p. https://doi.org/10.3133/b389

Lerner, A.J., Lucas, S.G., Spielmann, J.A., Krainer, K., Dimichele, W.A., Chaney, D.S., Schneider, J.W., Nelson, W.J., and Ivanov, A., 2009, The biota and paleoecology of the upper Pennsylvanian (Missourian) Tinajas locality, Socorro County, New Mexico, *in* Lueth, V., Lucas, S.G., and Chamberlin, R.M., eds., Geology of the Chupadera Mesa: New Mexico Geological Society Fall Field Conference Guidebook 60, p. 267–280. https://doi.org/10.56577/FFC-60.267

Linden, R.M., 1990, Allochthonous Permian rocks in the Socorro region, central New Mexico—A structural analysis of emplacement and deformation [PhD dissertation]: Socorro, New Mexico Institute of Mining and Technology, 104 p.

Long, K.R., van Gosen, B.S., Foley, N.K. and Cordier, D., 2010, The principal rare earth elements deposits of the United States—A summary of domestic deposits and a global perspective: U.S. Geological Survey Scientific Investigations Report 2010-5220, 104 p.

Loughlin, G.F., and Koschmann, A.H., 1942, Geology and ore deposits of the Magdalena mining district, New Mexico: U.S. Geological Survey Professional Paper 200, 168 p. https://doi.org/10.3133/pp200

Lovejoy, E.M.P., 1976, Geology of Cerro de Cristo Rey Uplift, Chihuahua and New Mexico: New Mexico Bureau of Mines and Mineral Resources Memoir 31, 82 p. https://doi.org/10.58799/M-31

Lozinsky, R.P., and Tedford, R.H., 1991, Geology and paleontology of the Santa Fe Group, southwestern Albuquerque Basin, Valencia County, New Mexico: New Mexico Bureau of Mines and Mineral Resources Bulletin 132, 35 p. https://doi.org/10.58799/B-132

Lucas, S.G., 1991, Triassic stratigraphy, paleontology and correlation, south-central New Mexico, *in* Barker, J.M., Kues, B.S., Austin, G.S., and Lucas, S.G., eds., Geology of the Sierra Blanca, Sacramento, and Capitan Ranges, New Mexico: New Mexico Geological Society Fall Field Conference Guidebook 42, p. 243–259. https://doi.org/10.56577/FFC-42.243

Lucas, S.G., 1993, The Chinle Group—Revised stratigraphy and biochronology of Upper Triassic nonmarine strata in the western United States: Museum of Northern Arizona Bulletin 59, p. 27–50.

Lucas, S.G., 2004, The Triassic and Jurassic systems in New Mexico, *in* Mack, G.H., and Giles, K.A., eds., The Geology of New Mexico—A geologic history: New Mexico Geological Society Special Publication 11, p. 137–152. https://doi.org/10.56577/SP-11

Lucas, S.G., and Anderson, O.J., 1998, Corals from the Upper Cretaceous of south-central New Mexico, *in* Mack, G.H., Austin, G.S., and Barker, J.M., eds., Las Cruces Country II: New Mexico Geological Society Fall Field Conference Guidebook 49, p. 205–207. https://doi.org/10.56577/FFC-49.205

Lucas, S.G., and Estep, J.W., 2000, Pennsylvanian selachians from the Cerros de Amado, central New Mexico, *in* Lucas, S.G., ed., New Mexico's fossil record 2: New Mexico Museum of Natural History and Science Bulletin 16, p. 21–27.

Lucas, S.G., and Hayden, S.N., 1991, Type section of the Permian Bernal Formation and the Permian–Triassic boundary in north-central New Mexico: New Mexico Geology, v. 13, no. 1, p. 9–15. https://doi.org/10.58799/NMG-v13n1.9

Lucas, S.G., and Krainer, K., 2004, The Red Tanks Member of the Bursum Formation in the Lucero Uplift and regional stratigraphy of the Bursum Formation in New Mexico, *in* Lucas, S.G., and Zeigler, K.E., eds., Carboniferous-Permian transition at Carrizo Arroyo, central New Mexico: New Mexico Museum of Natural History and Science Bulletin 25, p. 43–52.

Lucas, S.G., and Krainer, K., 2009, Pennsylvanian stratigraphy in the northern Oscura Mountains, Socorro County, New Mexico, *in* Lueth, V., Lucas, S.G., and Chamberlin, R.M., eds., Geology of the Chupadera Mesa: New Mexico Geological Society Fall Field Conference Guidebook 60, p. 153–166. https://doi.org/10.56577/FFC-60.153

Lucas, S.G., and Krainer, K., 2017, The Permian System east of Socorro, central New Mexico (USA), *in* Lucas, S.G., DiMichele, W.A. and Krainer, K., eds., Carboniferous-Permian transition in Socorro County, New Mexico: New Mexico Museum of Natural History and Science Bulletin 77, p. 231–261.

Lucas, S.G., and Tanner, L.H., 2021, Late Pennsylvanian calcareous paleosols from central New Mexico—Implications for paleoclimate: New Mexico Geology, v. 43, no. 1, p. 3–9. https://doi.org/10.58799/NMG-v43n1.3

Lucas, S.G., and Williamson, T.E., 1993, Eocene vertebrates and late Laramide stratigraphy of New Mexico, *in* Lucas, S.G., and Zidek, J., eds., Vertebrate paleontology in New Mexico: New Mexico Museum of Natural History and Science Bulletin, v. 2, p. 145–158.

Lucas, S.G., and Zeigler, K.E., 2004, Permian stratigraphy in the Lucero Uplift, central New Mexico, *in* Lucas, S.G., and Zeigler, K.E., eds., Carboniferous-Permian transition at Carrizo Arroyo, central New Mexico: New Mexico Museum of Natural History and Science Bulletin 25, p. 71–82.

Lucas, S.G., Hunt, A.P., and Kues, B.S., 1987, Stratigraphic nomenclature and correlation chart for northeastern New Mexico, *in* Clemons, R.E., King, W.E., Mack, G.H., and Zidek, J., eds., Northeastern New Mexico: New Mexico Geological Society Fall Field Conference Guidebook 38, p. 351–354. https://doi.org/10.56577/FFC-38.351

Lucas, S.G., Krainer, K., and Kues, B.S., 2002, Type section of the upper Carboniferous Bursum Formation, south-central New Mexico, and the Bursumian Stage, *in* Lueth, V.W., Giles, K.A., Lucas, S.G., Kues, B.S., Myers, R., and Ulmer-Scholle, D.S., eds., Geology of White Sands: New Mexico Geological Society Fall Field Conference Guidebook 53, p. 179–192. https://doi.org/10.56577/FFC-53.179

Lucas, S.G., Krainer, K., and Colpitts, Jr., R.M., 2005, Abo-Yeso (Lower Permian) stratigraphy in central New Mexico, *in* Lucas, S.G., Zeigler, K.E., and Spielmann, J.A., eds., The Permian of Central New Mexico: New Mexico Museum of Natural History and Science Bulletin 31, p. 101–117.

Lucas, S.G., Krainer, K. and Barrick, J.E., 2009a, Pennsylvanian stratigraphy and conodont biostratigraphy in the Cerros de Amado, Socorro County, New Mexico, *in* Lueth, V., Lucas, S.G., and Chamberlin, R.M., eds., Geology of the Chupadera Mesa: New Mexico Geological Society Fall Field Conference Guidebook 60, p. 183–212. https://doi.org/10.56577/FFC-60.183

Lucas, S.G., Dimichele, W.A., Krainer, K., Chaney, D.S., and Spielmann, J.A., 2009b, A coal-measure forest near Socorro, New Mexico, *in* Lueth, V., Lucas, S.G., and Chamberlin, R.M., eds., Geology of the Chupadera Mesa: New Mexico Geological Society Fall Field Conference Guidebook 60, p. 235–242. https://doi.org/10.56577/FFC-60.235

Lucas, S.G., Cather, S.M., Chamberlin, R.M., Lueth, V.W., Krainer, K., and Spielmann, J., 2009c, Quebradas country—Second-day road log from Socorro to Buffalo Well via Arroyo de la Parida and Cañoncito de la Uva, *in* Lueth, V., Lucas, S.G., and Chamberlin, R.M., eds., Geology of the Chupadera Mesa: New Mexico Geological Society Fall Field Conference Guidebook 60, p. 47–74. https://doi.org/10.56577/FFC-60.47

Lucas, S.G., Krainer, K., Chaney, D.S., DiMichele, W.A., Voigt, S., Berman, D.S., and Henrici, A.C., 2013a, The Lower Permian Abo Formation in central New Mexico, *in* Lucas, S.G., Nelson, J.W., DiMichele, W.A., Spielmann, J.A., Krainer, K., Barrick, J.E., Elrick, S., and Voigt, S., eds., The Carboniferous-Permian transition in central New Mexico: New Mexico Museum of Natural History and Science Bulletin 59, p. 161–180.

Lucas, S.G., Krainer, K., and Voigt, S., 2013b, The Lower Permian Yeso Group in central New Mexico, *in* Lucas, S.G., Nelson, J.W., DiMichele, W.A., Spielmann, J.A., Krainer, K., Barrick, J.E., Elrick, S., and Voigt, S., eds., The Carboniferous-Permian transition in central New Mexico: New Mexico Museum of Natural History and Science Bulletin 59, p. 181–199.

Lucas, S.G., Krainer, K., and Brose, R.J., 2013c, The Lower Permian Glorieta Sandstone in central New Mexico, *in* Lucas, S.G., Nelson, J.W., DiMichele, W.A., Spielmann, J.A., Krainer, K., Barrick, J.E., Elrick, S., and Voigt, S., eds., The Carboniferous-Permian transition in central New Mexico: New Mexico Museum of Natural History and Science, Bulletin 59, p. 201–211.

Lucas, S.G., Krainer, K., Oviatt, S.G., Vachard, D., Berman, D.S., and Henrici, A.C., 2016a, The Permian System at Abo Pass, central New Mexico, (USA), *in* Frey, B.A., Karlstrom, K.E., Lucas, S.G., Williams, S., Zeigler, K., McLemore, V., and Ulmer-Scholle, D.S., eds., Geology of the Belen Area: New Mexico Geological Society Fall Field Conference Guidebook 67, p. 313–350. https://doi.org/10.56577/FFC-67.313

Lucas, S.G., Allen, B.D., and Love, D.W., 2016b, Triassic-Jurassic stratigraphy on the Becker SW quadrangle and vicinity, Socorro County, New Mexico, *in* Frey, B.A., Karlstrom, K.E., Lucas, S.G., Williams, S., Zeigler, K., McLemore, V., and Ulmer-Scholle, D.S., eds., Geology of the Belen Area: New Mexico Geological Society Fall Field Conference Guidebook 67, p. 27–31. https://doi.org/10.56577/FFC-67

Lucas, S.G., Nelson, W.J., Krainer, K., and Elrick, S.D., 2019, The Cretaceous System in central Sierra County, New Mexico: New Mexico Geology, v. 41, no. 1, p. 3–39. https://doi.org/10.58799/NMG-v41n1.3

Lucas, S.G., Krainer, K., Barrick, J.E., Allen, B.D., and Nelson, W.J., 2022a, Pennsylvanian stratigraphy and biostratigraphy in the Cerros de Amado, Socorro County, New Mexico, *in* Koning, D.J., Hobbs, K.M., Phillips, F.M., Nelson, W.J., Cather, S.M., Jakle, A.C., and Van Der Werff, B., eds., Socorro Region III: New Mexico Geological Society Fall Field Conference Guidebook 72, p. 147–164. https://doi.org/10.56577/FFC-72.147

Lucas, S.G., Krainer, K., and Nelson, W.J., 2022b, Permian stratigraphy east of Socorro, central New Mexico, *in* Koning, D.J., Hobbs, K.M., Phillips, F.M., Nelson, W.J., Cather, S.M., Jakle, A.C., and Van Der Werff, B., eds., Socorro Region III: New Mexico Geological Society Fall Field Conference Guidebook 72, p. 187–201. https://doi.org/10.56577/FFC-72.187

Lueth, V., Lucas, S.G., and Chamberlin, R.M., eds., 2009, Geology of the Chupadera Mesa: New Mexico Geological Society Fall Field Conference Guidebook 60, 438 p. https://doi.org/10.56577/FFC-60

Lundin, E.R., 1992, Thin-skinned extensional tectonics on a salt detachment, northern Kwanza Basin, Angola: Marine and Petroleum Geology, v. 9, no. 4, p. 405–411. https://doi.org/10.1016/0264-8172(92)90051-F

Lynds, R.M., and Slattery, J.S., 2017, Correlation of Upper Cretaceous strata of Wyoming: Wyoming Geological Survey Stratigraphic Chart, Open-File Report 2017-3.

Machette, M.N., and Chamberlin, R.M., compilers, 2015, Fault number 2108b, Socorro Canyon fault zone, southern section, *in* Quaternary fault and fold database of the United States, U.S. Geological Survey: https://earthquakes.usgs.gov/hazards/qfaults (accessed July 2017).

Mack, G.H., and Bauer, E.M., 2014, Depositional environments, sediment dispersal, and provenance of the early Permian (Leonardian) Glorieta Sandstone, central New Mexico, *in* Rawling, G., McLemore, V.T., Timmons, S., and Dunbar, N., eds., Geology of the Sacramento Mountains Region: New Mexico Geological Society Fall Field Conference Guidebook 65, p. 261–271. https://doi.org/10.56577/FFC-65.261

Mack, G.H., and Dinterman, P.A., 2002, Depositional environments and paleogeography of the Lower Permian (Leonardian) Yeso and correlative formations in New Mexico: The Mountain Geologist, v. 39, p. 75–88.

Mack, G.H., McIntosh, W.C., Leeder, M.R., and Monger, H.C., 1996, Plio-Pleistocene pumice floods in the ancestral Rio Grande, southern Rio Grande rift, USA: Sedimentary Geology, v. 103, no. 1–2, p. 1–8. https://doi.org/10.1016/0037-0738(96)00009-7

Mack, G.H., Cole, D.R, and Treviño, L., 2000, The distribution and discrimination of shallow, authigenic carbonate in the Pliocene–Pleistocene Palomas Basin, southern Rio Grande rift: Geological Society of America Bulletin, v. 112, no. 5, p. 643–656. https://doi.org/10.1130/0016-7606(2000)112%3C643:TDADOS%3E2.0.CO;2

Mack, G.H., Hook, S., Giles, K.A., and Cobban, W.A., 2016, Sequence stratigraphy of the Mancos Shale, lower Tres Hermanos Formation, and coeval middle Cenomanian to middle Turonian strata, southern New Mexico, USA: Sedimentology, v. 63, no. 4, p. 781–808. https://doi.org/10.1111/sed.12238

MacKevett, Jr., E.M., 1963, Geology and ore deposits of the Bokan Mountain uranium-thorium area, southeastern Alaska: U.S. Geological Survey Bulletin 1154, 134 p. https://doi.org/10.3133/b1154

Mardirosian, C.A., 1971, Mining districts and mineral deposits of New Mexico (exclusive of oil and gas): Salt Lake City, Utah, Charles A. Mardirosian, scale 1:1,000,000.

Martinez, L.B., 1981, Coal, *in* Arnold, E.C., and Hill, J.M., compilers, New Mexico's energy resources '81—Annual report of Bureau of Geology in the Mining and Minerals Division of New Mexico Energy and Minerals Department: New Mexico Energy and Minerals Department, p. 43–44.

Mathews, G.W., 1978, Uranium occurrences in and related to plutonic igneous rocks, *in* Mickle, D.G., and Mathews, G.W., eds., Geological characteristics of environments favorable for uranium deposits: U.S. Department of Energy Report GJBX-67(78), p. 121–180.

Mauduit, T., Guerin, G., Brun, J.-P., and Lecanu, H., 1997, Raft tectonics—The effects of basal slope angle and sedimentation rate on progressive extension: Journal of Structural Geology, v. 19, no. 9, p. 1219–1230. https://doi.org/10.1016/S0191-8141(97)00037-0

Maulsby, J., 1981, Geology of the Rancho de Lopez area east of Socorro, New Mexico [MS thesis]: Socorro, New Mexico Institute of Mining and Technology, 85 p.

McAnulty, W.N., 1978, Fluorspar in New Mexico: New Mexico Bureau of Mines and Mineral Resources Memoir 34, 64 p. https://doi.org/10.58799/M-34

McGrath, D.B., and Hawley, J.W., 1987, Geomorphic evolution and soil-geomorphic relationships in the Socorro area, central New Mexico, *in* McLemore, V.T., and Bowie, M.R., eds., Guidebook to the Socorro area: New Mexico Bureau of Mines and Mineral Resources, p. 55–67.

McIntosh, W.C., and Bryan, C., 2000, Chronology and geochemistry of the Boot Heel volcanic field, New Mexico, *in* Lawton, T.F., McMillan, N.J., and McLemore, V.T., eds., Southwest Passage—A trip through the Phanerozoic: New Mexico Geological Society Fall Field Conference Guidebook 51, p. 157–174. https://doi.org/10.56577/FFC-51.157

McIntosh, W.C., Kedzie, L.L., and Sutter, J.F., 1991, Paleomagnetism and $^{40}Ar/^{39}Ar$ ages of ignimbrites, Mogollon–Datil volcanic field, southwestern New Mexico: New Mexico Bureau of Mines and Mineral Resources Bulletin 135, 79 p. https://doi.org/10.58799/B-135

McLemore, V.T., 1983a, Uranium in the Socorro area, *in* Chapin, C.E., and Callender, J.F., eds., Socorro Region II: New Mexico Geological Society Fall Field Conference Guidebook 34, p. 227–233. https://doi.org/10.56577/FFC-34.227

McLemore, V.T., 1983b, Uranium and thorium occurrences in New Mexico—Distribution, geology, production, and resources, with selected bibliography: New Mexico Bureau of Mines and Mineral Resources Open-File Report 183, 950 p. https://doi.org/10.58799/OFR-183

McLemore, V.T., 1999, La Bajada uranium-base metal deposit, Santa Fe County, New Mexico, *in* Pazzaglia, F.J., and Lucas, S.G., eds., Albuquerque Geology: New Mexico Geological Society Fall Field Conference Guidebook 50, p. 445–448. https://doi.org/10.56577/FFC-50.445

McLemore, V.T., 2017, Mining districts and prospect areas of New Mexico: New Mexico Bureau of Geology and Mineral Resources Resource Map 24, scale 1:1,000,000, 65 p. https://doi.org/10.58799/RM-24

McLemore, V.T., and Austin, G.S., 2017, Industrial minerals and rocks, *in* McLemore, V.T., Timmons, S., and Wilks, M., eds., Energy and Mineral Deposits in New Mexico: New Mexico Bureau of Geology and Mineral Resources Memoir 50/New Mexico Geological Society Special Publication 13, 115 p. https://doi.org/10.58799/M-50E

McLemore, V.T., and Chenoweth, W.L., 1989, Uranium resources in New Mexico: New Mexico Bureau of Mines and Minerals Resources Resource Map 18, scale 1:1,000,000, 36 p. https://doi.org/10.58799/RM-18

McLemore, V.T., and Chenoweth, W.C., 2017, Uranium resources, *in* McLemore, V.T., Timmons, S., and Wilks, M., eds., Energy and Mineral Deposits in New Mexico: New Mexico Bureau of Geology and Mineral Resources Memoir 50/New Mexico Geological Society Special Publication 13, 67 p. https://doi.org/10.58799/M-50C

McLemore, V.T., and Lueth, V., 2017, Metallic mineral deposits, *in* McLemore, V.T., Timmons, S., and Wilks, M., eds., Energy and Mineral Deposits in New Mexico: New Mexico Bureau of Geology and Mineral Resources Memoir 50/New Mexico Geological Society Special Publication 13, 79 p. https://doi.org/10.58799/M-50D

McLemore, V.T., Giordano, T.H., Lueth, V., and Witcher, J., 1998, Origin of barite-fluorite-galena deposits in the southern Rio Grande rift, New Mexico, *in* Mack, G.H., Austin, G.S., and Barker, J.M., eds., Las Cruces Country II: New Mexico Geological Society Fall Field Conference Guidebook 49, p. 251–263. https://doi.org/10.56577/FFC-49.251

McLemore, V.T., Hoffman, G., Smith, M., Mansell, M., and Wilks, M., 2005a, Mining districts of New Mexico: New Mexico Bureau of Geology and Mineral Resources Open-File Report 494, 1 sheet plus CD-ROM. https://doi.org/10.58799/OFR-494

McLemore, V.T., Krueger, C.B., Johnson, P., Raugust, J.S., Jones, G.E., Hoffman, G.K., and Wilks, M., 2005b, New Mexico Mines Database: Society of Mining, Exploration, and Metallurgy, and Mining Engineering, February, p. 42–47.

Mine Inspector for the Territory of New Mexico, 1894–1911, Annual reports to the Secretary of the Interior.

Mineral resources of the U.S., Calendar years 1883 and 1884, Albert Williams, Jr., Washington, D.C., Government Printing Office, p. 56, 170.

Mineral resources of the U.S. Calendar year 1887, 1888, David T. Day, Chief of Division of Mining and Statistics and Tech., Washington, D.C., Government Printing Office, p. 385.

Molenaar, C.M., 1974, Correlation of the Gallup Sandstone and associated formations, Upper Cretaceous, eastern San Juan and Acoma Basins, New Mexico, *in* Siemers, C.T., Woodward, L.A., and Callender, J.F., eds., Ghost Ranch: New Mexico Geological Society Fall Field Conference Guidebook 25, p. 251–258. https://doi.org/10.56577/FFC-25.251

Molenaar, C.M., 1983a, Major depositional cycles and regional correlations of Upper Cretaceous rocks, southern Colorado Plateau and adjacent areas: Rocky Mountain Section, Society of Economic Paleontologists and Mineralogists, p. 201–224.

Molenaar, C.M., 1983b, Principal reference section and correlation of Gallup Sandstone, northwestern New Mexico, *in* Hook, S.C., ed., Contributions to mid-Cretaceous paleontology and stratigraphy of New Mexico, Part II: New Mexico Bureau of Mines and Mineral Resources Circular 185, p. 29–47. https://doi.org/10.58799/C-185

Molenaar, C.M., and Baird, J.K., 1991, Stratigraphic cross sections of Upper Cretaceous rocks in the northern San Juan Basin, Southern Ute Indian Reservation, southwestern Colorado, *in* Zech, R.S., ed., Geologic framework and stratigraphy of Cretaceous and Tertiary rocks of the Southern Ute Indian Reservation, southwestern Colorado: U.S. Geological Survey Professional Paper 1505-C, 12 p. https://doi.org/10.3133/pp1505BC

Molenaar, C.M., Cobban, W.A., Merewether, E.A., Pillmore, C.L., Wolf, D.G., and Holbrook, J.M., 2002, Regional stratigraphic cross sections of Cretaceous rocks from east-central Arizona to the Oklahoma Panhandle: U.S. Geological Survey Miscellaneous Field Studies Map MF-2382.

Montañez, I.P., and Poulsen, C.J., 2013, The late Paleozoic ice age—An evolving paradigm: Annual Reviews of Earth and Planetary Sciences, v. 41, p. 629–656. https://doi.org/10.1146/annurev.earth.031208.100118

Moore, S.L., Turner, R.L., Blank, Jr., H.R., and Korzeb, S.L., 1988, Mineral resources of the Sierra de las Cañas wilderness study area, Socorro County, New Mexico: U.S. Geological Survey Bulletin 1734-D, 26 p. https://doi.org/10.3133/b1734D

Morgan, G.S., Lucas, S.G., and Love, D.W., 2009, Cenozoic vertebrates from Socorro County, central New Mexico, *in* Lueth, V., Lucas, S.G., and Chamberlin, R.M., eds., Geology of the Chupadera Mesa: New Mexico Geological Society Fall Field Conference Guidebook 60, p. 321–336. https://doi.org/10.56577/FFC-60.321

Murphy, J.W., Lucas, S.G., and Spielmann, J.A., 2007, Upper Cenomanian selachian assemblage from the Bridge Creek Member of the Mancos Shale, Socorro County, New Mexico [abstract]: New Mexico Geological Society Annual Spring Meeting, April 13, 2007, Macey Center, New Mexico Institute of Mining and Technology, Socorro, NM. https://doi.org/10.56577/SM-2007.2695

Needham, C.E., and Bates, R.L., 1943, Permian type sections in central New Mexico: Geological Society of America Bulletin, v. 54, no. 11, p. 1653–1668. https://doi.org/10.1130/GSAB-54-1653

Nelson, W.J., Lucas, S.G., Krainer, K., and Elrick, S.G., 2013, The Gray Mesa Formation (Middle Pennsylvanian) in New Mexico, *in* Lucas, S.G., Nelson, J.W., DiMichele, W.A., Spielmann, J.A., Krainer, K., Barrick, J.E., Elrick, S., and Voigt, S., eds., The Carboniferous-Permian transition in central New Mexico: New Mexico Museum of Natural History and Science Bulletin 59, p. 101–122.

Nelson, W.J., Elrick, S.D., Krainer, K., and Lucas, S.G., 2017, Facies changes in the Bursum Formation (Pennsylvanian–Permian) related to tectonic activity, Socorro area, New Mexico, *in* Lucas, S.G., DiMichele, W.A., and Krainer, K., eds., Carboniferous-Permian transition in Socorro County, New Mexico: New Mexico Museum of Natural History and Science Bulletin 77, p. 309–320.

Nickelson, H., 1979, Memoranda to the New Mexico Bureau of Mines and Mineral Resources, Reclamation evaluation for OSM, Abandoned Mine Lands Survey, Carthage field, unpublished notes, v. 2, p. 56–93.

NMBGMR, 2003, Geologic map of New Mexico: New Mexico Bureau of Geology and Mineral Resources, scale 1:500,000, 2 sheets. https://doi.org/10.58799/116894

North, R.M., and McLemore, V.T., 1986, Silver and gold occurrences in New Mexico: New Mexico Bureau of Mines and Mineral Resources Resource Map 15, scale 1:1,000,000, 32 p. https://doi.org/10.58799/RM-15

North, R.M., and McLemore, V.T., 1988, A classification of the precious metal deposits of New Mexico, *in* Bulk mineable precious metal deposits of the western United States symposium volume: Geological Society of Nevada, Reno, Symposium held April 6–8, 1987, p. 625–660.

North American Commission on Stratigraphic Nomenclature, 2005, North American stratigraphic code: American Association of Petroleum Geologists Bulletin, v. 89, no. 11, p. 1547–1591. https://doi.org/10.1306/07050504129

Nummedal, D., and Molenaar, C.M., 1995, Sequence stratigraphy of ramp-setting strand plain successions—The Gallup Sandstone, New Mexico; *in* Van Wagoner, J.C., and Bertram, G.T., eds., Sequence stratigraphy of foreland basin deposits from the Cretaceous of North America: American Association of Petroleum Geologists Memoir 64, p. 277–310.

Osburn, J.C., 1983, Coal resources of Socorro County, New Mexico, *in* Chapin, C.E., and Callender, J.F., eds., Socorro Region II: New Mexico Geological Society Fall Field Conference Guidebook 34, p. 223–226. https://doi.org/10.56577/FFC-34.223

Osburn, J.C., 1984, Geology of Pueblo Viejo Mesa quadrangle, Socorro and Cibola Counties, New Mexico: New Mexico Bureau of Mines and Mineral Resources Geologic Map 55, scale 1:24,000. https://doi.org/10.58799/GM-55

Osburn, G.R., and Chapin, C.E., 1983, Nomenclature for Cenozoic rocks of northeastern Mogollon–Datil volcanic field, New Mexico: New Mexico Bureau of Mines and Mineral Resources Stratigraphic Chart 1, 7 p., 1 sheet. https://doi.org/10.58799/SC-1

Otte, Jr., C., 1959, Late Pennsylvanian and early Permian stratigraphy of the northern Sacramento Mountains, Otero County, New Mexico: New Mexico Bureau of Mines and Mineral Resources Bulletin 50, 111 p. https://doi.org/10.58799/B-50

Partey, F., Lev, S., Casey, R., Widom, E., Lueth, V.W., and Rakovan, J., 2009, Source of fluorine and petrogenesis of the Rio Grande rift-type barite-fluorite-galena deposits: Economic Geology, v. 104, no. 4, p. 505–520. https://doi.org/10.2113/gsecongeo.104.4.505

Penge, J., Munns, J.W., Taylor, B., and Windle, T.M.F., 1999, Rift–raft tectonics—Examples of gravitational tectonics from the Zechstein basins of northwest Europe, *in* Fleet, A.J., and Boldy, S.A.R., eds., Petroleum geology of northwest Europe—Proceedings of the 5th conference: London, Geological Society Petroleum Geology Conference Series, v. 5, p. 201–213. https://doi.org/10.1144/0050201

Peterson, F., and Kirk, A.R., 1977, Correlation of the Cretaceous rocks in the San Juan, Black Mesa, Kaiparowits and Henry Basins, southern Colorado Plateau, *in* Fassett, J.E., and James, H.L., eds., San Juan Basin III: New Mexico Geological Society Fall Field Conference Guidebook 28, p. 167–178. https://doi.org/10.56577/FFC-28.167

Phillips, J.S., 1960, Sandstone-type copper deposits of the western United States [PhD dissertation]: Cambridge, Harvard University, 320 p.

Phillips, F.M., and Sion, B.D., 2022, Geomorphic surfaces of the Rio Grande valley in the vicinity of Socorro, New Mexico, *in* Koning, D.J., Hobbs, K.M., Phillips, F.M., Nelson, W.J., Cather, S.M., Jakle, A.C., and Van Der Werff, B., eds., Socorro Region III: New Mexico Geological Society Fall Field Conference Guidebook 72, p. 281–293. https://doi.org/10.56577/FFC-72.281

Pierson, C.T., Wenrich, K.J., Hannigan, B.J., and Machette, M.N., 1982, National Uranium Resource Evaluation, Socorro quadrangle, New Mexico: U.S. Department of Energy NURE report PGJ/F-068(82), 45 p.

Pike, W.S., 1947, Intertonguing marine and nonmarine Upper Cretaceous deposits of New Mexico, Arizona, and southwestern Colorado: Geological Society of America Memoir 24, 103 p. https://doi.org/10.1130/MEM24-p1

Pilcher, R.S., Murphy, R.T, and McDonough Ciosek, J., 2014, Jurassic raft tectonics in the northeastern Gulf of Mexico: Interpretation, v. 2, no. 4, SM39–SM55. https://doi.org/10.1190/INT-2014-0058.1

Planner, H.N., Fuka, M.A., Hanks, D.E., Hansel, J.M., Minor, M.M., Montoya, J.D., and Sandoval, W.F., 1981, Uranium hydrogeochemical and stream sediment reconnaissance for the Socorro NTMS quadrangle, New Mexico, including concentrations of forty-two additional elements: Los Alamos Scientific Laboratory Informal Report LA-8001-MS/U.S. Department of Energy NURE report GJBX-12(81), 145 p.

Pollock, C.J., Stewart, K.G., Hibbard J.P., Wallace, L., and Giral, R.A., 2004, Thrust wedge tectonics and strike-slip faulting in the Sierra Nacimiento, *in* Cather, S.M., Kelley, S.A., and McIntosh, W.C., eds., Tectonics, geochronology, and volcanism in the southern Rocky Mountains and the Rio Grande rift: New Mexico Bureau of Geology and Mineral Resources Bulletin 160, p. 97–111. https://doi.org/10.58799/B-160

Potter, S.C., 1970, Geology of Baca Canyon, Socorro County, New Mexico [MS thesis]: Tucson, University of Arizona, 54 p.

Pray, L.C., 1961, Geology of the Sacramento Mountains escarpment, Otero County, New Mexico: New Mexico Bureau of Mines and Mineral Resources Bulletin 35, 144 p. https://doi.org/10.58799/B-35

Rankin, C.H., 1944, Stratigraphy of the Colorado Group, Upper Cretaceous, in northern New Mexico: New Mexico Bureau of Mines and Mineral Resources Bulletin 20, 30 p. https://doi.org/10.58799/B-20

Read, A.S., Cather, S.M., Chamberlin, R.M., Connell, S.D., and Karlstrom, K.E., 2007, Preliminary geologic map of the Ladron Peak quadrangle, Socorro County, New Mexico: New Mexico Bureau of Geology and Mineral Resources Open-File Geologic Map 142, scale 1:24,000. https://doi.org/10.58799/OF-GM-142

Rejas, A., 1965, Geology of the Cerros de Amado area, Socorro County, New Mexico [MS thesis]: Socorro, New Mexico Institute of Mining and Technology, 128 p.

Reneau, S.L., and Dethier, D.P., 1996, Pliocene and Quaternary history of the Rio Grande, White Rock Canyon and vicinity, New Mexico, *in* Goff, F., Kues, B.S., Rogers, M.A., McFadden, L.D., and Gardner, J.N., eds, Jemez Mountains Region: New Mexico Geological Society Fall Field Conference Guidebook 47, p. 317–324. https://doi.org/10.56577/FFC-47.317

Ricketts, J.W., Kelley, S.A., Karlstrom, K.E., Schmandt, B., Donahue, M.S., and van Wijk, J., 2016, Synchronous opening of the Rio Grande rift ~20–10 Ma supported by apatite (U-Th)/He and fission-track thermochronology, and evaluation of possible driving mechanisms: Geological Society of America Bulletin, v. 128, no. 3–4, p. 397–424. https://doi.org/10.1130/B31223.1

Rothrock, H.E., Johnson, C.H., and Hahn, A.D., 1946, Fluorspar resources in New Mexico: New Mexico Bureau of Mines and Mineral Resources Bulletin 21, 245 p. https://doi.org/10.58799/B-21

Sanford, A.R., 1968, Gravity survey in central Socorro County, New Mexico: New Mexico Bureau of Mines and Mineral Resources Circular 91, 14 p. https://doi.org/10.58799/C-91

Schneider, J.W., Lucas, S.G., and Scholze, F., 2017, Late Pennsyslvanian Blattodea (Insecta) from near Socorro, New Mexico, *in* Lucas, S.G., DiMichele, W.A., and Krainer, K., eds., Carboniferous-Permian transition in Socorro County, New Mexico: New Mexico Museum of Natural History and Science Bulletin 77, p. 321–332.

Schweitzer, C.E., Feldmann, R.M., Kues, B.S., and Bridge, E.K., 2017, New Decapoda (Axiidea, Anomura, Brachyura) from the Turonian of New Mexico, USA: Neues Jahrbuch für Geologie und Paläontologie, v. 284, p. 89–115.

Scott, L.A., Elrick, M., Connell, S., and Karlstrom, K., 2005, Preliminary geologic map of the Scholle quadrangle, Valencia, Torrance, and Socorro Counties, New Mexico: New Mexico Bureau of Geology and Mineral Resources Open-File Geologic Map 99, scale 1:24,000. https://doi.org/10.58799/OF-GM-99

Seager, W.R., and Mack, G.H., 1998, Geology of the McLeod Tank quadrangle, Sierra and Doña Counties, New Mexico: New Mexico Bureau of Mines and Mineral Resources Geologic Map 77, scale 1:24,000. https://doi.org/10.58799/GM-77

Seager, W.R., and Mack, G.H., 2003, Geology of the Caballo Mountains, New Mexico: New Mexico Bureau of Geology and Mineral Resources Memoir 49, 135 p. https://doi.org/10.58799/M-49

Sealey, P.L., and Lucas, S.G., 2019, Late Cretaceous (Cenomanian-Campanian) ammonite systematic paleontology and biostratigraphy, southeastern San Juan Basin, Sandoval County, New Mexico: New Mexico Museum of Natural History and Science Bulletin 80, 245 p.

Siemers, W.T., 1978, The stratigraphy, petrology, and paleoenvironments of Pennsylvanian rocks in west-central New Mexico [PhD dissertation]: Socorro, New Mexico Institute of Mining and Technology, 275 p.

Siemers, W.T., 1983, The Pennsylvanian System, Socorro region, New Mexico—Stratigraphy, petrology, depositional environments, *in* Chapin, C.E., and Callender, J.F., eds., Socorro Region II: New Mexico Geological Society Fall Field Conference Guidebook 34, p 147–755. https://doi.org/10.56577/FFC-34.147

Sion, B.D., Phillips, F.M., Axen, G.J., Harrison, J.B.J., Love, D.W., and Zimmerer, M.J., 2020, Chronology of terraces in the Rio Grande rift, Socorro Basin, New Mexico—Implications for terrace formation: Geosphere, v. 16, no. 6, p. 1457–1478. https://doi.org/10.1130/GES02220.1

Smith, C.T., 1961, Triassic and Jurassic rocks of the Albuquerque area, *in* Northrop, S.A., ed., Albuquerque Country: New Mexico Geological Society Fall Field Conference Guidebook 12, p. 121–128. https://doi.org/10.56577/FFC-12.121

Smith, C.T., 1983, Structural problems along the east side of the Socorro constriction, Rio Grande rift, *in* Chapin, C.E., and Callender, J.F., eds., Socorro Region II: New Mexico Geological Society Fall Field Conference Guidebook 34, p. 103–109. https://doi.org/10.56577/FFC-34.103

Smith, C.T., Osburn, G.R., Chapin, C.E., Hawley, J.W., Osburn, J.C., Anderson, O.J., Rosen, S.D., Eggleston, T.L., and Cather, S.M., 1983, First-day road log from Socorro to Mesa del Yeso, Joyita Hills, Johnson Hill, Cerros de Amado, Loma de las Cañas, Jornada del Muerto, Carthage, and return to Socorro, *in* Chapin, C.E., and Callender, J.F., eds., Socorro Region II: New Mexico Geological Society Fall Field Conference Guidebook 34, p. 1–28. https://doi.org/10.56577/FFC-34.1

Soulé, J.H., 1956, Reconnaissance of the "red bed" copper deposits in southeastern Colorado and New Mexico: U.S. Bureau of Mines Information Circular 7740, 74 p.

Spiegel, Z., and Baldwin, B., 1963, Geology and water resources of the Santa Fe area, New Mexico: U.S. Geological Survey Water Supply Paper 1525, 258 p. https://doi.org/10.3133/wsp1525

Spielmann, J.A., and Lucas, S.G., 2009, Triassic stratigraphy and biostratigraphy in Socorro County, New Mexico, *in* Lueth, V., Lucas, S.G., and Chamberlin, R.M., eds., Geology of the Chupadera Mesa: New Mexico Geological Society Fall Field Conference Guidebook 60, p. 213–226. https://doi.org/10.56577/FFC-60.213

Spielmann, J.A., Pence, R., and Lucas, S.G., 2009, A nearshore vertebrate assemblage from the Late Cretaceous (Turonian) Atarque Sandstone, Socorro County, New Mexico, *in* Lueth, V., Lucas, S.G., and Chamberlin, R.M., eds., Geology of the Chupadera Mesa: New Mexico Geological Society Guidebook 60, p. 315–320. https://doi.org/10.56577/FFC-60.315

Spradlin, E.J., 1976, Stratigraphy of Tertiary volcanic rocks, Joyita Hills area, Socorro County, New Mexico [MS thesis]: Albuquerque, University of New Mexico, 73 p.

Stanesco, J.D., 1991, Sedimentology and depositional environments of the lower Permian Yeso Formation, northwestern New Mexico: U.S. Geological Survey Bulletin 1808-M, 12 p. https://doi.org/10.3133/b1808M

State Inspector of Mines, 1912–1968, Annual reports to the Governor of the State of New Mexico.

Stephenson, L.W., 1952, Larger invertebrate fossils of the Woodbine Formation (Cenomanian) of Texas, with decapod crustaceans from the Woodbine Formation of Texas: U.S. Geological Survey Professional Paper 242, 225 p. https://doi.org/10.3133/pp242

Stewart, J.H., Poole, F.G., and Wilson, R.F., 1972, Stratigraphy and origin of the Chinle Formation and related Upper Triassic strata of the Colorado Plateau region, with a section on sedimentary petrology and a section on conglomerate studies: U.S. Geological Survey Professional Paper 690, 336 p. https://doi.org/10.3133/pp690

Tabet, D.E., 1979, Geology of the Jornada del Muerto coal field, Socorro County, New Mexico: New Mexico Bureau of Mines and Mineral Resources Circular 168, 20 p. https://doi.org/10.58799/C-168

Tait, D.B., Ahlen, J.L., Gordon, A., Scott, G.L., Mots, W.L., and Spitler, M.E., 1962, Artesia Group of New Mexico and west Texas: American Association of Petroleum Geologists Bulletin, v. 46, no. 4, p. 504–517. https://doi.org/10.1306/BC74383B-16BE-11D7-8645000102C1865D

Talmage, S.B., and Wootton, T.P., 1937, The non-metallic mineral resources of New Mexico and their economic features (exclusive of fuels): New Mexico Bureau of Mines and Mineral Resources Bulletin 12, 159 p. https://doi.org/10.58799/B-12

Tanner, L.H., and Lucas, S.G., 2012, Carbonate facies of the Ojo Huelos Member, San Pedro Arroyo Member (Chinle Group), southern New Mexico—Paleoclimatic implications: Sedimentary Geology, v. 273–274, p. 73–90. https://doi.org/10.1016/j.sedgeo.2012.07.001

Tanner, L.H., and Lucas, S.G., 2013, Gallery of geology—Late Triassic pisolites in Socorro County, New Mexico: New Mexico Geology, v. 35, no. 1, p. 21–22. https://doi.org/10.58799/NMG-v35n1.21

Thompson, M.L., 1942, Pennsylvanian System in New Mexico: New Mexico Bureau of Mines and Mineral Resources Bulletin 17, 92 p. https://doi.org/10.58799/B-17

Thompson, T.B., 1988, Geology and uranium-thorium mineral deposits of the Bokan Mountain Granite Complex, southeastern Alaska: Ore Geology Reviews, v. 3, no. 1–3, p. 193–210. https://doi.org/10.1016/0169-1368(88)90018-2

Tonking, W.H., 1957, Geology of Puertecito quadrangle, Socorro County, New Mexico: New Mexico Institute of Mining and Technology, State Bureau of Mines and Mineral Resources Bulletin 42, 67 p. https://doi.org/10.58799/B-41

Turner, C.E., and Peterson, F., 2004, Reconstruction of the Upper Jurassic Morrison Formation extinct ecosystem—A synthesis: Sedimentary Geology, v. 167, no. 3–4, p. 309–355. https://doi.org/10.1016/j.sedgeo.2004.01.009

USGenWeb Archives, 2001, Carthage Branch, San Antonio to Carthage, Socorro County, New Mexico, by John M. Meade: http://files.usgwarchives.net/nm/socorro/history/carthage.txt (accessed May 2016).

Vachard, D., Krainer, K., and Lucas, S.G., 2015, Kungurian (late early Permian) algae, microproblematica, and smaller foraminifers from the Yeso Group and San Andres Formation (New Mexico, USA): Palaeontologia Electronica, v. 18.1, 21A. https://doi.org/10.26879/433

Varnes, D.J., 1978, Slope movement types and processes, *in* Schuster, R.L., and Krizek, R.J., eds., Landslides—Analysis and control: Washington, D.C., National Academy of Science, Transportation and Road Research Board Special Report 176, p. 11–33.

Vila, J.-M., Youssef, M.B., Bouhlel, S., Ghanmi, M., Kassa, S., Miaadi, F., 1998, Tectonique en radeaux au toit d'un "glacier de sel" sous-marin albien de Tunisie du Nord-Ouest—Exemple du secteur minier de Gueurn Halfaya: Comptes Rendus de l'Académie des Sciences, Series IIA, v. 327, p. 563–570.

Voigt, S., and Lucas, S.G., 2017, Early Permian tetrapod footprints from central New Mexico, *in* Lucas, S.G., DiMichele, W.A., and Krainer, K., eds., Carboniferous-Permian transition in Socorro County, New Mexico: New Mexico Museum of Natural History and Science Bulletin 77, p. 333–352.

Weissmann, G.S., Hartley, A.J., Nichols, G.J., Scuderi, L.A., Olson, M., Buehler, H., and Banteah, R., 2010, Fluvial form in modern continental sedimentary basins—The distributive fluvial system (DFS) paradigm: Geology, v. 38, no. 1, p. 39–42. https://doi.org/10.1130/G30242.1

Williams, F.E., 1966, Fluorspar deposits of New Mexico: U.S. Bureau of Mines Information Circular 8307, 143 p.

Wilpolt, R.H., and Wanek, A.A., 1951, Geology of the region from Socorro and San Antonio east to Chupadera Mesa, Socorro County, New Mexico: U.S. Geological Survey Oil and Gas Investigations Map 121, scale 1:62,500, 2 sheets. https://doi.org/10.3133/om121

Wilpolt, R.H., MacAlpin, A.J., Bates, R.I., and Vorbe, G., 1946, Geologic map and stratigraphic sections of Paleozoic rocks of Joyita Hills, Los Pinos Mountains, and northern Chupadera Mesa, Valencia, Torrance, and Socorro Counties, New Mexico: U.S. Geological Survey Oil and Gas Investigations Preliminary Map 61, scale 1:63,360, 1 sheet. https://doi.org/10.3133/om61

Winchester, D.E., 1920, Geology of Alamosa Creek valley, Socorro County, New Mexico, with special reference to the occurrence of oil and gas: U.S. Geological Survey Bulletin 716-A, 15 p. https://doi.org/10.3133/b716A

Wolberg, D.L., 1985, Selachians from the Atarque Sandstone Member of the Tres Hermanos Formation (Upper Cretaceous: Turonian), Sevilleta Grant near La Joya, Socorro County, New Mexico, *in* Wolberg, D.L., ed., Contributions to Late Cretaceous paleontology and stratigraphy of New Mexico—Part I: New Mexico Bureau of Mines and Mineral Resources Circular 195, p. 7–19. https://doi.org/10.58799/C-195

Wood, G.H., and Northrop, S.A., 1946, Geology of the Nacimiento Mountains, San Pedro Mountain, and adjacent plateaus in parts of Sandoval and Rio Arriba Counties, New Mexico: U.S. Geological Survey Oil and Gas Investigations Map OM-57, scale 1:95,000. https://doi.org/10.3133/om57

Woodward, L.A., Anderson, O.J., and Lucas, S.G., 1999, Late Paleozoic right-slip faults in the ancestral Rocky Mountains, *in* Pazzaglia, F.J., and Lucas, S.G., eds., Albuquerque Geology: New Mexico Geological Society Fall Field Conference Guidebook 50, p. 149–154. https://doi.org/10.56577/FFC-50.149

Ye, H., Royden, L., Burchfiel, C., and Schuepbach, M., 1996, Late Paleozoic deformation of interior North America—The greater ancestral Rocky Mountains: American Association of Petroleum Geologists Bulletin, v. 80, no. 9, p. 1397–1432. https://doi.org/10.1306/64ED9A4C-1724-11D7-8645000102C1865D

Zeigler, K.E., and Allen, B.D., 2010, Geologic map of the Bull Gap quadrangle, Lincoln County, New Mexico: New Mexico Bureau of Geology and Mineral Resources Open-File Geologic Map 210, scale 1:24,000. https://doi.org/10.58799/OF-GM-210

APPENDIX I: $^{40}AR/^{39}AR$ AGES FROM CONGLOMERATE CLASTS, LAVAS, AND IGNIMBRITES IN THE SOUTHERN JOYITA HILLS AND THE BLACKINGTON HILLS AREA

Appendix 1 is available for download at **https://geoinfo.nmt.edu/publications/monographs/memoirs/51/**

APPENDIX 2: CHEMICAL ANALYSES OF SELECTED MINERALIZED SAMPLES

Appendix 2 is available for download at **https://geoinfo.nmt.edu/publications/monographs/memoirs/51/**

APPENDIX 3: SUMMARY OF PUBLISHED AND UNPUBLISHED DATA ON MINES AND MILLS WITHIN THE QUEBRADAS AREA

Appendix 3 is available for download at https://geoinfo.nmt.edu/publications/monographs/memoirs/51/

New Mexico Bureau of Geology and Mineral Resources
A research and service division of New Mexico Tech
geoinfo.nmt.edu
801 Leroy Place
Socorro, NM 87801-4796
(575) 835-5490